Downloaded from orbit.dtu.dk on: May 01, 2024

DTU Library

Immunophenotyping and neoepitope mapping in relation to immunotherapy of cancer

Skadborg, Signe Koggersbøl

Publication date:
2023

Document Version
Publisher's PDF, also known as Version of record

Link back to DTU Orbit

Citation (APA):
Skadborg, S. K. (2023). *Immunophenotyping and neoepitope mapping in relation to immunotherapy of cancer*. DTU Health Technology.

General rights
Copyright and moral rights for the publications made accessible in the public portal are retained by the authors and/or other copyright owners and it is a condition of accessing publications that users recognise and abide by the legal requirements associated with these rights.

- Users may download and print one copy of any publication from the public portal for the purpose of private study or research.
- You may not further distribute the material or use it for any profit-making activity or commercial gain
- You may freely distribute the URL identifying the publication in the public portal

If you believe that this document breaches copyright please contact us providing details, and we will remove access to the work immediately and investigate your claim.

Immunophenotyping and neoepitope mapping in relation to immunotherapy of cancer

Signe Koggersbøl Skadborg

PhD thesis

February 2023

Title:	Immunophenotyping and neoepitope mapping in relation to immunotherapy of cancer
Author:	Signe Koggersbøl Skadborg
Department:	Department of Health technology, Technical University of Denmark
Supervisor:	Professor Sine Reker Hadrup
Co-supervisors:	Mohammad Kadivar, PhD Professor Ulrik Lassen, MD
Submitted:	14th of March 2023

Preface

This thesis was submitted in partial fulfillment to obtain PhD degree at the PhD school of Health technology at Technical University of Denmark (DTU). Research activities was conducted under supervision of Professor Sine Reker Hadrup, with the assistance of co-supervisors Mohammad Kadivar and Ulrik Lasssen, in the T cells and cancer group located at DTU, Kongens Lyngby.

The thesis consist of an introduction presenting the relevant scientific background to understand the scope of research, followed by two scientific manuscripts and finalized with an epilogue that concludes the research I have carried out between March 2020 on February 2023 in relation to scientific fields.

Signe Koggersbøl Skadborg

14th of March 2023

Abstract

Cancer immunotherapy, specifically immune checkpoint inhibitors (ICIs), has emerged as a promising approach for treating various types of cancer. ICIs work by blocking inhibitory signals within T cells caused by interacting with cancer cells, so called immune checkpoints. Immune checkpoint blockade allows the T cells to recognize and attack the cancer cells. However, not all patients respond to this therapy, which may be due to cancer heterogeneity and the tumor mutational burden (TMB). While TMB has been linked to immunotherapy efficacy, some patient with cancers known to have low TMB respond while some with high TMB do not, indicating TMB alone cannot predict response. In this PhD thesis, we evaluated the immune response to immunotherapy in cancer patients with both low and high TMB.

We analyzed samples from patients diagnosed with recurrent glioblastoma (GBM) who were treated with PD-1 targeting ICI therapy. GBM is a type of brain cancer with a relatively low TMB, and immunotherapy has historically been largely ineffective for these patients. We therefore investigated the tumor microenvironment (TME), and particularly the T cell phenotypes after ICI therapy. Our findings revealed a distinct profile of intratumoral T cells with indications of increased activation, but also a more differentiated and exhausted profile, which may contribute to induced ICI resistance. Nonetheless, we were able to demonstrate tumor reactivity in tumor-infiltrating lymphocytes (TILs) in a small subset of the patients. Neoantigen-reactive T cells (NARTs) were further detected in both the tumor and blood samples of these responsive patients, indicating a potential for an improved clinical response to immunotherapy in this subgroup of patients. However, combination therapy may be necessary to achieve optimal results. In contrast, melanoma patients exhibit a high TMB and have generally demonstrated favorable responses to ICI therapy, however some patients do not respond. To address this issue, we evaluated a neopeptide vaccine administered to advanced melanoma patients in combination with anti-PD-1 therapy, with the goal to increase the NART repertoire in these patients. Our results showed that the neopeptide vaccine was safe for use and capable of inducing a T cell response towards vaccine peptides, primarily driven by CD4 T cells. However, due to the limited size of the patient cohort, we are unable to draw definitive conclusions regarding the vaccine's potential to increase clinical response.

All together, these studies emphasize the need for personalized and combinational therapy, even within the same cancer type and stage.

Dansk Resumé

Immunterapi, specielt immune checkpoint-inhibitorer (ICI'er), har vist sig at være en lovende behandlingsform til forskellige typer kræft. ICI blokerer hæmmende signaler i T-celler forårsaget af interaktion med kræftceller, såkaldte immun checkpoints. Blokering af disse immun checkpoint gør det muligt for T-cellerne at genkende og angribe kræftcellerne. Det er dog ikke alle patienter, der reagerer på denne behandling, hvilket kan skyldes heterogenitet og tumormutationsbyrden (TMB). Mens TMB er blevet korreleret med effektiviteten af immunterapi, reagerer nogle patienter med kræftformer, selv om de er associeret med lav TMB, mens nogle med høj TMB ikke gør, hvilket indikerer, at TMB alene ikke kan forudsige respons. I denne ph.d.-afhandling evaluerede vi immunresponser i forbindelse med immunterapi hos kræftpatienter med både lav og høj TMB.

Vi analyserede prøver fra patienter diagnosticeret med recidiv glioblastom (GBM), som blev behandlet med anti- PD-1 ICI terapi. GBM er en type hjernekræft med en relativt lav TBM, og immunterapi har historisk set været ineffektiv for disse patienter. Vi undersøgte derfor tumormikromiljøet (TME), og især T-cellernes fænotype efter ICI-terapi. Vores resultater viste en profil af T-celler fra tumor som indikerede en øget aktivering, men også en mere differentieret T celle profil. Dette kan potentielt bidrage til induceret ICI-resistens. Ikke desto mindre var vi i stand til at påvise tumor-reaktivitet i tumorinfiltrerende lymfocytter i få af patienterne. Neoantigen-reaktive T-celler blev yderligere påvist i både tumor- og blodprøver fra disse patienter, hvilket indikerer et potentiale for et klinisk respons på immunterapi i denne undergruppe af patienter. En kombination af forskellige behandlingsformer kan dog være nødvendig for at opnå optimale resultater. I modsætning til GBM har patienter med modermærkekræft en høj TMB og har generelt vist at respondere godt på ICI-terapi, men der er stadig patienter som ikke viser klinisk respons. For at adressere dette problem undersøgte vi brugen af en neopeptid-vaccine administreret til patienter med fremskreden modermærkekræft i kombination med anti-PD-1-terapi, med det mål at øge repertoiret af neoantigen-reaktive T-celler hos disse patienter. Vores resultater viste, at neopeptid-vaccinen var sikker og i stand til at inducere et T-celle-respons mod vaccine-peptider, primært drevet af CD4 T-celler. Grundet den begrænsede patientkohorte var vi ikke i stand til at drage konklusioner vedrørende vaccinens potentiale til at øge et kliniske respons.

Tilsammen understreger disse undersøgelser behovet for personlig og kombinationsterapi, selv inden for samme kræfttype og -stadie.

Acknowledgements

First I would like to thank my supervisor Sine Reker Hadrup for giving me the opportunity to work as a PhD student in your group and gain a great amount of knowledge. I want to thank you for the supportive and trusting approach to your management and guidance. It has given me a large ballast for future projects and challenges. Thank you, Sine! I would like to thank my co-supervisors Ulrik Lassen and Mohammad Kadivar for the supervision on this journey. Mo, thank you for your support and cheering words and of course for the fun parties!

I want to express my gratitude to all the collaborators in this thesis. A special thanks to Sofie for being so cheerful and easy to work with, and to Simone for introducing me to the world of brain cancer and for the long nights at the flow cytometer.

A wholehearted thanks to all the patients who participated in the trials and donated tissue in the name of science.

I want to acknowledgement of all former, old and new colleagues at xTI. Thank you for making it a lovely and supportive place to work the last 3 years. Thank you Anni, Bente and Anna for introducing me to the lab, for all the help you provided and nice chats we have had. Thank you Marianne for your help in the administrative jungle. Thank you Annie and Kamilla for always being ready to help when I got stuck in R. A thanks to Lasse, Yogesh, Annie and Siri, for taking the time to proof reading my thesis, it was much appreciated. A big thank you to the R-hackers; Marie, Yogesh, Susana and of course Marcus for sharing the journey through the PhD struggles and success. Siri, Maria, Janine and Sara, thank you for all the comforting chats and shoulders to lean on, both in - and outside the lab. In general I want to thank the entire SRH group for all the talks and fun times at lunch breaks, conferences, outings, Friday bars and more, you are the best!

To my two guardian angles, Hofi and Micaela, thank you for always being there, and make sure my mental health is intact! To my great friends I can always count on, Christina, Francesco, Lea, Ea, Rebecca, Katarina and Christine who is still there even though time has been limited. To my loving family, for being a safe place where I can always find support and good advice, it means the world.

And finally Glynn, thank you for being my rock, even when you are on shaking grounds ♥

-Signe

Publications and Manuscripts

Includes in the thesis

Manuscript I

Signe Koggersbøl Skadborg*, Simone Maarup*, Arianna Daghi, Annie Borch, Sille Hendriksen, Jane Skøjth-Ramussen, Christina Yde, Benedikte Hasselbalch, Inge Marie Svane, Ulrik Lassen[+] & Sine Reker Hadrup[+], "Altered intratumoral immune composition after neoadjuvant Nivolumab in patients with recurrent Glioblastoma", *Manuscript in preparation*

Manuscript II

Signe Koggersbøl Skadborg*, Sofie Kirial Mørk*, Benedetta Albieri ,Arianna Draghi, Marie Christine Wulff Westergaard, Joachim Stoltenborg Granhøj, Mohammad Kadivar, Annie Borch, Nana Overgaard, Anders Bundgård Sørensen, Ida Svahn Rasmussen, Lars Vibe Andreasen, Christina Westmose Yde, Nis Nørgaard, Torben Lorentzen, Thomas Trolle, Christian Garde, Jens Friis-Nielsen, Dennis Christensen, Jens Vindahl Kringelum, Marco Donia, Sine Reker Hadrup & Inge Marie Svane, "Dose Escalation study of a Personalized Peptide-based Neoantigen Vaccine (EVX-01) in Patients with Metastatic Melanoma", *Manuscript in preparation*

Not includes in the thesis

Sofie Kirial Mørk, Mohammad Kadivar, Kalijn Fredrike Bol, Arianna Draghi, Marie Christine Wulff Westergaard, Signe Koggersbøl Skadborg, Nana Overgaard, Anders Bundgård Sørensen, Ida Svahn Rasmussen, Lars Vibe Andreasen, Christina Westmose Yde, Thomas Trolle, Christian Garde, Jens Friis-Nielsen, Nis Nørgaard, Dennis Christensen, Jens Vindahl Kringelum, Marco Donia, Sine Reker Hadrup & Inge Marie Svane, "Personalized therapy with peptide-based neoantigen vaccine (EVX-01) including a novel adjuvant, CAF®09b, in patients with metastatic melanoma", *Oncoimmunology,* 2022, 11 (1)

* These authors contributed equally

Abbreviations

ADCC	antibody-dependent cellular cytotoxicity
AI	artificial intelligence
APCs	antigen presenting cells
BBB	blood brain barrier
cDC	conventional DC
CNS	central nervous system
CTL	cytotoxic T lymphocyte
CTLA	cytotoxic T-lymphocyte–associated antigen
DAMPs	damage-associated molecular patterns
DCs	dendritic cells
EMA	european medicines agency
ER	endoplasmic reticulum
FasL	Fas ligand
FDA	food and drug administration
FGL-1	fibrinogen-like protein 1
HBV	hepatitis B virus
HPV	human papillomavirus
ICIs	immune checkpoint inhibitors
ICS	intracellular cytokine staining
IDO	Indoleamine-2,3-dioxygenase
IFN	interferon
LAG-3	lymphocyte activation gene 3
LN	lymph node
MAGE	melanoma antigen gene
MDSCs	myeloid derived suppressor cells
MHC	major histocompatibility complex
MHC-I	MHC class I
MHC-II	MHC class II
MS	multiple sclerosis
NARTs	neoantigen reactive T cells
NGS	next-generation sequencing
NK cells	natural killer cells
NLRs	NOD-like receptors
PAMPs	pathogen-associated molecular patterns
PAP	prostatic acid phosphatase
PD	programmed cell death protein
pMHC	peptide-MHC
poly I:C	polyinosinic–polycytidylic acid
PRR	pattern recognition receptors

SNV	single nucleotide variants
TAMs	tumor associated macrophages
T_{CM}	central memory T cell
TCR	T cell receptor
T_{eff}	effector T cells
T_{EM}	effector memory T cells
T_{EMRA}	T_{EM} re-expressing CD45RA
T_{EX}	exhausted T (T_{EX})
T_{FH} cell	follicular helper T cell
TGF	transforming growth factor
T_H	T helper cells
TIGIT	T cell immunoglobulin and ITIM domain
TIL	tumor infiltrated T lymphocyte
TIM	T-cell immunoglobulin and mucin domain 3
TLRs	toll-like receptors
TMB	tumor mutational burden
TME	tumor microenvironment
TNF	tumor necrosis factor
$T_{pre\text{-}EX}$	pre-exhausted T cells
Treg	T regulatory
T_{RM}	tissue resident memory T cells
TSA	tumor specific antigens
TAAs	tumor associated antigens
VEGF	vascular endothelial growth factor
β2m	beta-2 microglobulin

Table of content

Introduction

Chapter 1 | T cells and The Immune System

The immune system is the defense system of the body and its duty is to protect the body from foreign pathogens and clear out unhealthy cells. The immune system is comprised of barriers, signaling compounds and cells with various functions, and spans from epithelial- and mucosal surfaces, over the fast innate immune response to the highly specialized adaptive immune response (1). Imbalances in the immune system can lead to various diseases. An overactive immune system can cause autoimmune diseases where immune cells are attacking healthy cells. Examples could be an autoimmune response toward pancreatic beta cells where insulin is produced, which leads to the well-known disease, Type 1 Diabetes (T1D) (2). Another example is Multiple Sclerosis (MS), which is a chronic inflammation of the central nervous system (CNS) that can be induced by self-reactive immune cells causing myelin loss among other, which can lead to neurological disorder (3). However, autoimmune responses can also target less vital cells such as the hair follicles leading to hair loss known as alopecia (4). On the other hand, when the immune system fails to clear damaged and unhealthy neoplastic cells we can develop cancer. Cancer and the immune system will be the focus of this thesis, which I will elucidate more detailed in chapter 2, *Cancer Immunology*.

1.1 The interplay between innate and adaptive immune system

The cells and components of the innate immune system are responsible for the quick, first line of defense of the body. It is able to induce a rapid response when a pathogen intrudes within minutes or hours. When the innate immune system fails to clear the infection, it reports to the cells of the adaptive immune system, which will mount a strong and specialized response that instead can take days or weeks to fully activate (1). The innate immune cells can elicit fast responses due to invariant receptors called pattern recognition receptors (PRR), which can detect patterns that occurs on pathogens or is released from unhealthy cells. Such PRR comprise receptors like toll-like receptors (TLRs), NOD-like receptors (NLRs), C-type lectin receptors and more. PRRs recognize pathogen-associated molecular patterns (PAMPs) and damage-associated molecular patterns (DAMPs). PRRs are expressed on innate immune cells, including

macrophage and dendritic cells (DCs) (5). Macrophages reside in the tissue and can through binding of PRR engulf pathogens to clear the tissue. Additionally, macrophages also secrete biological active molecules, like chemokines and cytokines, to recruit and stimulate immune cells and induce inflammation at the infected site (6,7). DCs can, like macrophages, also engulf pathogens and contribute to the clearance of the infected site, although they are not as effective as macrophages. Their main function is to present information about the infection to adaptive immune cells. DCs are therefore thought to be the primary messengers between the innate and the adaptive immune system. DCs are specialized in processing extracellular pathogen or proteins and present them on surface molecules called Major histocompatibility complex (MHC) (8). The DCs migrate from the inflamed site to a secondary lymphoid organ, such as a lymph node (LN) located close by. This is the bridge between the innate and adaptive immune system, where DCs function as antigen presenting cells (APCs) and deliver information to the cells of the adaptive immune system, the lymphocytes; B cells and T cells (8) (Firgure 1).

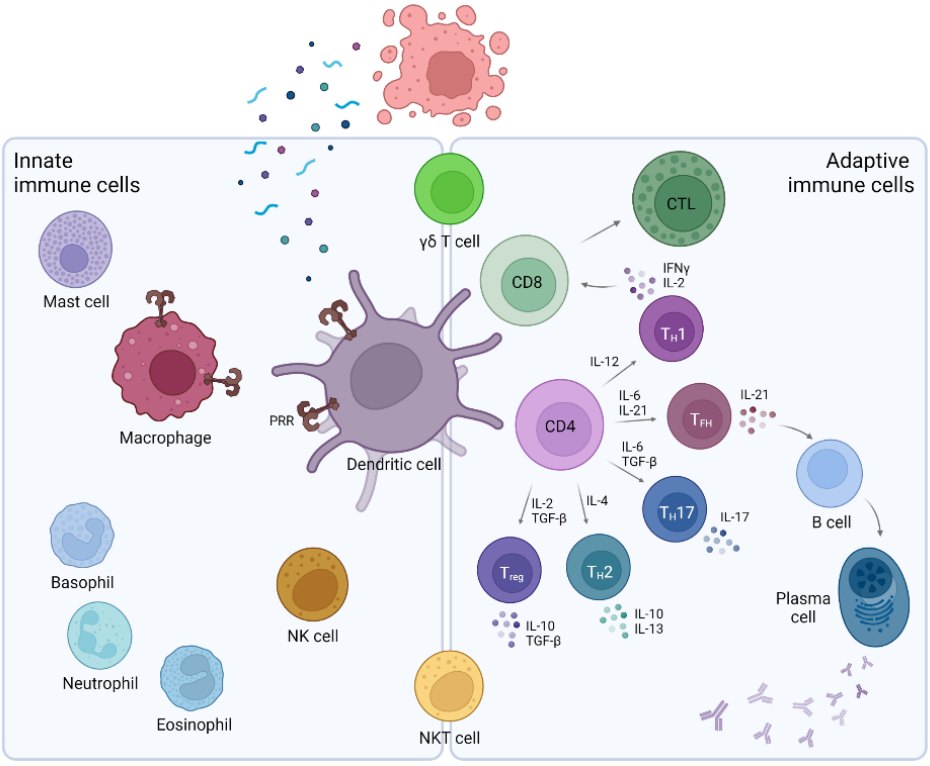

Figure 1 | Immune cells of the innate and adaptive immune cells. Innate immune cells are the first to provide an immune response protecting against infection or cancer. This comprise mast cells, granulocytes (neutrophils, basophils, eosinophils), NK cell cells, macrophages and dendritic cells (DCs). They act in a non-specific manner, and recognizes e.g. danger signals like DAMPs and PAMPs via pattern reconition receptors (PRR). DCs are delivering information from the infection or cancer site, to the adaptive immune cells, T cells and B cells. These immune cells can induce a highly specific and effective immune response. T cells differentiate into different subsets upon activation, defined by types of cytokine in the close environment. CD8 T cells traditionally differentiated into cytotoxic T cells (CTLs) and CD4 T cells can differentiate into different helper T cells (T_H) (T_H1, T_H2, T_H17, Treg, T_{FH}). T_H cells have different functions, e.g. help the maturation of B cell to plasma cells, in order to induce a humoral response (antibodies). NKT, (NK cells) and γδ T cell are innate-like lymphocytes. Figure inspired by Sara Hernández, PhD thesis (June 2022) Created with BioRender.com

Antigen receptors of T cells and B cells are, unlike PRR, highly specific. A naïve T cell in the LNs can become activated upon recognition of its cognate antigen presented on MHC molecules, when simultaneous co-stimulation is provided (9). Conventional T cell can be divided into two major sub-categories; cytotoxic CD8 T cells and helper CD4 T cells. The primary function of CD8 T cells is direct killing of their target, while CD4 T cells stimulate and support other immune cells (1). For example, a CD4 T cell can stimulate an immature B cell to enter the germinal center within the LN and undergo somatic hypermutation. Together with follicular DCs, CD4 T cells are also involved in the selection of mature B cells which will undergo further class-switching to become plasma cells or memory B cells (10). Plasma cells release highly specific antibodies that are a vital part of the humoral and fast response. Natural killer cells (NK cells), NKT cells and unconventional γδ T cells express Fc receptors, which can bind to the Fc region of an antibody. A pathogen or a cell which has been opsonized by antibodies can hereby be killed by NK cell or γδ T cells through antibody-dependent cellular cytotoxicity (ADCC) (11,12). NK, NKT and, γδ T cells belong to the lymphocyte family, but since they do not carry highly variable receptors like conventional T cell and B cell, they are considered a part of the innate immune system (13). Even though NK, NKT, and γδ T cells do not possess such highly specific receptor, they express various alternative receptors, which can induce killing of their targets. Moreover, they are also found to support the adaptive immune system through secretion of cytokines (14–16). The current thesis focuses on conventional αβ T cells, which carries the alpha and beta chain of the T cell receptor (TCR) and these will be referred to as T cells hereafter.

1.2 T cell development and recognition of the peptide-MHC complex

T cells derive from the lymphocyte precursor, which has been differentiated in the bone marrow. The lymphocyte precursor migrates to the thymus, and at this point, it do not express neither a TCR nor any of the two co-receptors, CD4 or CD8 (17). With the help from thymic epithelial cells, the lymphocyte precursor will differentiate into a T cell precursor which will start to express its TCR, and eventually become highly proliferative thymocyte. The thymocyte will go through TCR gene rearrangement during the proliferative state, where the V, (D) and J regions will undergo recombination and give rise multiple highly variable TCR clones. Thymocyte here gains a unique TCR and becomes double positive for the two co-receptors (18). The thymocytes need to go through two selection processes, a positive and a negative to become a naïve T cell. During the positive selection new hypermutated TCRs will be tested for their ability to bind to an MHC molecules. If a TCR recognizes an MHC class I (MHC-I) molecules, expressed by thymic epithelial cells, the co-receptor CD8 will be assisting the binding, and the thymocyte will become CD8 single positive. If the TCR recognizes an MHC class II (MHC-II) molecules, the co-receptor CD4 will be

selected and the thymocyte will become CD4 single positive. If the new TCR is not able to bind to either MHC-I or MHC-II, the thymocyte will die by neglect (19). Thymic epithelial cells and DCs are presenting self-peptides on their MHC-I and MHC-II to the single positive thymocytes for negative selection within the thymus. If the thymocyte binds strongly to the MHC presented self-peptide, it will undergo clonal deletion and die by programmed cell death, so-called apoptosis. Single positive thymocytes that do not bind or have a weak binding to a self-peptide MHC complex will become a naïve T cell and enter the periphery (17). This negative selection process is called central tolerance and is important to avoid the escape of autoreactive T cell into the periphery. In case an autoreactive T cell slips through the negative selection, peripheral tolerance will take over (20).

As mentioned, the peptide-MHC (pMHC) complex is important in the development and selection of T cell, but also for the T cell function. In humans it is known as the human leukocyte antigen (HLA). HLA genes are highly polymorphic and more than 25,000 alleles have been identified in 2020 (21). MHC will from hereon be used for simplicity. MHC-I is expressed on all nucleated cells of the body and serves both as an indication of a healthy cell and to present intracellular peptides derived from infection or mutations found in neoplastic cells. MHC-II is only expressed on APCs, which can take up extracellular pathogens or proteins through phagocytosis and degrade them for presentation on MHC-II molecules (1). A subset of the conventional DCs (cDC), are highly specialized in cross-presentation of extracellular proteins - the cDC1. The cDC1 subset can via cross-presentation both present antigen of the extracellular compound on MHC-I and MHC-II and are therefore important for the activation of CD8 and CD4 T cell in the secondary lymphoid organs(22). CD8 and CD4 T cells will recognize different peptides; CD8 T cells recognize short 8-11mer peptides, while CD4 T cells recognize longer peptides with 13-25 amino acid. This is reflected in the binding groove of the MHC-I and MHC-II. MHC-I has a closed and restricted binding groove, while MHC-II has an open binding groove resulting in a more flexible binding of peptides, which are also less restricted for the MHC-II alleles (23). Therefore, the peptide loading are also quite different (Figure 2).

For MHC-I, cytosolic proteins are processed and trimmed by the proteasome in the cytosol. The shorter peptides are hereafter transported into the endoplasmic reticulum (ER), where it is additionally trimmed. The transmembrane MHC-I molecules are synthesized and assembled in the ER. When the binding groove of the MHC-I is exposed, the short peptide can bind to MHC-I, whereafter it is transported through the Golgi apparatus (24). However, when an extracellular pathogen or protein is taken up by the APC, it will be degraded by lysosomal proteases after the phagosome or endosome fuses with lysosomes. MHC-II is also synthesized in the ER, wherein the binding groove of MHC-II is protected against binding of random

ER proteins. The MHC-II is transported through the Golgi apparatus before it within an endosome fuses with the phagosome or endosome containing degraded extracellular proteins. The longer peptides can now bind to the MHC-II binding groove(25,26). After peptide-loading will peptide-MHC molecules travel to the cell surface and be present to the extracellular surroundings.

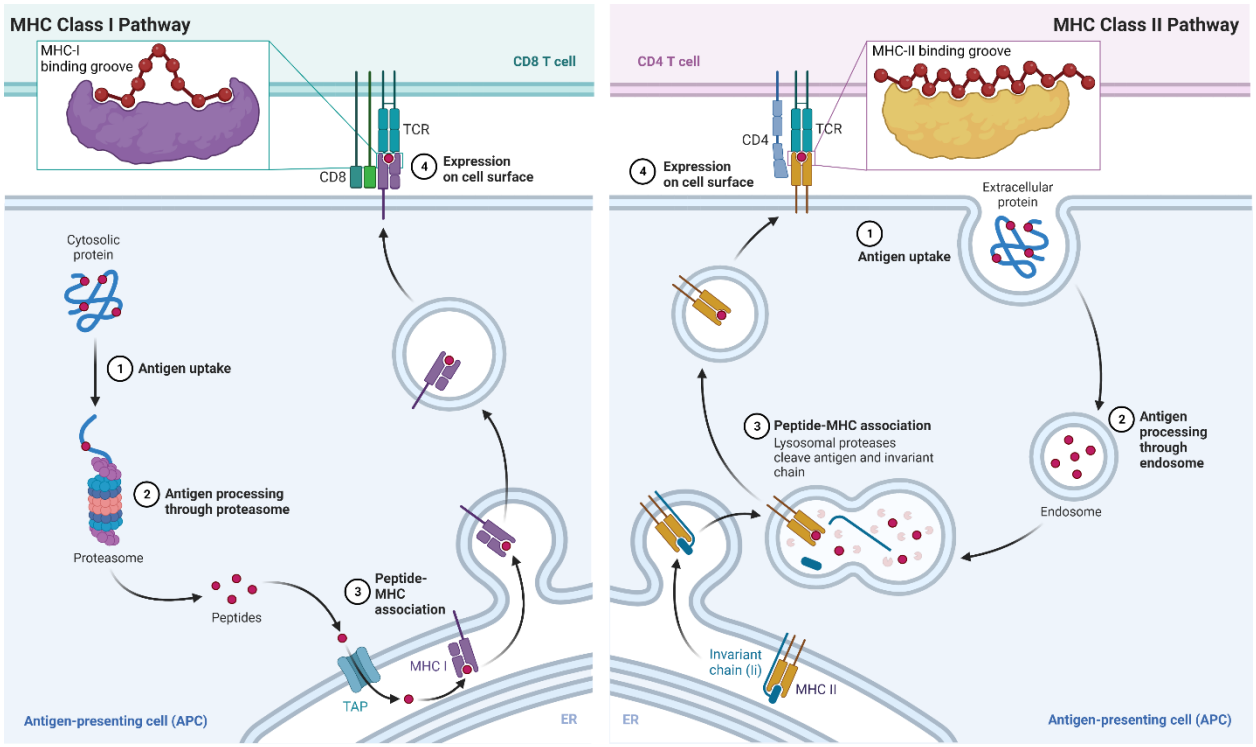

Figure 2 | antigen processing and peptide loading of MHC-I and MHC-II. MHC-I is expressed on the surface of nucleated cells and present peptides derived from intracellular proteins to CD8 T cells. Antigen processing for MHC-I involves degradation of intracellular proteins by the proteasome, followed by transport of the processed peptides into the endoplasmic reticulum (ER) by the transporter associated with antigen processing (TAP). In the ER, the peptides are loaded onto MHC-I molecules. MHC-II is expressed on the surface of professional antigen-presenting cells (APCs), and present peptides derived from extracellular proteins to CD4 T cells. Antigen processing for MHC-II involves the internalization of extracellular proteins via endocytosis or phagocytosis, followed by degradation in endosomes and lysosomes. The processed peptides are hereafter loaded onto MHC-II. The loaded MHC-peptide complexes are then transported to the cell surface for recognition by CD8 and CD4 T cells. Modified from BioRender template. Created with BioRender.com

1.3 T cells priming and activation

After maturation and thymic selection, the naïve T cells will travel to the secondary lymphoid organs, e.g. the LNs, where the naïve T cells are searching for their cognate antigen presented by an APC. When a naïve T cell has found its' antigen, the priming and activation of the T cell can begin. The naïve T cell need three signals for its primary activation; 1) antigen recognition through TCR:MHC binding, 2) Co-stimulation, e.g. binding of the co-stimulatory molecule CD28 to CD80/CD86 and 3) differentiation of the T cell through cytokine stimulation (27) (Figure 3).

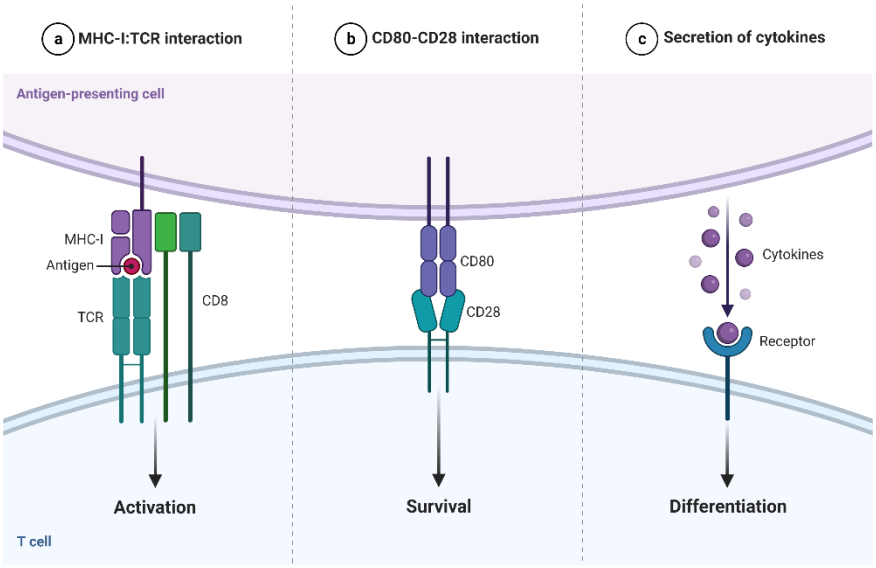

Figure 3 | T cell priming and activation . T cells need to receive three signal for the initial priming and activation. 1) TCR recognition of the cognate antigen presented on MHC. 2) Interaction between co-stimulatory molecules expressed on T cells (e.g. CD28) and APCs (e.g. CD80/CD86). Absence of this co-stimulation would result in T cell anergy or programmed cell death. 3) Cytokine signaling expressed by the APC and surrounding cells in the close environment. This will lead to differentiation of the T cell as well as expansion (e.g. IL-2). Modified from BioRender template. Created with BioRender.com

A naïve T cell will recognizes its' antigen through TCR binding to the pMHC complex. The TCR:MHC interaction is stabilized by the co-receptors, CD4 or CD8. The CD3 complex is additionally essential for TCR signaling and is therefore widely used as a universal marker for T cells, as it ubiquitously expressed on T cells (28). The co-receptor binding to pMHC induces a recruitment of additional factors to the immunological synapses and will thereby also help T cell activation (29). Together with the co-stimulatory signal through CD28 engagement with CD80/CD86, the T cells will become activated. During the initial priming of the T cell, it needs the third signal to be differentiated into its destined type of the effector T cell. CD4 T cells can polarize into different subsets of T helper (T_H) cells, which will have different functions in the immune response (30) (Figure 1). T_H1, – 2 and – 17 will mainly be found and act in the periphery, while the follicular helper T (T_{FH}) cell assists the maturation of B cell in the LN, and is responsible in the production antibodies for the humoral response, as described earlier (10). Additionally, T regulatory (Treg) cells exhibit a regulatory role by dampening immune responses, e.g. after clearance of a pathogen and to maintain peripheral self-tolerance (31). Furthermore, Treg cells also play a role in suppression of anti-tumor immune responses and will be elaborate in the next chapter, *Cancer Immunology*.

CD4 T cells are differentiated into T_H1 cells in the presence of IL-12 and IFNg. T_H1 cells will start producing IFNγ which will serve as a positive feedback and further differentiation into the T_H1 cell subtype. T_H1 cells also support polarization of the naïve CD8 T cell to the cytotoxic T lymphocyte (CTL) through secretion of IFNg and IL-2 (30). As the name indicates, CTLs are cytotoxic cells that inspect cells of the body for MHC-I presentation of intracellular antigens, and will recognizes non-self, such as antigens related to infection

or malignancies. Upon TCR recognition of its cognate antigen, the CD8 positive CTL can secrete cytotoxic molecules, namely perforin and granzyme B. Perforin will form pores in the target cell allowing granzyme B to enter and induce apoptosis through activation of the caspase pathway. CTLs can also induce apoptosis through cross-linking Fas ligand (FasL) to Fas expressed by the target cell but is acting much slower (32). Additionally, an indirect killing of target cells can be obtained through release of tumor necrosis factor(TNF) -α and interferon (IFN)-γ (27).

Naïve T cells are in a quiescent state before priming, to avoid activation and expansion when encountering a cognate antigen in the periphery. This will keep a relative number of the naïve T cell clones during steady-state, and also contributes to the mechanisms of self-tolerance (33). Another contributor of self-tolerance is T cell anergy, which can be induced during and after T cell priming due to lack of co-stimulatory signaling, a tolerogenic TCR activation(33). In the periphery the anergic state of a T cell can be sustained during chronic inflammation, due to continued antigen exposure, leading to low production of IL-2 and TNF (34).

1.4 Peripheral T cell differentiation

After priming and activation, T cells enter the periphery. Peripheral T cell differentiation are initiated upon antigen recognition, whereafter the T cell goes through clonal expansion. This allows the T cells to differentiate into effector T (T_{eff}) cells, which will perform the effector function of the given T cell subtype. After clearance of the target, a small fraction of the expanded T cells will become memory T cell and maintain a long-lasting antigen response. The remaining T_{eff} will contract and undergo apoptosis. A population of memory T cells are maintained, to evoke a rapid and functional response towards known antigens (35).

CD45 is a common marker for leukocytes. In T cells, CD45 is thought to be involved in the regulation of TCR activation (36). Different isotype forms are expressed on T cells depending on their differentiation status. The isotype form CD45RA is expressed in naïve T cells. After priming and activation, the T cells downregulate expression of CD45RA, and upregulates expression of another isoform, CD45RO (37). Together with the expression of the chemokine receptor CCR7, the T cells' differentiation state can be determined. CCR7 is highly expressed on naïve T cells. CCR7 expression will allow them to home to the LNs, as mature DCs, e.g. cDC1, secrete the cognate chemokine, CCL19 (38). T memory cells can be divided in to two groups based on their level of differentiation; central memory T (T_{CM}) cell and effector memory T (T_{EM}) cells (39). T_{CM} cells express CCR7 and are therefore able to migrate to the LN to be activated, while

T_{EM} has downregulated CCR7 expression and therefore remains in the periphery. T_{CM} cells are less differentiated and keep a higher proliferative capacity, while T_{EM} cells are at later stages of differentiation and instead hold a higher cytotoxic capacity as they are more specialized (35). Taken together, T_{CM} cells are therefore thought to be better at handling systemic infections, while T_{EM} would clear infections in peripheral organs (40). Tissue resident memory T (T_{RM}) cells appear to be a subtype of T_{EM} cells, which stays in the tissue instead of entering circulation after clearance. T_{RM} cells express the integrins CD103 and CD49a which helps the T cells to enter the given tissue, and CD69 that is expressed immediately after TCR recognition, to retain the T cells in the tissue (41,42) (Figure 4).

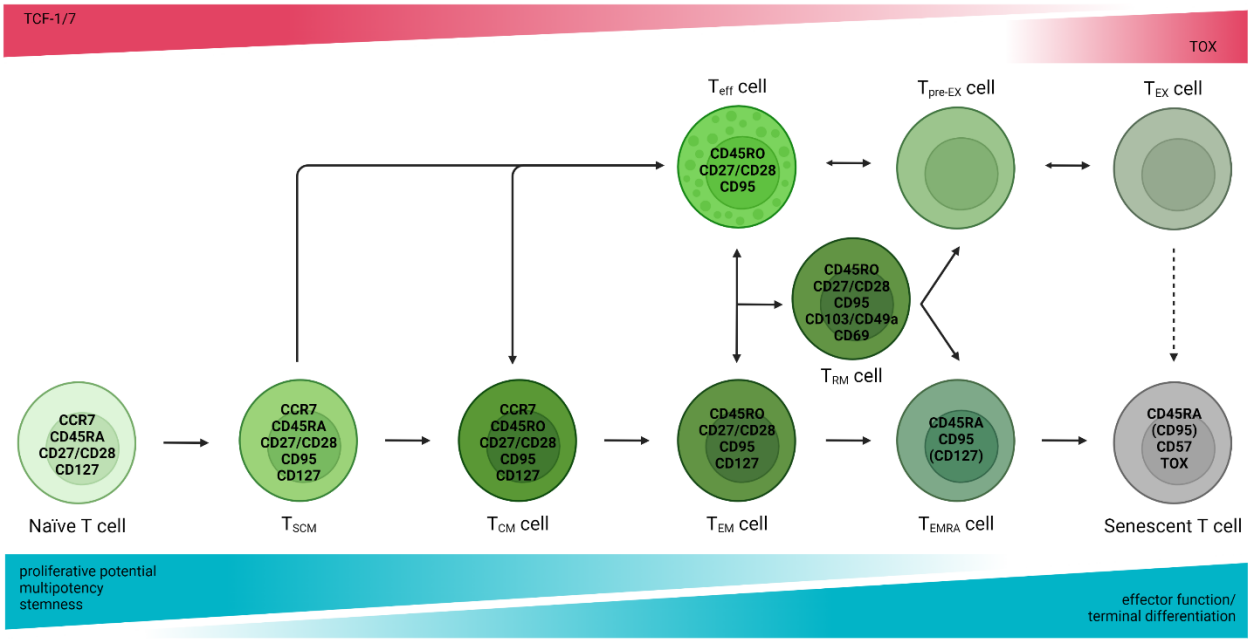

Figure 4 | Overview of T cells differentiation. A schematic presentation of T cell differentiation and marker expression defining the different stages of differentiation from a naïve T cell to an exhausted or senescent T cell. The diminishing red lines are depicting expressing level of the transcription factors, TCF1/7 and TOX. The different differentiation stages of T cells are thoroughly described in the text. In short, upon activation naïve T cells differentiate into effector T cells (T_{eff}), these are short lived and only a small faction persist at memory T cells, for long-term immune responses (T_{CM}, T_{EM}). Some of these can become tissue-resident and thus reside in peripheral tissue instead of circulating (T_{RM}). Effector and memory T cells can also acquire an exhausted profile over time or due to a continuing TCR activation. These T cells has a drastically reduced effector function (T_{EMRA}, T_{pre-EX}, T_{EX}). Created with BioRender.com

Due to the rapid contraction after clearance, T_{eff} cells do not occur during steady-state, however terminal differentiation of effector and effector memory cells can persist in the circulation. These cells are T_{eff} cells that have re-expressed CD45RA, thereof the name T_{EMRA} cells, and are mainly found among CD8 T cells (35). This subpopulation has a low TCR activation with the reexpression of CD45RA, and a low proliferative capacity, which can be measured by the expression of the transcription factor Ki67 (43).

During chronic inflammation, e.g. due to infection or tumor escape, a continued antigen presentation can lead to T cell exhaustion (44). A T cell memory response can fail to be developed during a constant TCR stimulation, leading to a specific antigen repertoire will consist mainly of exhausted T (T_{EX}) cells, and no memory T cells. Some T_{EX} cells can still be functional, but to a much lower extend, with low levels of cytokine production and high expression of so-called inhibitory checkpoint molecules (33). Inhibitory checkpoint molecules, is a part of the checkpoints for self-tolerance, as they upon ligand engagement can inhibit T cell activation through intracellular signaling (45). Various inhibitory molecules or checkpoint molecules have been identified, such as PD-1, CTLA-4, TIM-3, LAG-3, TIGIT, etc. Many of these are now also targeted when developing therapies, which will elaborated in the chapter *Cancer Immune Therapies*. T_{EX} cells are different from anergic T cells (described above), though they appear similar in the landscape of surface markers. Hypo-responsiveness of the anergic T cell is due to co-receptor deficiency, while T_{EX} cells has decrease response due to chronic stimulation of the TCR in the presence of co-stimulation(33). However, T_{EX} cells appears to have transcription factor-expression pattern including downregulation of TCF1 and upregulation of TOX, which might be involved in the survival from T_{eff} cells to T_{EX}. The potential functionality of T_{EX} cells can be predicted based on TCF1 expression, which appears to have stem-cell like properties (46,47). TCF1-expressing T_{EX} cells can therefore be termed as $T_{pre\text{-}EX}$ cell and can potentially benefit from blockade of the inhibitory checkpoint molecules (48). T_{EX} cells are longer lived than T_{eff} and could therefore from evolutionary perspective help to control a chronic infection. On the other hand exhaustion and inhibition could also ensure reduced tissue damage and autoreactivity (33). When T cells reach a terminally differentiated stage, they have lost their proliferative capacity due to the short telomeres. They belong to the T_{EMRA} cell population and can be defined by expression of CD57, which correlates with the appearance short telomeres (49,50). They have downregulated the co-receptors CD27 and CD28, but the senescent T cells can secrete large amount of pro- or anti-inflammatory cytokines in contrast to T_{EX} cells. Senescent T cells will accumulate during aging but also during chronic inflammation (33).

Overall, T cells are a highly diverse group of immune cells, with many different functions and destinies. T cell immunity is a complex and fine-tuned system, and this chapter has only touched upon a fraction of their remarkable functions in the adaptive immune system.

Chapter 2 | Cancer Immunology

Cancer is a name for a relatively heterogeneous group of diseases, which appears in many different forms depending on which part of the body it develops. Common for all cancer types is that they arise due to mutations in the genome. Mutations can occur in any cell of the body, which can cause cells to hyper-proliferate and induce tumor formation with invasion of vital organs. Cancer is therefore considered as a genetic disease. Mutations can arise due to environmental factors like; UV light radiation, chemical carcinogen and pathogenic infections as well as life style factors such as; alcohol consumption, obesity and smoking, but mutations also arise during normal cell division(51). Mutations can occur without causing any harm to the cell thanks to the DNA repair machinery, otherwise tumor suppressor genes will ensure the cell will undergo cellular arrest or apoptosis, and hereby inducing intrinsic tumor suppression. However, environmental and lifestyle factors can also impair the DNA repair machinery, which can contribute an increase in mutational load over time. Mutations can hit essential genes in the cell proliferation machinery and induce tumor formation, through gain-of-function mutations in proto-oncogenes, responsible for anti-apoptotic and proliferative signaling, or through loss-of-function mutations in tumor suppressor genes, responsible for pro-apoptotic and anti-proliferative signaling (52).

Our body is a fine tuned system and several mechanism and cells are responsible for clearing neoplastic cells and avoid malignant tumor formations. In 2000, Douglas Hanahan and Robert Weinberg first reviewed and defined hallmarks of cancer, containing acquired function for survival, proliferation and dissemination of cancer cells (53). In 2011, they revised these six hallmarks and added two enabling characteristics; *genome instability and mutation* and *tumor promoting inflammation*, as well as two additional emerging hallmarks; *deregulating cellular energetics* and *avoiding immune destruction*(54). These new hallmarks and characteristics, made it clear that immune cells and – factors are not only taking part in cancer elimination, but are also contributing to sustaining the tumor and induce tumor growth. The interplay between the immune system and tumor formation will be elaborated in this chapter.

2.1 Cancer immunoediting

Over a century ago Paul Ehrlich proposed that the immune system could reduce the occurrence of carcinomas (55–57). This little seed led to the hypothesis of “cancer immunosurveillance”, suggested by F. M. Burnet and L. Thomas in parallel from the 1950s (57–59). The concept of immunosurveillance implied that frequently arising neoplastic cells would be rejected by the immune system, and thereby avoid

formation of tumors. This hypothesis was further revised in the start of the new millennium by Schreiber and Dunn who described the idea of cancer immunoediting, which comprise the three interchangeable phases; elimination, equilibrium and escape, also known as the 3 E's (60,61) (Figure 5). This process was shown experimentally by Shankaran et al. reported in 2001. They demonstrated that immune compromised mice were more susceptible to tumor growth upon carcinogenic stimulus than wild type mice, supporting the immunosurveillance concept. However, they also showed that tumors grown in immune competent mice were less immunogenic than tumors from immune compromised mice, resulting in tumor growth upon transplantation into wild type mice. They therefore suggested that the immune system contributes to the sculpturing of tumor towards immune escape in an immunoediting process (62). This advocates that the immune system not only takes part in the initial elimination of neoplastic cells, but also during the development of tumors.

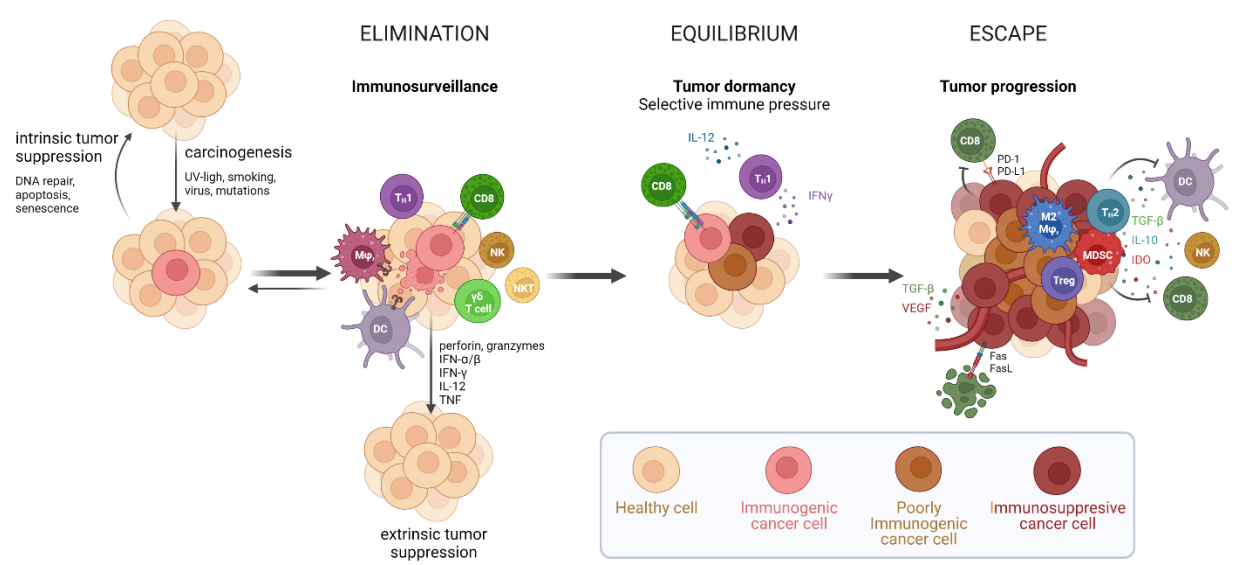

Figure 5 | Cancer immunoediting. Cancer cells develops when the intrinsic tumor suppression fails. This is when cancer immunoediting begins, which comprise up to three phases. 1) *Elimination*; cancer cell can be eradicated by immune cells from the innate and adaptive immune system due to immunosurveillance. 2) When the immune system is not able to eliminate cancer cells, tumor formation occurs and the cancer enters the *equilibrium* phase. The adaptive immune cells are able to control the out-growth of the tumor. However, the immune cells can induce a Darwinian selection pressure on cancer cells during this potentially long phases. 3) Eventually, the tumor can enter the *escape* phase where the cancer cell has become poorly immunogenic and even acquire immunosuppressive function, including recruitment of immunosuppressive cell to the tumor microenvironment. Figure inspired by (63). Created with BioRender.com

The elimination phase entails immunosurveillance by the innate and adaptive immune cells, which will form a response to eliminate cancerous cells. Cancer cells release danger signal, like DAMP, leading to a fast immune response by the innate immune cells, including macrophages, DCs, NK cells, γδ T cells, NKT cells, followed by an adaptive response by CD8 T cells and CD4 T cells, especially T_H1 cells. These will all create an anti-cancer environment, through secretion of pro-inflammatory cytokines and effector

molecules, including INFa/b, IFNg, IL-2, IL-12, TNF, Perforin and more (60,63). Specifically, CD8 T cell are the main driver of tumor control(64) through recognition of antigens presented on the cancer cells, including tumor associated antigens (TAAs) or tumor specific antigens (TSA). When the immune cells reach complete clearance of cancer cells through the extrinsic tumor suppression, a full protection against tumor development is reached. However, if the first immune response is not able to clear out cancer cells, a tumor will start to form and enters the equilibrium phase. Here the tumor will exist in a state of dormancy, which can last over several years. During this phase, adaptive immune cells will keep the tumor in check, by creating a dynamic balance between tumor growth and immune control. To this end, this is also where immunoediting begins and a Darwinian evolution of cancer cells will take place, favoring immune resistant cancer-cell clones. Over time, the tumor can enter the third phase – escape. The cancer cells have now developed mechanisms to escape immune recognition and created an anti-inflammatory microenvironment, allowing the tumor to grow and potentially disseminate (60).

2.2 Tumor microenvironment

The tumor microenvironment (TME) of solid tumors is extremely complex and consist of a highly heterogeneous composition of various cells. Cancer cells are of course the primary and driving factor within the tumor microenvironment, however the mass formation also require structural support, such as endothelial cells forming blood- and lymphatic vessel, stromal cells, epithelial cells, extracellular matrix and of course cells of immune system (65).

As described above the cells of the adaptive immune system have a great impact on shaping the tumor. To this end, several acquired intrinsic and extrinsic mechanisms have been identified in cancer and other tumor cells that allows them to escape immune recognition. During an inflammatory state such as cancer CD8 T cells and T_H1 cells produce the cytokine IFNg, which stimulates MHC-I signaling, and thereby makes their target cell more visible for antigen recognition. However, cancer cells can down regulate their expression of MHC-I, through mutations or epigenetic modifications in genes encoding beta-2 microglobulin (β2m) or in genes involved anywhere in the MHC-I pathway and thereby induce “loss of HLA”. While CD8 T cells are not able to detect and kill such cancer cells, NK cell can identify them through their recognition of “missing-self”, which causes NK cell to lose inhibitory signals and thus induce cancer-cell- killing (66). Moreover, tumor cells can further express a variety of immunosuppressive molecules, such as IL-10, transforming growth factor (TGF)-β, vascular endothelial growth factor (VEGF), Indoleamine-2,3-dioxygenase (IDO) (67). TGF-β and VEGF are both growth factors which induces

endothelial growth leading to the formation of blood vessel (68). Blood vessel formation not only allows nutrition and oxygen flow to the tumor as well as recruitment of pro-inflammatory immune cells but also allows immunosuppressive cells, such as Treg cells and myeloid derived suppressor cells (MDSCs) (69). Moreover, immune cells residing in the TME can also become differentiated towards an immune suppressive subtype, such as T_H2 cells or M2-like macrophages also defined as tumor associated macrophages (TAMs). Such immunosuppressive cells can contribute to the expression of anti-inflammatory molecules. TAMs have been skewed to secrete IL-10 instead of IL-12, which suppress activation of CD8 T cells, while Treg cells and T_H2 cells also are sources of IL-10 and TGF-β (67). This can lead to upregulation of FasL and down regulation of Fas on cancer cells, which will revert the direction of killing and instead induce apoptosis in differentiated T cells that express Fas (70). Furthermore IL-10 and TGF-β can also inhibit DC maturation leading to a decreased T cell activation and potential formation of anergic T cell due to lack of DC provided co-stimulation (71). IDO, which can be expressed by MDSCs, can both suppress T_{eff} and promote activation of Treg cells (72). In addition to secretion of anti-inflammatory cytokines, Treg cells also express high amount of IL-2 receptors on their surface which "steal" IL-2 from surrounding T cells in the TME. The reduction of IL-2 in the TME will lead to a decreased proliferation of remaining T cells, such as CD8 T cells (73). Moreover, the presence of TGF-β will regulate the cytotoxic capacity of CD8 T cells and NK cell by down regulating the expression of perforins and granzymes, while it will also retain CD8 T_{eff} cells in the TME by increasing surface expression of the integrin CD103 (74). This might result in a continuous exposure of the T cells to its cognate antigen and can induce T cell exhaustion as described in the previous chapter, and upregulation of inhibitory checkpoint molecules.

Inhibitory check point molecules on T cells

Upon activation, T cells will express inhibitory checkpoint molecules, in order to regulate their immune response. However, overstimulation of a T cell will result in increased expression of various inhibitory checkpoint molecules. This skews the differentiation from T_{eff} cell towards T_{EX} cells resulting in loss of T cell effector functions (33). Many different check point molecules have been described, including cytotoxic T-lymphocyte–associated antigen (CTLA)-4, Programmed Cell Death Protein (PD)-1, T cell immunoglobulin and ITIM domain (TIGIT), Lymphocyte activation gene (LAG)-3, T-cell immunoglobulin and mucin domain (TIM)-3 and more, which will act through inhibition of various co-stimulatory pathways (75) (Figure 6).

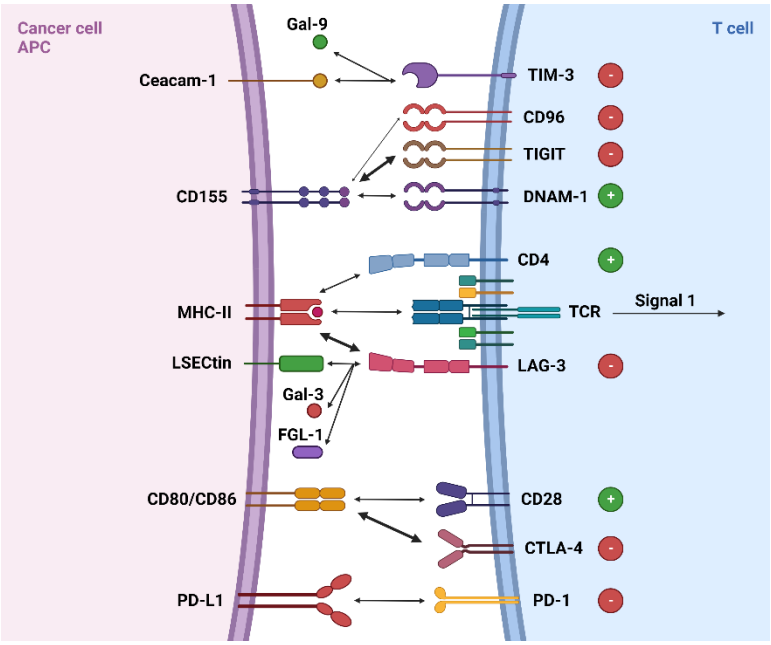

Figure 6 | Immune checkpoint molecules. An overview of selected immune checkpoint molecules found to be expressed on T cells, upon activation and exhaustion. Engagement of the checkpoint molecule with its ligand induces an inhibitory signal in the T cells. This is a mechanism of tolerance. The ligands can be expressed on APCs and/or on peripheral tissue. Cancer cells are known to exploit this inhibitory pathway and avoid T cell killing through up-regulation of such ligands. Some Immune checkpoint molecules function in a competing manner for binding of a ligand of a co-stimulatory molecules. This includes CTLA-4 competing with CD28 for binding of CD80/CD86, LAG-3 competing with CD4 for binding of MHC-II and TIGIT competing with DNAM-1(CD226) for binding of CD155. Other checkpoint molecules are dependent on up-regulation of their ligand on the opposing cells (PD-1, TIM-3, LAG-3). Figure inspired by (75). Created with BioRender.com

CTLA-4 is competing with CD28 for binding of CD80/CD86, however with a much higher affinity. Thus, when CTLA-4 is expressed it will surpass the binding by CD28, and hereby inhibit the co-stimulatory signal. Treg cells are expressing high levels of CTLA-4 due to their expression of the transcription factor FoxP3. The high levels of CTLA-4 on Treg cells will compete with other T cells for the binding of CD28 to CD80/CD86, and hereby regulate an immune response (76). Similar to CTLA-4, TIGIT are also competing for binding of CD155 expressed on APC or target cells. TIGIT is competing with the co-stimulatory receptor CD226 (DNAM-1), and has a higher affinity for CD155 than CD226. Thereby, TIGIT inhibit the stimulatory signal from CD226 (77). Less is known about the inhibitory check point molecule, LAG-3. It has been demonstrated that LAG-3 binding to MHC-II induces an inhibitory response in the T cell. Thus it is thought to compete with the binding of CD4 to MHC-II. However, LAG-3 is also found to be expressed on CD8 T cells. Therefore, other ligands for LAG-3 has been suggested, including the membrane bound LSECtin and the soluble molecules; galectin-3 and fibrinogen-like protein 1 (FGL-1), all identified in various tumors (78,79). Unlike the check point molecules mentioned above, PD-1 will not directly compete for binding in order to inhibit a co-stimulatory signal. It will instead bind its ligands PD-L1 and PD-L2, expressed by target cells and immune cells. PD-1 will upon ligand-induced activation intrinsically inhibit CD28 co-stimulatory signaling (76,80). Finally TIM-3, can bind to the membrane bound Ceacam-1 or the soluble galectin-9. TIM-3 activation appears to have more function, including inhibition of TCR activation as well as regulating T_H1 cell responses by inducing cell death (81,82). Such check point molecules have been shown to be promising therapeutic targets for cancer and will be elaborated in *Cancer Immunotherapy*.

Chapter 3 | Tumor antigens

T cells as previously mentioned are the main driver for direct cancer cell killing. Tumor antigens are displayed in a peptide-MHC complex on the surface of a cancer cell, where it can be recognized by T cells. The dissimilarity between tumor antigen and self-antigen is the driver of a strong T cell response. Thus, Tumor antigens can be separated into two groups; tumor associated antigens (TAA) and tumor specific antigens (TSA) (83) (Figure 7).

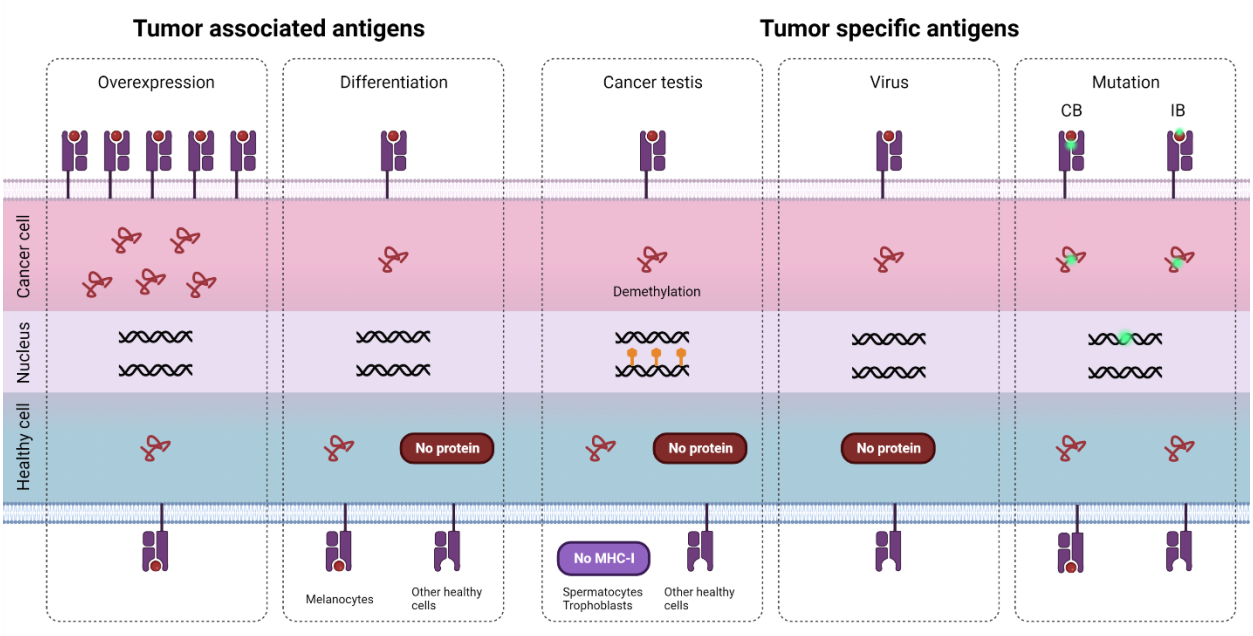

Figure 7 | 5 classes of tumor antigens recognized by T cells. Tumor associated antigens (TAAs) provides low tumor specificity as TAA are also expressed on healthy cells. TAAs includes overexpressed antigens and differentiation antigens, which are only expressed in differentiated cells in healthy tissue such as melanocytes, and therefore also in cancer cells originating from this tissue. Tumor specific antigens (TSA) provides high tumor specificity as these are only expressed in cancer cells and not in healthy tissue. TSAs includes Cancer testis antigens, which can be expressed on tumor cell due to demethylation, viral antigens that can be expressed upon infection of oncogenic viruses, and mutated antigens. Mutated antigens comprise conserved binders (CB), where the mutation modifies a peptide that previously binds to a MHC, and improved binders (IB), where the mutation allows a peptide to bind to MHC. Figure inspired by (83). Created with BioRender.com

TAAs are antigens with low tumor specificity, as the antigens are also found in healthy tissue. Specific T cells recognizing such antigens must therefore escape central tolerance in order to induce an immune response. There are two types of such TAA. 1) Overexpressed antigens which can induce a T cell response due to extremely high expression level of self-antigen on a cancer cell compared to healthy cells (83). HER2/neu is highly expressed in breast cancer and ovarian cancer, which would consequently express high levels HER2/neu derived antigen. HER2/neu antigen specific T cells have also been identified, indicating a

tumor response based on overexpression of self-antigen (84). 2) Differentiated antigens refers to antigens which are expressed on cancer cells and in healthy tissue, but only in the tissue of the cancer cell origin. A protein expressed in melanoma cell as well as in healthy melanocytes, called Melan-A (or MART-1), gives rise to a population of Melan-A specific T cells. Such T cells have been found both in melanoma patients and also as a naïve population in healthy individuals (85–87).

While TAAs comprise self-antigens, TSAs includes antigens which are only tumor specific, and therefore not presented in healthy tissue. They can therefore elicit a highly tumor specific immune response. 1) Cancer germline genes are only expressed in germ cells, which do not express MHC molecules, thus not presenting cancer germline antigens (also known as Cancer testis antigens). The cancer germline genes are epigenetically suppressed in healthy tissue. However many cancer types have been shown to express such cancer germline antigens, due to demethylation of the genes (88). A common example of cancer germ line genes is the Melanoma Antigen Gene (MAGE) protein family, expressed in many different cancers, including melanoma, lung cancer, breast cancer and prostate cancer (83). 2) Oncogenic virus can integrate their genetic material into the host cell's genome, and hereby induce uncontrollable cell growth and tumor formation. The newly introduced oncoviral genes can give rise to antigens that are only expressed by cancer cells. Oncoviral antigens, such as antigens from human papillomavirus (HPV), are shared between patients, and therefore making it easier to treat and even prevent such cancers with prophylactic vaccines (89). 3) Finally somatic mutation can give rise to highly immunogenic antigens – so-called neoantigens, as they can introduce altered amino acid sequences (non-synonymous mutations) (90). Somatic mutation can either generate a new MHC binder, where the wild type peptide was not able to bind the MHC (improved binder), or the mutation can alter an existing MHC binder and thereby elicit a TCR recognition (conserved binder).

3.1 Neoantigens

Neoantigens are the result of cancer-regulated irregularities of the genome. Neoantigens can be formed by gene fusions or non-synonymous mutations caused by single nucleotide variants (SNV) or larger alterations of the genome such as frameshift mutations due to an insertion or deletion (indels). Tumor mutational burden (TMB) varies between different cancer types but also within the same cancer type, which illustrates how patient specific neoantigens are. The cancer types with the highest mutational burden are melanoma and lung cancer, where environmental factors, such as UV light exposure and smoking respectively, are known to increase the risk of these cancers significantly. On the other hand

glioblastoma has a comparably lower mutational burden, where no clear correlation between environmental factors and glioblastoma has been shown (90) (Figure 8).

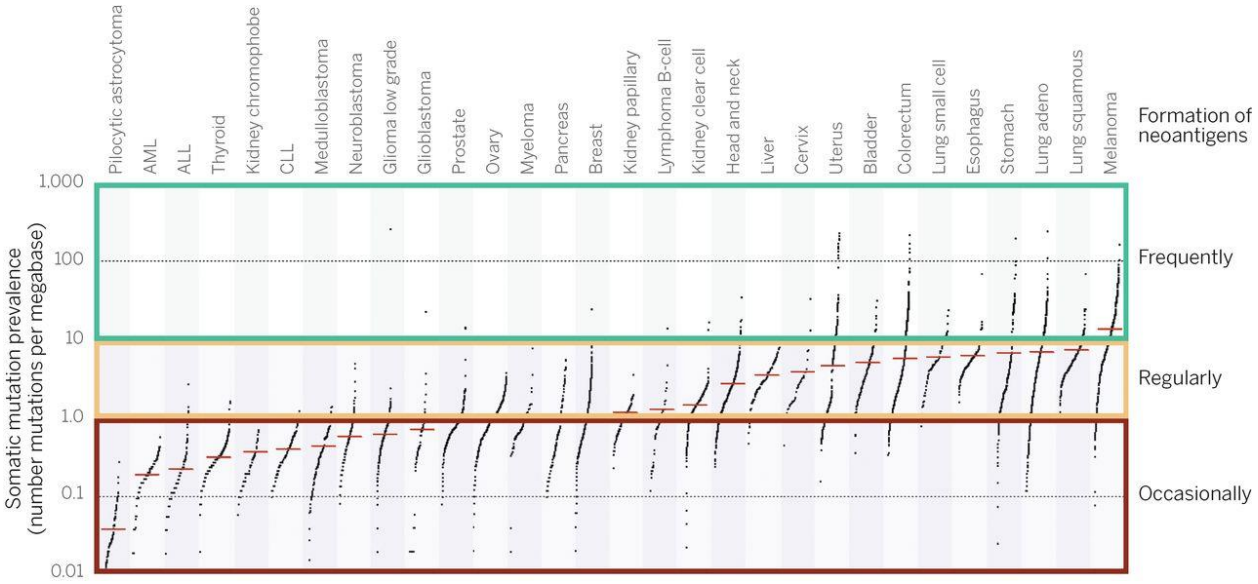

Figure 8 | Tumor mutational burden across different cancer types. Somatic mutations in individual tumors. Black dots represent one tumor sample and red horizontal lines marks the median number of somatic mutations. Cancers are ordered from low median number of somatic mutations to high median numbers. ALL, acute lymphoblastic leukaemia; AML, acute myeloid leukaemia; CLL, chronic lymphocytic leukaemia. From (90).

The mutational burden of a tumor has previously been thought to positively correlate with the immunogenicity of the tumor and also better clinical outcome after immunotherapy (91,92). However, several factors come into play; among others the "quality" of the neoantigen presented on the cancer cells. Both the binding affinity of the peptide to the MHC molecules, as well as potential tolerance toward the peptides can influence the immunogenicity of a neoantigen. Wild-type peptides for improved binders have not been presented prior to the mutation, and tolerance should therefore exist towards these peptides. However, conserved binders are more likely to be overlooked by the immune system due to a higher self-similarity with the wild type peptide and thus due to tolerance. Improved binders might therefore be more immunogenic than conserved binders (93). SNV are the most abundant mutation and is also the most studied, but improved binders are more likely to emerge from frameshift mutations (94,95).

An increasing interest has evolved toward neoantigens over the last decades, in search for personalized treatment strategies, but also in search for answers to why clinical effect of immune therapies sometimes do not appear. We do not only see a large heterogeneity between patients, but we also see it within a single tumor. Mutations in tumor cells can be defined by the terms; clonal mutations and sub-clonal

mutations. Clonal mutations occur during tumor formation, while sub-clonal mutations appear in cancer cells further down the evolutionary timeline of the tumor (96). A lower heterogeneity and high frequency of clonal mutations are associated with increased overall survival, also in context with immune therapy (97,98). Driver mutations are mutations that induce essential function of the cancer cell proliferation and survival, such as gain-of-function mutations in proto-oncogenes or loss of function in tumor suppressor genes (99). Though driver mutations are primarily thought to dominate the clonal mutations, they are also found in sub-clonal mutations, especially within Glioblastoma patients (100,101). Furthermore, sub-clonal driver mutations are correlated with progressive disease (102).

3.2 Prediction and detection of neoantigen reactive T cells

With increasing advances in sequencing technologies, the interest for neoepitopes has grown. Neoepitopes are defined as mutated peptides (neopeptides) that can bind to MHC and elicit a T cell response. The field is well-established within MHC-I binding neoepitopes, but MHC-II binding neoepitopes are also now studied intensively. In this chapter, neoepitopes refers to MHC-I binders. Neoepitope prediction field is especially of great interest for production of therapeutic patient-specific neopeptide vaccines, which will be elaborated in next chapter, *Cancer Immunotherapy*. However, it is only a small fraction of the predicted neoepitopes, which can be detected by autologous CD8 T cells (93,103). Several *in silico* prediction tool has been developed for neoepitope prediction. In general, the strategy for neoepitope prediction is to identify somatic mutations by comparing Whole Genome Sequencing (WGS) - or Whole Exome Sequencing (WES) data from tumor to WGS/WES data from healthy tissue, such as blood. Furthermore, the expression level of the mutated gene is measured based on RNA sequencing of the tumor tissue, in order to filter out mutated genes that are not expressed in the tumor (104). Sequencing data are additionally used to type HLA-alleles of the given patient. HLA binding affinity of the mutated neopepides are predicted with tools like netMHCpan (105), where HLA binding affinity, EL%rank, below 0.5 indicate strong binders and EL%rank below 2 indicates weak binders (106). A pool of potential predicted neoepitopes can be selected with the use of HLA binding and expression level from RNA sequencing, and patient derived T cells can be screened for neoantigen reactive T cells (NARTs), for final identification of true immunogenic neoepitopes.

It is as mentioned not all mutations that are expressed in the cancer cells, but it is also not all expressed mutated peptides that are presented or even elicit an immune response. In the context of e.g. neopeptide vaccines, it is therefore important to identify the immunogenic peptides, to improve prediction tools and

hereby narrow down the pool of potential neoepitopes. Several different techniques can be used for identification of immunogenic peptides and vary in complexity. Low technology methods comprise detection of cytokine secretion following intro peptide stimulation by e.g. ELISPOT or intra cellular cytokine staining using flow cytometry. Both assays rely on cytokine release, e.g. INF-γ and TNF-α, and have relatively low sensitivity and screening capacity is also considerably low. However, both MHC-I and –II binding peptides can be screened by these assays. Along with the development and improvement of *in vitro* MHC-I folding, pMHC-based screening technologies have been developed (107). Instead of folding each MHC-I molecule with each individual peptide, methods where MHC refolding with UV-cleavable ligands (108), dipeptides (109,110), and as empty MHC molecules with a stabilizing disulfide bond in the binding groove (111) have been established over the last few decades. Instead, these refolded MHC-I molecules permit peptide exchange or direct peptide loading, respectively. pMHC-based detection of NARTs comprises fluorochrome-labeled multimers, that allows detection via flow cytometry and to stabilize the low affinity binding between TCR and pMHC (112). Low through-put single detection of NARTs was initially used due to limitations within the flow cytometry field. However, combinatorial encoding of fluorescently-labelled pMHC tetramer was first described by Hadrup et al. in 2009 (113). This then allowed simultaneous screening of around 40 pMHC specificities, by labeling the individual pMHCs with a specific combination of two fluorophores. In recent years, a high through-put screening method was developed, where pMHC are multimerized on a dextran backbone. The individual pMHC multimer is labelled with a DNA barcode and a common fluorophore. DNA barcoding instead allows detection of more than 1000 individual pMHCs (114) (Figure 9).

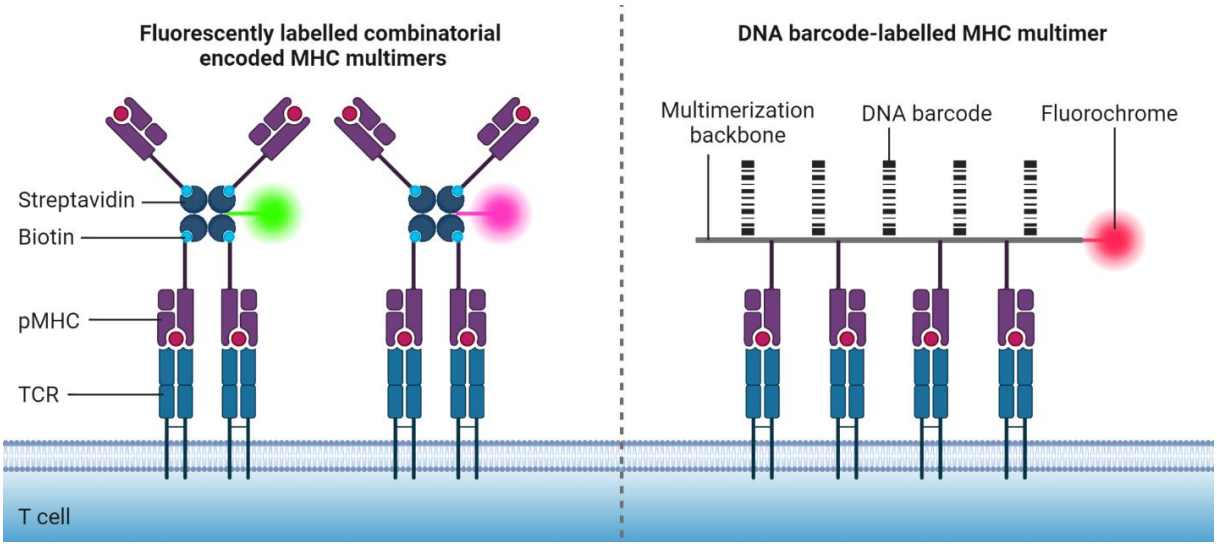

Figure 9 | pMHC-based screening methods for NART detection. Detection of NARTs with fluorescently labelled combinatorial encoded pMHC tetramers (left) and DNA barcoded-labelled MHC multimer (right). Figure inspired by (107). Created by BioRender.com

Chapter 4 | Cancer Immunotherapy

First-line treatment of primary cancer is surgical removal of the cancerous tissue. However, when cancer reaches an advanced stage, chemotherapy and radiotherapy may be utilized to eradicate inoperable cancerous tissue. Since these treatment options target both healthy and cancerous cells, they can result in considerable toxicity. To this end, cancer immunotherapies have gained traction over the last decades as a treatment option for cancer. As defined in the previous chapter, cells of the immune system play an essential role in protection against cancer. Nonetheless, cancer cells evolve several immune escape mechanisms due to a Darwinian selection pressure created by the immune cells, resulting in hampered anti-cancer immune responses. Cancer immunotherapies aim to unleash the impairment of immune cell function and hereby boost and restore the body's natural defense against cancer. Although immunotherapy is perceived as a new and promising approach to cancer treatment, it was actually first used over a century ago. Around 1900, William Coley developed a vaccine known as *Coley's Toxin*. Coley discovered that bacterial infections at the site of tumor lesions cured sarcoma patients. He therefore developed a vaccine with the toxins from two bacterial strains to induce a harmless "infection" at the tumor site (115,116). In the 1980s, clinical trials with cytokine administration were setup to examine the promising preclinical anti-tumor activity that had previously been shown (117–119). Modest clinical benefits were shown in clinical trial after therapy with the cytokines IFN-α or IL-2. But in a few cases, these therapies let to complete remission and long lasting response in metastatic patients, who had not responded to any other therapies. Yet, severe toxicity was related to the administration of these cytokine (120–123). Importantly, these limited yet remarkable clinical outcomes of cytokine administration have paved the way for the application of immunotherapy in the treatment of cancer, several decades after the development of *Coley's Toxin*.

As described in the previous chapters, a number of events must be initiated to induce an effective immune response against cancer. Altogether, these event can form a *Cancer-immunity cycle*. In short, the steps of the cancer-immunity cycle include a release of neoantigens from cancerous cells. DCs will take up and process such extracellular proteins or peptides and migrate to the LN to present the neoantigens on MHC-I and MHC-II to T cells. Neoantigen-presentation can lead to priming and activation of T cells, which then migrate and infiltrate the tumor tissue. The cytotoxic T cells will here recognize their cognate neoantigens expressed by cancer cells and kill their target. Finally, the killing of cancer cells will lead to a release and spreading of additional neoantigens, which hereby concludes the circle (124). Several inhibitory factors

and pathways have been identified within the different steps of the cancer-immunity cycle. Such inhibitory mechanisms serve as regulatory system to maintain peripheral tolerance, though they can also impede an immune response towards cancer. Consequently, a broad variety of immunotherapies, acting within the different steps have been developed since the 1980s (Figure 10) (124).

Immunotherapy can be categorized according to their mechanism of action as either active or passive

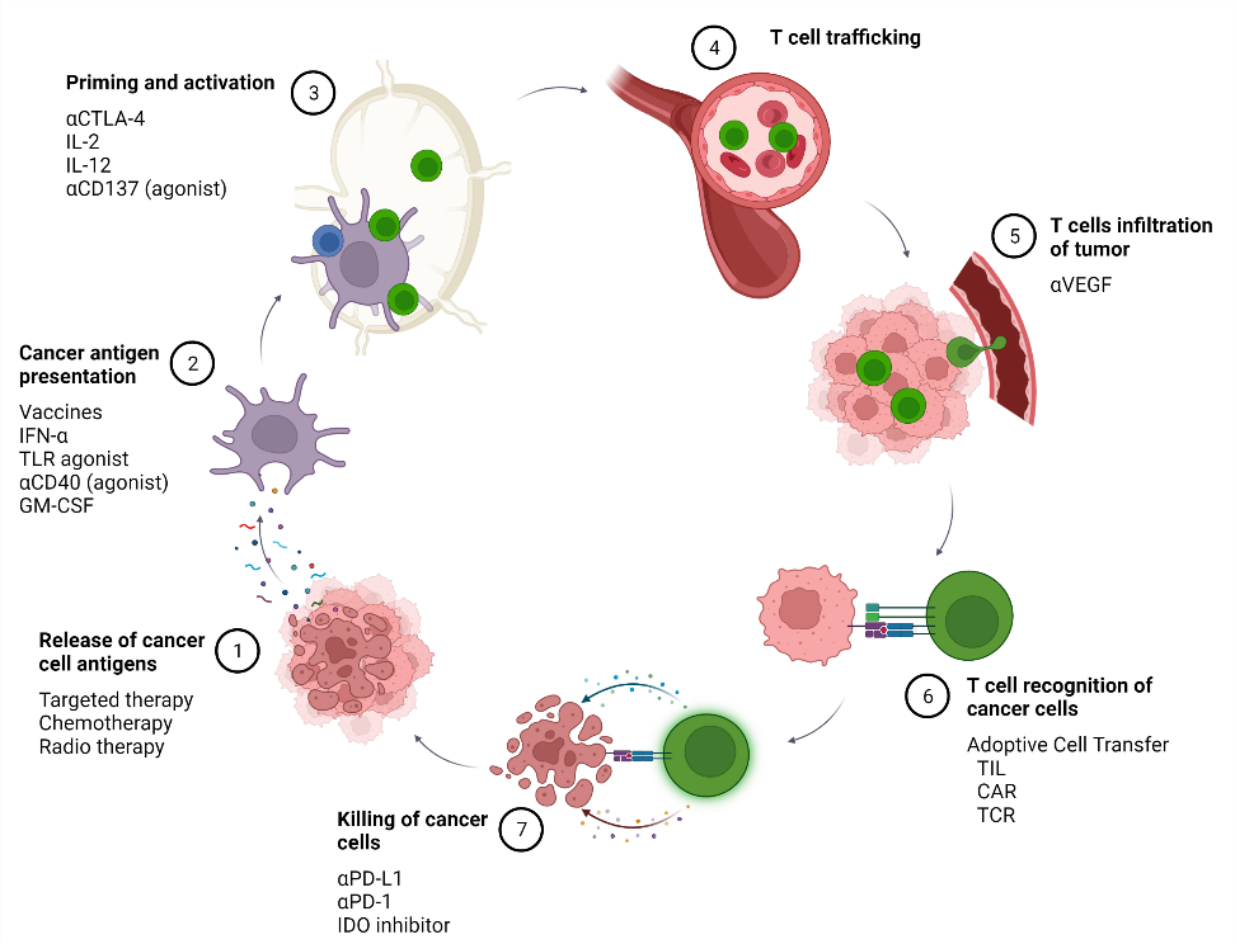

Figure 10 | Cancer-immunity cycle. 7 events leading to an anti-cancer T cells response, depicted as a cancer-immunity cycle. 1) Cancer cells release antigens. 2) Antigen uptake and presentation by DCs. 3) DC priming and activation of T cells upon DC migration to the lymph node. 4) T cell trafficking. 5) T cell infiltration from the periphery into the tumor lesion. 6) T cells recognize their cognate target expressed on cancer cells. 7) T cell induced killing of cancer cells. This concludes the cycle. Immunotherapy has been developed for almost all steps in the cancer-immunity circle to help inducing an immune response towards the tumor. Figure inspired by (124). Created with BioRender.com

immunotherapies (Figure 11). Passive immunotherapies include *ex vivo* produced molecules or activated cells, such as cytokines, tumor-targeting monoclonal antibodies, and various adoptive cell transfer therapies, which can create an anti-tumor immune response in patients with a weak or unresponsive immune system. Active immunotherapies function by stimulating an immune response *in vivo* and can

potentially create a long-lasting memory response in patients. Active immunotherapies include oncolytic viruses – creating similar effects to *Coley's Toxin*, cancer vaccines and immune checkpoint inhibitors (125).

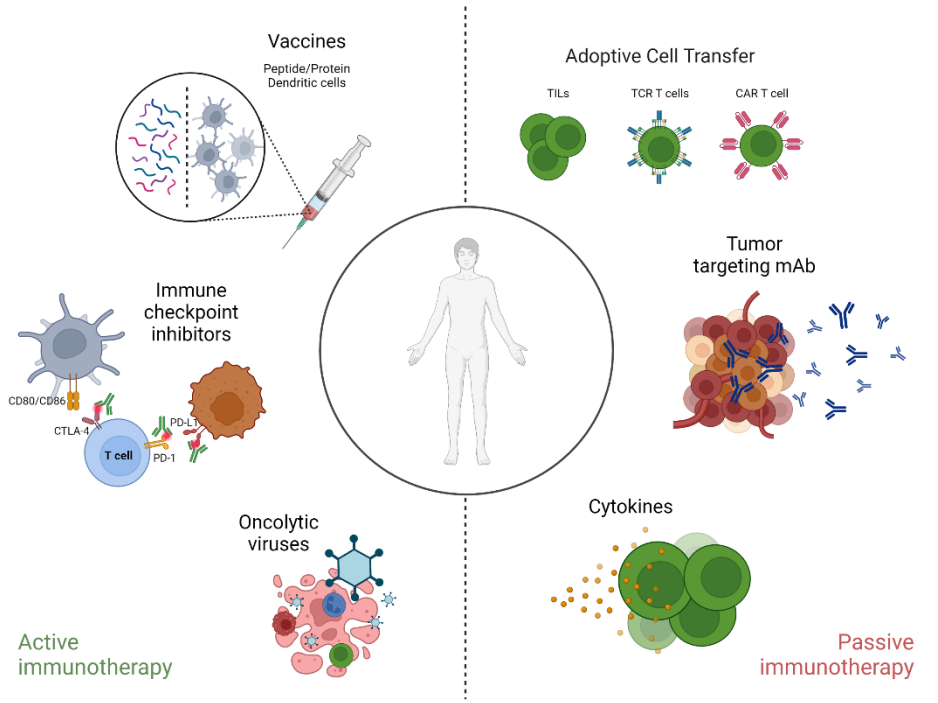

Figure 11| Immunotherapies categorized as passive and active. Cancer immune-therapies can be categorized as active immunotherapies (left) including; Vaccines, immune checkpoint inhibitors (ICIs) and oncolytic viruses or as passive immunotherapies (right) including, adoptive cells transfer, tumor-targeting monoclonal antibodies (mAb) and cytokines. Created with BioRender.com

4.1 Immune Checkpoint inhibitors

Immune checkpoint inhibitors (ICIs) are monoclonal antibodies targeting immune checkpoint molecules. As previously described, immune checkpoint molecules are crucial for maintaining peripheral tolerance, however, they can be exploited by cancer cells to evade immunosurveillance. ICIs has been designed to block the inhibitory axis between effector cells and tumor cells or APCs, and unleash effector cell activation. An *in vivo* study in 1996, showed the great potential of blocking the co-inhibitory molecule, CTLA-4, resulting in tumor regression and subsequent tumor protection (126). This groundbreaking finding established the foundation of ICI therapy, which is widely used today. The CTLA-4/CD80 and PD-1/PD-L1 axes are best characterized and broadly utilized targets for ICI (Figure 12).

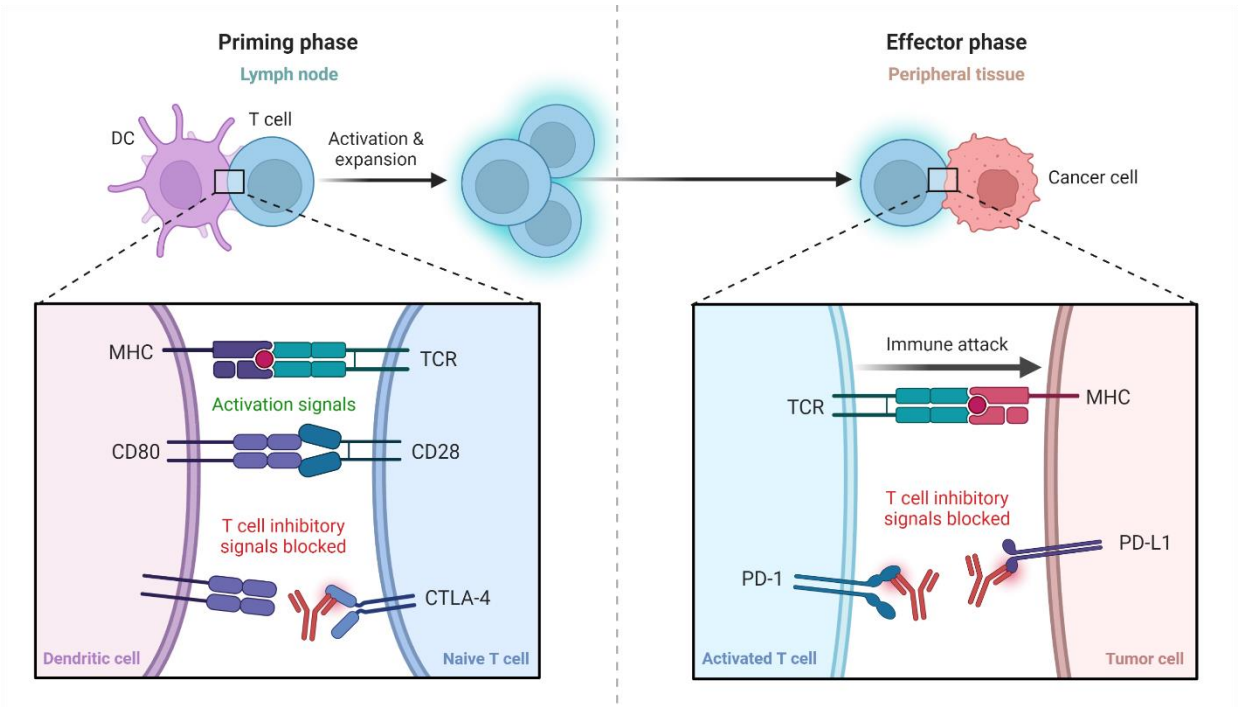

Figure 12 | Immune check point inhibitors. The two most common targets for checkpoint inhibition are the CTLA-4/CD80 axis and the PD-1/PD-L1. Immune checkpoint inhibitors (ICI) are monoclonal antibodies (red), that block the interaction between CTLA-4/CD80 or PD-1/PD-L1. This will allow T cell activation as the inhibitory signal will be broken. CTLA-4 blockade will allow initial priming and activation of T cells in the lymph node, PD-1/PD-L1 blockade primarily allows activation of T cells in the peripheral tissue. Modified from BioRender template. Created with BioRender.com

Blocking CTLA-4 will primarily influence the inhibitory interaction between T cells and APCs in the T cell priming phase, and will therefore unleash the initial priming and activation of T cells taking place in lymphoid tissue. Tolerance is hereby broken and T cells can proliferate regardless of TCR specificity, also due to a decreased suppression by Treg cells (76,127). PD-1 was simultaneously discovered to induce regulatory functions in T cells, rather than being involved in programmed cells death as first suggested (128,129). The cognate ligand for PD-1 is PD-L1, also known as B7-H1, and was identified shortly after discovering the functions of PD-1 (130,131). PD-L1 is normally expressed in healthy cells to induce tolerance and avoid autoimmune responses, however, cancer cells has been shown to exploit this mechanism through overexpression of PD-L1, thereby inhibit T cell-mediated cancer cell killing (132). In contrast to CTLA-4-targeting ICIs, targeting the PD-1/PD-L1 axis unleashes the local T cell response in peripheral tissue, including tumor tissue, rather than the early immune response formed in lymphoid tissue (133). Since their discovery, a range of clinical trials with ICIs targeting both CTLA-4 and PD-1/PD-L1 have shown increased survival in various types of cancer (134). Thus, ICI therapy has attained the most prominent role within cancer immunotherapies as an off-the-shelf product. In 2011, Ipilimumab, a

monoclonal antibody targeting CLTA-4, was the first ICI to be approved for patients with malignant melanoma (135). Since then, particularly PD-1/PD-L1 ICIs have been approved for a broad variety of cancer types, both as second or first-line therapies, including melanoma, lung cancers, renal cell carcinoma, head and neck squamous cell cancer, bladder cancer (136,137). Since ICI therapy blocks a regulatory mechanism and breaks peripheral tolerance, a systemic increase in the activity of the immune system occurs. This hyper active immune system can lead to inflammatory side-effects, called immune-related adverse events (138). Due to its interference in early T cell activation in lymphoid tissues, more severe side effects have been observed after anti-CTLA-4 therapy than anti-PD-1/anti-PD-L1 therapy (138,139). Moreover, studies have shown that anti-PD1-1 therapies (Pembrolizumab and Nivolumab) was associated with increased overall and progression free survival and lower risk of severe adverse events compared to chemotherapy in patients with advanced NSCLC and melanoma (140,141).

Even though ICI therapy has shown promising responses in cancer patients, there is still a large fraction who do not respond. Several immunological factors can influence the clinical outcome following ICI therapy. As described earlier (1.4 Peripheral T cell differentiation) the differentiation status of T cells has been suggested to be important for the clinical response to ICI therapy (48). Terminally differentiated or exhausted T cells (T_{EX}, high TOX expression) are not able to regain their cytotoxic capacity upon immune check point blockade, whereas pre-exhausted T cells ($T_{pre\text{-}EX}$) are thought to maintain cytotoxic capacity (high TCF-1 expression), while being impaired primarily due to upregulation of inhibitory molecules (142,143). Thus, it is believed the ICI would benefit patient with a TME containing such cells. Resistance can also be acquired following ICI treatment, e.g. due to upregulation of additional inhibitory immune checkpoints on T cells, such as LAG-3 and TIM-3 (144) and CD39, which is expressed upon TCR activation. CD39 expression has been used to differentiate tumor-reactive T cells from bystander T cells in the TME (145), but it has also been associated with exhausted and dysfunctional T cells (146). Additionally, increased expression of CD39 together with CD73, are also found to contribute to an anti-inflammatory TME, through the conversion of ATP to adenosine (147,148). Increased adenosine in the TME can induce a shift from production of pro-inflammatory cytokines to anti-inflammatory cytokine, and can also inhibit activation of immune cells and their migration to the TME (148).

Among the most important factors for successful ICI therapy targeting e.g. PD-1/PD-L1, is of course PD-L1 expression in the TME (149) and infiltration of tumor-specific T cells, which is correlated with positive clinical outcome of ICI (150,151). Thus, the use of vaccination to boost the repertoire of such tumor specific T cells have been increasingly studied over the last decade.

4.2 Cancer vaccines

Cancer vaccines are mainly therapeutic vaccines, that aim to induce or boost an existing cancer-specific immune response, but also includes two approved prophylactic vaccines that have been shown to successfully prevent cancers caused by infection with Hepatitis B virus (HBV) and HPV (152). However, when targeting cancers that are not caused by virus infection, the tumor antigens typically have a lower immunogenicity making it more difficult to induce a tumor immune response through vaccination. Additionally, it is of great importance to induce a CD8 T cells response, rather than a humoral response, as is the case for traditional virus vaccines (153).

Therapeutic cancer vaccines can be divided into four categories based on their delivery; cell-based, virus-based, nucleic acid-based and peptide-based. Sipuleucel-T, is one of the only two therapeutic cancer vaccine that has been approved for cancer by the Food and Drug Administration (FDA) and the European Medicines Agency (EMA) in 2010 and 2013, respectively, although approval has later been withdrawn by EMA. Sipuleucel-T is a cell-based vaccine approved for prostate cancer and involves autologous APCs that have been *ex vivo* activated with prostatic acid phosphatase (PAP) fused to GM-CSF (154). PAP is a differentiation TAA that has been found overexpressed in prostatic cancer (155) and GM-CSF is a cytokine that promotes maturation and differentiation of APCs (156). Additional therapeutic TAA cancer vaccines has not reach FDA or EMA approval since then, most likely due to challenges with high tolerance as well as low tumor specificity (157). Advances in high-throughput sequencing technologies, such as next-generation sequencing (NGS) and identification of antigen-specific T cells have provided data for development of computational prediction tools. Artificial intelligence (AI) prediction tools can predict the *neopeptidome* of individual patients based on HLA-type and identification of tumor specific mutations as previously described (158). Although the tumor-specificity should decrease the risk of tolerance, there are various complication associated with vaccines targeting potential neoepitopes. The heterogeneity within the tumor makes it difficult to broadly target all tumor clones, and clonal mutations could therefore be preferable to target. To overcome this, neoepitope-targeting vaccines therefore includes several and up to dozens of targets in the individual vaccines (159), as well as both CD4 and CD8 T cell epitopes. Although CD8 T cells are found to be important in immunosurveillance and cancer eradication, CD4 T cells responses are also found to be important for both the priming of CD8 T cells, but also as effector cells in within the TME (160,161).

Nucleic acid-based cancer vaccines, including mRNA- and DNA-encoding neoepitopes, act through intracellular expression of selected neoepitopes. This provides a direct access to the MHC-I presentation pathway and CD8 T cell responses are therefore easier to obtain, along with a CD4 T cell response following MHC-II presentation (159). Peptide vaccines can comprise both long and short peptides, where long peptides usually both embeds CD4 and CD8 T cells epitopes, while short peptides would only include CD8 T cell epitopes. Short peptides (8-11 amino acid) have a shorter half-life, and is therefore degraded faster *in vivo* than long peptides (162). They do not require antigen processing and can therefore be loaded directly onto MHC-I on APCs, or other nucleated cells, and hereby induce CD8+ T cell responses. However, there is a great risk of developing tolerance or anergy in targeted CD8 T cells due to the lack of co-stimulation, thus adjuvants delivering co-stimulatory signaling is highly needed (163). Additionally, short peptide-based neoepitope vaccines are restricted by MHC polymorphism due to the limitation of peptide length. Thus, a broad and strong immune response is hard to obtain with neoepitope vaccines (159). On the other hand, long peptides (>15 amino acids) need to be taken up by APCs and intracellularly processed in order to be presented as potential CD4 and CD8 T cells epitopes on MHC-II and -I, respectively. To this end, long peptides are needed to induce a memory response following vaccination (164). However, long neopeptide has shown to primarily induce CD4 T cell responses (165,166). Adjuvants that can induce cross-presentation in DCs are therefore of great interest, in order to prime and activate neoepitope specific CD8 T cells. TLR agonist are widely investigated as adjuvants for peptide-based cancer vaccines, including the TLR3 agonist(159). TLR3 binds to double stranded RNA or the synthetically produced TLR3 agonist polyinosinic–polycytidylic acid (poly I:C). TLR-3 is highly expressed on cDC1s and upon engagement of the TLR3 agonist cDC1s induce maturation and upregulation of co-stimulatory molecules and contributes to cDC1 cross-presentation (167,168). The adjuvant CAF09b, used is in the vaccine studied in **Manuscript II**, includes poly I:C in the adjuvant construct and have been shown to induce CD8 T cell responses towards various peptides in mice (169).

Peptide-vaccines targeting neoepitopes are generally shown to be save to use, possibly due to the tumor-specific cytotoxicity (170,171). Neopeptide vaccines have been investigated in the combination with ICI and have shown promising results in a preclinical setting (172). However, increased survival found in a human setting still remains to be established. Neopeptide vaccines could potentially benefit the outcome of ICI in cancer types with low TMB. A peptide vaccine targeting neoepitopes in glioblastoma patient, has for example shown to activate T cells responses (170). However, neopeptide vaccines are an exclusively personalize immunotherapy, which is both costly and time consuming to produce. The latter which might be critical for the relative to the disease status of the patient.

Research objectives

The overall research objective was to identify and evaluate immunological effect of immunotherapy in different patients with two different types of cancer. The common immune cell of interest in the two studies is the T cell, the main effector cell of anti-cancer immune responses.

Manuscript I

Altered intratumoral immune composition after neoadjuvant Nivolumab treatment in patients with recurrent Glioblastoma.

The research objective of this study was to investigate the impact of anti-PD-1 ICI therapy, Nivolumab, on the tumor microenvironment (TME) in GBM patients with recurrent disease. We examined the presence of T cells and Nivolumab in tumor tissue and characterized the phenotype of intratumoral T cells. Additionally, we evaluated the reactivity of expanded tumor infiltrated T lymphocytes (TILs) towards autologous tumor and examined blood and TILs for neoantigen reactive CD8 T cells.

Manuscript II

Dose Escalation study of a Personalized Peptide-based Neoantigen Vaccine (EVX-01) in Patients with Metastatic Melanoma.

The aim of this study was to investigate safety and efficacy of a neopeptide vaccines in combination with anti-PD-1 ICI therapy administered to advanced melanoma patients. This was done by evaluating the safety of the vaccine in three increasing dose levels. Next, we examined the vaccine specific T cells responses, before and after vaccination, including the presence CD8 T cells specific to both vaccine-embedded and other neopetides. Finally, we assessed the clinical an immunological outcomes of the neopeptide vaccine in relation to neopeptide prediction.

Manuscript I

Altered intratumoral immune composition after neoadjuvant Nivolumab in patients with recurrent Glioblastoma

Signe Koggersbøl Skadborg[1*], Simone Maarup[2,3*], Arianna Daghi[3], Annie Borch[1], Sille Hendriksen[1], Jane Skøjth-Ramussen[4], Christina Yde[5], Benedikte Hasselbalch[2], Inge Marie Svane[3], Ulrik Lassen[2+], Sine Reker Hadrup[1+]

[*] These authors contributed equally

[+] These authors contributed equally

1 Experimental and Translational Immunology, Department of Health Technology, Technical University of Denmark, Kgs. Lyngby, Denmark

2 DCCC Brain Tumor Center, Department of Oncology, Copenhagen University Hospital Rigshospitalet, Copenhagen, Denmark

3 National Center for Cancer Immune Therapy, CCIT-DK, Copenhagen University Hospital Herlev Hospital, Herlev, Denmark

4 Neurosurgical Department, Copenhagen University Hospital, Copenhagen, Denmark

5 Center of Genomic Medicine, Copenhagen University Hospital, Copenhagen, Denmark

Altered intratumoral immune composition after neoadjuvant Nivolumab treatment in patients with recurrent Glioblastoma

Signe Koggersbøl Skadborg[1*], Simone Maarup[2,3*], Arianna Daghi[3], Annie Borch[1], Sille Hendriksen[1], Jane Skøjth-Ramussen[4], Christina Yde[5], Benedikte Hasselbalch[2], Inge Marie Svane[3], Ulrik Lassen[2*], Sine Reker Hadrup[1*]

1 Experimental and Translational Immunology, Department of Health Technology, Technical University of Denmark, Kgs. Lyngby, Denmark

2 DCCC Brain Tumor Center, Department of Oncology, Copenhagen University Hospital Rigshospitalet, Copenhagen, Denmark

3 National Center for Cancer Immune Therapy, CCIT-DK, Copenhagen University Hospital Herlev Hospital, Herlev, Denmark

4 Neurosurgical Department, Copenhagen University Hospital, Copenhagen, Denmark

5 Center of Genomic Medicine, Copenhagen University Hospital, Copenhagen, Denmark

* These authors contributed equally

ABSTRACT

Glioblastoma (GBM) is an aggressive brain tumor with a dismal prognosis, and consequently substantial efforts are driven toward developing new and efficacious treatment options. In this context, immunotherapy is being explored, but it is still unresolved to what extend systemic immunotherapy treatment can reach and modify the tumor microenvironment in the brain.

To explore this further, we evaluated changes in immune characteristics in tumor and blood samples from patients with recurrent GBM who received Nivolumab and Bevacizumab. A patient cohort was treated with one dose of neoadjuvant Nivolumab seven days prior to surgery, and immune characteristics of the tumor was compared to a control patient group, only receiving surgical resection without Nivolumab treatment.

Nivolumab-bound T cells was detected in tumor tissue after seven days of treatment, and we observed increased frequencies of activated but also differentiated CD4+ and CD8+ T cell phenotypes in tumor from Nivolumab-treated patients, compared to the non-treated control patients. Furthermore, we demonstrated that tumor infiltrating lymphocytes (TILs) from Nivolumab-treated patients showed cytolytic activity towards autologous tumor digest, and that patients mounted neoantigen reactive CD8+ T cells in both tumor and blood. Our results suggest that Nivolumab had reached the tumor and induced important changes in the tumor immune microenvironment within the short time span.

ABBRIVIATIONS

BBB	Blood Brain Barrier
CNS	Central Nervous System
CSF	Cerebral Spinal Fluid
DEA	Differential Expression Analysis
DMSO	Dimethylsulfoxid
FACS	Fluorescence Activating Cell Sorting
FBS	Fetal Bovine Serum
FFPE	Formalin Fixed Paraffin Embedded
GBM	Glioblastoma
GO	Gene Ontology Database
GSEA	Gene Set Enrichment Analysis
ICS	Intracellular Staining
ISF	Interstitial Fluid ISF
kDA	Kilo Dalton
MFI	Median Fluorescence Intensity
NART	Neoantigen Reactive CD8 T cell
NIVO	Nivolumab treated patients
ON	Over Night
OS	Overall Survival
PBMC	Peripheral Blood Mononuclear Cell
PFS	Frogression Free Survival
REP TIL	Rapid Expanded TIL
TIL	Tumor Infiltrating Lymphocyte
TME	Tumor Microenvironment
VART	Virus Antigen Reactive T cell
WES	Whole Exome Sequencing
WGS	Whole Genome Sequencing
YTIL	Young TIL

INTRODUCTION

At primary diagnosis glioblastoma patients are treated with maximal surgery, radiation and concomitant Temozolomide (1), however, when relapse occur no standard treatment is available (2). Even though numerous treatment strategies has been explored, OS remains at 14.6 months (1). Therefore, new treatment options are urgently needed, and immunotherapy is one strategy being explored, that may show promise in selected patients (3,4).

The brain is determined as an immune privileged organ, which has been equated with no passage of peripheral immune cells to the parenchyma of the brain (5). However, it has been shown that communication with the peripheral immune system occurs, including cellular exchange. It is known that T cells can be primed in the meningeal area of the brain (6), however knowledge of the route of entry and presence of effector T cells, in the parenchyma or tumor tissue localized in the brain, is minimal. However, it has been shown in mice that cerebral spinal fluid (CSF) and interstitial fluid (ISF) are drained via CNS draining lymphatic vessel to the deep cervical lymph node which suggests an alternative route for immune surveillance of the brain (7–9).

Immunotherapy has revolutionized cancer treatment, but yet, many cancer types, including glioblastoma (GBM) are unresponsive to current immunotherapeutic strategies (10–12). The effect of immune-checkpoint inhibition has been sparse in GBM and it has been questioned, if the checkpoint-blocking antibodies would pass the blood brain barrier (BBB) sufficiently to enter the tumor microenvironment (13). Nivolumab is a 146 kDa molecule, while the molecules that are believed to freely pass the BBB measures between 400-500 Dalton (13). It has earlier been shown that the BBB is compromised in some areas of individual primary brain tumors, but other areas within the same tumor show intact BBB (14,15). Additionally, some glioblastoma tumors have high collagen levels,resulting in a tumor grid of collagen amour, which can challenge the penetration capacity (16). Together these characteristics may limit the penetrance of Nivolumab and effector immune cells, and hence compromise the effect of immunotherapy GBM.

Checkpoint inhibitors have shown great result in brain cancer mouse models (17,18), but when the treatment is moved to the human setting, the impressive responses are not translated (19). Therefore it is of great importance to understand the impact of checkpoint inhibition on a cellular level in the human setting. In this study, we have explored the intratumoral presence of Nivolumab and its effect on the phenotypic profile of intratumoral and peripheral T cells. We examined the tumor reactivity of expanded

tumor infiltrated lymphocytes (TILs) and the presence of neoantigen reactive CD8 T cells in GBM lessions and peripheral blood.

METHODS AND MATERIAL

Trial design

CA209-9UP is a phase II open-label, two-armed translational study of Nivolumab and Bevacizumab for recurrent GBM, where Stupp's regime has proven ineffective (1). In total 44 patients (4 screen failures) were included in a surgical arm (arm A, N=20) and non-surgical arm (arm B, N=20) depending on the possibility of salvage neurosurgical resection (Figure 1). All patients received 240mg Nivolumab and 10mg/kg Bevacizumab every two weeks. The arm A also received neoadjuvant 240mg Nivolumab seven days prior surgery. In total 44 patients were included by January 2021, follow-up was ended May 2022. The trial was approved by the Danish Ethical Committee (EudraCT 2017-003925-13), written consents were obtained with the possibility to withdraw consent at any time. Additionally, control patients (N=10) with recurrent glioblastoma undergoing neurosurgical resection were included. The controls did not receive neoadjuvant treatment in the recurrent setting therefore the fresh tumor tissue was untreated.

Patient material

RNA/DNA extraction from tumor tissue or blood

Paired samples from primary and recurrent tumors were available from the arm A; Recurrent tumor samples were collected and stored in RNAlater (Thermo Fischer Scientific) immediately after resection. Archival tissue from autologous primary tumor was available as fresh frozen tissue or formalin fixed paraffin embedded (FFPE) tissue. Blood samples for germline DNA were collected in Streck- and EDTA vials. DNA and RNA were extracted from fresh frozen tissue by AllPrep RNA/DNA/Protein Mini Kit (Qiagen). RNA was further DNase treated with RNeasy mini kit (Qiagen). DNA and RNA were extracted from FFPE slides by GeneRead DNA FFPE kit (Qiagen) and Agencourt FormaPure Reagent Kit (Beckman Coulter), respectively. DNA from blood for germline whole exome sequencing (WES) was extracted by ReliaPrep Large Volume HT gDNA isolation system (Promega). Manufacturers' instructions were followed for all kits. Bioanalyzer 2100 with the 6000 RNA Nano and Pico Assay was used to evaluate the RNA quality. RNA was quantified using DeNovix Spectrophotometer. DNA was quantified using Qubit Fluorometric Quantification (Thermo Fisher Scientific). All sequencing was performed using a NovaSeq S4 flow cell

(Illumina) on an Illumina NovaSeq 6000 machine. Library preparation for WES was done by SureSelect Clinical Research Exome (Agilent) and WGS by Illumina DNA PCR-free prep (Illumina).

Peripheral blood mononuclear cells (PBMCs)

Peripheral blood samples were collected from patients at several time points (Figure 1); baseline/prior to treatment (T1), after 8 weeks (T3) and 16 weeks (T4). One additional blood sample was collected 3 weeks post neoadjuvant Nivolumab (T2) in arm A – 2 weeks after surgery. Peripheral blood mononuclear cells (PBMCs) were isolated using Lymphoprep density gradient (Takeda) and cryopreserved in 10% DSMO (Herlev Hospital Pharmacy) and 90% human serum (H4522, Sigma-Aldrich/Merck KGaA) using controlled-rate freezing (Cool-Cells, Biocision) in -80 °C, and later stored in -140 °C (Figure 1).

Tumor infiltrating lymphocyte in vitro expansion

Young Tumor infiltrating lymphocytes (YTILs) were expanded from resected tumor tissue. Tumor tissue was cut into 1-3 mm3 fragments and plated in wells of a 24 well-plate with 2 mL complete media consisting of 90% RPMI-1640 plus GlutaMAX and 25 mM HEPES (72400-021, Gibco, Thermo Fisher Scientific), 10% heat-inactivated human AB serum (H4522-100ML, Sigma-Aldrich/Merck KGaA, Darmstadt, Germany), 100 U/mL penicillin, 100 µg/mL streptomycin (15140122, Gibco, Thermo Fisher Scientific, Waltham, MA), 1.25 µg/mL Amphotericin B (Fungizone®, Bristol-Myers-Squibb, New York, NY), and 6000 IU/mL of rhIL-2 (Proleukin®, Novartis). Plates were incubated at 37 °C with 5% CO2 and were inspected every other day from day 5 to investigate extrusion and proliferation of lymphocytes. Half of the media was replaced with fresh complete media every other day after day 5. Cells were split when needed, harvested after 3-6 weeks and cryopreserved as described above. (20,21)

Rapid expanded Tumor Infiltrating lymphocytes (REP TILs) were expanded from 100,000 YTILs (just harvested or thawed). When biopsies were sparse REP TILs were prioritized over young TILs due to higher success rate in production of REP TILs than young TILs. Frozen young TILs were thawed and rested overnight prior to the REP. Young TILs were co-cultured with feeder cells and 30ng/mL anti-CD3 (clone: OKT-3, Miltenyi Biotec) in 10mL complete media and 10mL rapid expansion media, which consisted of AIM-V (Thermo Fisher Scientific, 0870112DK) and Fungizone® 1.25 µg/ml supplemented with 6000 IU rhIL-2/ml in T25 flasks (Cat. No. 156367, Thermo Fischer Scientific). Feeder cells (PBMCs) from minimum three donors were thawed and irradiated by 40 Gy (Gammacell 3000 Elan, MDS Nordion). REP cultures were incubated at 37 °C with 5% CO2 for 5 days. Hereafter half of the media was replaced with 10mL mixed media (consisting of 1:1; complete media:rapid expansion media). According to growth the cultures were

moved to larger flasks and rapid expansion media replaced over the next 14 days. REP TILs were harvested and cryopreserved as mentioned above. (20,21)

Tumor digest (single cell suspension)

Fresh tumor samples from the surgery room were transported in media (RPMI-1640 plus GlutaMAX and 25mM HEPES (Cat. No 72400-021, Gibco, Thermo Fisher Scientific) supplemented with 100 U/mL penicillin and 100 µg/mL streptomycin (Pen Strep, Cat No 15140122, Gibco, Thermo Fisher Scientific)) on ice. The fresh tumor tissue were dissected under sterile conditions into fragments after the macroscopical vessels were removed. Tumor fragments were then placed in T80 flask with 25 mL of digesting media consisting of 100 mL RPMI-1640 plus GlutaMAX and 25mM HEPES supplemented with 1% Pen/Strep, 1 mg/mL Collagenase (Cat No C5138-100MG, Sigma-Aldrich), 0.025 mg/mL Dornase alfa (Pulmozyme®, Genentech), and placed overnight on a magnetic stirrer at room temperature. After minimum 18 hours the digested tumor fragments were filtered through 70 µM filter to obtain single cell suspension. Single cells were cryopreserved as aforementioned.

Phenotyping by flow cytometry

Cryopreserved PBMCs, YTILs, REP TILs and tumor digest were thawed and washed once in RPMI 1640 Medium with 10% fetal bovine serum (FBS) for cellular staining. Tumor digest was thawed and rested overnight in X-vivo 15 (Lonza) with 5% heat-inactivated sterile filtered human serum (HS, Sigma-Aldrich) to regain surface-marker expression after enzymatic digestion. PBMCs, YTILs and REP TILs were thawed immediately before staining. PBMC and tumor digest were washed twice in PBS with 2% FBS (FACS buffer), stained with a panel of fluorochrome conjugated antibodies for surface markers (Supplementary Table 1) for 30 minutes (dark, 4 °C), and cells were washed twice in FACS buffer. For staining of intracellular (ICS) marker in panel B, we used the eBioscience™ Foxp3/Transcription Factor Staining Buffer Set (Invitrogen) following manufacturer's protocol. Fixation/permeabilization working solution was added to surface stained PBMCs and - tumor digest and incubated overnight (dark, 4 °C). Cells were washed twice in 1X Permeabilization Buffer and antibodies for intracellular markers were added and cells were stained for 30 minutes and hereafter washed twice with 1X Permeabilization Buffer. PBMCs and digest stained with panel A (surface markers) were fixated in 1% PFA. Samples were resuspended in FACS buffer and acquired on LSRFortessa (BD bioscience).

Analysis of flow cytometry data

Analysis of PBMCs and tumor digest

Tumor digest contained much debris and lymphocyte counts varied between patients. Samples with less than 30 events in the parent populations (CD4+ T cells or CD8+ T cells) were not included in the analysis. Number of events in parent population per patient samples are shown in Supplementary Figure 1a. Flow cytometry data was analyzed in FlowJo v10.8.1. Manual gating was performed as depicted in Supplementary Figure 1b.

Unpaired t-test was used to compare means of two groups and performed with a 95% confidence interval. * = p<0.05, ** = p<0.01, *** = p<0.001, **** = p<0.0001.

Median Fluorescence Intensity (MFI) fold change

In order to compare expression level of markers analyzed by flow cytometry, adjusted MFI fold change was calculated from MFI of positive population (MFIpos) and MFI of negative population (MFIneg) for each of the markers of interest as followed;

$$MFI\ fold\ change = \frac{MFIpos + 1000}{MFIneg + 1000}$$

As MFIneg could have a negative value, we added 1000 to each MFIpos and MFIneg and hereafter calculated the fold change MFI based on adjusted numbers. Samples with parent population ($CD4^+$ T cells or $CD8^+$ T cells) less than 30 events were not included in the analysis. MFI fold change was set to 1 for samples with a positive population less than 10 events.

TIL Reactivity Assay

YTILs and REP TILs were tested for reactivity against autologous and allogenic tumor digest with cytokine intracellular staining. TILs were thawed in pulmozyme buffer (RPMI-1640+ GlutaMAX and 25mM HEPES (Cat. No 72400-021, Gibco, Thermo Fisher Scientific) supplemented with 100 U/mL penicillin, and 100 µg/mL streptomycin (Pen/Strep, Cat No 15140122, Gibco, Thermo Fisher Scientific), 0.5mL of Magnesium chloride (Herlev Hospital Pharmacy and 0.025 mg/mL dornase alfa (Pulmozyme®, Genentech)) washed and cultured RPMI+ Pen/Strep+ 10% Human Serum (HS) with a concentration of 2-4x10^6 cells/mL. TILs were incubated and rested overnight. Tumor digest were thawed in pulmozyme buffer and washed. Cells from tumor digest were counted and resuspended in RPMI-1640+ Pen/Strep+ 10% HS in a concentration of 2x10^6 cells/mL. TILs were washed and resuspended in RPMI-1640+ Pen/Strep+ 10% HS in a

concentration of $3x10^6$ cells/mL. TILs and digest cells were co-cultured in a ratio of 3:1 by adding 100µL TILs suspension and 50µL autologous or allogenic tumor digest suspension in a sterile 96 well plate (Cat. No. 163320, Thermo Scientific). GolgiPlug (Cat. No. 51-2301KZ, BD Biosciences), GolgiStop (Cat. No. 51-2092KZ, BD Biosciences) and anti-CD107a (BD Biosciences) were added according to manufacturer's recommendations and RPMI-1640+ Pen/Strep+ 10% HS was added up to a total volume of 200µL per well. TILs stimulated with PMA/ionomycin (25ng/0.5uM) (Cat. No. P1585-1MG, Sigma Aldrich /Cat. No. 13909-1ML, Sigma Aldrich) or 0.4uL Leukocyte Activating Cocktail (BD biosciences) were used as positive controls. TILs alone and TILs cultured with allogenic tumor digest were used as negative controls. Melanoma tumor cell line without MHC class I and II expressions due to Beta-2 Microglobulin or CIITA knockout by CRISPR-associated protein 9 (CAS9) was additionally used as negative controls, both previously described (20,22). The co-cultures were incubated for 8 hours in a humidified incubator 37°C with 5% CO_2 and then stained as described above (Supplementary Table 1, panel C or D). Stained cells were acquired on the LSRFortessa or NovoCyte Quanteon Flow Cytometer (Aigilent, Sata Clara, CA) and analyzed with FlowJo 10.6.1 or 10.8.1.

Transcriptomics

Preprocessing of the RNA sequencing FASTQ files was done using trimming with TrimGalore 0.6.4 (23) which was combined with Cutadapt (24) and FastQC version 0.11.9 (25). Kallisto Quant version 0.46.0 (26) was used to align the trimmed reads to GRCh38 (27). Differential expression analysis (DEA) performed with DeSeq2 version 1.30.1 (28) and the results with genes and log-fold change was used as input to a Gene Set Enrichment Analysis (GSEA) with clusterprofiler packages from R version 4.2.2 (29) and then the Gene Ontology database (GO) and KEEG database was applied. Complexity heatmap version 2.10 (30) were used for the heatmap in Figure 5A and 6C and enrich figures were made with geasqplot2 from enrichplot (31).

Detection of Neoantigen reactive T cells in PBMCs and TILs

Neoantigens were predicted with the following pipeline; The mutations are detected by the GATK4 best practice(32). Firstly, the WES reads were trimmed using TrimGalore 0.6.4(23) combined with Cutadapt (24) and FastQC 0.11.9(25) with a minimum length of 50 bp, and else default settings. The trimmed reads were aligned to the human reference genome, GRCh38(27) using BWA-MEM 0.7.16a(33) followed by the pre-processing steps including MarkDuplicate and base re-calibrator(32). Somatic variant calling called using MuTect2(34) with filtering of panal of normal (PON) and contamination filter from GTAK best

practice. MuPexi(35) were used to predict neoepitope candidate which were filtered by the expression of the corresponding gene obtained from kaillisto version 0.46.0(26) and the binding to the corresponding HLA-allele predicted with NetMHCPan 4.1(36). The patient specific HLA-allele were typed used Razers3 (version 3.4)(37) followed by OptiType version 1.2(38). The criteria for selecting neoepitope candidates were expression level >= 0.1 TPM and then top 100 of the best EL%Rank to the HLA allele but only including HLA binders. Neoantigens were predicted for both primary and recurrent tumor.

PBMCs, Young TILs and REP TILs were screened neoantigen reactive CD8 T cells (NARTs) and virus antigen reactive T cells (VARTs) using DNA barcode-labelled peptide-MHC I multimers (39). In short DNA barcode-labelled peptide-MHC I multimers are assembled, so each DNA barcode is specific for each pMHC in the neoantigen panel. The multimers are build on a dextran backbone, which is labelled by a fluorochrome (NARTs: PE, VARTs: APC). Patient samples were stained with a patient specific pool of pMHC multimers, together with CD8 and CD3 antibodies (Supplementary Table 1). PE and APC labelled CD8+ T cell are hereafter sorted by Fluorescence activating cell sorting (FACS) on FACSAria (BD). DNA barcodes in the sorted cells were hereafter amplified by PCR. A baseline sample from the multimer pool was also amplified as a reference. PCR products were sequenced by Primbio and sequencing results were hereafter analysed in Barracoda (39). Output files from Barracoda included information on the fold change of enriched DNA barcodes in the sorted samples compared to the baseline and whether the enrichment is significant. A fold change (log2) over 2 and $p < 0.001$ was set as threshold for a significantly enriched DNA barcode, wherefrom the T cell recognition of pMHC was annotated.

Verification peptide reactivity

Peptides detected by NARTs was verified by peptide specific expansion of patient PBMCs. PBMCs were co-cultured with a pool of reactive peptides for 14 days. PBMCs were cultured in X-vivo (Lonza) with 5% human serum. Peptides were added at day 0 with a concentration of 10 ug/ml per peptide. PBMCs were additionally stimulated with 40 IU/ml IL-2, and 0.5ug/ml purified anti-CD28 (BD, clone: CD28.2). Media with IL-2 was changed twice per week. PBMCs expanded with peptides were hereafter stained with single tetramers to validate the pMHC specificity of the given T cell cultures. Each tetramer was fluorchrome labelled with both PE and APC. PBMC samples was analysed by LSRFortessa (BD) and gated in FlowJo v10.

RESULTS

To investigate if Nivolumab could influence the immune-cellular signatures in recurrent GBM patients, blood and tumor samples were collected from 40 patients. Twenty patients had neurological tumor resection (arm A), while the remaining 20 received medical treatment only (arm B). From arm A, 19 tumor digests resulted in 15 YTILs, 16 REP TILs, and 1 tumor cell line. In addition, tumor biopsies were collected from 10 non-treated control patients with recurrent glioblastoma, resulting in 10 tumor digests, 8 YTILs, and 10 REP TILs (Figure 1 and Supplementary Table 2).

Intratumoral T cells from patients in arm A (NIVO) was compared to intratumoral T cells from control patients. Blood samples from arm A and arm B was additionally studied for the long-term effect of combinational therapy with Nivolumab and Bevacizumab, and to examine the role of continuous tumor presence (Arm B) versus tumor removal (Arm A).

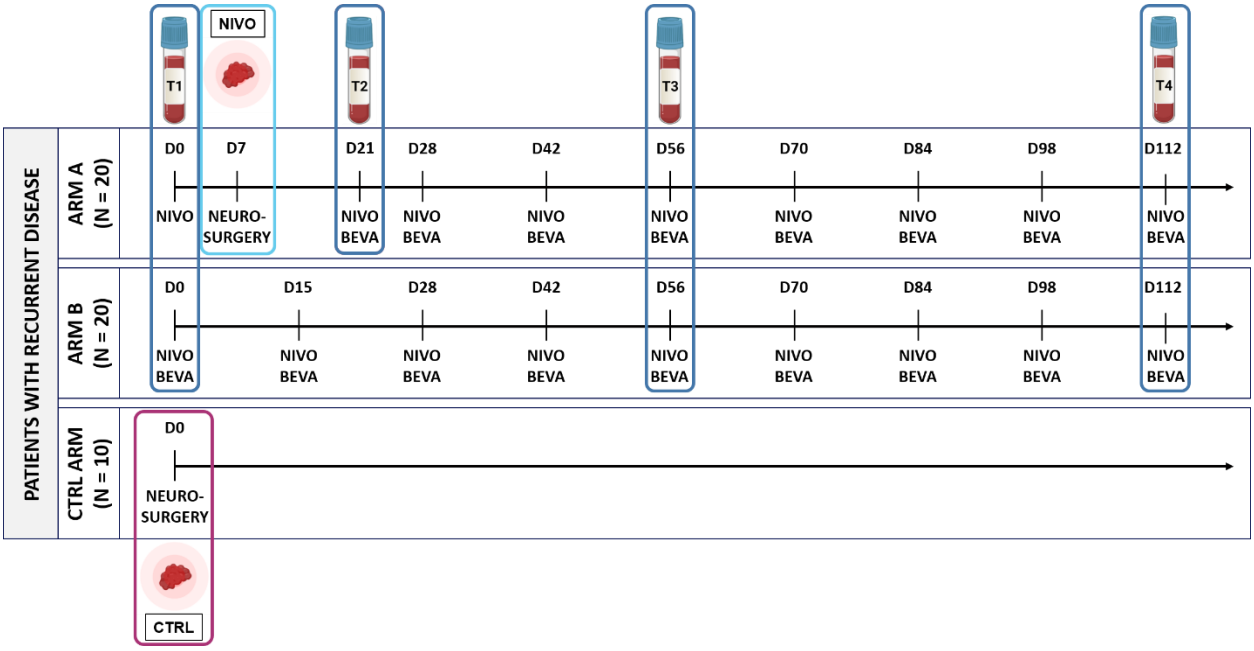

Figure 1 | Clinical setup. Timeline showing administration of treatment with Nivolumab (NIVO) and Bevacizumab (BEVA), including time points of sampling blood and tumor tissue. Treated patients included a surgical arm (arm A) and non-surgical arm (arm B), and all patients received Nivolumab and Bevacizumab every two weeks. Patients in arm A also received neoadjuvant Nivolumab seven days prior surgery. Control patients with recurrent glioblastoma undergoing neurosurgical resection were additionally included. Controls did not undergo neoadjuvant treatment in the recurrent setting, thus tumor tissue remained untreated. Additionally, blood samples were collected from treated patients at D0 as baseline (T1), after 8 weeks (T3) and 16 weeks (T4). An additional blood sample was collected 3 weeks post neoadjuvant Nivolumab (T2) from patients in arm A – 2 weeks after surgery

Intratumoral detection of Nivolumab and tissue resident T cells

Tumor samples were analyzed to evaluate Nivolumab's ability to penetrate the tumor microenvironment (TME). To detect Nivolumab binding to PD-1 on T cell surfaces we applied a fluorochrome-conjugated anti-IgG4, while free PD-1 molecules was determined by a regular fluorochrome-conjugated aPD-1 antibody (Figure 2a).

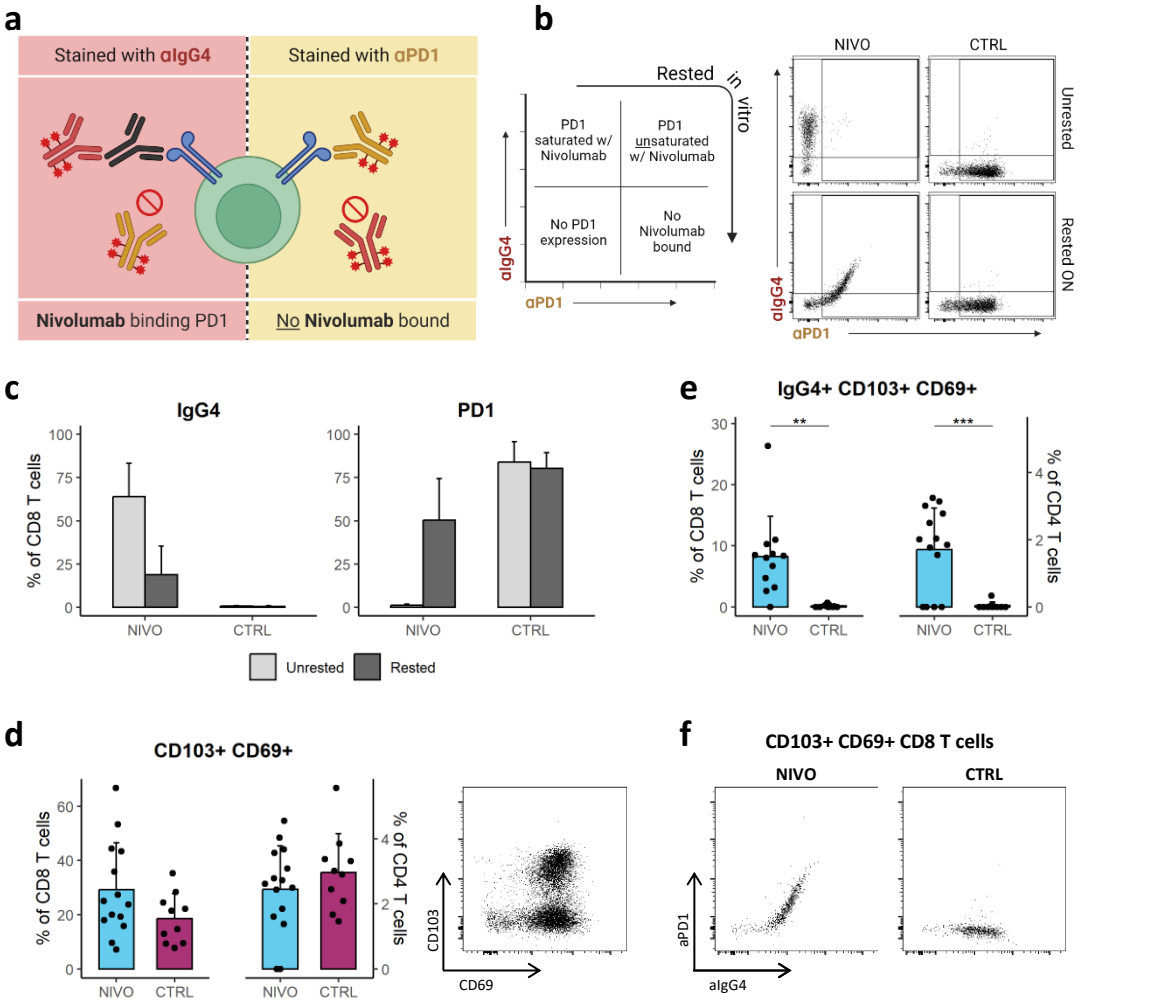

Figure 2 | Intratumoral detection of Nivolumab and tissue resident T cells. a) Illustrative explanation for PD1 and Nivolumab antibody(Ab)-detection; Nivolumab bound to PD1 was detected with an fluorochrome-conjugated anti-IgG4 Ab (red) binding to the Fc region of Nivolumab (black Ab), while free PD1 molecules were detected with fluorochrome-labelled anti-PD1 Ab (yellow). **b)** Explanation of dot plot showing Nivolumab binding and saturation (left), representative flow cytometry dot plots of unrested and rested tumor digest stained with aPD1 and aIgG4, showing a complete Nivolumab saturation of intratumoral T cells in unrested tumor digest from Nivolumab-treated (NIVO) patient, which is partly lost after resting. Intratumoral T cells from control(CTRL) patients do not bind aIgG4 (right). **c)** Frequency of CD8+ T cells stained with aIgG4 (Nivolumab bound) and aPD1 (free PD1 molecules) in unrested (light grey) and rested (dark grey) tumor digest. **d)** Frequency of CD8+ and CD4+ T cells co-expressing the markers of tissue residency, CD69 and CD103, in Tumor digest from NIVO patients (light blue) and CTRL patients (purple) (left). Representative plot of intratumoral CD8+ T cells expressing CD69 and CD103 (right). **e)** Frequency of CD8+ and CD4+ T cells binding Nivolumab (aIgG4) that are tissue resident T cells. **f)** Representative plots from NIVO and CTRL patients showing tissue resident CD8+ T cells from rested tumor digest binding aPD1 and aIgG4. Means were compared between NIVO and CTRL using unpaired t-test , * = p<0.05, ** = p<0.01, *** = p<0.001, **** = p<0.0001.

Tumor digests were rested overnight to re-express certain T cell surface markers lost during tissue digestion. Before rest, T cells were only binding aIgG4, indicating all PD-1 molecules were bound to Nivolumab. After rest, T cells bind both aPD-1 and aIgG4, indicating surface presence of new PD-1 molecules during the resting period, or loss of Nivolumab binding. T cells from control patients only bound aPD-1, confirming that IgG4 binding is specific to Nivolumab (Figure 2b and 2c). Tumor digests were stained for CD103 and CD69 to confirm that T cells found in the tumor digest included tissue resident T cells. Both markers were expressed on both CD4+ and CD8+ T cells in the tumor digest, with no difference in frequencies between patients in NIVO and control patients. Importantly, CD103 and CD69 co-expression was also detected within Nivolumab-bound T cells. Altogether, this suggests that Nivolumab has penetrated the tumor tissue as free molecules and can hereby bind to tissue-resident T cells within the tumor (Figure 2e and 2f).

CNS homing and T cells activation in TME and blood

Next we searched for T cells in both tumor and blood that expressed a central nervous system (CNS) homing profile. The chemokine receptors CD183 and CD195 has previously been correlated with CNS homing in neurological inflammation (40,41). As cancer is also an inflammatory disease we investigated the expression of the two chemokine receptors, CD183 (CXCR3) and CD195 (CCR5). The frequency of CD4+ T cells co-expressing CD183 and CD195 was higher in NIVO treated tumors compared to controls, while stable for CD8+ T cells (Figure 3a). Furthermore, a significantly higher MFI fold change was found within both CD4+ and CD8+ T cells for both CD183 and CD195 in the tumor of NIVO patients, indicating enhanced expression of these marker following treatment (Figure 3b). This coincided with PBMCs showing a trend towards lower frequency of both CD4 and CD8 T cells that co-expresses the two chemokine receptors (Supplementary figure 2). . Together, this suggests that Nivolumab can reinforce CNS recruitment, with increased expression level of the two chemokine receptors on T cells in tumor digest from after Nivolumab treatment compared to controls. Interestingly, in blood we also observed a difference in chemokine expressing CD8+ T cells between Nivolumab treated patients who had their tumor removed (arm A) and the tumor bearing patients (arm B). We found that PBMCs from arm B had significantly higher frequencies of CD183+ CD195+ T cells within the CD8 population at T1 and T4 compared to arm A (Figure 3c). The larger fraction of this migratory phenotype suggests a more pronounced neurological inflammation patients in arm B.

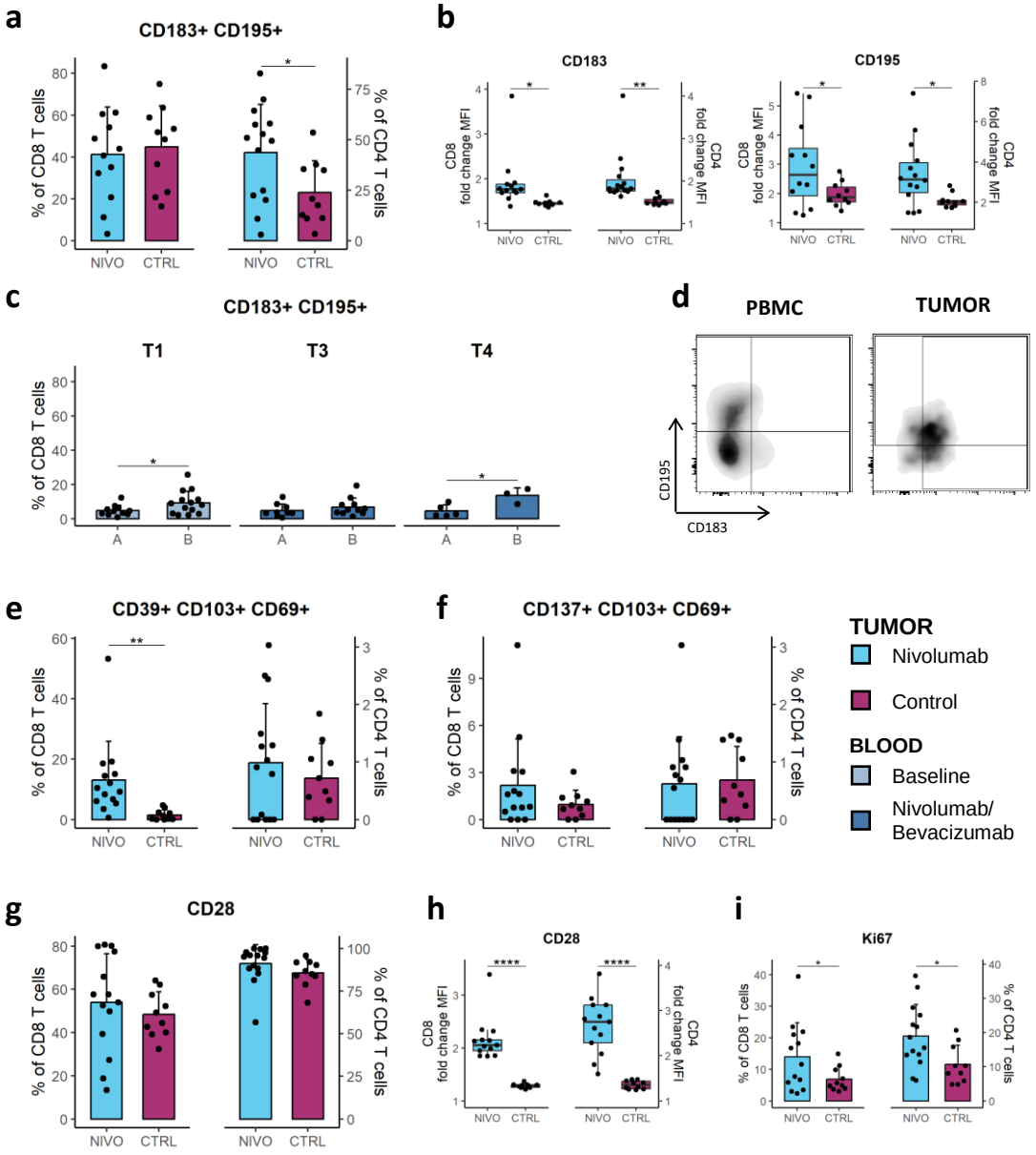

Figure 3 | CNS-homing, activation and proliferation in tumor tissue and blood. a) Frequency of CD8+ and CD4+ T cells co-expressing the chemokine receptors, CD183 (CXCR3) and CD195 (CCR5) in tumor tissue of Nivolumab-treated (NIVO) and control (CTRL) patients, for indication of CNS homing. **b)** Fold change in median fluorescent intensity (MFI) between the positive and negative population in T cells stained for CD183 and CD195. MFI fold change indicate the change in expression level of the two markers in NIVO and CTRL patients. **c)** Frequency of CD8+ T cells co-expressing CD183 and CD195 in blood samples from T1 (Day 0), T3 (8 weeks) and T4 (16 weeks). Frequencies are compared between the surgical arm (arm A) and the tumor bearing arm (arm B). **d)** Representative flow cytometry plot of CD195 and CD183 staining in blood (PBMCs) and tumor. **e)** Frequency of tissue resident T cells expressing the marker of activation CD39 among intratumoral CD8+ and CD4+ T cells. **f)** Frequency of tissue resident T cells expressing the marker of activation CD137 among intratumoral CD8+ and CD4+ T cells. **g)** Frequency of T cells expressing the co-stimulatory receptor CD28 among intratumoral CD8+ and CD4+ T cells. **h)** MFI fold change of CD28 staining of intratumoral CD8+ and CD4+ T cells. **i)** Frequency of T cells expressing the marker of proliferation Ki67 among intratumoral CD8+ and CD4+ T cells. Means were compared between NIVO and CTRL (Tumor), and between arm A and arm B (blood) using unpaired t-test . * = p<0.05, ** = p<0.01, *** = p<0.001, **** = p<0.0001.

As we found that a CNS homing potential could be observed among T cells in both blood and tumor, we further evaluated the activation status of intratumoral T cells after Nivolumab exposure. T cells co-expressing CD39 (a marker of recent T cell activation) and the tissue resident markers, CD103 and CD69 were only present in tumor tissue. We found significantly higher frequencies of such activated tissue-resident T cells within the CD8+ T cell population in NIVO tumors tissue compared to tumor tissue from control patients, a similar tendency was also found within CD4+ T cells but in a much lower frequency level (Figure 3e). Tissue resident T cells expressing the early activation marker CD137 (4-1BB), were also found in low frequencies within both CD8+ and CD4+ T cells, and tended to increase in CD8+ T cells after Nivolumab treatment (Figure 3f). Furthermore, the frequency of T cells in the tumor expressing the co-stimulatory molecule, CD28 did not significantly change with NIVO treatment (Figure 3g), but such T cells demonstrated strong treatment-associated upregulation of the surface expression of this co-stimulatory marker (Figure 3h). Finally, enhanced proliferation was observed among both intratumoral CD8+ and CD4+ T cells following Nivolumab treatment, based on the detection of Ki67 expression (figure 3i).

In summary, T cells in tumor following treatment with Nivolumab have increased CNS-homing profile, and a higher frequency of T cells with status of activation and proliferation compared to tumors from untreated control patients.

Increased intratumoral T cell differentiation after Nivolumab treatment

T cell expression of inhibitory molecules and markers of differentiation including PD-1, TIGIT, LAG-3, TIM-3 and CTLA-4 were examined to evaluate potential Nivolumab induced changes in blood (PBMCs) and tumor (digest). PD-1 expression was measured using both aPD-1 and aIgG4 staining antibodies. The kinetics of Nivolumab binding is shown in figure 4a, where PBMC derived CD8+ T cells are stained with aPD-1 and aIgG4. At baseline (T1) PD-1 molecules on T cells was stained only by aPD-1, while after Nivolumab administration, PD-1 molecules were instead stained by aIgG4. The sum of the T cell populations stained by either aPD-1 or aIgG4 was therefore defined as the PD-1+ population, in order to compare expression of PD-1 between time points and patient groups. A significant drop in frequencies of PD-1 expressing CD8+ T cells was observed in PBMCs after NIVO treatment (T2, T3, T4), and a similar trend was observed within CD4 T cells (Figure 4b). This drop in PD1 expressing CD8+ T cells in the NIVO treated patients was similarly detected in the tumor (Figure 4c). Taken together, Nivolumab appears to induce a downregulation of PD-1 expression in T cells, or selective loss of PD1 expressing T cells.

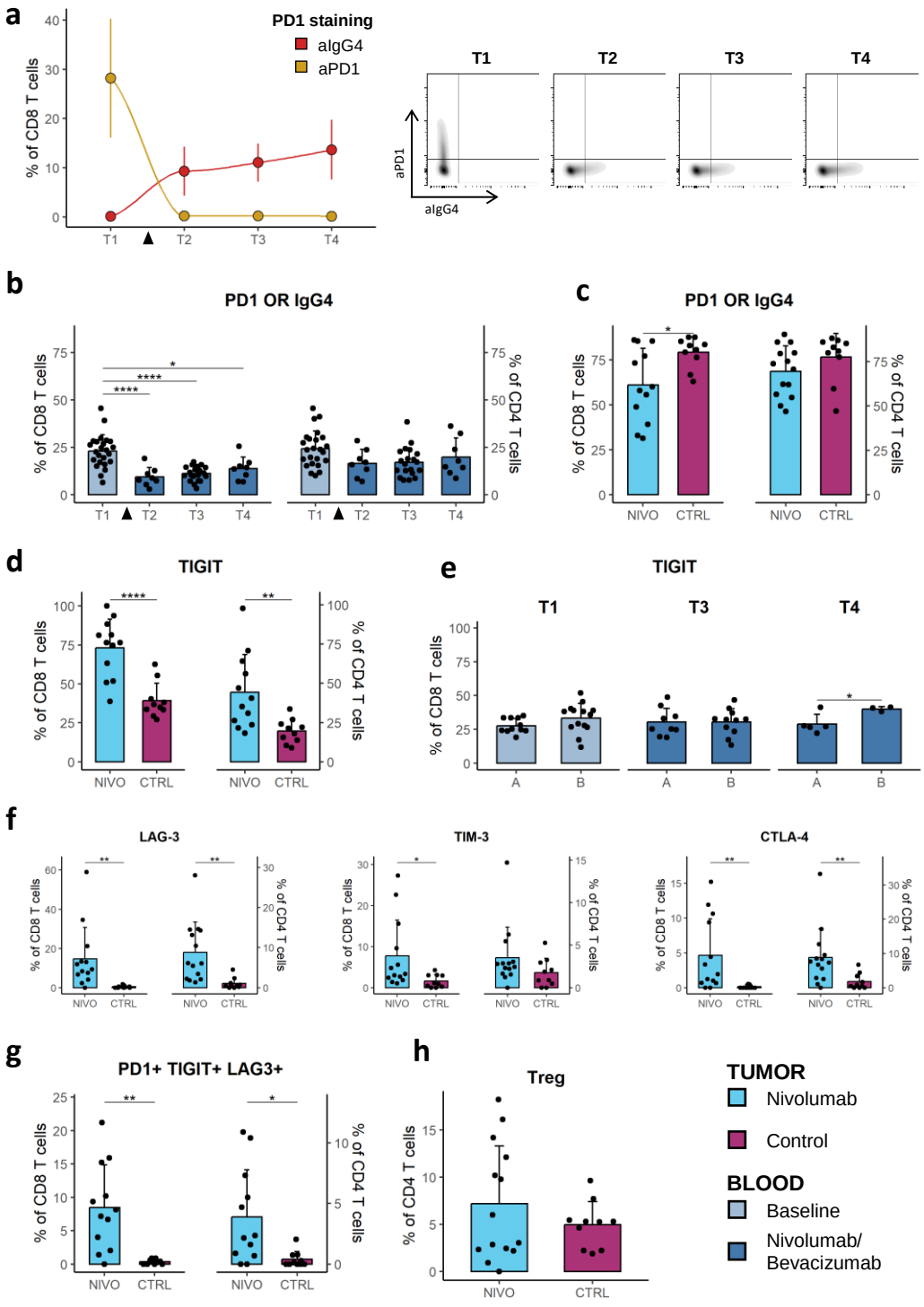
a
PD1 staining
aIgG4
aPD1
% of CD8 T cells
T1
T2
T3
T4
aPD1
aIgG4
b
PD1 OR IgG4
% of CD8 T cells
% of CD4 T cells
c
PD1 OR IgG4
NIVO
CTRL
d
TIGIT
e
TIGIT
f
LAG-3
TIM-3
CTLA-4
g
PD1+ TIGIT+ LAG3+
h
Treg
TUMOR
Nivolumab
Control
BLOOD
Baseline
Nivolumab/
Bevacizumab

Figure 4 | Nivolumab induced differentiation of T cells. a) The kinetics of Nivolumab binding. CD8+ T cells derived from blood collected before (T1) and after (T2, T3, T4) Nivolumab administration stained with aPD1 (yellow) and aIgG4 (red). **b)** Frequency of a collected PD1+ population (based on aPD1 and aIgG4 staining) within PBMC derived T cells collected at different time points of the treatment. **c)** Frequency of the collected PD1+ population within intratumoral T cells from Nivolumab-treated (NIVO) and control (CTRL) patients. **d)** Frequency of intratumoral T cells from NIVO and CTRL patients expressing the inhibitory molecule, TIGIT. **e)** Frequency of CD8+ T cells expressing TIGIT from blood samples at T1 (Day 0), T3 (8 weeks) and T4 (16 weeks). Frequencies are compared between the surgical arm (arm A) and the tumor bearing arm (arm B). **f)** Frequency of intratumoral T cells from NIVO and CTRL patients expressing the inhibitory molecules, LAG-3, TIM-3 and CTLA-4. **g)** Frequency of intratumoral T cells co-expressing the three most common inhibitory molecules, PD1+, TIGIT+ and LAG-3 from NIVO and CTRL patients. **h)** Frequency Treg cell among intratumoral CD4+ T cells from NIVO and CTRL patients. Means were compared between NIVO and CTRL (Tumor), and between arm A and arm B, and the four time points T1, T2, T3, T4 (blood) using unpaired t-test . * = $p<0.05$, ** = $p<0.01$, *** = $p<0.001$, **** = $p<0.0001$.

When investigating expression of other checkpoint molecules (TIGIT, LAG-3, TIM-3 and CTLA-4), this loss of PD1 expression seems to be counteracted by a general increased in these. Higher frequencies of T cells expressing TIGIT, LAG-3, TIM-3 and CTLA-4 was observed in tumor tissue from NIVO patients compared to untreated control patients. The frequencies of T cells expressing TIGIT are significantly higher in tumors following Nivolumab treatment, both in the CD8+ and CD4+ T cells populations (Figure 4d). Interestingly, when comparing the frequency of TIGIT+ T cells in blood between arm A (surgical arm) and arm B (tumor bearing arm), significantly higher frequencies of CD8 T cells expressing TIGIT is found in arm B in time point 4 (T4) (Figure 4e). This could indicate that there is an ongoing exhaustion of T cells from arm B, as the tumor is still present and chronic inflammation of the tumor tissue can be mirrored in a peripheral upregulation of TIGIT. Moreover, there was a significantly higher percentage of T cells expressing LAG-3, TIM-3 (CD8+), CTLA-4 in tumor digest following Nivolumab treatment (Figure 4f). For these markers limited differences was observed in PBMCs (Supplementary Figure 2). Interestingly, when analyzing co-expression the three most commonly expressed checkpoint molecules on intratumoral T cells (PD-1, TIGIT and LAG-3), very low percentages were found in control patient, but they significantly increased in NIVO patients (Figure 4g). This demonstrated that intratumoral T cells from the Nivolumab treated patients were more differentiated compared control patients. Additionally, it suggests a compensatory upregulation of other checkpoint inhibition molecules, especially TIGIT, when PD-1 blocking takes place in GBM. Finally, Treg levels were low in tissue from controls, but highly heterogeneous between NIVO patients (Figure 4g), indicating an induced anti-inflammatory tumor microenvironment (TME) after Nivolumab administration for a fraction of the patients.

Intratumoral gene expression analysis in Nivolumab treated patients vs controls

Transcriptomic data obtained from the recurrent tumor samples were compared between NIVO and control patients to investigate potential changes in the TME. From a differential expression analysis (DEA)

we found 1,716 differential overexpressed genes and 260 genes which were differential under-expressed in the Nivolumab treated patients compared to controls (Figure 5a).

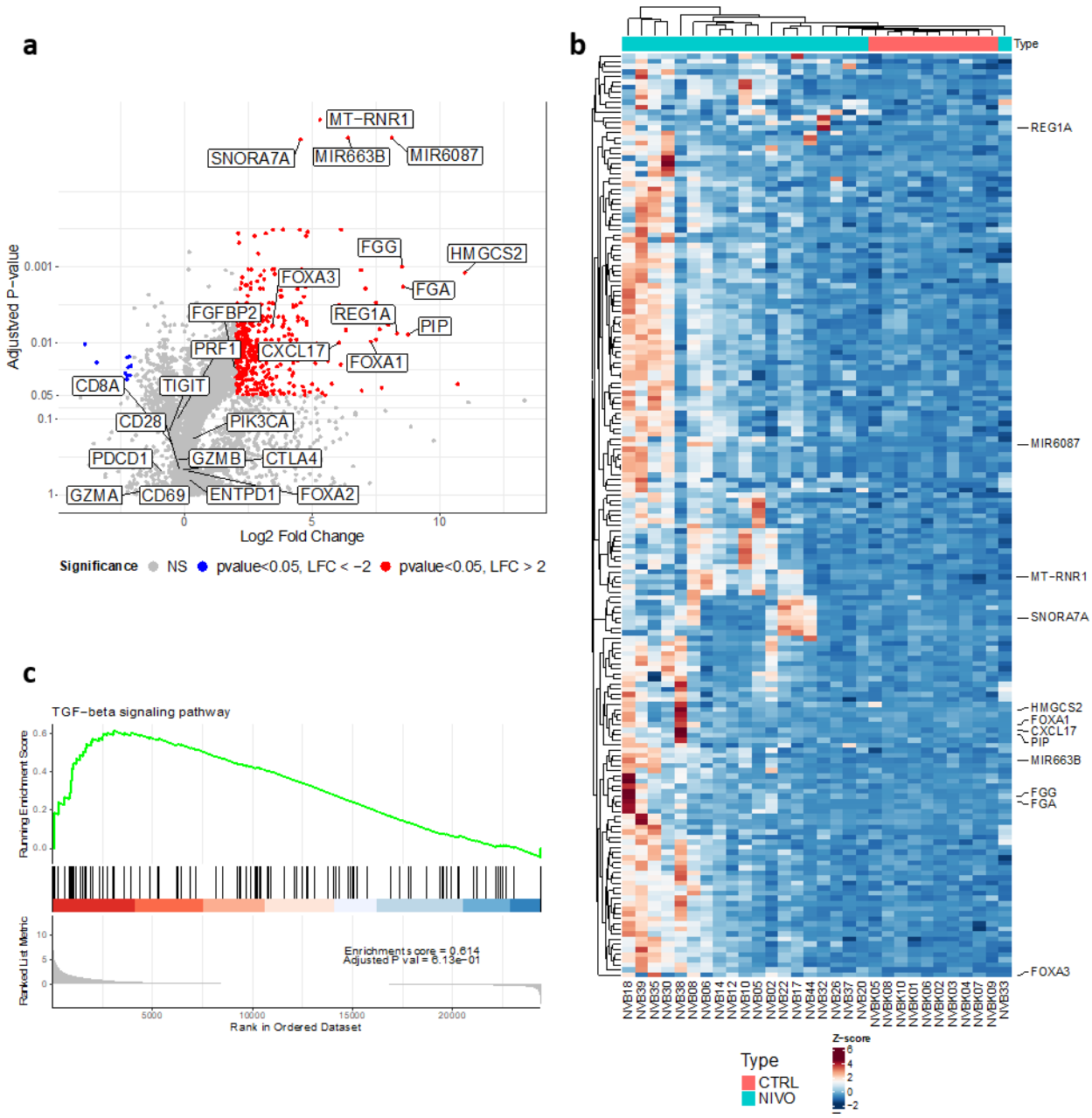

Figure 5 | Transcriptomic comparison of Nivolumab treated patients versus control. a) Volcano plot showing 1,716 differential overexpressed in red with an adjusted p-value < 0.05 and log2 fold change > 2. Additionally, there were found 260 under-expressed genes in blue with adjusted p-value < 0.05 and log2 fold change < -2. The highlighted genes consist of the most up/down regulated genes and few immune-related genes of interest. Additionally, the genes asses by in flow cytometry are highlighted. **b)** The most significantly differential expressed genes from the volcano figure with adjusted p-value < 0.01 and log2 fold change > 2 or < -2 were illustrated with a heatmap with unsupervised clustering. Highlighted genes are significantly over and under-expressed genes highlighted in a). **c)** A gene set enrichment analysis showed that the TGF-β pathway were differential over-expressed in the Nivolumab treated patients shown in an enrichment figure.

Neither of the investigated genes in the phenotype analysis described above were found significant expressed in the DEA. Though, it should be noted that transcriptomics data are based on bulk RNA including all cell types in the TME, why an upregulation of T cell activation and differentiation markers might be overshadowed due to low T cell infiltration. Most significantly overexpressed genes are related to cancer progression (MT-RNR1, SNOR7A, MIR663B, MIR6087, FGG, FGA, HMGCS2, PIP, REG1A) rather than being related to immune response induced by Nivolumab administration. Nevertheless, genes related to inflammation including Forkhead Box A (FOXA) genes and CXCL17 were also found to be significantly overexpressed. Additionally, FGFBP2 is significantly overexpressed, and is related to T cell effector function (Figure 5a). Despite the majority of significantly, highly overexpressed genes are related to cancer progression rather than inflammation, an unsupervised clustering resulted in separation of the Nivolumab treated patients compared to untreated controls (Figure 5b). Genes enriched in the DEA were compared to the KEEG database and the TGF-β pathway were found to be enriched in NIVO patients (Figure 5c). Taken together, transcriptomic data showed the same tendency as detected by surface expression; Nivolumab has a cellular impact on the TME with a sign of T cell activation, which can result in upregulation of inhibitory pathways, such as TGF-β.

Autologous tumor reactivity of TILs

We challenged the tumor-reactive capacity of expanded TILs, using intracellular cytokine staining of TILs after co-culture with autologous tumor digest. Reactivity in REP TILs against autologous tumor digest was demonstrated in four Nivolumab treated patients (NVB02, NVB05, NVB08, NVB10) out of 16 patients. However, when we tested the tumor digest from NVB08 against arbitrary allogenic REP TILs, reactivity was unanimously detected (data not shown), indicating reactivity in TILs were not tumor specific. REP TILs from patient NVB02 and NVB05 showed clear responses among both CD4+ and CD8+ T cells. For patient NVB10, we detected a small response only among CD8+ T cells in REP TILs (Figure 6a and Supplementary Figure 5). Overall tumor reactivity ranged between 1.2-13.6% reactive $CD8^+$ TILs and between 6.3-10.9 % reactive $CD4^+$ TILs (excluding NVB08) (Figure 6a). To assess whether T cell reactivity could influence patient outcome, we evaluated the median overall survival (OS) of patients with reactive T cells (NVB02, NVB05, NVB10) to 18.0 months and PFS of 12.2 months. This is numerical higher than the rest of NIVO patients with corresponding OS of 11.7 months progression free survival (PFS) of 4.7 months, respectively (Supplementary Figure 5b). However, the difference is not significant based on the small study cohort applicable to T cell reactivity analyses, and hence the results warrant further studies.

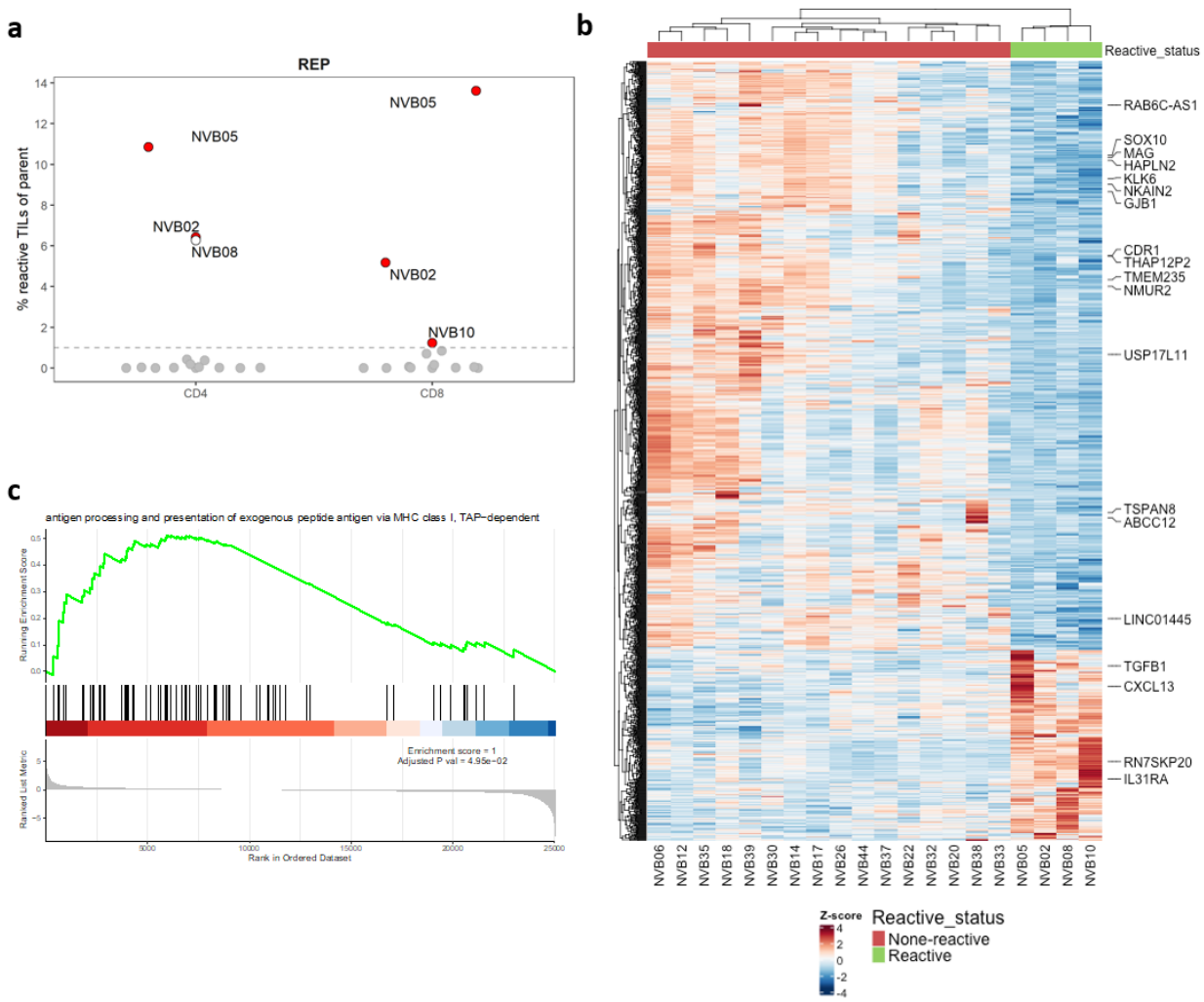

Figure 6| Comparison of patients with reactive T cells versus non-reactive T cells. a) Reactivity towards autologous tumor digest detected in rapid expanded tumor infiltrating lymphocytes (REP TILs). TILs where co-cultured with autologous tumor digest for 8 hours and hereafter intracellularly stained for TFN-α, IFN-γ, CD137 and CD107a. TILs expressing at least two of the markers, where defined as reactive. Background reactivity (TILs alone) are subtracted and hereafter patients with more than 1% reactive TILs are defined as reactive. Patients with tumor reactive TILs are highlighted in red. Patient NVB08 had reactive TILs, but it appeared not to be tumor specific, this patient is therefore marked with an open circle. Patients without tumor reactive TILs are marked in grey. **b)** 372 differential over-expressed and 1,150 differential under-expressed genes were found in patients with reactive T cells by differential expression analysis with adjusted p-value < 0.05. These differential expressed genes were Illustrated by heatmap showing that patients with reactive and non-reactive T cells were defining the two first unsupervised clusters. The highlighted genes consist of the most up/down regulated genes and include some immune-related genes of interest. **C)** A gene set enrichment analysis was made from the differential expression analysis and enriched pathway in antigen presentation on MHC-1 was found for patients with reactive T-cells.

Transcriptomics analyses were performed to investigate differences in the tumor microenvironment between patients with tumor reactivity in TILs, compared to the rest of arm A. The DEA showed 1,522 differential expressed genes and the reactive patients (NVB02, NVB05, NVB08, NVB10) defined the first cluster-split, showing a large difference between the TME in the reactive and non-reactive patients. Among the overexpressed genes we found in the patients with reactive TILs was; TGFβ1, CXCL13 and

IL31RA, which all can be related to inflammation (Figure 6b). A gene set enrichment analysis further demonstrated a differential overexpressed pathways involved in the MHC-I peptide presentation (Figure 6c) in patient with reactive TILs. Additionally, when considering surface expression of the T cell markers described above, we find a tendency for higher frequency of T cells expressing CD28, and the inhibitory receptor TIGIT among intratumoral T cells from patients with reactive TILs compared to the remaining NIVO patients. Additionally, we also found significantly higher frequency of Treg cell among CD4+ T cells in the reactive patients (Supplementary Figure 5c). In summary, the TME of these patients has a different gene-expression profile than the remaining NIVO patients, and an expression profile with a higher potential for effector T cell activation due to increased MHC-I peptide presentation, and higher frequency of CD8+ T cells expressing CD28. Increased gene-expression of TGF-beta, and higher frequencies of TIGIT+ CD8+ T cells and Tregs cells might therefore be an immune suppressive response caused by the T cell activation.

Neoantigen reactive T cells (NARTs) in PBMCs and TILs

Tissue from patients with tumor reactive TILs (NVB02, NVB05, NVB08, NVB10) was further evaluated to determine the antigen recognition potentially related to such anti-tumor reactivity. Neoepitopes was predicted from the sequencing data from the primary and recurrent, resulting in a total of 97-173 potential neoepitopes for each patient. We screened PBMCs, Young TILs and REP TILs for neoantigen reactive CD8+ T cells (NARTs) using this library of predicted neoepitope and virus antigen reactive CD8+ T cells (VARTs), using fluorescent and DNA barcode-labelled peptide-bound MHC I multimers. We identified NART populations against 2-6 such neoepitope-MHC per patient in PBMCs and/or TILs (Figure 7a, and Supplementary Figure 6). The number of responses are shown in Figure 7b and sum of estimated frequencies of NARTs and VARTs are shown in Figure 7b for each blood sample time point as well as for the TILs. When looking at the dynamics of number of responses towards neoantigens, there appears to be an increase after Nivolumab distribution (T2) for patient NVB02 and NVB05, which hereafter persist. The same pattern was observed for sum of estimated frequencies at T2 and T3, especially for NVB02. Neoantigen responses were only found at baseline (T1) and T3 in PBMCs from NVB10. However, number and size of responses appears to increase at T3. Neoepitope responses were only detected in TILs from NVB02 and NVB05, where both the number of responses, but also estimated frequencies are increased in REP TILs compared to Young TILs, mostly dominant in TILs from NVB02. The number of responses towards virus peptides in PBMCs remains relatively consistent throughout the treatment period, as does the sum of frequency of VARTs. This demonstrates that the assay is stable between different samples. All

specificities was confirmed by 14 days patient-specific peptide stimulation of PBMCs. All previously detected neoantigen was detected in at least one time point in expanded PBMCs by tetramers staining of each of the detected pMHCs (Supplementary Figure 7).

In summary, we screened for NARTs in YTILs, REP TILs and PBMCs. We found NARTs in TILs from NBV02 and NVB05. This coincide with NVB02 and NVB05 having the highest frequencies of reactive CD8+ TILs upon tumor challenge, while NVB10 has a relatively low CD8+ TIL response and NVB08 had no CD8+ TIL response (see Figure 6a). Importantly, we also detected NARTs in blood samples, confirming an interaction between the brain tumor and the peripheral immune system. Interestingly, we also detected a boost of NARTs in blood after Nivolumab distribution, which aligns with previous observations from other cancer cohorts (42).

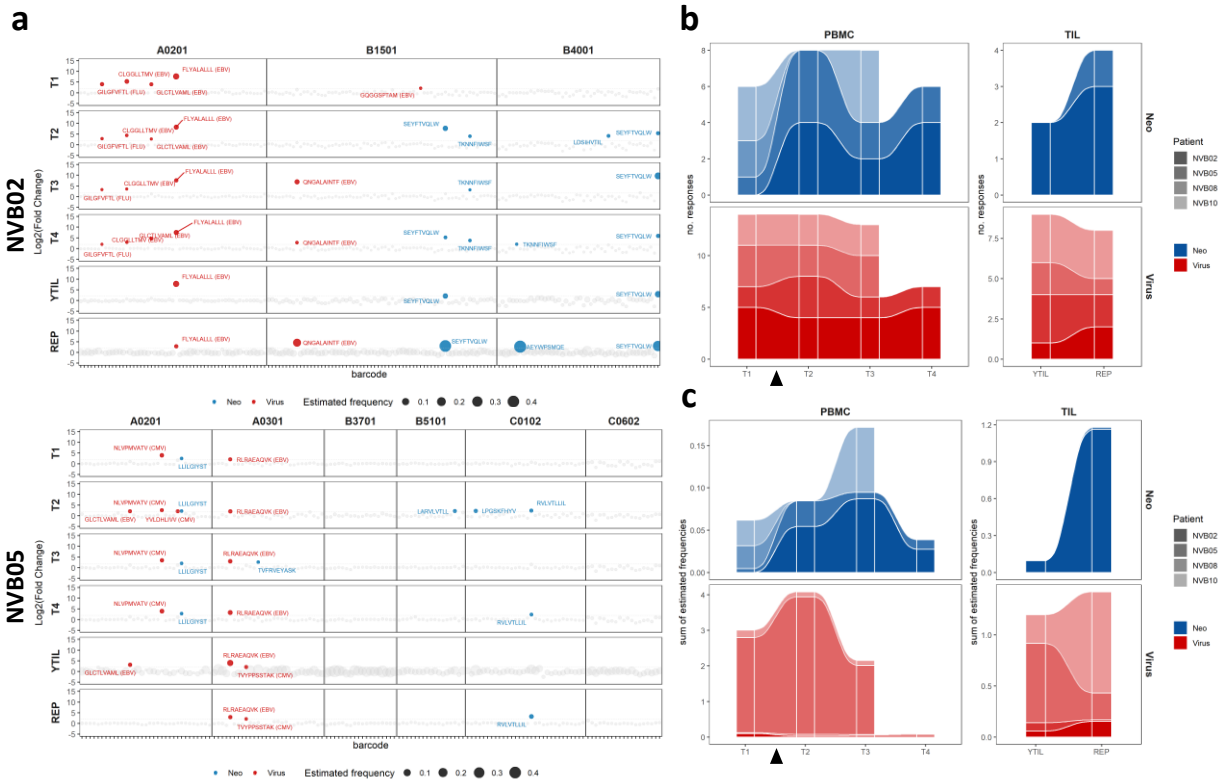

Figure 7 | Detection of neo-antigen reactive CD8 T cells (NARTs). a) Screening output for patient NVB02 and NVB05. Significantly enriched ($p < 0.001$, Log2 fold change > 2) barcoded pMHC multimers are colored and labelled with the immunogenic peptide sequence. Virus antigens are marked in red and neoantigens are marked in blue. The dot size represents an estimated frequency of CD8+ T cells for each NART. Grey dots are all pMHC multimers that where not significantly enriched after sample staining. Specificities are shown for each blood sample timepoint; T1 (Day 0), T2 (3 weeks), T3 (8 weeks), T4 (16 weeks), and for YTIL (young TILs) and REP TILs. The screened pMHC are additionally divided based on HLA type. **b)** Number of responses towards different neoantigens (blue) and virus antigens (red). Individual patients are marked in different shades of the respective color. The plot is further divided in PBMC and TILs. There was no significant difference between blood-sample time points or between YTILs and REP TILs **c)** Sum of estimated frequency of NARTs recognizing different neoantigens (blue) and virus antigens (red). There was also no significant difference between bloodsample time points or between YTILs and REP TILs

When examining the origin of the immunogenic neoepitopes and found a tendency of enrichment (p=0.06, propotion z-test) of immunogenic peptides, which was predicted from both primary and recurrent tumor (4.3%), compared to immunogenic peptides only predicted from one of the tumors (1.6%) (Supplementary Figure 8a). Interestingly, we observed three neoepitopes recognized by NART, which originated from the same frameshift mutation from the gene; NF1 (Supplementary Figure 8b), suggesting extraordinary immunogenicity of this genetic alterations, and open a possibility to explore this further as a potential shared neoantigen source.

DISCUSSION

Researchers are still in the early stages of understanding the immune system of the brain, and very little is known about peripheral immune cells' role in brain. This study examined intratumoral T cells in patients with recurrent glioblastoma, by evaluating the cellular impact of neo-adjuvant Nivolumab (aPD-1) treatment. Moreover, we studied the long-term effect of Nivolumab and Bevacizumab (aVEGF) treatment on peripheral T cells in patient who did (arm A) and did not (arm B) receive resection of their recurrent tumor.

We confirmed the presence of Nivolumab in blood and importantly also in tumor tissue. To our knowledge, it has not yet been demonstrated that Nivolumab can be found intratumorally in primary brain cancers. It can be questioned whether Nivolumab have entered the tumor as free molecules or only by binding to T cells. The BBB strongly regulates passage of larger molecules and cells into the brain tissue through tight junction (13), however, it has also been shown that the BBB in GBM can be disrupted and become more permeable in these tight junctions, which support both scenarios (14,15). We found that PD-1 molecules on all intratumoral T cells were saturated by Nivolumab in unrested digest, this also included tissue resident T cell within tumor tissue. Thus our results implies that Nivolumab can penetrate the tumor as free molecule. Previously, Osa et al. found that Nivolumab bound to T cells where lost, when Nivolumab-pretreated T cells were cultured in Nivolumab free medium for more than 24 hour. Moreover, they showed that decreased concentrations of Nivolumab in plasma correlated with drop in level of Nivolumab-bound T cells in blood from patient with non-small cell lung cancer (43). Comparing our results to these findings indicates that Nivolumab has been in excess in the TME as intratumoral T cells were

saturated by Nivolumab, which further support that Nivolumab can enter the GBM microenvironment as a molecule alone.

We found that Nivolumab administration had a phenotypical impact on T cells both in the tumor and also in the periphery, but we could also observe an effect on the TME.

Firstly, intratumoral T cells had higher expression level of the chemokine receptors CD183 and CD195 following Nivolumab administration. It has previous been shown that T cells co-expressing CD195 and CD183 can be detected in CSF and PBMCs of Multiple Sclerosis patients and other cases of neurological inflammation, but not in non-inflammatory neurological diseases (40,41). To this end, our results indicate that a recruitment to the GBM tumor is boosted due to increased inflammation caused by Nivolumab administration. Additionally, we found that Nivolumab treated patients who did not have their tumor removed (arm B) had higher frequencies of CD8+ T cells expressing CD183 and CD195 in the blood compared to the tumor resected arm (armA). This is an interesting observation, as it supports that peripheral T cell are actively being recruited to the brain due to neurological inflammation also in a cancer setting. However, it should be investigated further by analyzing the level of CNS homing T cells in the blood as well as in the CSF of the two patient groups.

Furthermore, intratumoral T cells was found to have higher frequency of cells expressing markers of activation. CD137, also known as 4-1BB, is expressed on T cells upon antigen recognition and activation (44). CD137+ tissue resident (69+/CD103+) CD8+ T cells were found in seemingly higher frequencies in digest after Nivolumab treatment. However, it should be noted that they still appeared in low frequencies in the tumor digest, which could be explained by a transient expression upon TCR recognition (45). While CD137 expression both increases and attenuates quickly after stimulation, CD39 are lately - and more persistently expressed upon T cell activation (45–48). CD39 co-expressed with the tissue resident marker CD103 has previously been identified as a unique CD8+ T cell population within the TME, which were then found to be enriched for tumor-reactive T cells as well as correlating with longer survival for HNSCC patients (49). We demonstrated increased frequencies of CD39+ tissue resident CD8+ T cells in tumor digest from Nivolumab-treated patients compared to controls. Thus, collectively PD-1- blocking have most likely led to an increased TCR activation of intratumoral T cells, also supported by overexpression of FGFBP2, a gene related to T cell cytotoxicity (50,51). Futhermore, the co-stimulatory molecule, CD28 were expressed on the majority of intratumoral T cells, though there was a substantial diversity in the frequency of CD28+ CD8+ T cell within the Nivolumab-treated group. Previous studies shows that CD28+ T cell responds well to PD-1 therapy and that loss of CD28 on CD8 T cells is a marker for un-responsive patients

(52,53). Interestingly, we found that patients with higher frequency of CD8+ T cells expressing CD28 had seemingly longer PFS and OS after recurrence. This was only evident for Nivolumab treated patients and not controls (Supplementary Figure 9), why CD28 frequency among effector T cells could indicate a successful treatment. In addition, PD-1 acts primarily by inhibiting the co-stimulatory signal through CD28, rather than TCR signaling (54). We found that CD28 expression was significantly higher on intratumoral T cells following Nivolumab administration. Thus, it could be speculated whether Nivolumab treatment not only result in blocking of the inhibitory signaling, but also allow T cells to increase expression of CD28 and unleash co-stimulation. Co-stimulation and activation would lead to expansion and proliferation of tumor specific T cell clones, supported by higher frequency of Ki67+ intratumoral T cells within Nivolumab treated patients.

Even though we find an upregulation of activation and proliferation within intratumoral T cells following Nivolumab treatment, an anti-inflammatory TME appeared to be boosted, perhaps due to a wave of induced cytotoxic response caused by PD-1 blocking. Analysis of transcriptomic data showed an enrichment of the TGF-β pathway in the TME of Nivolumab treated patients. CD39 expression is known to be upregulated in the presence of TGF-β (49,55,56). In addition, CD39 have also been described to have a regulatory function, as it together with CD73 generates adenosine from ATP, which also contributes to an anti-inflammatory TME (57). Interestingly, PD-1 expression was measured in lower frequencies of intratumoral CD8+ T cells in Nivolumab-treated patients compared to controls. A similar effect of Nivolumab was detected in blood, with a decrease in the frequency of T cells expressing PD-1 after Nivolumab administration (Figure 4b and 4c). This could be due to endocytosis of the receptor after Nivolumab binding, as the case is for other receptors after engagement of their target(58,59), but it needs to be evaluated further. However, a compensatory upregulation of additional inhibitory checkpoint molecules, including LAG-3, TIM-3, CTLA-3 and TIGIT, were detected within intratumoral T cells following Nivolumab administration, and thus potentially contribute to drug resistance (60). In particular, TIGIT are expressed on a larger fraction of T cells, and could therefore be a relevant co-target as has previously been suggested (61,62). Altogether our results implies that Nivolumab have in fact reached the tumor tissue within approximately 7 days and have had an impact on T cell activation and their differentiation as well as an effect on the TME.

Next, we were able to detect tumor specific reactivity in REP TILs from 19% (3 out of 16) of Nivolumab treated patient. Interestingly, we found a clear difference in the TME landscape of patients with reactive TILs compared to the remaining Nivolumab treated patients based on transcriptomic data. Specifically,

we found a gene set enrichment of the pathway involved in antigen processing and presentation on MHC class I. This could indicate an ongoing presentation of potential immunogenic neoepitopes to T cells within the TME of these patients, providing a potential for CD8 T cell mediated cancer cell killing (63,64). We therefore examined the tumor specificity of the reactive TILs further, by screening PBMCs and TILs for the presence of neoantigen reactive CD8 T cells (NARTs). We were only able to detect NARTs in TILs from two patients which matched with the patients who showed the highest reactivity against tumor. Interestingly, the NARTs detected in these patients (NVB02 and NVB05) were specific to neoantigens found in both the primary and recurrent tumor, potentially representing clonal mutation. In fact, we detected three immunogenic neoepitopes from patient NVB05 arriving from a frameshift mutation in NF1. This frameshift mutation has previously been described to be related to high T cell infiltration in gliomas (65). Previously, the T cell infiltration and quality of neoantigens and thereby the potential to induce a potent tumor specific T cell response has also been correlated with longer survival for GBM patients (66). Our results supports this with a higher PFS and OS after recurrence for patients with tumor reactive TILs, compared to the remaining patients in the Nivolumab treated group, though it was not significant presumably due a small patient group. Additionally, the frequency of CD28 among intratumoral CD8 T cells were also seemingly higher for patients with tumor reactive TILs, supporting that CD28 expression can indicate successful Nivolumab therapy. Personalized neoantigen vaccines has therefore also been tested in order to induce and boost the NART repertoire in GBM patients also in patients with low mutational burden, but despite tumor infiltration of vaccine-induced NARTs, immune suppressive factors diminished the immune response(67,68). In line we found that expression of inhibitory molecule TIGIT and Treg cell where also detected in higher frequency among CD8+ and CD4+ T cells respectively, in the reactive patients, along with over expression of TGFB1. This supports the need for combination therapy to overcome such compensatory immune inhibition and improve treatment outcome for these patients.

Finally, an increasing number if observations suggests that the peripheral immune system play a role in the immunosurveillance of the brain (6–9). This is additionally supported by a study identifying GBM specific NARTs in blood (69). Similarly, we are also able to detect NARTs in blood from the patient with tumor reactive TILs. In fact, both the number and the sum of estimated frequency of the NARTs increased after Nivolumab treatment. In line, therapy targeting the PD-1/PD-L1 axis, like Nivolumab has previously been showed to boost the number NARTs in PBMC (42). Thus, the effect of Nivolumab in patients with an existing GBM reactive T cell response can also entail an increase in NARTs potentially due to epitope spreading after an induced cytotoxic tumor response.

In conclusion, we reported that Nivolumab can reached the TME of GBM patients. After only 7 days, an effect could be observed on both intratumoral T cell and in the gene expressing profile of the TME. We found that intratumoral T cells had both an increased activated and but also a differentiated phenotype, and the TME showed both indication of cytotoxic response, but also an immunosuppressive profile. Furthermore, we found tumor reactive TILs from three Nivolumab-treated patients, where NARTs were identified in samples from all three patient. These patients had longer PFS and OS and high frequencies of CD28+ CD8+ T cells, however anti-inflammatory factors were also induced. Importantly, NARTs could be detected in PBMC and appeared to be boosted in after Nivolumab administration. Altogether, to improve immunotherapies for GBM we need to consider the complexity of the tumor and the resistance mechanism induced after PD-1 blockade. It is likely that some patients will benefit from this treatment, why it is important to identify the characteristics associated to clinical responses, as well as offering selected patients a combination therapy to overcome the adaptable resistance mechanisms.

REFERENCES

1. Stupp R, Mason WP, van den Bent MJ, Weller M, Fisher B, Taphoorn MJB, et al. Radiotherapy plus Concomitant and Adjuvant Temozolomide for Glioblastoma. N Engl J Med. 2005;352(10):987–96.

2. Wen PY, Weller M, Lee EQ, Alexander BM, Barnholtz-Sloan JS, Barthel FP, et al. Glioblastoma in adults: a Society for Neuro-Oncology (SNO) and European Society of Neuro-Oncology (EANO) consensus review on current management and future directions. Neuro Oncol. 2020;22(8):1073.

3. Schalper KA, Rodriguez-Ruiz ME, Diez-Valle R, López-Janeiro A, Porciuncula A, Idoate MA, et al. Neoadjuvant nivolumab modifies the tumor immune microenvironment in resectable glioblastoma. Nat Med. 2019;25(3):470–6.

4. Arrieta VA, Chen AX, Kane JR, Kang SJ, Kassab C, Dmello C, et al. ERK1/2 phosphorylation predicts survival following anti-PD-1 immunotherapy in recurrent glioblastoma. Nat cancer. 2021;2(12):1372.

5. Medawar PB. Immunity to Homologous Grafted Skin. III. The Fate of Skin Homographs Transplanted to the Brain, to Subcutaneous Tissue, and to the Anterior Chamber of the Eye. Br J Exp Pathol. 1948;29(1):58.

6. Bartholomäus I, Kawakami N, Odoardi F, Schläger C, Miljkovic D, Ellwart JW, et al. Effector T cell interactions with meningeal vascular structures in nascent autoimmune CNS lesions. Nature. 2009;462(7269):94–8.

7. Louveau A, Smirnov I, Keyes TJ, Eccles JD, Rouhani SJ, Peske JD, et al. Structural and functional features of central nervous system lymphatic vessels. Nature. 2015;523(7560):337–41.

8. Aspelund A, Antila S, Proulx ST, Karlsen TV, Karaman S, Detmar M, et al. A dural lymphatic vascular system that drains brain interstitial fluid and macromolecules. J Exp Med. 2015;212(7):991–9.

9. das Neves SP, Delivanoglou N, Da Mesquita S. CNS-Draining Meningeal Lymphatic Vasculature: Roles, Conundrums and Future Challenges. Front Pharmacol. 2021;12.

10. Nayak L, Molinaro AM, Peters K, Clarke JL, Jordan JT, de Groot J, et al. Randomized Phase II and Biomarker Study of Pembrolizumab plus Bevacizumab versus Pembrolizumab Alone for Patients

with Recurrent Glioblastoma. Clin Cancer Res. 2021;27(4):1048–57.

11. Reardon DA, Kim TM, Frenel JS, Simonelli M, Lopez J, Subramaniam DS, et al. Treatment with pembrolizumab in programmed death ligand 1–positive recurrent glioblastoma: Results from the multicohort phase 1 KEYNOTE-028 trial. Cancer. 2021;127(10):1620–9.

12. Larkin J, Chiarion-Sileni V, Gonzalez R, Grob J-J, Rutkowski P, Lao CD, et al. Five-Year Survival with Combined Nivolumab and Ipilimumab in Advanced Melanoma. N Engl J Med. 2019;381(16):1535–46.

13. Pluim D, Ros W, van Bussel MTJ, Brandsma D, Beijnen JH, Schellens JHM. Enzyme linked immunosorbent assay for the quantification of nivolumab and pembrolizumab in human serum and cerebrospinal fluid. J Pharm Biomed Anal. 2019 Feb 5;164:128–34.

14. Liebner S, Fischmann A, Rascher G, Duffner F, Grote EH, Kalbacher H, et al. Claudin-1 and claudin-5 expression and tight junction morphology are altered in blood vessels of human glioblastoma multiforme. Acta Neuropathol. 2000;100(3):323–31.

15. Wolburg H, Wolburg-Buchholz K, Kraus J, Rascher-Eggstein G, Liebner S, Hamm S, et al. Localization of claudin-3 in tight junctions of the blood-brain barrier is selectively lost during experimental autoimmune encephalomyelitis and human glioblastoma multiforme. Acta Neuropathol. 2003;105(6):586–92.

16. Pointer KB, Clark PA, Schroeder AB, Salamat MS, Eliceiri KW, Kuo JS. Association of collagen architecture with glioblastoma patient survival. J Neurosurg. 2017;126(6):1812.

17. Reardon DA, Gokhale PC, Klein SR, Ligon KL, Rodig SJ, Ramkissoon SH, et al. Glioblastoma eradication following immune checkpoint blockade in an orthotopic, immunocompetent model. Cancer Immunol Res. 2016;4(2):124–35.

18. Park J, Kim CG, Shim JK, Kim JH, Lee H, Lee JE, et al. Effect of combined anti-PD-1 and temozolomide therapy in glioblastoma. Oncoimmunology. 2018;8(1).

19. Reardon DA, Brandes AA, Omuro A, Mulholland P, Lim M, Wick A, et al. Effect of Nivolumab vs Bevacizumab in Patients With Recurrent Glioblastoma: The CheckMate 143 Phase 3 Randomized Clinical Trial. JAMA Oncol. 2020;6(7):1003–10.

20. Donia M, Junker N, Ellebaek E, Andersen MH, Straten PT, Svane IM. Characterization and

comparison of “standard” and “young” tumour-infiltrating lymphocytes for adoptive cell therapy at a Danish translational research institution. Scand J Immunol. 2012;75(2):157–67.

21. Andersen R, Borch TH, Draghi A, Gokuldass A, Rana AHM, Pedersen M, et al. T cells isolated from patients with checkpoint inhibitor-resistant melanoma are functional and can mediate tumor regression. Ann Oncol. 2018;29(7):1575–81.

22. Draghi A, Chamberlain CA, Khan S, Papp K, Lauss M, Soraggi S, et al. Rapid Identification of the Tumor-Specific Reactive TIL Repertoire via Combined Detection of CD137, TNF, and IFNγ, Following Recognition of Autologous Tumor-Antigens. Front Immunol. 2021 Oct 11;12:4236.

23. Krueger F. Trim Galore [Internet]. 2019 [cited 2022 Feb 7]. Available from: https://github.com/FelixKrueger/TrimGalore

24. Martin M. Cutadapt removes adapter sequences from high-throughput sequencing reads. EMBnet.journal. 2011;17(1).

25. Andrews S. FastQC [Internet]. 2019 [cited 2022 Feb 7]. Available from: https://www.bioinformatics.babraham.ac.uk/ projects/fastqc

26. Lab P. Kallisto [Internet]. 2019 [cited 2022 Feb 9]. Available from: https://pachterlab.github.io/kallisto/

27. Consortium GR. Genome Reference Consortium Human Build 38 patch release 14 (GRCh38.p14) [Internet]. 2022 [cited 2022 Jul 4]. Available from: https://www.ncbi.nlm.nih.gov/assembly/GCF_000001405.40

28. Love MI, Huber W, Anders S. Moderated estimation of fold change and dispersion for RNA-seq data with DESeq2. Genome Biol. 2014;15(12).

29. Wu T, Hu E, Xu S, Chen M, Guo P, Dai Z, et al. clusterProfiler 4.0: A universal enrichment tool for interpreting omics data. Innov. 2021;2(3).

30. Gu Z, Eils R, Schlesner M. Complex heatmaps reveal patterns and correlations in multidimensional genomic data. Bioinformatics. 2016;32(18).

31. Yu G. Visualization of functional enrichment result. R package version 1.10.2. Mol Ther Nucleic Acids. 2021;

32. McKenna A, Hanna M, Banks E, Sivachenko A, Cibulskis K, Kernytsky A, et al. The Genome Analysis Toolkit: a MapReduce framework for analyzing next-generation DNA sequencing data. Genome Res. 2010;20.

33. Li H. Aligning sequence reads, clone sequences and assembly contigs with BWA-MEM. arXiv Prepr arXiv. 2013;

34. Cibulskis K, Lawrence MS, Carter SL, Sivachenko A, Jaffe D, Sougnez C, et al. Sensitive detection of somatic point mutations in impure and heterogeneous cancer samples. Nat Biotechnol. 2013;31(3).

35. Bjerregaard AM, Nielsen M, Hadrup SR, Szallasi Z, Eklund AC. MuPeXI: prediction of neo-epitopes from tumor sequencing data. Cancer Immunol Immunother. 2017 Sep 1;66(9):1123–30.

36. Reynisson B, Alvarez B, Paul S, Peters B, Nielsen M. NetMHCpan-4.1 and NetMHCIIpan-4.0: Improved predictions of MHC antigen presentation by concurrent motif deconvolution and integration of MS MHC eluted ligand data. Nucleic Acids Res. 2021;48(W1).

37. Weese D, Holtgrewe M, Reinert K. RazerS 3: Faster, fully sensitive read mapping. Bioinformatics. 2012;28(20).

38. Szolek A, Schubert B, Mohr C, Sturm M, Feldhahn M, Kohlbacher O. OptiType: precision HLA typing from next-generation sequencing data. Bioinformatics. 2014;30(23):3310.

39. Bentzen AK, Marquard AM, Lyngaa R, Saini SK, Ramskov S, Donia M, et al. Large-scale detection of antigen-specific T cells using peptide-MHC-I multimers labeled with DNA barcodes. Nat Biotechnol. 2016 Oct 1;34(10):1037–45.

40. Giunti D, Borsellino G, Benelli R, Marchese M, Capello E, Valle MT, et al. Phenotypic and functional analysis of T cells homing into the CSF of subjects with inflammatory diseases of the CNS. J Leukoc Biol. 2003;73(5):584–90.

41. Teleshova N, Pashenkov M, Huang YM, Söderström M, Kivisäkk P, Kostulas V, et al. Multiple sclerosis and optic neuritis: CCR5 and CXCR3 expressing T cells are augmented in blood and cerebrospinal fluid. J Neurol. 2002;249(6):723–9.

42. Holm JS, Funt SA, Borch A, Munk KK, Bjerregaard AM, Reading JL, et al. Neoantigen-specific CD8 T cell responses in the peripheral blood following PD-L1 blockade might predict therapy outcome

in metastatic urothelial carcinoma. Nat Commun. 2022;13(1).

43. Osa A, Uenami T, Koyama S, Fujimoto K, Okuzaki D, Takimoto T, et al. Clinical implications of monitoring nivolumab immunokinetics in non–small cell lung cancer patients. JCI Insight. 2018;3(19).

44. Wolfl M, Kuball J, Ho WY, Nguyen H, Manley TJ, Bleakley M, et al. Activation-induced expression of CD137 permits detection, isolation, and expansion of the full repertoire of CD8+ T cells responding to antigen without requiring knowledge of epitope specificities. Blood. 2007;110(1):201–10.

45. Chow A, Uddin FZ, Liu M, Dobrin A, Nabet BY, Mangarin L, et al. The ectonucleotidase CD39 identifies tumor-reactive CD8+ T cells predictive of immune checkpoint blockade efficacy in human lung cancer. Immunity. 2023;56(1):93–106.

46. Kverneland AH, Chamberlain CA, Borch TH, Nielsen M, Mørk SK, Kjeldsen JW, et al. Adoptive cell therapy with tumor-infiltrating lymphocytes supported by checkpoint inhibition across multiple solid cancer types. J Immunother Cancer. 2021;9(10):3499.

47. Krishna S, Lowery FJ, Copeland AR, Bahadiroglu E, Mukherjee R, Jia L, et al. Stem-like CD8 T cells mediate response of adoptive cell immunotherapy against human cancer. Science (80-). 2020;370(6522):1328.

48. Kortekaas KE, Santegoets SJ, Sturm G, Ehsan I, van Egmond SL, Finotello F, et al. CD39 identifies the CD4+ tumor-specific T-cell population in human cancer. Cancer Immunol Res. 2020;8(10):1311–21.

49. Duhen T, Duhen R, Montler R, Moses J, Moudgil T, De Miranda NF, et al. Co-expression of CD39 and CD103 identifies tumor-reactive CD8 T cells in human solid tumors. Nat Commun. 2018;9(1):1–13.

50. Voskoboinik I, Smyth MJ, Trapani JA. Perforin-mediated target-cell death and immune homeostasis. Vol. 6, Nature Reviews Immunology. 2006.

51. Zheng C, Zheng L, Yoo JK, Guo H, Zhang Y, Guo X, et al. Landscape of Infiltrating T Cells in Liver Cancer Revealed by Single-Cell Sequencing. Cell. 2017;169(7).

52. Kim KH, Kim HK, Kim HD, Kim CG, Lee H, Han JW, et al. PD-1 blockade-unresponsive human

tumor-infiltrating CD8+ T cells are marked by loss of CD28 expression and rescued by IL-15. Cell Mol Immunol. 2021;18(2).

53. Kamphorst AO, Wieland A, Nasti T, Yang S, Zhang R, Barber DL, et al. Rescue of exhausted CD8 T cells by PD-1 targeted therapies is CD28-dependent. Science (80-). 2017;355(6332):1423.

54. Hui E, Cheung J, Zhu J, Su X, Taylor MJ, Wallweber HA, et al. T cell costimulatory receptor CD28 is a primary target for PD-1-mediated inhibition. Science (80-). 2017;355(6332):1428–33.

55. Baghbani E, Noorolyai S, Shanehbandi D, Mokhtarzadeh A, Aghebati-Maleki L, Shahgoli VK, et al. Regulation of immune responses through CD39 and CD73 in cancer: Novel checkpoints. Life Sci. 2021;282:119826.

56. Peres RS, Donate PB, Talbot J, Cecilio NT, Lobo PR, Machado CC, et al. TGF-β signalling defect is linked to low CD39 expression on regulatory T cells and methotrexate resistance in rheumatoid arthritis. J Autoimmun. 2018;90.

57. Arab S, Hadjati J. Adenosine blockage in tumor microenvironment and improvement of cancer immunotherapy. Immune Netw. 2019;19(4).

58. Cendrowski J, Mamińska A, Miaczynska M. Endocytic regulation of cytokine receptor signaling. Cytokine Growth Factor Rev. 2016;32:63–73.

59. Saad E Ben, Oroya A, Rudd CE. Abstract 6528: Anti-PD-1 induces the endocytosis of the co-receptor from the surface of T-cells: Nivolumab is more effective than Pembrolizumab. Cancer Res. 2020;80(16_Supplement).

60. Jenkins RW, Barbie DA, Flaherty KT. Mechanisms of resistance to immune checkpoint inhibitors. Br J Cancer. 2018;118(1).

61. Hung AL, Maxwell R, Theodros D, Belcaid Z, Mathios D, Luksik AS, et al. TIGIT and PD-1 dual checkpoint blockade enhances antitumor immunity and survival in GBM. Oncoimmunology. 2018;7(8).

62. Raphael I, Kumar R, McCarl LH, Shoger K, Wang L, Sandlesh P, et al. TIGIT and PD-1 Immune Checkpoint Pathways Are Associated With Patient Outcome and Anti-Tumor Immunity in Glioblastoma. Front Immunol. 2021;12.

63. Dhatchinamoorthy K, Colbert JD, Rock KL. Cancer Immune Evasion Through Loss of MHC Class I

Antigen Presentation. Front Immunol. 2021;12.

64. Lee MY, Jeon JW, Sievers C, Allen CT. Antigen processing and presentation in cancer immunotherapy. J Immunother cancer. 2020;8(2).

65. Lobbous M, Bernstock JD, Coffee E, Friedman GK, Metrock LK, Chagoya G, et al. An update on neurofibromatosis type 1-associated gliomas. Cancers (Basel). 2020;12(1).

66. Zhang J, Caruso FP, Sa JK, Justesen S, Nam DH, Sims P, et al. The combination of neoantigen quality and T lymphocyte infiltrates identifies glioblastomas with the longest survival. Commun Biol. 2019;2(1).

67. Hilf N, Kuttruff-Coqui S, Frenzel K, Bukur V, Stevanović S, Gouttefangeas C, et al. Actively personalized vaccination trial for newly diagnosed glioblastoma. Nature. 2019;565(7738).

68. Keskin DB, Anandappa AJ, Sun J, Tirosh I, Mathewson ND, Li S, et al. Neoantigen vaccine generates intratumoral T cell responses in phase Ib glioblastoma trial. Nature. 2019;565(7738).

69. Leko V, Cafri G, Yossef R, Paria B, Hill V, Gurusamy D, et al. Identification of neoantigen-reactive T lymphocytes in the peripheral blood of a patient with glioblastoma. J Immunother Cancer. 2021;9(7).

SUPPLEMENTARY MATERIAL

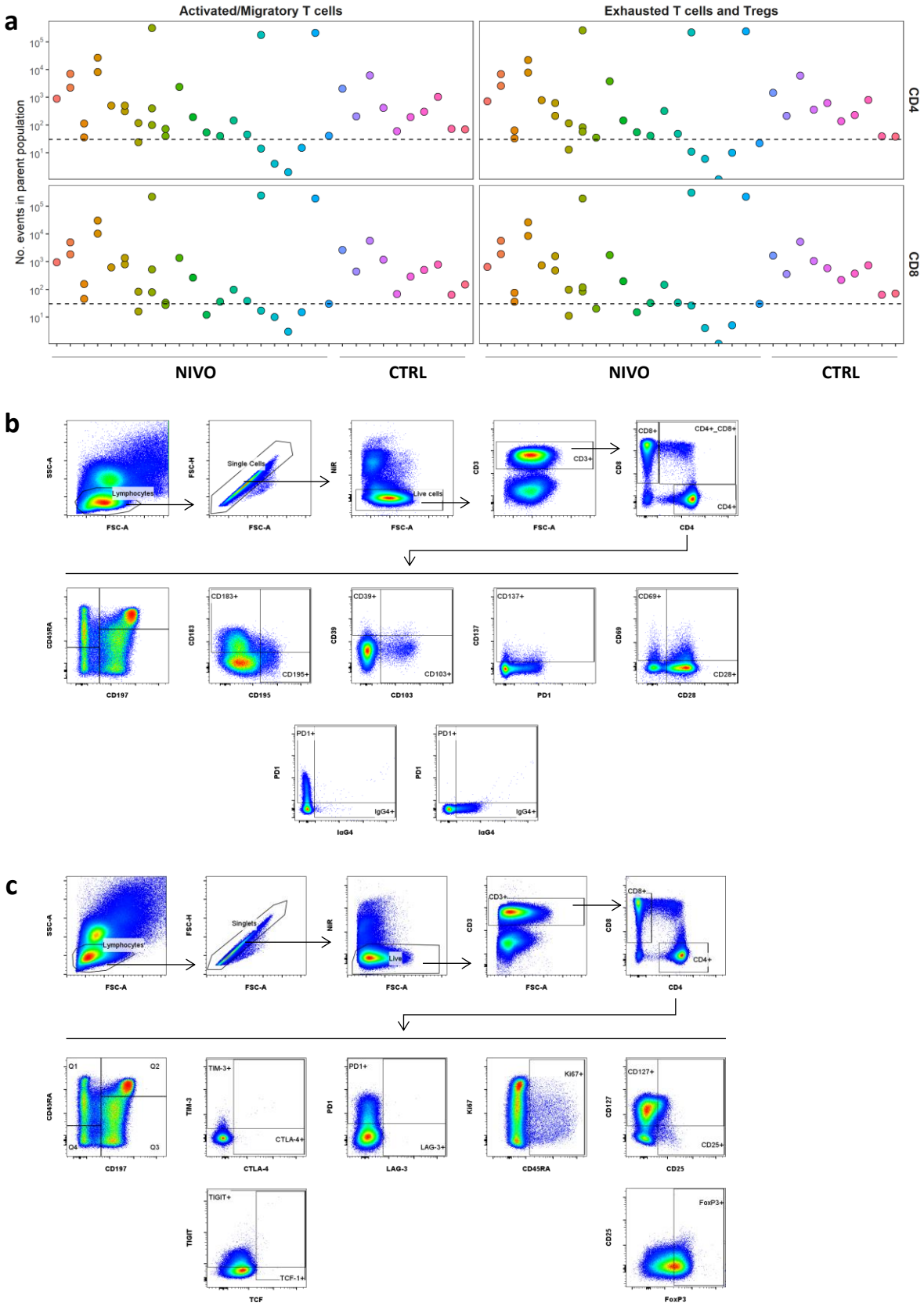

Supplementary Figure 1 | Flow cytometry analysis. a) Number of events of the parent (CD4 and CD8) population in tumor digest from NIVO and control patients. The horizontal line indicates cut-off value of 30 events. Parent population with < 30 events was not included in the analysis of flow cytometry data. Tumor digest was analysed with two flow cytometry panels ("Activated/Migratory T cells" and "Exhausted T cells and Tregs") **b)** Gating strategy for peripheral blood mononuclear cells (PBMCs) and tumor digest analysed with Panel A, "Activated/Migratory T cells" and **c)** Panel B, "Exhausted T cells and Tregs". b) and c) shows representative plots for gated PBMCs.

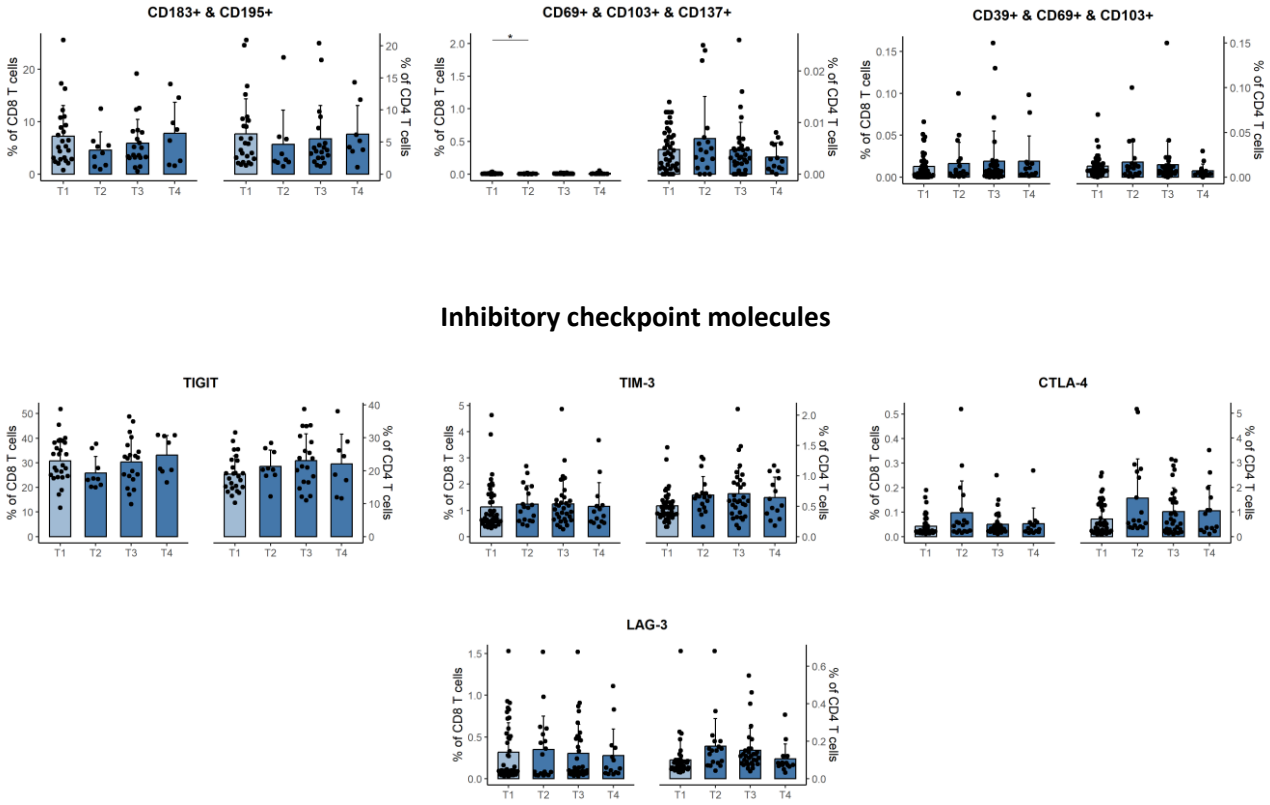

Supplementary Figure 2 | CNS homing - and activation markers and inhibitory checkpoint molecules on PBMC derived T cells. Frequency of CD8+ and CD4+T cells expressing various markers and molecules in blood samples from T1 (Day 0), T2 (3 weeks), T3 (8 weeks) and T4 (16 weeks).

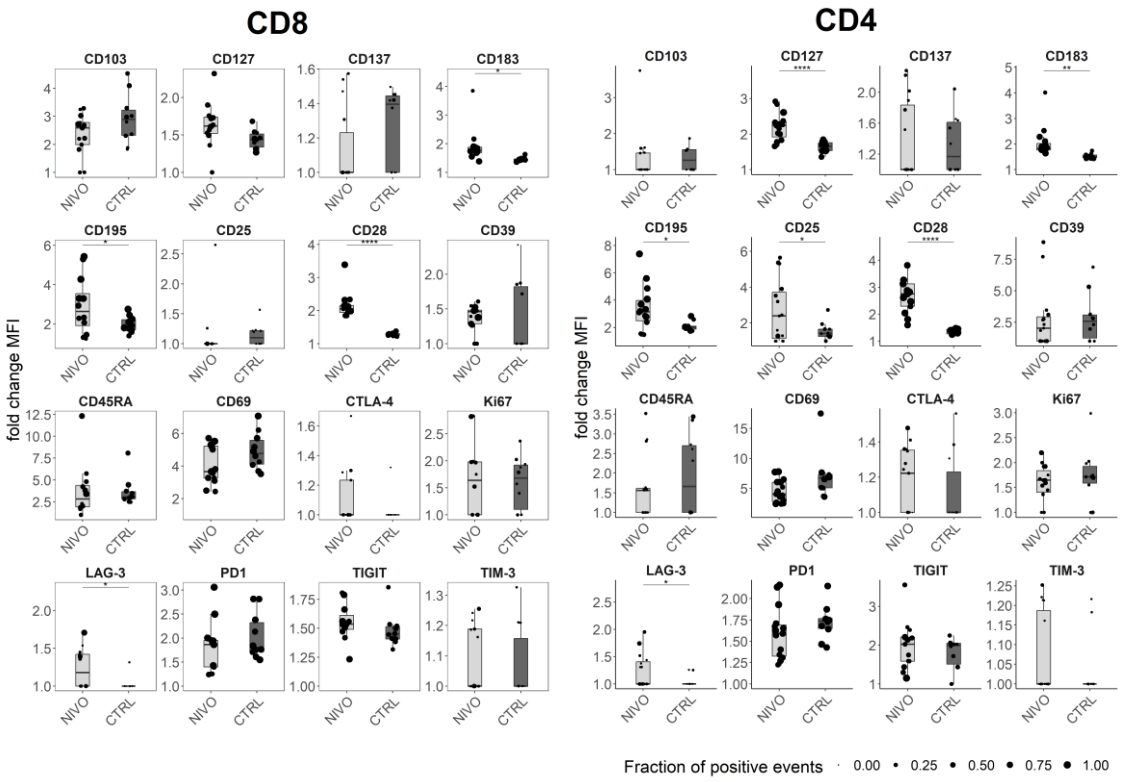

Supplementary Figure 3| Fold change of median fluorescent intensity (MFI) of all investigated markers. MFI fold change for all investigated markers expressed intratumoral CD8+ and CD4 T cells for Nivolumab-treated patients. Means were compared between NIVO and CTRL (Tumor) using unpaired t-test . * = p<0.05, ** = p<0.01, *** = p<0.001, **** = p<0.0001.

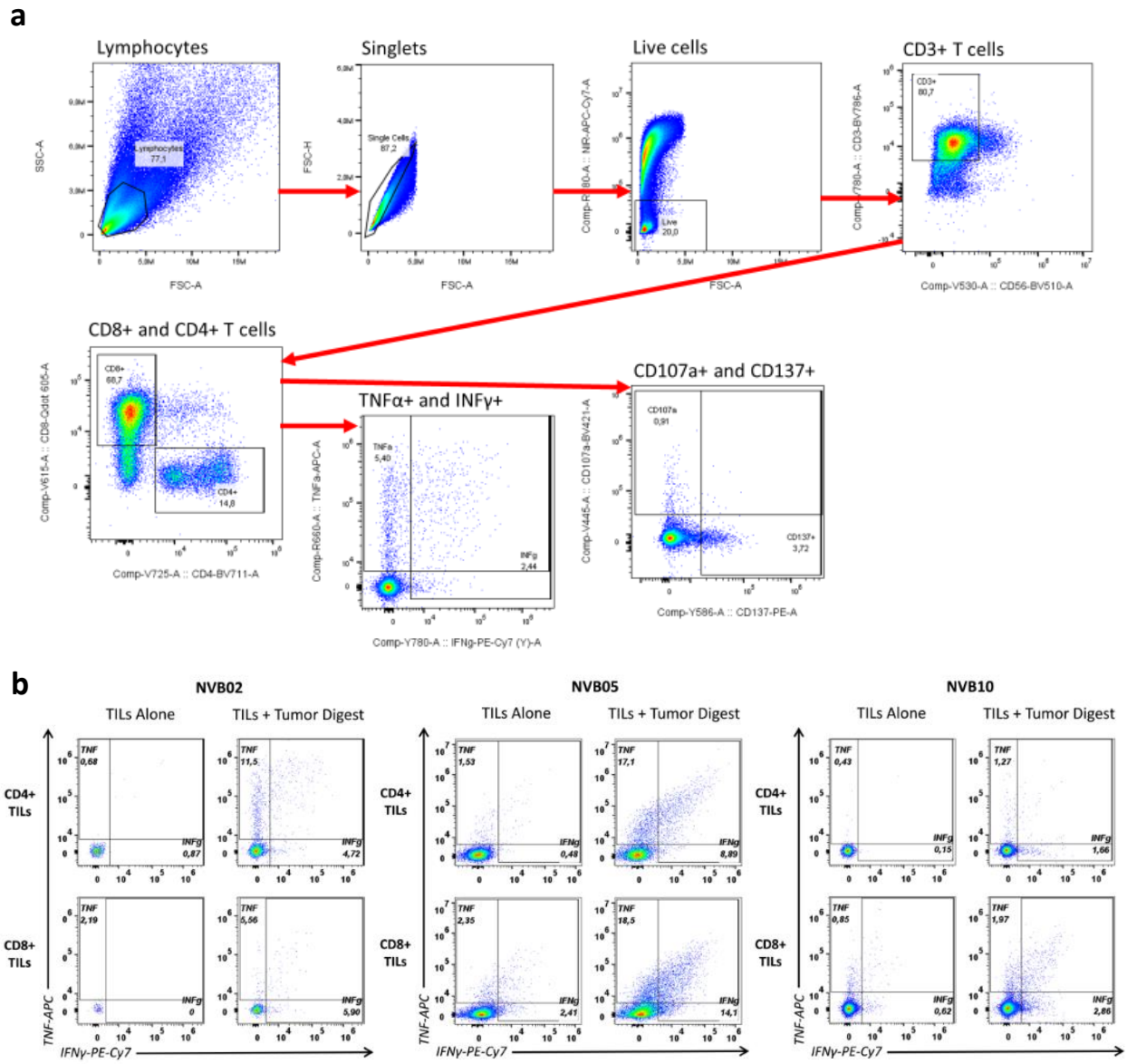

Supplementary Figure 4 | Gating strategy for T cell reactivity assay. TILs where co-cultured with autologous tumor digest for 8 hours and hereafter intracellularly stained for TFN-α, IFN-γ, CD137 and CD107a. **a)** Gating strategy of TILs in the reactivity assay. **b)** flow cytometry dotplot for patient with tumpor specific reactive TILs, showing TFN-α and IFN-γ expression in CD4+ and CD8+ T cells after co-culture with autologous tumor digest or TILs alone.

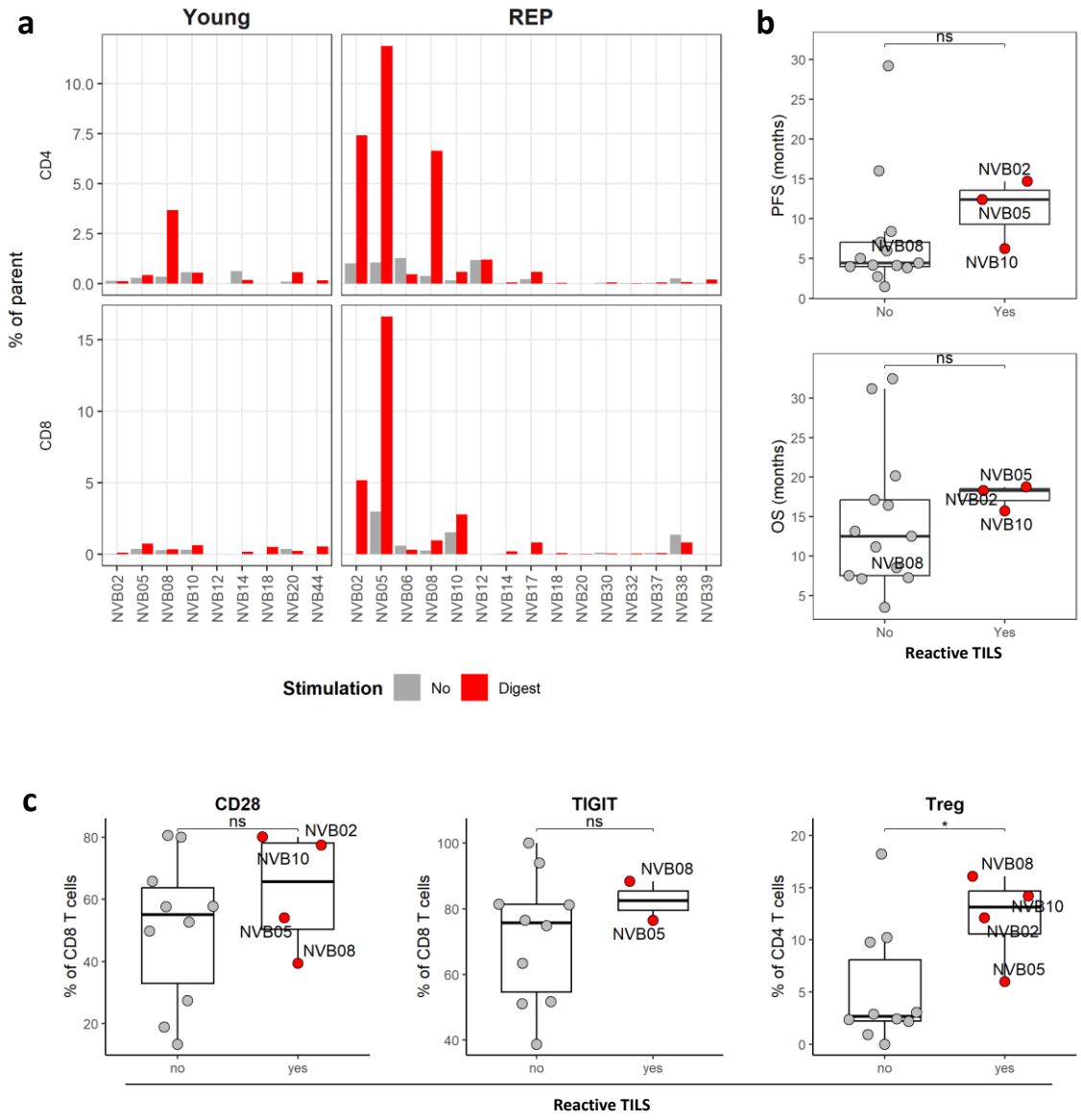

Supplementary Figure 5| Tumor reactive TILs. a) Raw frequency of tumor reactive TILs; reactivity in Young TILs (YTILs) and REP TILs including background reactivity (TILs alone, grey) and co-cultures with tumor digest (red) for all tested patients. **b)** Progression free survival (PFS) and overall survival (OS) in a recurrent setting stratified in reactive (Yes) and non-reactive (No) patients within the Nivolumab-treated (NIVO) patient group. **c)** Frequency of intratumoral CD8+ T cells expressing CD28 and TIGIT, and frequency of Treg cell among CD4 T cells stratified in reactive and non-reactive patient within the NIVO patient group. Means were compared between patients with reactive and non-reactive TILs using unpaired t-test . * = p<0.05, ** = p<0.01, *** = p<0.001, **** = p<0.0001.

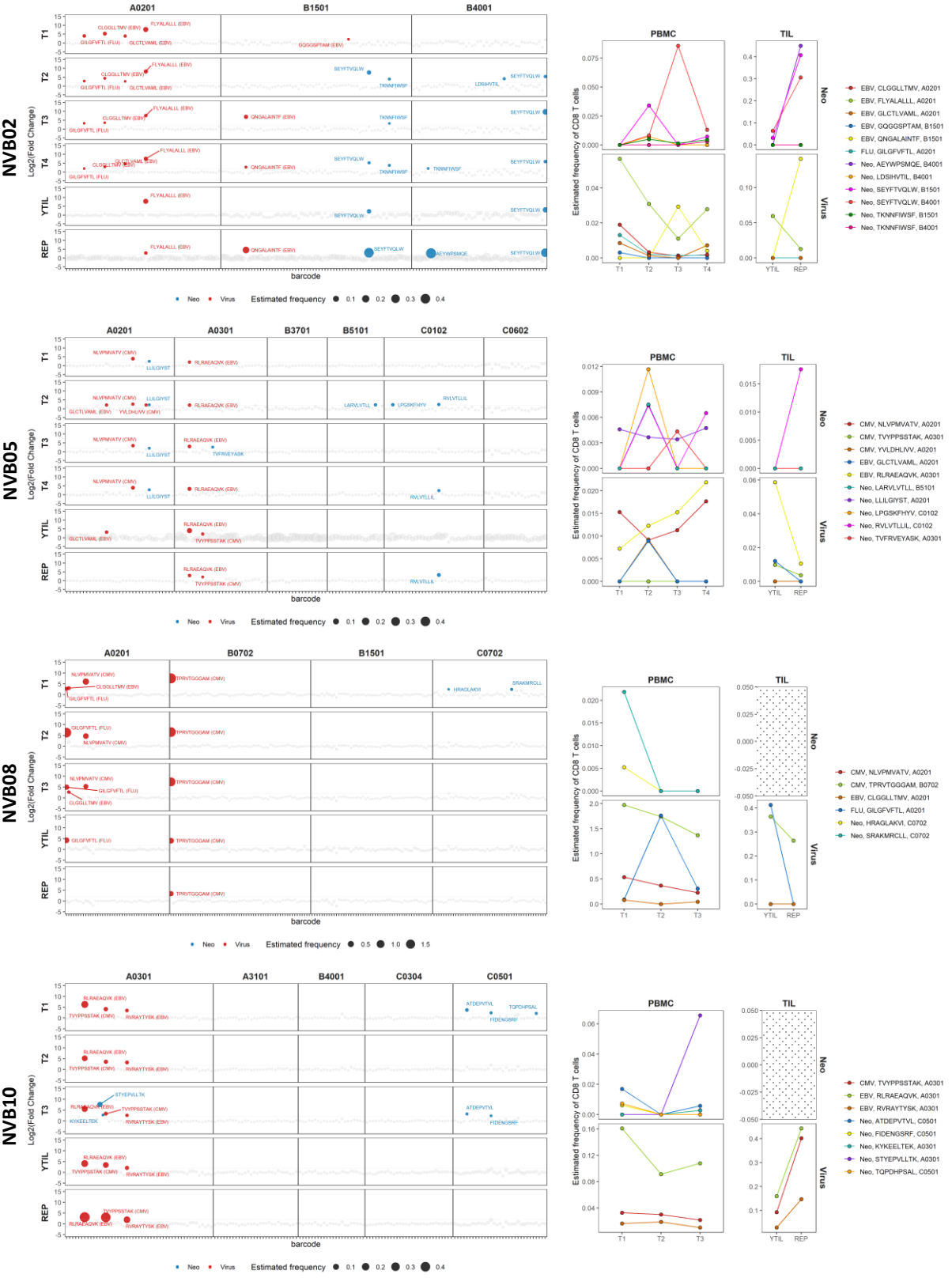
NVB02
A0201
B1501
B4001
T1
T2
T3
T4
YTIL
REP
Log2(Fold Change)
barcode
Neo
Virus
Estimated frequency
PBMC
TIL
Estimated frequency of CD8 T cells
Neo
Virus
EBV, CLGGLLTMV, A0201
EBV, FLYALALLL, A0201
EBV, GLCTLVAML, A0201
EBV, GQGGSPTAM, B1501
EBV, QNGALAINTF, B1501
FLU, GILGFVFTL, A0201
Neo, AEYWPSMQE, B4001
Neo, LDSIHVTIL, B4001
Neo, SEYFTVQLW, B1501
Neo, SEYFTVQLW, B4001
Neo, TKNNFIWSF, B1501
Neo, TKNNFIWSF, B4001
NVB05
A0201
A0301
B3701
B5101
C0102
C0602
CMV, NLVPMVATV, A0201
CMV, TVYPPSSTAK, A0301
CMV, YVLDHLIVV, A0201
EBV, GLCTLVAML, A0201
EBV, RLRAEAQVK, A0301
Neo, LARVLVTLL, B5101
Neo, LLILGIYST, A0201
Neo, LPGSKFHYV, C0102
Neo, RVLVTLLIL, C0102
Neo, TVFRVEYASK, A0301
NVB08
A0201
B0702
B1501
C0702
CMV, NLVPMVATV, A0201
CMV, TPRVTGGGAM, B0702
EBV, CLGGLLTMV, A0201
FLU, GILGFVFTL, A0201
Neo, HRAGLAKVI, C0702
Neo, SRAKMRCLL, C0702
NVB10
A0301
A3101
B4001
C0304
C0501
CMV, TVYPPSSTAK, A0301
EBV, RLRAEAQVK, A0301
EBV, RVRAYTYSK, A0301
Neo, ATDEPVTVL, C0501
Neo, FIDENGSRF, C0501
Neo, KYKEELTEK, A0301
Neo, STYEPVLLTK, A0301
Neo, TQPDHPSAL, C0501

Supplementary Figure 6 | detection of NARTs in YTILs, REP TILs and ex vivo PBMCs. Screening output for all patients with reactive TILs. Significantly enriched ($p < 0.001$, Log2 fold change > 2) enriched barcoded pMHC multimers are colored and labelled with the immunogenic peptide sequence. Virus antigens are marked in red and neoantigens are marked in blue. The dot size represents an estimated frequency of CD8+ T cells for each NART. Grey dots are all pMHC multimers that where not significantly enriched after sample staining. Specificities are shown for each blood sample time point; T1 (Day 0), T2 (3 weeks), T3 (8 weeks), T4 (16 weeks), and for YTIL (young TILs) and REP TILs. The screened pMHC are additionally divided based on HLA type. (left). The estimate frequency is shown for each specificity in PBMCs and TILs (right).

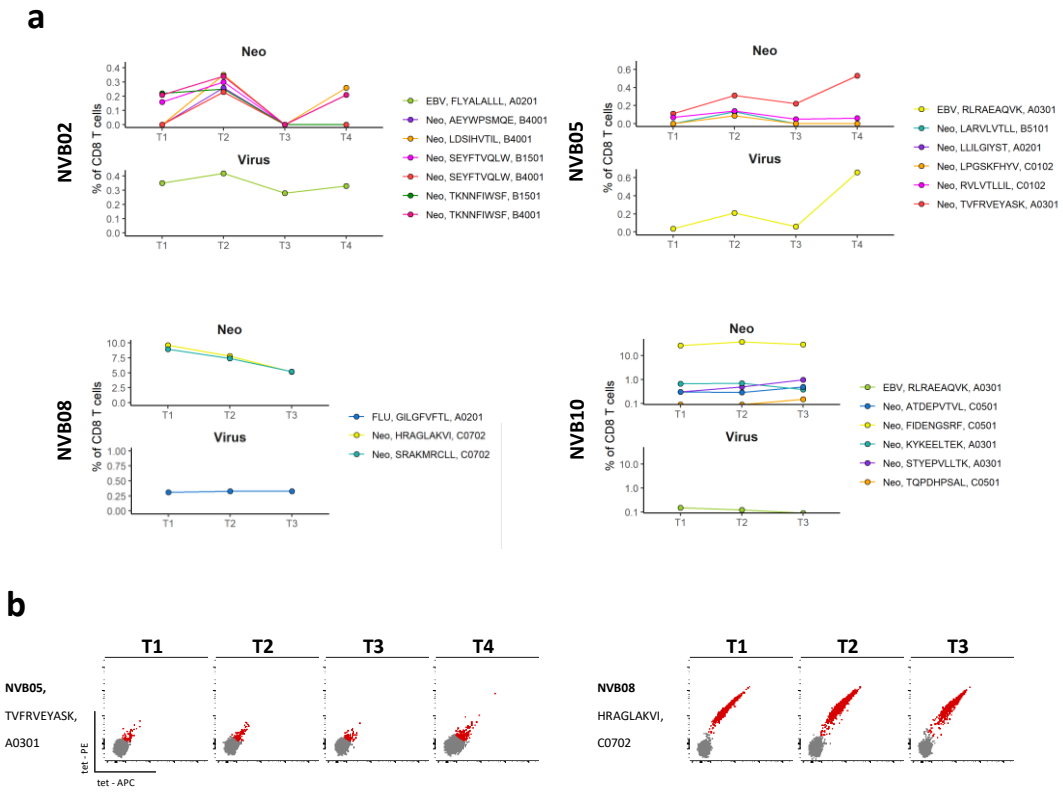

Supplementary Figure 7 | verification of detected NARTs. PBMCs were expanded with a pool of the detected immunogenic peptides over 14 days. Expanded PBMCs were hereafter stained with pMHC tetramers specific for the immunogenic peptides. **a)** Frequencies of expanded NART within CD8+ T cells from expanded PBMCs deriving from the blood sample time points, T1, T2, T3 and T4. **b)** Representative plots for expanded NARTs from patient NVB05 and NVB08.

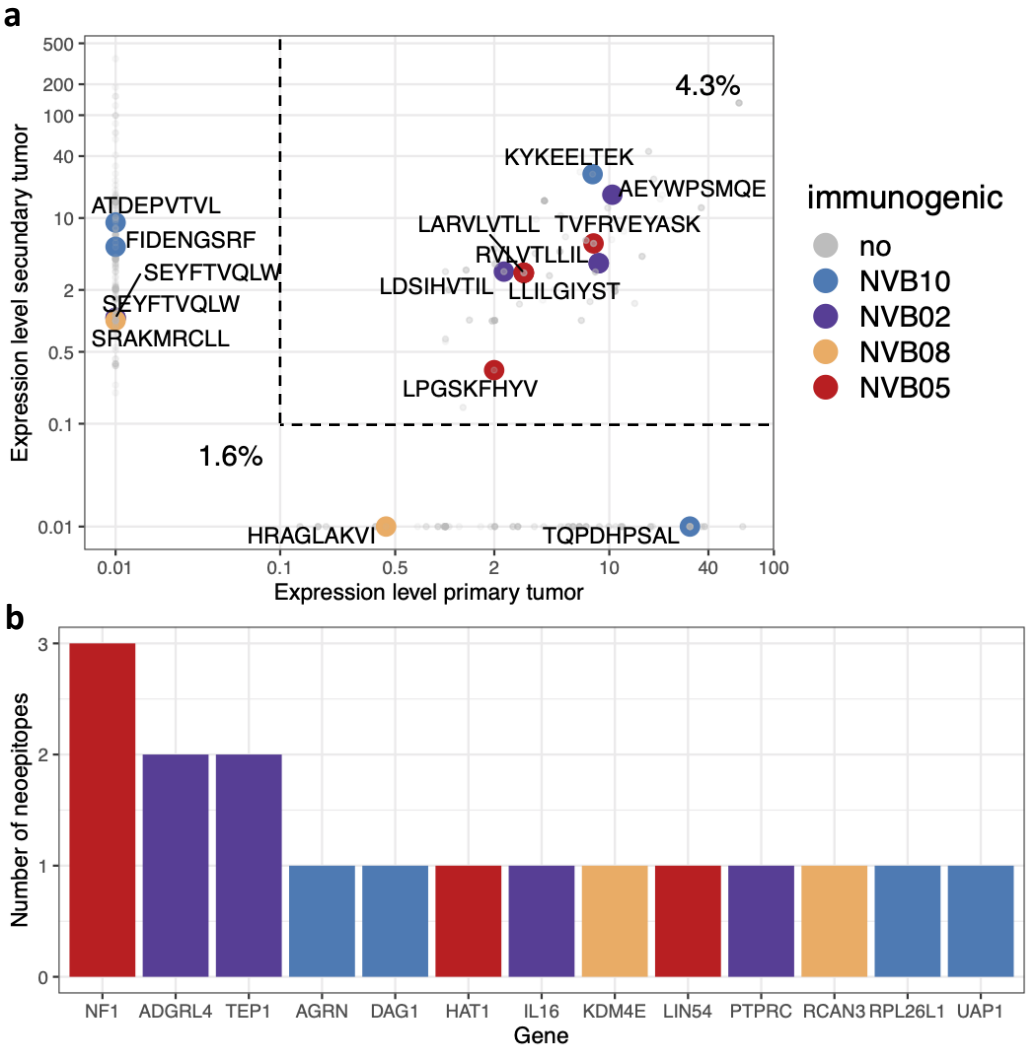

Supplementary Figure 8 | Immunogenic vs. non-immunogenic neoepitopes. a) Expression level of the mutation found in primary vs. secondary tumor. 4.3 % of the peptides which are found in both primary and secondary tumors are found immunogenic, whereas only 1.6 % of peptide found in only one of the tumor samples are found immunogenic. This is borderline significant (p=0.6) with a proportion z-test. Grey dots represents screened non-immunogenic peptides and the colored dotes represents immunogenic peptides **b)** The number of immunogenic neoepitopes and the gene the mutation is found in.

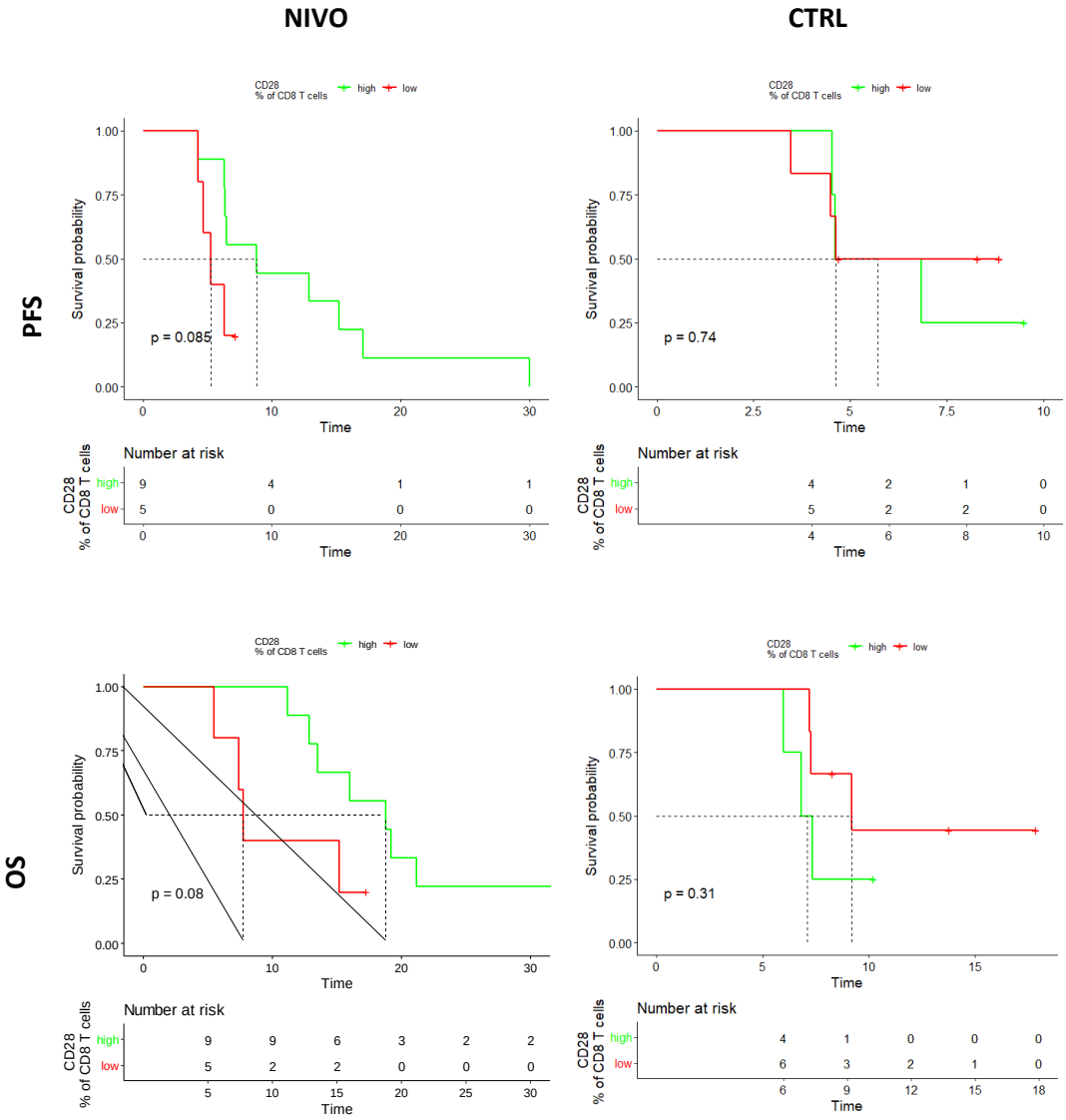

Supplementary Figure 9 | Progression free survival and overall survival related to frequency of CD8+ T cells expressing CD28. Kaplan-Meier curve of progression free survival (PFS) and overall survival (OS) in the recurrent setting for patients with high and low frequency of intratumoral CD8+ T cells expressing CD28 within both Nivolumab-treated (NIVO) and control (CTRL) patients.

Supplementary Table 1 | Flow cytometry staining panels

Marker	Flourochrome	Clone	Dilution	Company	Type
Panel A: Activated T cells					
CD3	FITC	SK7	1:10	BD Biosciences	Surface
CD4	BUV395	M-T477	1:320	BD Biosciences	Surface
CD8	BV480	RPA-T8	1:80	BD Biosciences	Surface
CD28	BUV737	CD28.2	1:80	BD Biosciences	Surface
CD39	BV786	TU66	1:40	BD Biosciences	Surface
CD45RA	BV421	HI100	1:160	BD Biosciences	Surface
CD69	PE-Cy7	L78	1:40	BD Biosciences	Surface
CD103	PerCP eFlour710	Ber-ACT8	1:20	Invitrogen	Surface
CD137	PE-Cy5	4B4-1	1:40	BD Biosciences	Surface
CD183 (CXCR3)	BV711	G025H7	1:40	Biolegend	Surface
CD197 (CCR7)	APC	G043H7	1:20	Biolegend	Surface
CD279 (PD1)	PE-CF594	EH12.1	1:80	BD Biosciences	Surface
IgG4	PE	HP6025	1:40	SouthernBiotech	Surface
CD195(CCR5)	BV650	3A9	1:40	BD Biosciences	Surface
Live	NiR		1:1000	Invitrogen	Surface
Panel B: Exhausted T cells and Tregs					
CD3	FITC	SK7	1:10	BD Biosciences	Surface
CD4	BUV395	M-T477	1:320	BD Biosciences	Surface
CD8	BV480	RPA-T8	1:80	BD Biosciences	Surface
CD25	BV711	BC96	1:40	Biolegend	Surface
CD45RA	BV421	HI100	1:160	BD Biosciences	Surface
CD127	APC-R700	HIL-7R-M21	1:40	BD Biosciences	Surface
CD152 (CTLA-4)	PE-Cy5	BNI3	1:20	BD Biosciences	Surface
CD197 (CCR7)	APC	G043H7	1:20	Biolegend	Surface
CD223 (LAG-3)	BV650	11C3C65	1:160	Biolegend	Surface
CD279 (PD1)	PE-CF594	EH12.1	1:80	BD Biosciences	Surface
CD366 (TIM-3)	PE-Cy7	F38-2E2	1:80	Biolegend	Surface
FoxP3	PE	259D/C7	1:10	BD Biosciences	IC
Ki67	BV786	B56	1:40	BD Biosciences	IC
TIGIT	BV605	A15153G	1:20	Biolegend	Surface
Live	NiR		1:1000		Surface
Panel C: Multicytokines Intracellular Staining Panel					
CD3	FITC	SK7	1:10	BD Biosciences	Surface
CD4	BUV395	M-T477	1:320	BD Biosciences	Surface
CD8	BV480	RPA-T8	1:80	BD Biosciences	Surface
TNF-α	PE-Cy7	MAb11	1:20	Biolegend	IC
IFN-γ	APC	25723.11	1:20	BD Biosciences	IC
CD137 (4-1BB)	BUV737	4B4-1	01:40	BD Biosciences	IC
Live	NiR		1:1000		Surface
Panel C: Multicytokines Intracellular Staining Panel					
CD137	PE	4B4-1		BD Biosciences	IC
IFNγ	PE-Cy7	B27		BD Biosciences	IC
TNF	APC	MAb11		BD Biosciences	IC
Live	APC-Cy7	None		Thermo Fisher Scientific	Surface
CD107a	BV421	H4A3		BD Biosciences	IC
CD56	BV510	NCAM16.2		BD Biosciences	Surface
CD8	Qdot 605	3B5		Thermo Fisher Scientific	Surface
CD4	BV711	SK3		BD Biosciences	Surface
CD3	BV786	SK7		BD Biosciences	Surface

Supplementary Table 2 | Tissue overview

Pseudonym	**Tumor digest (single cell suspension)**	**Young TILs[1]**	**REP TILs[1]**	**Tumor cell line**
NVB02	x	x	x	Not available
NVB05	x	x	x	X
NVB06	x	x	x	Failed
NVB08	x	x	x	Not available
NVB10	x	x	x	Not available
NVB12	x	x	x	Not available
NVB14	x	x	x	Failed
NVB17	x	Not available	x	Not available
NVB18	x	x	x	Not available
NVB20	x	x	X	Not available
NVB22	x	x	Failed	Not available
NVB26	x	x	Not possible[2]	Failed
NVB30	x	Not possible[2]	x	Not available
NVB32	x	X	x	Not available
NVB33	Not available	Not possible[2]	Not possible[2]	Not available
NVB35	x	x	Failed	Not available
NVB37	x	Not possible[2]	x	Not available
NVB38	x	Failed	x	Not available
NVB39	x	x	x	Not available
NVB44	x	x	x	Not available
K_01	X	X	X	Not available
K_02	X	X	X	Not available
K_03	X	X	X	Not available
K_04	X	X	X	Not available
K_05	X	X	X	Not available
K_06	X	X	X	Not available
K_07	X	X	X	Not available
K_08	X	X	X	Not available
K_09	X	Failed[2]	X	Not available
K_10	x	Failed[2]	X	Not available

Manuscript II

Dose Escalation study of a Personalized Peptide-based Neoantigen Vaccine (EVX-01) in Patients with Metastatic Melanoma.

Signe Koggersbøl Skadborg[2*], Sofie Kirial Mørk[1*], Benedetta Albieri[1] ,Arianna Draghi[1], Marie Christine Wulff Westergaard[1], Joachim Stoltenborg Granhøj[1], Mohammad Kadivar[2], Annie Borch[2], Nana Overgaard[2], Anders Bundgård Sørensen[3], Ida Svahn Rasmussen[4], Lars Vibe Andreasen[4], Christina Westmose Yde[5], Nis Nørgaard[6], Torben Lorentzen[7], Thomas Trolle[3], Christian Garde[3], Jens Friis-Nielsen[3], Dennis Christensen[4], Jens Vindahl Kringelum[3], Marco Donia[1], Sine Reker Hadrup[2], Inge Marie Svane[1]

* These authors contributed equally

1 National Center for Cancer Immune Therapy (CCIT-DK), Department of Oncology, Copenhagen University Hospital, Herlev, Denmark

2 Technical University of Denmark – DTU, HEALTH TECH, Department of Health Technology, Lyngby, Denmark

3 Evaxion Biotech A/S, Denmark

4 Center for Vaccine Research, Statens Serum Institut, Copenhagen, Denmark

5 Genomic Medicine Rigshospitalet, Copenhagen, Denmark

6 Department of Urology, Copenhagen University Hospital, Herlev, Denmark

7 Department of gastroenterology, Gastroenheden, Copenhagen University Hospital, Herlev, Denmark

Dose Escalation study of a Personalized Peptide-based Neoantigen Vaccine (EVX-01) in Patients with Metastatic Melanoma.

Authors: Signe Koggersbøl Skadborg[2*], Sofie Kirial Mørk[1*], Benedetta Albieri[1] ,Arianna Draghi[1], Marie Christine Wulff Westergaard[1], Joachim Stoltenborg Granhøj[1], Mohammad Kadivar[2], Annie Borch[2], Nana Overgaard[2], Anders Bundgård Sørensen[3], Ida Svahn Rasmussen[4], Lars Vibe Andreasen[4], Christina Westmose Yde[5], Nis Nørgaard[6], Torben Lorentzen[7], Thomas Trolle[3], Christian Garde[3], Jens Friis-Nielsen[3], Dennis Christensen[4], Jens Vindahl Kringelum[3], Marco Donia[1], Sine Reker Hadrup[2], Inge Marie Svane[1]

* These authors contributed equally

Affiliations: [1]National Center for Cancer Immune Therapy (CCIT-DK), Department of Oncology, Copenhagen University Hospital, Herlev, Denmark; [2]Technical University of Denmark – DTU, HEALTH TECH, Department of Health Technology, Lyngby, Denmark; [3]Evaxion Biotech A/S, Denmark; [4]Center for Vaccine Research, Statens Serum Institut, Copenhagen, Denmark, [5]Genomic Medicine Rigshospitalet, Copenhagen, Denmark, [6]Department of Urology, Copenhagen University Hospital, Herlev, Denmark, [7]Department of gastroenterology, Gastroenheden, Copenhagen University Hospital, Herlev, Denmark.

Correspondence addressed to: Inge Marie Svane, National Center for Cancer Immune Therapy (CCIT-DK), Copenhagen University Hospital, Borgmester Ib Juuls Vej 25C, 5th floor, 2730, Herlev, Denmark, phone: +4538682131, fax: +4538683457, email: Inge.Marie.Svane@regionh.dk

Keywords: personalized therapy, neoantigen, immune response, cancer vaccine, immunotherapy

Conflicts of interest: Marco Donia has received honoraria for lectures from Roche and Novartis (past two years). Inge Marie Svane has received honoraria for lectures and consultancies from Novartis, Roche, MSD, BMS and Pierre Fabre. CCIT-DK has been granted economic support for personal wages from Evaxion Biotech A/S, Denmark. SRH is cofounder of PokeACell and is the co-inventor of several licensed patents. TT, ABS, CG, JFN, and JVK are employees of Evaxion Biotech A/S and have a financial interest in the company. All other authors have declared that they have no conflict of interest.

ABSTRACT

Background

Neoantigens originate from mutations in cancer cells, and several studies have demonstrated that they can potentially serve as targets to T cell-mediated anti-tumor-immunity via personalized neopeptide vaccines. The personalized peptide-based neoantigen vaccine, EVX-01, combined with the novel adjuvant, CAF®09b, has previously been published to be safe and able to elicit EVX-01-specific T cell responses in patients with metastatic melanoma. Additional dose-escalation studies were carried out to further evaluate the feasibility of increased vaccine dosages (NCT03715985).

Methods

Patients with metastatic melanoma on anti-PD1 (pembrolizumab) therapy were treated in two additional cohorts with increasing (two-fold and four-fold) vaccine dosage. Tumor-derived neoantigen encoding peptides were selected by the AI platform PIONEER™ and used in personalized therapeutic cancer vaccines, EVX-01. Vaccines were administered every second week for a total of 6 vaccinations (three intraperitoneal and three intramuscular). The primary endpoint was safety. Additional endpoints included immunological and objective responses.

Results

No additional vaccine related severe adverse events (AE) were observed during dose escalation of EVX-01 in combination with pembrolizumab 2 mg/kg, q3w. Two patients at the third dose level developed grade 3 toxicity most likely related to pembrolizumab. 8 out of 12 patients had objective response (6 PR and 2 CR) overall in the trial, including all four patients at the highest dose level. EVX-01 elicited increased peptide-specific T cell response in all treated patients. Responses were detected in both CD4+ and CD8+ T cells. A significant correlation between the PIONEER prediction score and induced T cell immunogenicity was detected, while better clinical responses was correlated with larger numbers of immunogenic EVX-01 peptides.

Conclusion

Dose escalation of EVX-01 was shown to be safe. Objective tumor responses were observed at all dose levels. In addition, immunization elicited vaccine-specific CD8+ and CD4+ T cell responses in patients from all dose levels examined. However, the anti-tumor efficacy of EVX-01 in combination with PD-1 warrants further study.

INTRODUCTION

Immune checkpoint inhibitors (ICIs) has provided major treatment advantages for solid cancers.(1) Especially the ICI targeting PD1/PDL1 axis, releasing anti-tumor cytotoxicy within the tumor are now the standard treatment for several cancers, including melanoma.(2) Still, there are patients who do not benefit from the ICI therapy (3). The tumor mutational burden (TMB) has been suggested to be a predictive factor the treatment outcome of immune therapy(4,5), however it is of greater importance whether mutations give rise to immunogenic MHC presented neoantigens (6). The lack of response observed in most cancer patients is perhaps related to a limited development of T cell responses against cancer cells. Therefore, combining ICI with a personalized neopeptide cancer vaccine to elicit neoantigen-specific T cell responses could be an attractive therapeutic option.

Several clinical trials are currently evaluating personalized vaccines against neoepitopes in combination with ICIs (NCT02950766 and NCT03289962)(7). Differences in the peptide components' dose and/or structure can profoundly affect T cell activation and function (8–10). Thus, efficacy and risk of toxicity might rely on the 'correct' choice of peptide and adjuvant and the administered amount of both components. In a recent study(11), three different dosages of human telomerase reverse transcriptase vaccines (UV1) were investigated in patients with non-small cell lung cancer (NSCLC), and they found a positive correlation between the highest dosage (700µg) with both immune response and overall survival (OS). Another study showed that a high dosage Melan-A/ELA peptide vaccine in patients with metastatic melanoma would induce early selection of Melan-A-specific CD8+ T cells of increased functional capability(10). However, none of the studies evaluating vaccination with neopeptides(7) addresses the effects or risk of vaccine dosage choice.

Additionally, peptide vaccines have been shown to boost T cell responses effectively. However, several clinical studies reports a primary boost of CD4+ T cells cells, rather than effector CD8 T cells(12,13). However, *in vivo* studies suggests different strategies to induces CD8 T cells boost (14,15). The CAF09 adjuvant used in this study has been shown to boost CD8 T cells responses when delivered by intraperitoneal injection compared to intramuscular injections(16).

We have previously reported interim data related to production and feasibility of the EVX-01 neoantigen targeting peptide vaccine(17). Here, we report the complete findings for the phase I study, including dose escalation evaluation. In this study, patients were vaccinated metastatic melanoma with the neopeptide vaccine, EVX-01 at 3 different dose escalation level (500ug, 1000ug and 2000ug), while keeping the adjuvant level stable. The patients received aPD1 ICI before and throughout the vaccination. We followed

the safety of the vaccine, and it was found to be safe at all three dose levels. We further examined the clinical and cellular response to the vaccine. The CD4 and CD8 immune response towards vaccine peptides was measured before, during and after vaccination. Immune responses were hereafter compared to vaccine doses and clinical outcomes.

PATIENTS, MATERIALS, AND METHODS

Patients

Included patients had biopsy-verified advanced unresectable melanoma. Patients were planned to either begin first-line treatment with an aPD1 checkpoint inhibitor (group A) or had already been treated with an aPD1 agent for at least four months with stable disease (SD) and who qualified for continued treatment with aPD1 (group B). Additional inclusion criteria included; ≥ 1 measurable lesion as per investigator-assessed Response Evaluation Criteria in Solid Tumors (RECIST v.1.1); an Eastern Cooperative Oncology Group (ECOG) performance status of 0 or 1; adequate organ function; and tumor tissue available for whole-exome sequencing (WES). Critical exclusion criteria included: Severe autoimmune disease; previous severe immune-related AE.

Trial design

This is a clinical first-in-man phase I trial (EudraCT No. 2018-002892-16) and clinicaltrial.gov (NCT03715985). It was conducted at the National Center for Cancer Immune Therapy (CCIT-DK) and the Department of Oncology, Copenhagen University Hospital, Herlev, Denmark. The study protocol was approved by the Ethics Committee and the Danish Medicines Agency and conducted following the Helsinki agreement (18) and guidelines for Good Clinical Practice (GCP)(19). All patients signed informed consent before inclusion.

The trial was amended to include EVX-01 dose-escalation cohorts. The trial was closed after inclusion at three dose levels.

Included patients were treated with an aPD1 agent according to local guidelines. When the personalized EVX-01 vaccine production was finished, it was added to the treatment schedule (Figure 1a). The patients received EVX-01 treatment every two weeks, six treatments in total. The first three vaccines were administered as IP injections, and the last three vaccines were administered as IM injections.

Three dose level groups was included in the trial. At least two vaccine doses was administered to patient 1 and 2, before additional patients could start treatment. Dose level 1 (lowest dose) included five patients,

three patients received the doubled dosage (dose level 2). Again no vaccine-related grade 3-4 AEs should occur at the first two vaccinations before the next patient could initiate treatment. This also applied to the four patients at the quadruple vaccine dosage (dose level 3).

The study's primary endpoints were safety and tolerability of the treatment in three different vaccine dosages based on the observation of AEs according to the NCI Common Terminology Criteria for Adverse Events (CTCAE version 4.0). The secondary endpoints were feasibility of manufacturing a personalized neoantigen-based vaccine within six to eight weeks of inclusion via the AI PIONEER™ production pipeline and evaluating the immune response before, during, and after treatment with the personalized neoantigen vaccine (EVX-01). The tertiary endpoints included efficacy, and was evaluated by best overall response (BOR), progression-free survival (PFS), and overall survival (OS).

Assessments in the study were based on physical examination, ECOG performance status, vital signs (pre- and post-treatment), and blood samples to warrant the safety of the participants. Imaging (CT scan or PET-CT) was done at baseline, and every three months (preferable between the third and fourth vaccination), followed by imaging every 12 weeks to evaluate the clinical efficacy of the trial treatment. Tumors were evaluated following the RECIST v. 1.1 criteria. Tumor biopsies were obtained at baseline (obligatory), shortly before the initial vaccination and just after the final vaccination (voluntary).

Interim results from dose level 1 have previously been published(17).

Design of personalized neoantigen vaccines

Personalized neoantigen vaccines was predicted and developed with The PIONEER™ platform by Evaxion Biotech. Whole-exome sequencing (WES) data from healthy and tumor tissue, mRNA sequencing data from tumor tissue, and human leukocyte antigen (HLA) typing data from healthy tissue were used to predict the neopeptides. They were ranked by 1) the potential to bind MHC, 2) expression levels, and 3) the clonality. Manufacturing of personalized neoantigen vaccine is described in detail in the manuscript: Personalized therapy with peptide-based neoantigen vaccine (EVX-01) including a novel adjuvant, CAF®09b, in patients with metastatic melanoma(17).

CAF®09b supply and final vaccine formulation at all dose levels

Each EVX-01 vaccine comprises 5-10 synthetically manufactured peptides (NPV-dp001) mixed with the CAF®09b adjuvant. Formulation of every EVX-01 vaccine with CAF®09b was done at CCIT shortly before administration (at the most two hours) as follows; a total of 1.08 mL sterile filtered Tris reconstitution buffer was added to 0.12 mL sterile filtered NPV-dp001 and thoroughly mixed. Following this step, 1 mL

of the peptide solution was added to a 2R vial containing 1.0 mL CAF®09b 2500/500/125. Following this, the final vaccine product (500 µg of total peptide in 0.5 ml) could be drawn into a syringe. At dose level 2, patients received 1000 µg of total peptide, administered as either 2 x 0.5 ml (IM) or 1.0 ml (IP). At dose level 3, patients received 2000 µg of total peptide, administered as either 2 x 1.0 ml (IM) or 2.0 ml (IP). Initial individual peptide dose was chosen based on the experience from a clinical trial performed at DK-CCIT (EudraCT No.: 2015-003719-39) (manuscript in preparation).

Peripheral Blood Mononuclear Cells isolation and pre-stimulation

Peripheral blood mononuclear cells (PBMC) were obtained from peripheral blood at different time points: At baseline (which for group A is before aPD1 therapy) (T1), before first vaccination (T2), after three vaccinations (T3), six vaccinations (T4) and follow-up (FU). First, PBMCs were separated with gradient-centrifugation with Lymphoprep (Takeda). PBMCs were cryopreserved in 90% human AB serum (Sigma Aldrich, Ref. No H4522-100ml) and 10% DMSO, and stored at -140 ºC until use.

Before screening for peptide recognition, the PBMCs were pre-stimulated with EVX-01 peptides. PBMCs were thawed and cultivated in X-vivo media (X-vivo 15 + 5% human serum) supplemented with IL-15(10 ng/ml) and IL-21(50 ng/ml) (Preprotech) as culture media. At day 1, pooled vaccine peptides (final concentration 20ug/ml) were added to the cell cultures in base media. From day 2, the culture media was supplemented with IL-2 (40 IU/ml) (Preprotech). The cells were cultivated for 14 days and rested for 1-3 days in X-vivo media.

Skin-test infiltrating lymphocytes

A delayed-type hypersensitivity (DTH) skin test (voluntary) was done approximately two weeks after the six vaccinations (Figure 3a). Volunteering patients received two intradermal injections of the EVX-01 peptides, one injection with trisaminomethan (TRIS) buffer and Dimethyl sulfoxide (DMSO) as a negative control on the back. After 48 hours, 5mm punch biopsies were obtained from each injection site. The tissue was transported directly to the laboratory for skin test-infiltrating lymphocytes (SKILs) culture. The tissue biopsies were divided into 1-3 mm3 fragments, placed in separate wells of a 24 well-culture plate, with medium (90% RPMI-1640 plus GlutaMAX and 25mM HEPES), 10% heat-inactivated AB Human serum (HS; Sigma-Aldrich), 100 U/ml penicillin, and 100 µg/ml streptomycin (Pen Strep, Thermo Fisher Scientific), 1.25 µg/ml Amphotericin B (Fungizone, Bristol-Myers Squibb) and 100 IU/ml rhIL-2 (Proleukin, Novartis). Plates were incubated at 37°C, and 1/2 of the medium was replaced at day five and thereafter three times weekly. After three to six weeks, pooled SKILs were cryopreserved or further expanded with Rapid

Expansion Protocol(20). Before screening for peptide recognition, the SKILs were thawed and rested overnight in RPMI-1640, 10% heat-inactivated AB Human serum, 100 U/ml penicillin, and 100 µg/ml streptomycin.

Tumor-infiltrating lymphocytes and tumor cell lines

As previously described(21), fresh tumor tissue was collected and transported to the laboratory for tumor-infiltrating lymphocytes (TILs) culture. In short, to obtain minimally-expanded TILs, the tumor biopsies were divided into 1-3 mm3 fragments and placed in separate wells of a 24 well-culture plate, with medium (90% RPMI-1640 plus GlutaMAX and 25mM HEPES), 10% HS, 100 U/ml penicillin, and 100 µg/ml streptomycin, 1.25 µg/ml Amphotericin B and 6000 IU/ml rhIL-2, for 3 to 6 weeks. Minimally-expanded TILs were then pooled and either cryopreserved or further expanded according to a standard 14-day rapid expansion protocol (REP)(21). Autologous tumor cell lines (TCLs) were established via serial passage of adherent cells from the same tumor biopsies(22). The TCLs were routinely tested negative for mycoplasma (AppliChem; Darmstadt, Germany), and the number of passages between collection and use in the described experiments was <10.

T cell activation assay by IFNγ ELISPOT

Using the IFNγ ELISPOT assay, we screened for peptide recognition by T cells in both PBMCs and SKILs. This is thoroughly described in the interim report(17). 96-well ELISPOT plates were prepared by coating with IFNγ capture antibody. For TILs and SKILs, 100,000 effector cells and 10,000 isolated autologous monocytes were added per well. For PBMCs, 300,000 effector cells were added per well. Pooled and single vaccine peptides were added at a 20 µg/ml concentration and 0.5 – 5 µg/ml, respectively, as well as a positive control, Phytohaemagglutinin P (PHA). Negative controls for SKILs: T cells + monocytes without peptide, T cells + monocytes with irrelevant peptide, monocytes + peptide pool, and T cells alone. Negative controls for PBMCs were: PBMCs without peptides, and PBMCs + irrelevant peptide (conc: 1ug/ml, sequence: GDVKIHAHKVVLANISPYFKAMFTGNL). After incubation overnight, cells were removed, IFNγ biotinylated detection antibody was added, followed by addition of Streptavidin-HRP, and finally, AEC substrate was used for spot formation. Spots were counted by the ImmunoSpot Series 2.0 Analyzer (CTL Analyzer; Bonn, Germany). A positive response was defined when the counted number of spots for the tested peptides exceeded the background (irrelevant peptides) spot number plus three times the standard deviation of the background with at least ten spots over the background(17).

T cell activation assay: Intracellular flow cytometry

PBMCs (peptide-specific activation)

Rested PBMCs were cultured in a 96-well plate (2-3x10^6 cells/well) and restimulated with the vaccine peptide pool (20ug/ml) or irrelevant peptide (1ug/ml) in X-vivo media. Afterward, the cells were incubated in a 37°C incubator for 2 hours. After 2 hours, Golgi mix containing; GolgiPlug™, GolgiStop™ (dilution 1:1000, BD biosciences), CD107a (dilution 1:40, BD biosciences), and X-vivo media were added to the cells hereafter incubated for 6 hours. The cells were washed and stained with Live/Dead Fixable Dead Cell Stain Near-IR (Thermo Fisher) and Surface antibodies; CD3, CD4, CD8 (BD biosciences). Then the cells were fixed and permeabilized by using Foxp3/Transcription Factor Staining Buffer Set (Invitrogen). Next, the cells were intracellularly stained for TNF-α (Biolegend), IFNγ, and CD137 (BD biosciences). Cells were analyzed using the LSRFortessa^{TM} (BD biosciences), and flow cytometry data were analyzed by FlowJo version 10 (Becton Dickinson). Reactivity of the T cells was seen as a percentage of live CD8+ or CD4+ T cells staining positive for at least two of four markers (TNF-α, IFNγ, CD137, and CD107a). Irrelevant peptides with effector cells were used as an unstimulated control.

SKILs and TILS (peptide-specific activation)

Prior to the initiation of the assays, SKILs and TILs were thawed and rested overnight. EVX-01-specific T cell activation was evaluated with an 8-hour co-culture at 37°C of effector cells (TILs or SKILs) and peptides in the presence of autologous monocytes. The SKIL to monocyte ratio was 10:1. The single peptides and peptide pool were added with a final concentration of 0.5 µg/mL alongside as a positive control (PMA+Ionomycin) and a negative control (irrelevant peptide). After 2 hours of co-culture, Anti-human CD107a antibody, Brefeldin A (dilution of 1:1000, GolgiPlug™) and Monensin (dilution of 1:1000, GolgiStop™) were added. After 8 hours of incubation, the cells were washed two times with DPBS (Sigma-Aldrich/Merck KGaA) and stained with live/dead reagents, as well as antibodies used for surface markers. Afterward, the cells were washed, fixed, and permeabilized overnight using the FoxP3/Transcription Factor Staining Buffer Set (eBiosciences, Thermo Fisher Scientific). Following, the cells were stained with antibodies binding to intracellular targets. Cells were then analyzed on a NovoCyte Quanteon™ Flow Cytometer and analyzed with FlowJo version 10 (Becton Dickinson). The definition of T cell reactivity was the percentage of live CD8+ or CD4+ T cells staining positive for at least two of four markers (TNF-α, IFNγ, CD107a, CD137) minus the background (unstimulated control). Further details can be found in the interim manuscript(17).

Detection of peptide specific CD8+ T cells by combinatorial fluorochrome encoding of pMHC multimers

8-11mer minimal peptides was predicted from every EVX-01 peptide (22-27mer) by NetMHCpan 4.1(23), based in patient specific HLA type. EVX-01 derived minimal peptides were selected per patient based on EL%rank < 2. A selection process was performed to reduce the number of peptides; we selected top 30-41 peptides with lowest EL%rank, grouped by the long EVX-01 peptides and the patient specific HLA alleles. (Supplementary figure 6). Few EVX-01 peptides did not include HLA class I binders (EL%rank < 2), why no minimal peptides were not included for these peptides. A panel of fluorochrome-labelled peptide-MHC (pMHC) tetramers was assembled for each patient, with each pMHC having a unique identifiable fluorochrome combination, as previously described(24,25). EVX-01 prestimulated PBMCs for all collected time point was stained with the patient specific pMHC tetramer panel, analysed on LSR fortessa (BD) and gated in FlowJo™ v10.

Detection of peptide specific CD8 T cells using DNA barcode-labelled peptide-MHC I multimers

Selected patients (Patient 1, 2, 3, 4, 8 and 9) was screened for the broad presence of neo-antigen reactive CD8+ T cells (NARTs) and virus-reactive CD8+ T cells (VARTs). Patient specific neopeptides was predicted with two different prediction pipelines, PIONEER™ and MuPeXi(26). Top 100 peptides from each prediction pipeline was selected. Additionally, minimal EVX-01 peptides described above and virus peptides was added to the patient specific panel of peptides resulting in a total of 145-231 unique peptide-MHC combinations per patient . Ex vivo PBMC, TILs and SKILs was screened for CD8+ T cell recognition using the patient specific peptide panels, loaded into barcode labeled pMHC-multimer complexes(27). In short, pMHCs and a short unique DNA barcode are both bound to fluorochrome (PE: neo antigens, APC: virus antigens) labelled dextran molecules, creating a DNA barcode-labelled peptide-MHC I multimer, which is unique for each peptide-MHC combination. The above mentioned tissue were stained with a panel of these multimers, in combination with an CD8(BD, RPA-T8) and CD3 (BD, clone SK7) antibody. PE and APC fluorochrome-labelled CD8+ T cells were sorted on the FACSAria (BD). DNA barcodes bound to the sorted cells were hereafter amplified by PCR, as were a reference DNA barcode baseline sample from the collected pMHC multimer panel that the cells were stained with. Amplified barcodes from sorted cells and baseline was hereafter sequences by PrimBio. Sequence results was uploaded to Barracoda(27) for analysis, together with various information on primers, DNA barcodes, DNA barcode annotation for pMHC and information on samples identification. Output files includes log2 fold change of sorted barcodes compared to baseline barcodes and the related p value to determine significantly pMHC complexes among the sorted cells. Here, barcode-pMHC multimers were used to select pMHC complexes possible

recognized by T cells in the pool (between 7-41 pMHC complexes), while this more restricted library of pMHC was included for analyses using combinatorial fluorochrome encoding of pMHCs as described above.

RESULTS

Patients with metastatic melanoma were vaccinated with personalized neopeptide vaccine, EVX-01. Injections of the vaccines was done first IP and hereafter IM. During vaccine production time, patients were treated with aPD1 ICI, which continued during vaccination. The length of vaccine production time from baseline biopsy until first vaccination ranged from 51 to 70 days for all 12 patients (Table 1). The trial was designed to investigate the safety and immunologic response following EVX-01 vaccination. Three dose levels were included: Dose level 1: 500 ug/peptide, 5 patients (previously reported), Dose level 2: 1000µg/peptide, 3 patients and Dose level 3: 2000µg/peptide, 4 patients.

Table 1 | Patient characteristics

Patient	Age at inclusion	Sex	Group A or B	Disease stage	Baseline LDH	Biomarkers	Dosage	Days from biopsy until first vaccine
1	81	male	A	M1b	259	PD-L1 > 1 % and <50% BRAF mutation	single	56
2	49	female	B	M1c	147	PD-L1 > 1% BRAF mutation	single	51
3	61	male	A	M1c	118	PD-L1 > 1% and < 2% BRAF negative	single	53
4	84	female	A	M1a	184	PD-L1 5% BRAF muation	single	57
5	79	female	A	M1b	835	PD-L1 < 1% BRAF negative	single	60
6	71	female	B	M1a	116	PD-L1 < 1% BRAF mutation	double	62
7	84	female	B	M1b	239	PD-L1 > 1% BRAF negative	double	56
8	64	female	B	M1a	180	PD-L1 < 1% BRAF mutation	double	60
9	59	female	A	M1b	160	PD-L1 > 50% BRAF positive	quadruple	53
10	70	female	A	M1c	201	PD-L1 > 50% BRAF negative	quadruple	70
11	67	female	A	M1a	210	PD-L1 negative BRAF positive	quadruple	57
12	74	male	A	M1c	223	PD-L1 > 1% BRAF positive	quadruple	56

Safety

Patients were enrolled from January 2019 to October 2021. Demographics and baseline disease characteristics of the patients are listed in Table 1.

Table 2 |Adverse reaction within 14 days of vaccination at middle and high dosage levels

	Middle dose group (n = 3)		high dose group (n = 4)	
All adverse reactions within 0-14 days				
	IP	**IM**	**IP**	**IM**
Any	12	3	13	12
Grade 2	1	0	2	2
Grade 3	0	0	0	3
Injection site adverse reactions within 0-14 days				
	IP	**IM**	**IP**	**IM**
Pain grade 1	2	0	6	4
Systemic adverse reactions witin 0-14 days				
	IP	**IM**	**IP**	**IM**
Abdominal pain grade 1	1	0	0	0
Abdominal pain grade 2	1	0	0	0
Chils grade 1	0	0	1	0
Cough grade 1	1	0	0	0
Fatigue grade 1	1	1	1	2
Fatigue grade 2	0	0	1	1
Fever grade 1	2	0	0	0
Flu like symptoms grad 1	0	0	3	0
Headache grade 1	0	0	0	1
Joint pain grade 1	0	0	1	0
Joint pain grade 2	0	0	1	0
Nausea grade 1	3	1	0	0
Vomiting grade 1	2	1	1	0
Edema grade 2	0	0	0	1
Myositis grade 3	0	0	0	1
Adrenal insufficiency grade 3	0	0	0	1
Papilledema grade 1	0	0	1	0
Nefritis grade 3	0	0	0	1

As previously reported 5 patients were enrolled at dose level 1 (lowest dose). Four patients were in group A (aPD1 naïve) and patient 2 was in group B (SD on aPD1). Most AE observed was grade 1, except for patient 2 who experienced grade 2 fatigue after first vaccination.(17)

At dose level 2, three patients were enrolled, all from group B, and every participant received all six vaccinations. One patient experienced grade 2 abdominal pain after IP injection. No severe vaccine-related AE was seen at this dose level.

Four patients were then enrolled at dose level 3, and all were in group A. Patient 11 developed grade 3 immune-related myositis and adrenal insufficiency after 6 vaccinations and 6 treatments of ICI. Patient 12 developed grade 3 immune-related nephritis after 4 vaccinations and 5 series of ICI. These side effects are most likely related to the ICI treatment.

In summary, most AEs were grade 1, except for four reactions (abdominal pain, fatigue, edema and joint pain), which were registered as grade 2, and two reactions (nephritis and myositis) were registered as grade 3, but is most likely related to ICI (Table 2). The most frequent events were pain at the injection site, fatigue, and nausea. The treatment was therefore well tolerated despite dosage escalation. Both patients with grade 3 side effects stopped treatment with ICI. Between the two vaccination routes, a tendency of more side effects was seen after IP injections than after IM injections.

Clinical efficacy

The best overall tumor responses were found in six patients with PR (patients 1, 3, 8, 9, 10 and 12) and two with CR (patient 2 and 11). Thus, eight of twelve patients treated with the combination of aPD1 and EVX-01 vaccination achieved objective response (Figure 1b).

At dose level 1 three patients had objective response with best overall response (BOR) comprising 2 PR and 1 CR. Duration of response (DOR) for patient 1 was 28 months, for patient 2 10 months, and 5 months for patient 3 with PR who unfortunately died from treatment unrelated reasons.

At dose level 2 patient 8 was the only patient with an objective response. This patient had been treated with ten cycles of aPD1 at time of inclusion with SD as best response. Seven months from the first vaccination, the patient had PR (60% regression in target lesions) with DOR of 9 months. The patient developed temporary complete regression in target lesions (100 %) and a stable non-target lesion (Supplementary figure 1).

At dose level 3 all four patients obtained objective response with BOR comprising 3 PR and 1 CR. DOR for patient 9, 10 and 12 were 8, 4 and 2 months respectively. Patient 11 have ongoing CR for 16 months. Off notice, patient 10 had PR after only 1 vaccination but developed PD shortly after the sixth vaccine similar patient 11 showed CR after 1 vaccination.

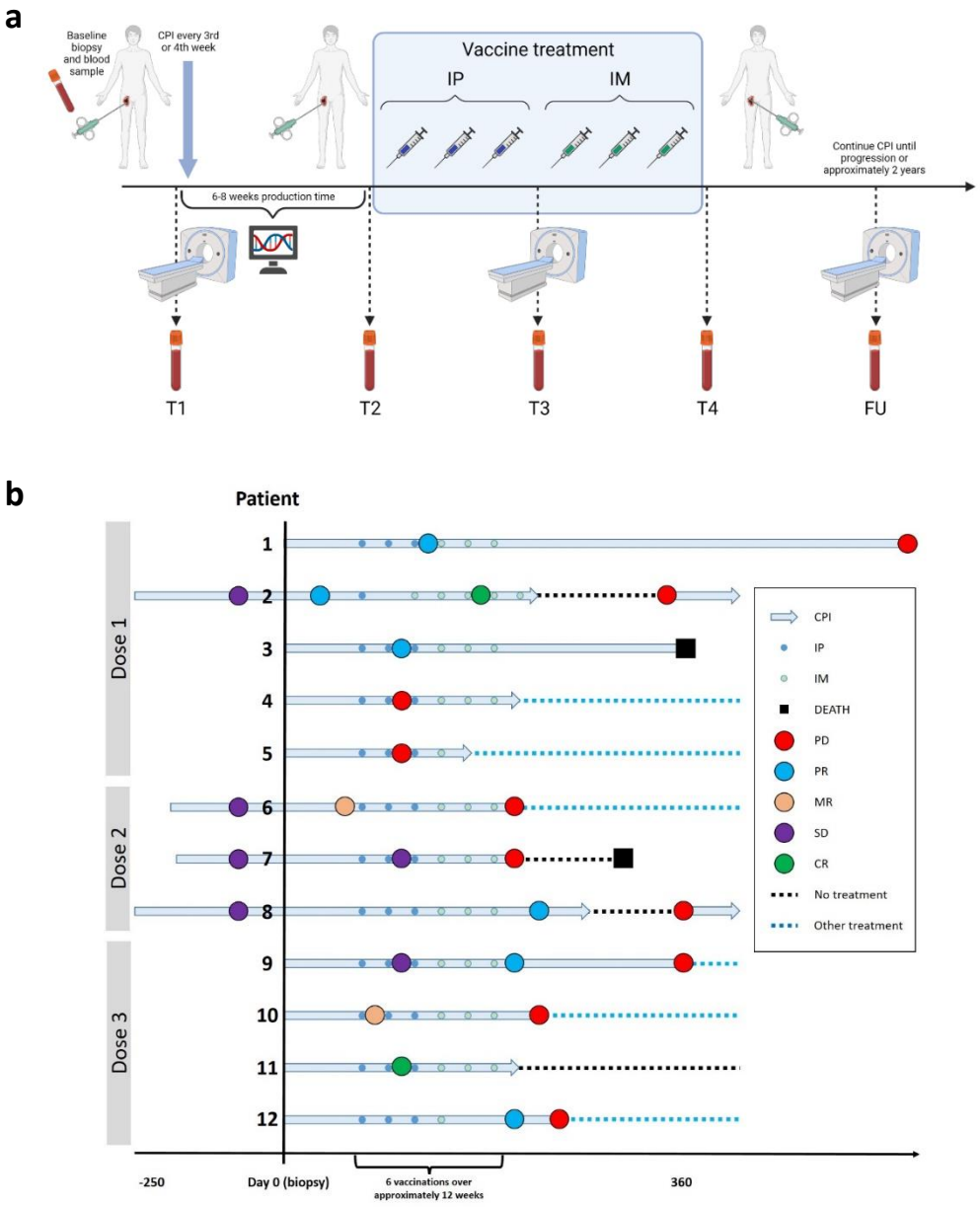

Figure 1 | clinical setup and - response. a) Clinical setup; Biopsy, PET/CT scan, and blood samples were collected at baseline (T1). Treatment with aPD1 was either initiated around the first biopsy (group A) or had already been initiated for at least four months before the biopsy (group B). EVX-01 vaccination was administered approximately at week 6-8 and every second week for six vaccinations in total (3 IM + 3 IP). Tumor biopsies were performed (if possible) at T2 and T4. In addition, radiographic imaging was done every 12 weeks. Blood samples were collected from T1 to T4, and thereafter every 12 week. Figure created with BioRender.com **b)** Overview of patient inclusion: checkpoint inhibitor (CPI) initiation, baseline biopsy (day 0), vaccine treatment, and follow-up information of the twelve patients at three different dose levels. Small blue and green dots indicate either IP vaccinations or IM vaccinations, respectively. The depiction of disease condition and patient status are indicated in various colors. PD – Progressive Disease (red), PR; Partial Response (blue), MR;Mixed Response (salmon), SD; Stable Disease (purple), CR; Complete Response (green).

EVX-01-specific T cell responses before and after vaccination

EVX-01-specific T cell responses were evaluated by both IFNγ Elispot and intracellular cytokine staining (ICS) analysed by flow cytometry. T cell reactivity to the vaccine was evaluated at baseline before aPD1 initiation (T1), before vaccine initiation (T2), and after administration of vaccine EVX-01 (T3 = after 3 vaccines, IP) (T4 = after 3 vaccines, IM, a total of 6 vaccine doses).

Detecting single peptide responses by Elispot

The frequency of responses detected by Elispot before vaccination (Pre, T1 and T2), after vaccination (Post, T3 and T4) and in follow up samples (FU1-FU5) are shown in table 3. Blood samples from all 12 patients was analysed by IFNγ ELIspot assay, where EVX-01 prestimulated PBMCs were restimulated with single EVX-01 peptides. We observed vaccine-induced T cell responses in all patients. A total of 90 peptides were included in the vaccines covering the 12 patients. We measured peptide-induced INFγ secretion in pre-stimulated PBMCs towards 54 of these EVX-01 peptides (60 %). Among these, peptide-induced INFγ secretion towards 42 of the 90 peptides was only detected after vaccination, hence representing de-novo responses (47%). The three dose levels have similar frequencies of total responses (mean: 61.2%, SD: 8.8) and de-novo responses (mean 46 %, SD: 7.3). Dose level 2 had the highest frequencies of total responses, however dose level 1 had the highest level of de novo responses.

Table 3 | Overview – number of IFN-γ T cells responses to EVX-01 peptides measured by Elispot

Dose level	Total resoponses (n)	De novo Responses (n)	Total peptides	Total responses (%)	De novo Responses (%)
All	54	42	90	60	47
Dose 1	26	22	41	63	54
Dose 2	11	7	16	69	44
Dose 3	17	13	33	52	39
			mean	61.2	46
			SD	8.8	7.3

Elispot responses for each patient are shown in figure 2a. EVX-01 responses are generally small and low frequent throughout the three dose levels before vaccination (T1 and T2). After vaccination (T3 and T4) responses are observed in all patients, and we detect an increase in response size (sum of spots) compared to responses before vaccination. Across all patients, the highest response frequency was detected at dose level 1 and the largest response size was found in dose level 3. Responses are generally detected in all follow up samples, but a decrease in both frequency and size of responses is observed over time (Figure 2a). Notably, patient 8 has a persistent response towards peptide 2, which is also detected at T1 before vaccination. (Supplementary figure 2).

The level of T cell responses towards single peptides was grouped based on the vaccination dose. Post vaccination we see an increase in the level of T cell responses with an increase in peptide dose. EVX-01 peptides delivered in a dose of 200 ug and 400 ug per peptide generated a significantly higher size of response (number of delta spots) compared to peptides delivered with a dose of 50 ug per peptide. We observed the same tendency in the follow up samples, where we detected significantly higher responses toward peptides delivered with a dose of 200 ug per peptide (Figure 2b, Supplementary Figure 6).

CD4+ or CD8+ driven response measured by ICS

We evaluated whether the EVX-01-specific T cell responses were dominated by CD4+ or CD8+ T cell reactivity. To do so, EVX-01 pre-stimulated PBMCs were restimulated with patient-specific EVX-01 peptide pools. Restimulated PBMCs were intracellular stained for INFγ, TNFα, CD137 and CD107a to detect T cell reactivity against the peptide pool using flow cytometry. EVX-01 reactive CD4+ T cells were observed in all 12 patients after vaccine administration at TP3 and TP4. The most pronounced response was detected in patient 7 at T4. CD4+ T cells responses persist in follow up samples, however frequency of reactive CD4+ T cells decreases with time. EVX-01 reactive CD8+ T cell were detected in 5 patients at T3 and T4 (patient 3, 5, 7, 8 and 9). Additionally, CD8+ T cell reactivity was detected in samples from patient 6 and 10 at FU1. A total of 7 patient sample showed a CD8+ response after vaccination. CD8+ T cell responses was not detected after FU1, except in patient 8, where a response was detected in both FU2 an FU3. Patient 8 did also give rise to the largest CD8 T cells response. Minor reactivity was detected before vaccination (T1 and T2) in both CD4+ and CD8+ cells. There was no obvious difference in size of reactivity between the three dose levels, but the largest CD4 and CD8 T cell derived response was found in dose level 2, after IM vaccinations (T4). Finally, we observed the most robust and largest responses in CD4+ T cell, which clearly dominates the EVX-01 response. (Figure2c). In summary, 12 out of 12 patient (100%) showed a CD4+ T cell reactivity against EVX-01 peptides, while CD8+ T cell reactivity was demonstrated in 7 out of 12 patients (58 %) and with much lower frequencies of reactive CD8+ T cells compared to CD4+ T cells.

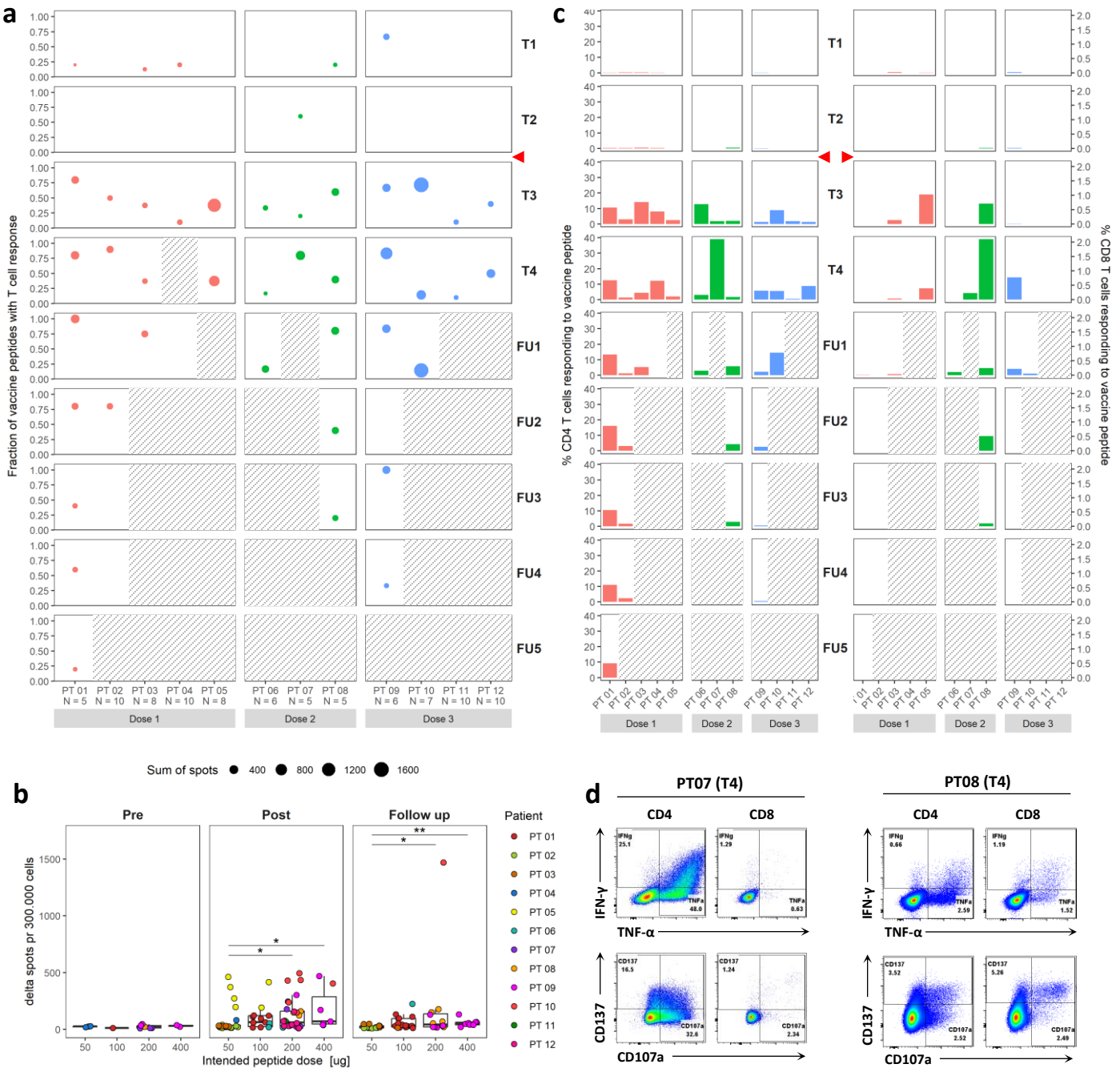

Figure 2| EVX-01-specific PBMC derived T cell responses analyzed by Elispot and ICS. a) An overview of all patient IFN-γ responses detected by Elispot from all three dose levels and all time points. Red dots represent dose level 1, green dots dose level 2, and blue dots dose level 3. The height of the dots on the y-axis represent the fraction of single vaccine peptides with a T cell response out of total peptides pr. patient. The total number of single peptides (N) are stated under the patient number at the X-axis. The size of the dots represents the sum of the spot after subtraction of the background (Irrelevant peptide). This only includes spots from single peptide stimulation, which induce positive responses. Grey scattered boxes indicate time points which were not analysed. **b)** The intended vaccine dose of the single EVX-01 peptides vs delta spots for peptides with T cell response (background stimulated with irrelevant peptide has been subtracted). Responses has been divided in pre vaccination (T1 and T2), post vaccination (T3 and T4) and Follow up (all FU time points). Each dot represent a single peptide response detected with Elispot. Means was compared between peptide dose groups using Kruskal-Wallis test. Significant difference is indicated with asterisks (* $p<0.05$, ** $p<0.01$) **c)** T cell responses was tested after re-stimulation with pool vaccine peptides and stained intracellularly for IFN-γ, TNF-α, CD107a and CD137. The percentage of T cell which are positive for at least two of mentioned markers are shown in an overview of EVX-01-specific CD4+ and CD8+ T cells in all patient responses from all three dose levels and all time points. Red bars represent dose level 1, green bars dose level 2, and blue bars dose level 3. Bars show specific CD4+ and CD8+ T cells. Background response has been subtracted. Grey scattered boxes indicate time points which were not analysed. **d)** Flow cytometry dotplots for CD4+ and CD8+ T cells stained for IFN-γ, TNF-α, CD107a and CD137. The dotplots are shown for patient 7 with the highest CD4+ T cell response at T4, and patient 8 with the highest CD8+ T cell response at T4.

EVX-01-specific T cells migration

A Delayed-Type Hypersensitivity (DTH) skin test was performed in six patients (patients 2, 6, 7, 8, 9 and 11) to investigated if EVX-01-specific T cells would migrate towards intra dermally injected EVX-01 peptides. This might give an indication of the tumor infiltrating ability of the vaccine specific T cells. We evaluated the presence of EVX-01-specific T cells in SKILs by IFNγ ELISPOT and ICS. We observed reactivity against individual EVX-01 peptides in the SKILs from patients 2, 6, 8 and 11 by Elispot. (Figure 3b).

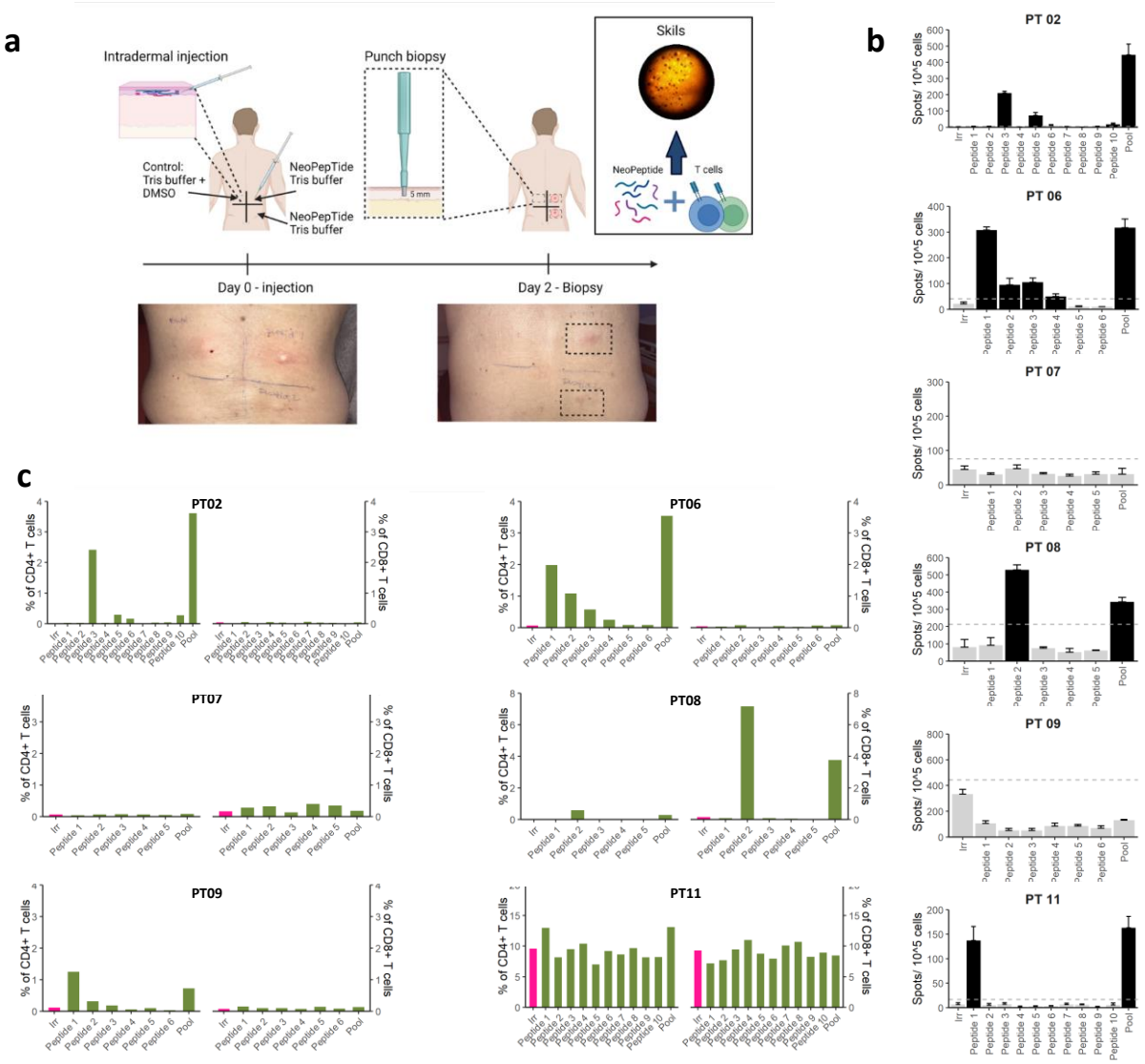

Figure 3| EVX-01 reactive SKIL derived T cell. a) DTH skin test was done approximately two weeks after the last vaccination. Two intradermal injections of the EVX-01 peptides and one control (DSMO) injection were administered on day 0 (approximately two weeks from the last vaccination). After 48 hours, 5mm punch biopsies were taken from the three injections site. The tissue was then transported to the laboratory for SKILs culture. Minimally expanded SKILs were expanded from tissue fragments for 3 to 6 weeks. Created with BioRender.com. EVX-01-specific T cell responses in SKILs (skin-test infiltrating lymphocytes) in patients 2 (dose level 1), 6, 7, 8 (dose level 2), and 9, 11 (dose level 3). **b)** Elispot responses were examined in SKILs at T4 (after six vaccinations) from six patients. SKILs were co-cultured with EVX-01 peptide pool and individual EVX-01 peptides. Black bars represent significant responses, grey bars are not significant. The dotted line indicated the threshold value for a significant response; background(irrelevant peptide) plus 3xSD of the background and at least 10 spots over background response **c)** T cells specific towards EVX-01 peptides were identified in SKILs, which were re-stimulated with EVX-01 peptide pool (green), single vaccine peptides (green) or irrelevant peptide (pink) for 8 hours.

Using ICS after 8-hour EVX-01 single peptide stimulation, we could confirm a CD4+ T cell response in these 4 patients, while only patient 8 showed a CD8+ T cell response in the SKILs. Furthermore, a low EVX-01 specific response was detected in CD4+ SKILs for patient 9, but there was no response detected for patient 7. (Figure 3c) Responses to single peptides in ICS matched responses detected in SKILs using Elispot. The responses detected in SKILs had also been detected in PBMC with Elispot, except for peptide 2 and peptide 4 detected in SKILs from patient 6 (Supplementary figure 2). For patient 6, a tumor cell line was established from a tumor biopsy collected before vaccination (T2). Therefore, tumor-specific SKIL responses were measured by Elispot and ICS. No tumor-specific SKIL responses were detected (data not shown).

In summary, SKIL reactivity analysed in Elispot and ICS assays match our results from EVX-01 prestimulated PBMC. Additionally, tumor biopsies were collected both before (T1 and T2) and after (T4) vaccination from 3 patients (patients 1, 6, and 7). TILs were successfully expanded from all tumor biopsies, but no reactivity was detected when these TILs were exposed to EVX-01 (data not shown).

Vaccine related neoantigen recognizing CD8+ T cell in expanded PBMCs

EVX-01 expanded PBMCs were screened for CD8+ T cells reactive towards epitopes within the EVX-01 peptides. CD8+ T cells which were found to be reactive towards minimal peptides predicted from EVX-01 are defined as VaccNARTs (vaccine-related neoantigen recognizing CD8+ T cells). The presence of VaccNARTs was examined by staining with peptide-MHC I tetramers. MHC I binders were predicted from long vaccine binders shown in supplementary figure 6. VaccNARTs were gated in clusters due to cross reactivity among minimal vaccine peptide with overlapping sequence identity (Supplementary Figure 6). Figure 4a shows the frequency of CD8+ T cells, VaccNART, recognizing clusters of vaccine derived minimal epitopes. We did not detect any overall increase in frequency after vaccination (Figure 4a, Supplementary Figure 7, Supplementary Table 1). However, VaccNARTs for a few selected peptides were increased after vaccination. In patient 6, a strong enhancement of low-level pre-existing T cell recognition was observed towards minimal peptides derived from vaccine-peptide 2 and 6. In patient 8, VaccNARTs were observed against a minimal peptide derived from vaccine-peptide 3, this response was increased after ICI treatment T2, and again after IM vaccine injection T4. (Figure 4b and c)

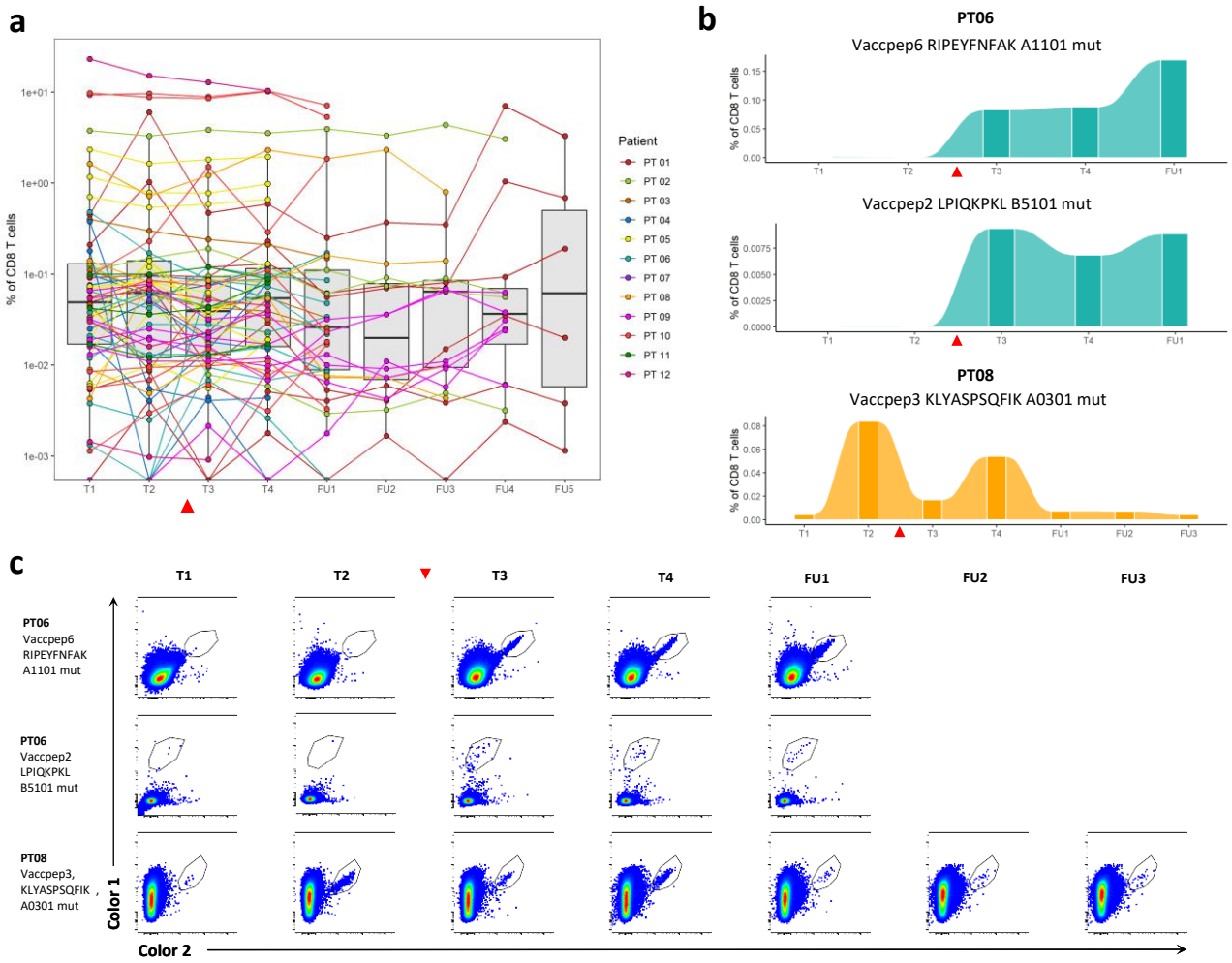

Figure 4 | EVX-01 prestimulated PBMCs derived CD8 T cells screened for EVX-01 CD8 epitopes. EVX-01 prestimulated PBMC were screened for EVX-01 specific CD8 T cells (VaccNARTs) using fluorochrome labelled pMHC-multimers. VaccNARTs are gated in clusters with one or more specificities due to overlap cross reactivity between sequences. **a)** The frequency of VaccNART clusters detected in EVX-01 expanded PBMC from different time points. Each dot represent a cluster which are colored according to patient. The single clusters are connected with lines between time points to follow the single clusters dynamics. Boxplots summarize the distribution and median of clusters within single timepoints. The red triangles indicated before and after vaccination initiation. **b)** The frequency of selected VaccNART clusters with only one specificity, from patient 6 and patient 8. EVX-01 peptide number (Vaccpep), short peptide sequence, HLA, and whether the short peptide includes the mutated region of the Vaccpep (mut) is shown above the graphs. **c)** Flow cytometry dotplots showing the VaccNART populations shown in b), y-axis and x-axis show the binding of the specific pMHCs marked with different fluorochrome colors.

Neoepitope spreading after vaccination

Potential neoepitopes were predicted based on tumor-specific mutations, hence also covering neopeptides beyond those embedded in the EVX-01 vaccine-peptides. CD8+ T cells that recognized predicted neopeptides are categoriesed as either VaccNARTs (recognizing vaccine-embedded sequences) or NARTs (recognizing non-vaccine-embedded neoepitopes). Ex vivo PBMCs and expanded TILs and SKILs was screened for NARTs, VaccNARTs and VARTs, in samples from patient 1, 2, 3, 4, 8 and 9. We did not observe any overall increase in frequencies of NARTs after vaccination, and hence no signs of epitopes

spreading (Figure 5a). Few NARTs were only detected after ICI (T2) in PBMC or TILs (Supplementary figure 9). In patient 9, a NART population was detected in PBMC after IM vaccination (T4), but also in TILs at baseline (T1) (Figure 5c and Supplementary figure 9), hence representing a pre-existing T cell response. The number of specific NART responses are roughly stable in tissue samples (TILs and SKILs) and in PBMCs before and after vaccination (Figure 5b). No epitope spreading was observed caused by neither ICI nor vaccination, but rather a small boost of pre-existing responses after ICI.

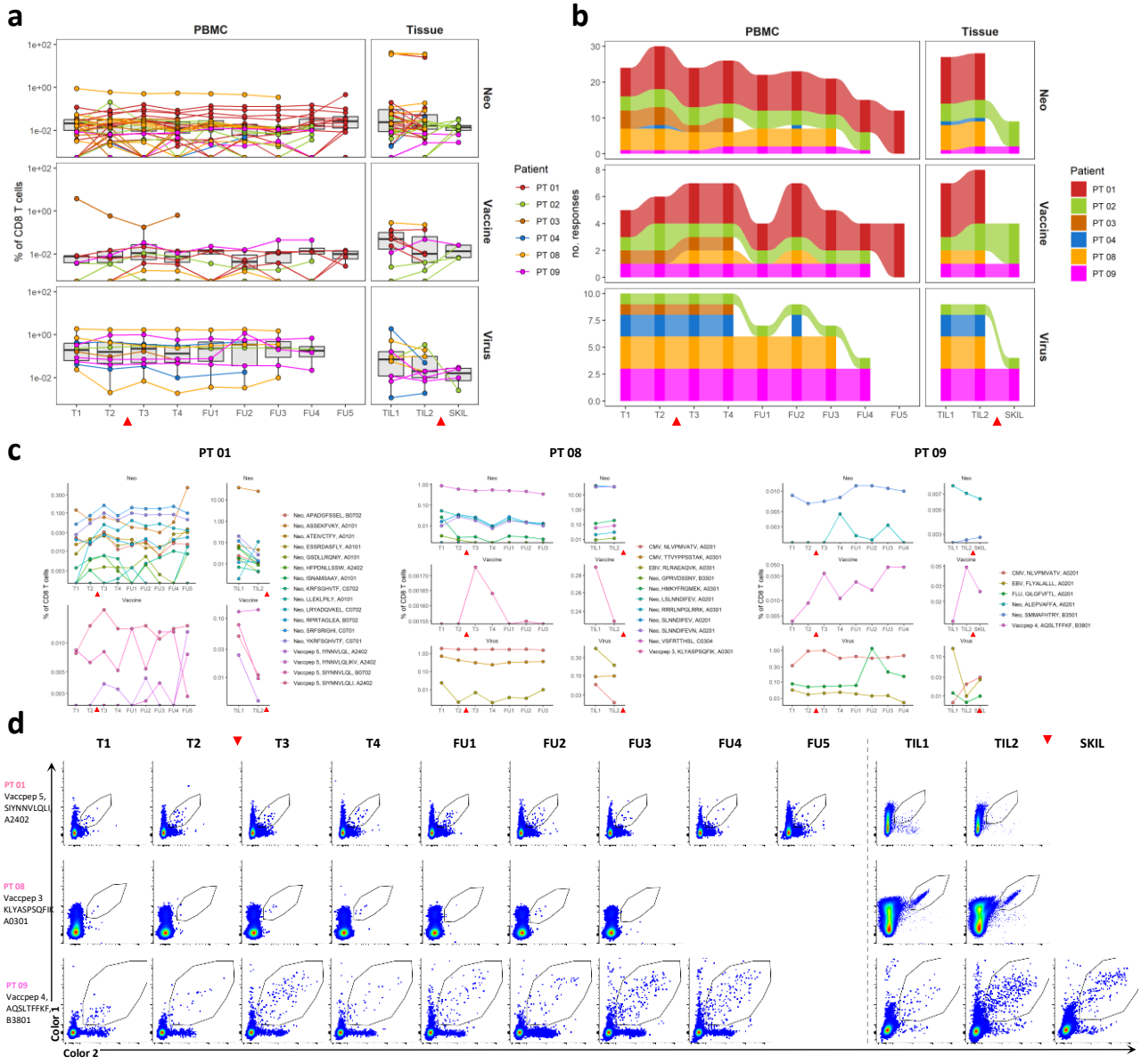

Figure 5 | Analysis of epitope spreading detected in *ex vivo* PBMCs, and expanded TILs and SKILs. Ex vivo PBMC and expanded TILs and SKILs were screened for neoepitope specific CD8+ T cells and virus specific CD8+ T cells (VARTs). Neoepitope specific CD8+ T cells were devided into two categories; CD8+ T cells recognizing EVX-01-embedded neopeptides, are referred to as VaccNARTs (also described in figure 4) and CD8+ T cells recognizing the remaining non-EVX-01-embedded neopeptides, are referred to as NARTs. **a)** The frequency of NARTs (Neo), VaccNART (Vaccine) and VARTs (Virus) detected in *ex vivo* PBMC from each time point and TILs from time point T1 and T2, and SKILs. Each dot represent a specific CD8+ T cells population which are colored according to patient. The single populations are connected with lines between time point to follow the dynamics. Boxplots summarize the distribution and median of clusters within single time points. The red triangles indicated before and after vaccination initiation. **b) T**he number of different responses detected by NARTs, VaccNARTs and VARTs within *ex vivo* PBMCs and expanded TILs and SKILs. The colors indicates each of the screened patients, to follow the flow in number of responses, within the patients **c)** The frequency of NARTs, VaccNARTs and VARTs shown for selected patients, showing the single populations dynamics over time **c)** Flow cytometry dotplots showing selected VaccNART populations. The y-axis and x-axis show the binding of the specific pMHCs marked with different fluorochrome colors.

VaccNARTs were studied to identify a boost or de novo responses after vaccination. Frequency and number of VaccNARTs generally appeared to have a small increase first after ICI (T2) and then again after vaccination (T3) (Figure 5a and 5b). Similar to NARTs, new VaccNARTs detected in PBMCs after vaccination was also detected in TILs from tumor biopsies taken before vaccination (Figure 5c, 5d and Supplementary figure 9). VaccNARTs were also found in SKILs, from both patients where these where available (patient 2 and 9), and patient 2 had larger frequency of VaccNART in SKILs compared to TILs (T1 and T2). All together, the EVX-01 vaccine appears to boost pre-existing VaccNART responses rather than creating de novo CD8+ T cell responses. Finally, frequency and number of VARTs was stably detected in PBMCs over time and was also detected in TILs and SKILs, demonstrating assay stability between time points (Figure 5a and 5b).

Balance of T cell recognition and functional immune responses

Immune analyses conducted on EVX-01 expanded PBMCs using Elispot and ICS were compared to determine the balance of functional responses (Elispot) and T cell recognition (MHC tetramer binding) Comparison was done for patient 1, 2, 3, 4, 8 and 9, who were screened for VaccNARTs in ex vivo PBMCs. As shown in figure 6a, the largest overlap in EVX-01 detected peptides are found in T3 and T4 samples, and decreases in FU samples. However, all EVX-01 peptides detected by VaccNARTs have also induced an Elispot response at, at least, one of the time points. We detected a CD8+ T cell reactivity by ICS in 3 of the 6 selected patients, patient 3, 8 and 9 (Figure 2c and Supplementary figure 3), and patient specific VaccNARTs were identified in all of those three patients. VaccNARTs were identified in two additional patients, patient 1 and 3, while neither CD8+ T cells reactivity nor VaccNARTs were identified in patient 4 (Figure 6b).

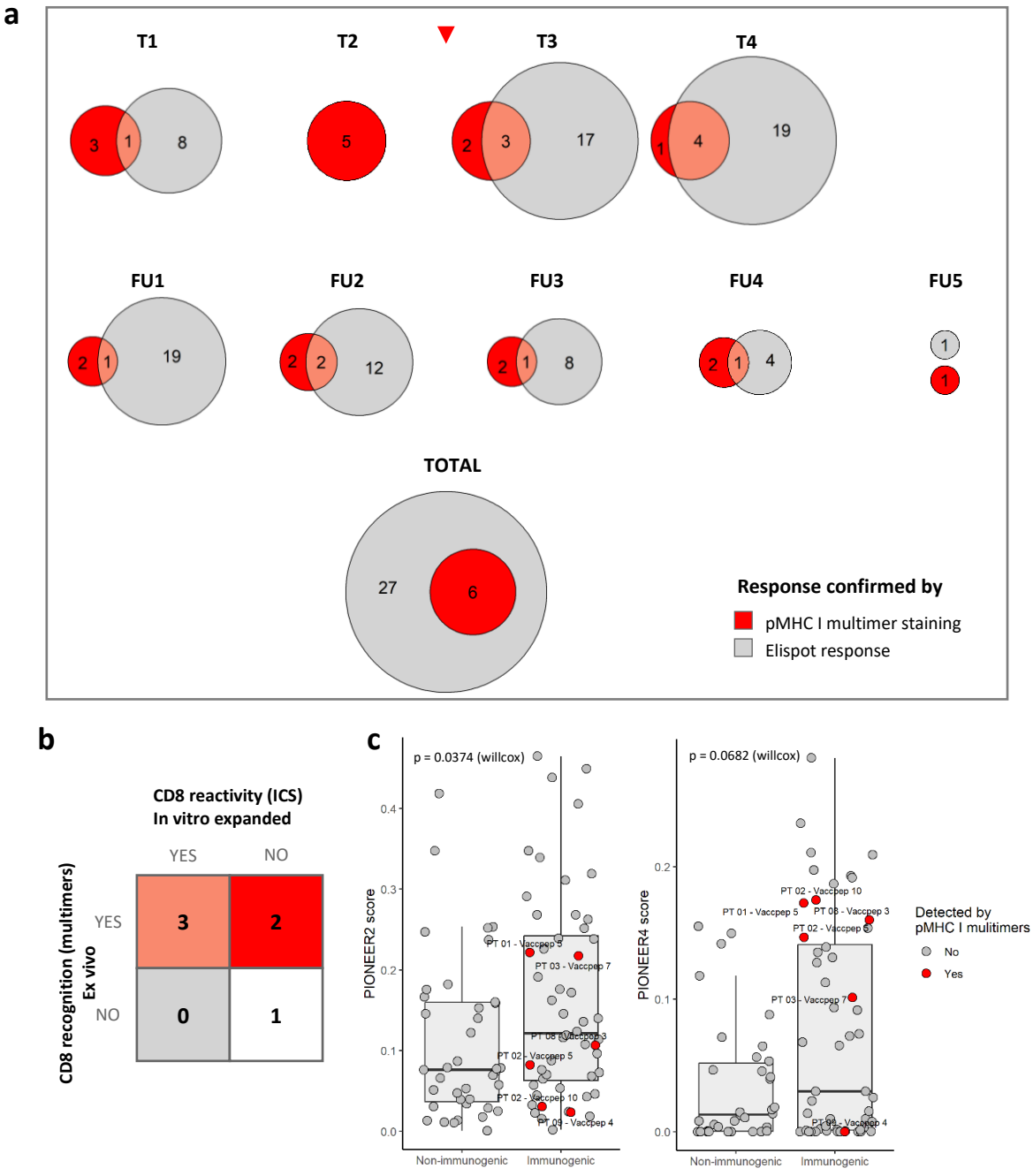

Figure 6| The balance of T cell recognition and functional immune responses. a) Venn diagrams showing the overlap of functional responses towards EVX-01 peptides detect by Elispot in expanded PBMCs (grey) and EVX-01 responses detected by the pMHC-I multimers in *ex vivo* PBMCs (red). The overlap of EVX-01 responses are shown for each time point, and for all time points collected (total) **b)** Number of patients with a functional EVX-01 CD8+ T cell responses detected by ICS compared to number of patients with EVX-01 responses detected by the pMHC-I multimers in *ex vivo* PBMCs. **c)** Prediction scores for EVX-01 peptides inducing functional responses detected by Elispot (immunogenic) compared to non-immunogenic EVX-01 peptides. Prediction scored for both PIONEER2 and PIONEER4 is shown. EVX-01 responses detected by the pMHC-I multimers in ex vivo PBMCs are marked in red. A t test was used to test the difference between immunogenic and non-immunogenic EVX-01 peptides' prediction scores, p-values are shown in the

Finally, prediction scores obtained from PIONEER^{TM} prediction of EVX-01 peptides were compared between immunogenic and non-immunogenic EVX-01 peptides defined by Elispot response. As shown in figure 6c, prediction score from PIONEER2 shows a significant split between the two categories, where immunogenic peptides obtained a higher prediction score. EVX-01 peptides detected by VaccNARTs are marked in the plot, where they spread out between high and low prediction scores. PIONEER4 prediction scores appeared to have better split, with significantly higher prediction scores for immunogenic peptides, additionally VaccNART detected EVX-01 peptides are all found within the highest prediction scores, except for peptide 4 from patient 9. (Figure 6c)

Clinical responses reflected in immune analyses

We compared the level of T cell responses with the BOR of the patients. We observed that patient who was vaccinated with a higher number of immunogenic EXV-01 peptides had a better clinical outcome. This was both true when looking at responses detected in post vaccination samples (T3 and T4) and in follow up samples (FU) (Figure 7a).

However, we did not find any positive impact on the clinical outcome when compared to the size of Elispot response (Supplementary figure 10a), or the ICS detected responses neither in CD4+ T cells nor of CD8+ T cells. (Figure 7b) Interestingly, the prediction scores are clearly highest for EVX-01 peptides in clinical responders (CR/PR), both for PIONEER2 and PIONEER4. PIONEER 4 drags down the prediction score for patients with stable disease (SD) and progressive disease (PD). (Figure7c) Furthermore, PIONEER4 prediction scores obtains a better prediction score for CR, when only looking at prediction scores for immunogenic EVX-01 peptides (Supplementary figure 10b). Overall the best predictor for good clinical response is the number of immunogenic peptides contained in the EVX-01 vaccine and the prediction of such peptides are performed best using PIONEER 4.

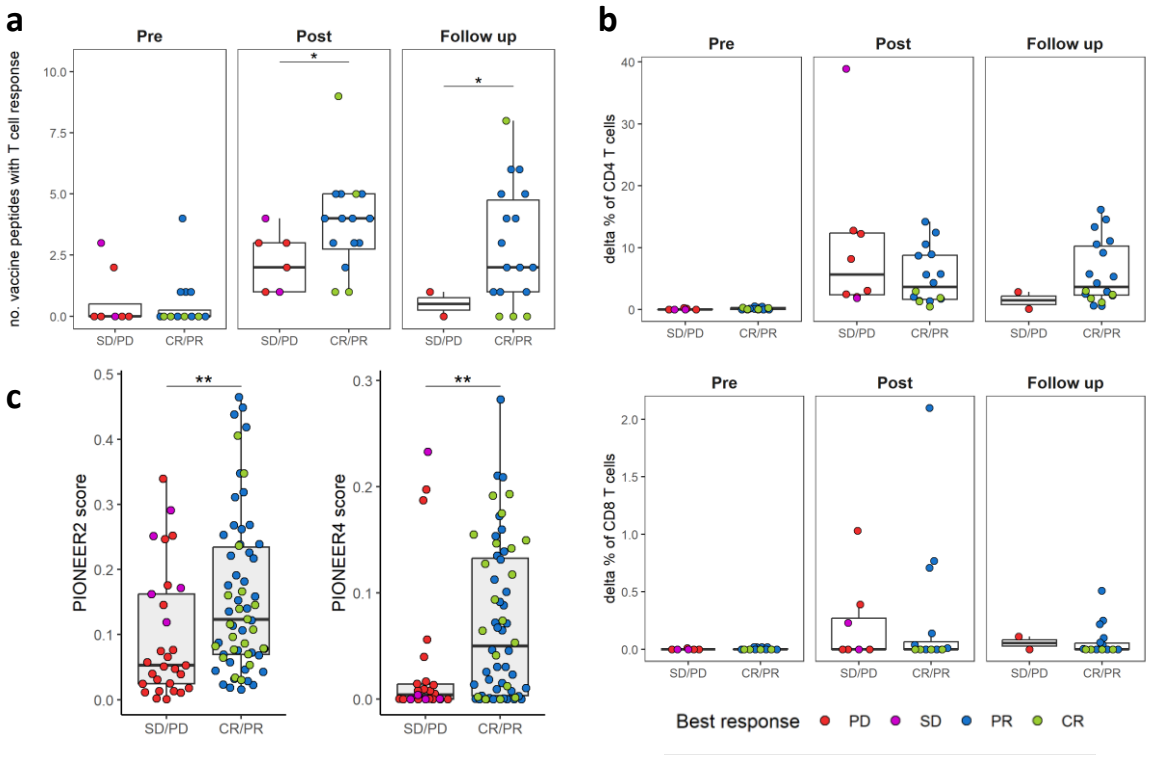

Figure 7| Clinical responses reflected immune analyses and prediction scores. Patient clinical outcomes was grouped in good response; CR- Complete Response and PR - Partial Response, and bad response; SD -Stable Disease and PD – Progressive Disease. Immune responses detected before vaccination (Pre), during and after vaccination (Post) and in follow up samples are grouped and compared to the clinical outcomes of the patients. **a)** The number of EVX-01 peptides with T cell responses detected by Elispot were compared for patients with good responses and bad responses. **b)** The frequency of functional CD4+ and CD8+ T cells responses towards EVX-01 vaccine detected by ICS was compared the two patient groups. **c)** The prediction scores for all EVX-01 peptides (both from PIONEER2 and PIONEER4) was compared between patients with good responses and – bad responses. Means was compared between response groups using t test. Significant difference is indicated with asterisks (* - p<0.05, ** - p<0.01)

DISCUSSION

In this study, patients with metastatic melanoma were recruited for treatment with a personalized neopeptide vaccine, EVX01 in combination with ICI therapy. Here we address the safety of the vaccine in three escalating dose levels. We found the treatment was safe at increased dose levels. Two serious events were observed in two patients in the highest dose group, but most likely caused by ICI treatment. Thus, we show that the combination of the EVX-01 vaccine in combination with aPD1 only adds mild side effects comparable to aPD1 treatment alone and similar clinical trials(7). This is in contrast to the known high risk of severe toxicity (>50% grade 3-4 AEs) for the combination of aPD1 and aCTLA4(28). Of 12 patients included at the three dose levels in this phase I study, eight showed an objective response (CR and PR). All patients initiated aPD1 treatment prior to the addition of the EVX-01 vaccine, and it is therefore not possible to conclude the potential clinical benefit of adding the vaccine, from this study.

This is in line with Ott et al. who also observed responses in melanoma patients treated with both aPD1 and their neoantigen vaccine(7). Patient 8 had SD at baseline after ICI treatment and developed PR after six vaccinations, which could indicate that the EVX-01 vaccine boosted anti-tumor efficacy. However, the treatment of more patients with SD before EVX-01 vaccination would be needed to document this potential effect. A larger and randomized trial is needed to investigate the potential clinical benefit of EVX-01 combined with aPD1 over ICI alone.

We found robust EVX-01-specific T cell responses in all patients, but no apparent differences between the three dose levels (Figure 2a). We found that the vaccination dosage of the single peptide can impact on the size of response, as we observed larger Elispot responses for peptides vaccinated with a higher dose of the single EVX-01 peptides (Figure 2b). Similar results were seen in a recent study, where patients receiving the highest vaccine dose developed a stronger immune response(29). In contrast, other studies have reported that lower dosage creates a better immunogenic response than a high dosage(30). However, every EVX-01 vaccine is personalized and therefore contains different neopeptides, with individual immunogenicity and avidity, which could explain differences in optimal dose levels. Of note, we observe that the fraction of de novo responses, defined by peptides that are not detected before vaccination, were decreasing during dose escalation (Table 3). It could be speculated whether the increase in vaccination dose, leads to a better activation of pre-existing dormant specific T cells.

The immunogenic responses were dominated by CD4 responses, which is similar to observations from other trials also reporting CD4+ T cell dominated responses (7,12,13,31). EVX-01-specific CD8+ T cell responses were detected at all dose levels, with the highest response at dose level 2 in patient 8. Furthermore, patient 8 is also the only patient that had a persistent CD8+ T cell response in follow up samples, while CD4+ T cells demonstrated long-lasting responses after vaccine termination. Perhaps the dominating CD4+ T cell responses play a role in priming and enhancing CD8+ T cells(32,33), why it might be more pronounced than the CD8+ T cell response. It has previously been described that, IP administration route in mouse models, induced stronger CD8+ T cell responses(16). However, we could not confirm an increase of CD8 T cell response after IP administration (T3) compared to IM administration (T4). In fact, patient 8 with the most dominant CD8 response, showed the highest response at T4 (IM). However, a larger cohort should be evaluated to investigate this in depth. Additionally, if the administration routes had been reversed, the immune response could show a different pattern supporting previous mouse studies.

Vaccine-specific neoepitope reactive CD8 T cells (VaccNARTs) was low frequent in expanded PBMCs. Two vaccine induced responses was detected in patient 6 at low frequencies after vaccination (T3). However, these two peptides were not detected by Elispot, indicating that these CD8+ T cell driven immune response were too small to be detected in Elispot. A recent in vivo study have shown impressive CD8+ T cell responses, when vaccinated with 29mer peptide comprising a MHC class I epitopes conjoined with a universal helper epitope, P30(15). Therefore, the absence of larger CD8+ T cell response could be due to long vaccine peptide spanning the native peptides around the neoepitope rather than a helper epitope, as shown by Swartz et al(15). However, the long vaccine peptides was chosen as they can contain both CD4 and CD8 epitopes and as they are less likely to be silenced by immune tolerance or degradation(34,35). A more pronounced CD8+ T cell response could potentially also be detected if using short EVX-01 peptide pool for assay stimulation– however this was not feasible due to tissue limitations.

We examined CD8+ T cell responses ex vivo in PBMCs, to investigate the effect of EVX-01 vaccine unbiased by pre-stimulation. Minor neoepitope spreading within non-vaccine-related predicted neo-peptides was detected in few patients. This was most pronounced after ICI corresponding to previous report showing ICI-induced increase in the number of NARTs in blood(36).

We further evaluated the scores obtained with the AI prediction tool, PIONEER^{TM} used for prediction of EVX-01 peptides, with our vitro results. The newest version of PIONEER^{TM} (v4) had a larger split between immunogenic and non-immunogenic based on prediction scores, together with a better placement of VaccNART detected EVX-01 peptides (Figure 6c). These results taken together with a better positive correlation between clinical outcome and prediction score(Figure 7c and Supplementary figure 10b), the newer version of PIONEER^{TM} are seemingly better at predicting immunogenic peptides with both CD4+ and CD8+ T cell responses. A new cohort could therefore benefit from the observed improvement of vaccine prediction tool.

Finally, we found that a higher fraction and number of immunogenic EVX-01 peptides, was correlated with clinical response (Figure7a, Supplementary figure 11). It appears that the number of immunogenic peptides are of importance for clinical response and longer PFS, rather than the size of response towards single vaccine embedded peptides. A broader T cell responses will reduce the risk of tumor escape through antigen loss (6,37).

In conclusion, personalized immunotherapy is a promising approach in cancer treatment. We demonstrated that EVX-01, a personal neoantigen vaccine at three different dose levels is safe, and

capable of eliciting T cell responses in a clinical setting where patients received concurrent standard immune therapy (ICI). We detected both CD8+ and CD4+ T cell responses towards corresponding vaccine peptides and found that the number of immunogenic peptides was the only predictor for a clinical response and longer PFS. Objective responses were observed in metastatic-melanoma patients at all three dose levels. However, larger trials are warranted for further evaluation of clinical efficacy.

ACKNOWLEDGEMENT

We thank all the patients who participated in the study. We are very grateful to the Kennedy center (Genomic Center) staff for support and assistance. In addition, we thank the staff at Gastroenheden Herlev for performing needle biopsies; the staff at the Department of Urology at Herlev Hospital for performing ultrasound-guided intraperitoneal vaccinations; the PIONEER operations team for designing the personalized neoantigen vaccines; the staff at Evaxion for assay development and data interpretation; the laboratory technicians for invaluable help with handling blood samples and the vaccine preparation; the staff at SSI for data analysis and data interpretation; the Department of Oncology, Herlev Hospital, physicians and nurses for their support and loving care of the patients.

FUNDING

These works were supported by research grants by Innovation Fond Denmark and the Danish Cancer Society (Knæk Cancer).

REFERENCES

1. Bagchi S, Yuan R, Engleman EG. Immune Checkpoint Inhibitors for the Treatment of Cancer: Clinical Impact and Mechanisms of Response and Resistance. Annu Rev Pathol Mech Dis. 2021;16:223–49.
2. Twomey JD, Zhang B. Cancer Immunotherapy Update: FDA-Approved Checkpoint Inhibitors and Companion Diagnostics. AAPS J. 2021;23(2):1–11.
3. Esfahani K, Roudaia L, Buhlaiga N, Del Rincon S V., Papneja N, Miller WH. A review of cancer immunotherapy: From the past, to the present, to the future. Curr Oncol. 2020;27(S2):87–97.
4. Snyder A, Makarov V, Merghoub T, Yuan J, Zaretsky JM, Desrichard A, et al. Genetic Basis for Clinical Response to CTLA-4 Blockade in Melanoma. N Engl J Med. 2014;371(23).
5. Rizvi NA, Hellmann MD, Snyder A, Kvistborg P, Makarov V, Havel JJ, et al. Mutational landscape determines sensitivity to PD-1 blockade in non–small cell lung cancer. Science. 2015;348(6230):124.
6. Jardim DL, Goodman A, de Melo Gagliato D, Kurzrock R. The Challenges of Tumor Mutational Burden as an Immunotherapy Biomarker. Cancer Cell. 2021;39(2).
7. Ott PA, Hu-Lieskovan S, Chmielowski B, Govindan R, Naing A, Bhardwaj N, et al. A Phase Ib Trial of Personalized Neoantigen Therapy Plus Anti-PD-1 in Patients with Advanced Melanoma, Non-small Cell Lung Cancer, or Bladder Cancer. Cell. 2020;183(2):347–62.
8. Liu W, Tang H, Li L, Wang X, Yu Z, Li J. Peptide-based therapeutic cancer vaccine: Current trends in clinical application. Cell Prolif. 2021 May;54(5):1–16.
9. Leggatt GR. Peptide dose and/or structure in vaccines as a determinant of T cell responses. Vaccines. 2014;2(3):537–48.
10. Carretero-Iglesia L, Couturaud B, Baumgaertner P, Schmidt J, Maby-El Hajjami H, Speiser DE, et al. High Peptide Dose Vaccination Promotes the Early Selection of Tumor Antigen-Specific CD8 T-Cells of Enhanced Functional Competence. Front Immunol. 2020;10(January):1–16.
11. Lőrincz O, Tóth J, Molnár L, Miklós I, Pántya K, Megyesi M, et al. In Silico Model Estimates the Clinical Trial Outcome of Cancer Vaccines. Cells. 2021 Nov;10(11):3048.
12. Ott PA, Hu Z, Keskin DB, Shukla SA, Sun J, Bozym DJ, et al. An immunogenic personal neoantigen vaccine for patients with melanoma. Nature. 2017;547(7662).
13. Awad MM, Govindan R, Balogh KN, Spigel DR, Garon EB, Bushway ME, et al. Personalized neoantigen vaccine NEO-PV-01 with chemotherapy and anti-PD-1 as first-line treatment for non-squamous non-small cell lung cancer. Cancer Cell. 2022;40(9):1010–26.
14. Reintjens NRM, Tondini E, De Jong AR, Meeuwenoord NJ, Chiodo F, Peterse E, et al. Self-Adjuvanting Cancer Vaccines from Conjugation-Ready Lipid A Analogues and Synthetic Long Peptides. J Med Chem. 2020;63(20).
15. Swartz AM, Congdon KL, Nair SK, Li QJ, Herndon JE, Suryadevara CM, et al. A conjoined universal helper epitope can unveil antitumor effects of a neoantigen vaccine targeting an MHC class I-restricted neoepitope. npj Vaccines. 2021;6(1).

16. Schmidt ST, Khadke S, Korsholm KS, Perrie Y, Rades T, Andersen P, et al. The administration route is decisive for the ability of the vaccine adjuvant CAF09 to induce antigen-specific CD8+ T-cell responses: The immunological consequences of the biodistribution profile. J Control Release. 2016;239:107.

17. Mørk SK, Kadivar M, Bol KF, Draghi A, Westergaard MCW, Skadborg SK, et al. Personalized therapy with peptide-based neoantigen vaccine (EVX-01) including a novel adjuvant, CAF®09b, in patients with metastatic melanoma. Oncoimmunology. 2022;11(1).

18. WMA DECLARATION OF HELSINKI – ETHICAL PRINCIPLES FOR MEDICAL RESEARCH INVOLVING HUMAN SUBJECTS.

19. GCP. GCP guidelines.

20. Donia M, Junker N, Ellebaek E, Andersen MH, Straten PT, Svane IM. Characterization and Comparison of 'Standard' and 'Young' Tumour-Infiltrating Lymphocytes for Adoptive Cell Therapy at a Danish Translational Research Institution. Scand J Immunol. 2012;75(2):157–67.

21. Andersen R, Borch TH, Draghi A, Gokuldass A, Rana AHM, Pedersen M, et al. T cells isolated from patients with checkpoint inhibitor-resistant melanoma are functional and can mediate tumor regression. Ann Oncol. 2018;29(7):1575–81.

22. Donia M, Junker N, Ellebaek E, Andersen MH, Straten PT, Svane IM. Characterization and comparison of "standard" and "young" tumour-infiltrating lymphocytes for adoptive cell therapy at a Danish translational research institution. Scand J Immunol. 2012;75(2):157–67.

23. Reynisson B, Alvarez B, Paul S, Peters B, Nielsen M. NetMHCpan-4.1 and NetMHCIIpan-4.0: Improved predictions of MHC antigen presentation by concurrent motif deconvolution and integration of MS MHC eluted ligand data. Nucleic Acids Res. 2021;48(W1).

24. Andersen RS, Kvistborg P, Mørch Frøsig T, Pedersen NW, Lyngaa R, Bakker AH, et al. Parallel detection of antigen-specific t cell responses by combinatorial encoding of MHC multimers. Nat Protoc. 2012;7(5).

25. Hadrup SR, Bakker AH, Shu CJ, Andersen RS, van Veluw J, Hombrink P, et al. Parallel detection of antigen-specific T-cell responses by multidimensional encoding of MHC multimers. Nat Methods. 2009;6(7).

26. Bjerregaard AM, Nielsen M, Hadrup SR, Szallasi Z, Eklund AC. MuPeXI: prediction of neo-epitopes from tumor sequencing data. Cancer Immunol Immunother. 2017 Sep 1;66(9):1123–30.

27. Bentzen AK, Marquard AM, Lyngaa R, Saini SK, Ramskov S, Donia M, et al. Large-scale detection of antigen-specific T cells using peptide-MHC-I multimers labeled with DNA barcodes. Nat Biotechnol. 2016 Oct 1;34(10):1037–45.

28. Wolchok JD, Kluger H, Callahan MK, Postow MA, Rizvi NA, Lesokhin AM, et al. Nivolumab plus Ipilimumab in Advanced Melanoma. N Engl J Med. 2013 Jul;369(2):122–33.

29. Brunsvig PF, Guren TK, Nyakas M, Steinfeldt-Reisse CH, Rasch W, Kyte JA, et al. Long-Term Outcomes of a Phase I Study With UV1, a Second Generation Telomerase Based Vaccine, in Patients With Advanced Non-Small Cell Lung Cancer. Front Immunol. 2020;11.

30. Rhodes S. Dose finding for new vaccines: The role for immunostimulation/ immunodynamic

modelling. HHS public access J Theor Biol. 2019;465:51–5.

31. Sahin U, Derhovanessian E, Miller M, Kloke BP, Simon P, Löwer M, et al. Personalized RNA mutanome vaccines mobilize poly-specific therapeutic immunity against cancer. Nature. 2017;547(7662).

32. Krawczyk CM, Shen H, Pearce EJ. Memory CD4 T cells enhance primary CD8 T-cell responses. Infect Immun. 2007;75(7).

33. Phares TW, Stohlman SA, Hwang M, Min B, Hinton DR, Bergmann CC. CD4 T Cells Promote CD8 T Cell Immunity at the Priming and Effector Site during Viral Encephalitis. J Virol. 2012;86(5).

34. Aldous AR, Dong JZ. Personalized neoantigen vaccines: A new approach to cancer immunotherapy. Bioorganic Med Chem. 2018;26(10).

35. Slingluff CL. The present and future of peptide vaccines for cancer: Single or multiple, long or short, alone or in combination? Cancer J. 2011;17(5).

36. Holm JS, Funt SA, Borch A, Munk KK, Bjerregaard AM, Reading JL, et al. Neoantigen-specific CD8 T cell responses in the peripheral blood following PD-L1 blockade might predict therapy outcome in metastatic urothelial carcinoma. Nat Commun. 2022;13(1).

37. Lang F, Schrörs B, Löwer M, Türeci Ö, Sahin U. Identification of neoantigens for individualized therapeutic cancer vaccines. Nat Rev Drug Discov. 2022;21(4).

SUPPLEMENTARY MATERIAL

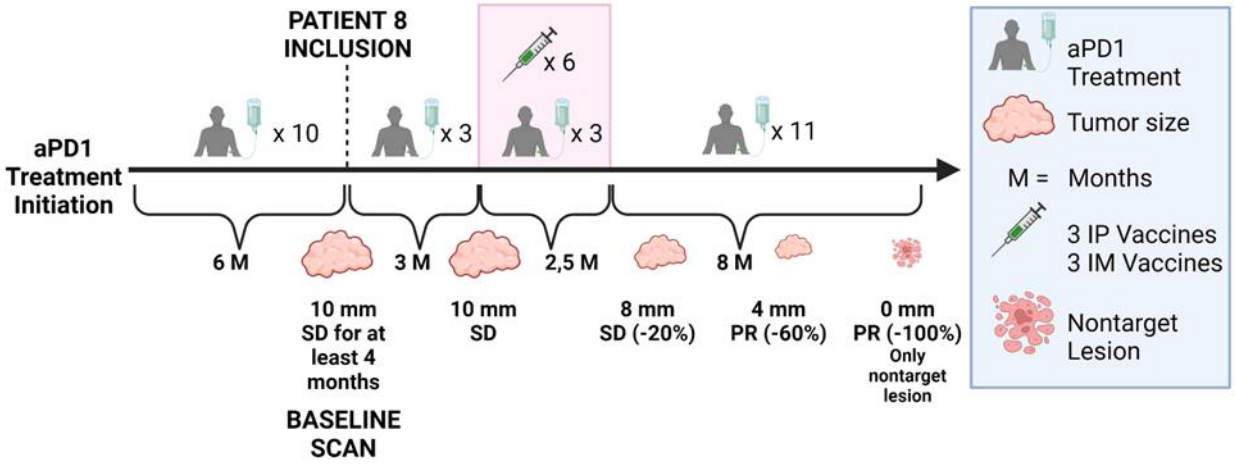

Supplementary Figure 1 | Tumor response in patient 8 during treatment timeline. The patient was included after ten aPD-1 treatments. The patient was evaluated to have had SD for at least four months before inclusion. During vaccine production, the patient received additional three aPD1 treatments. Control scan placed after the first vaccination still showed SD. After additional six vaccinations and three aPD-1 treatments, the control scan showed tumor regression, which continued 11 months from the first vaccination. The scan showed complete regression in the target lesion but still visible non-target lesions, so we define the state as PR and not complete response (CR). Figure created with BioRender.com

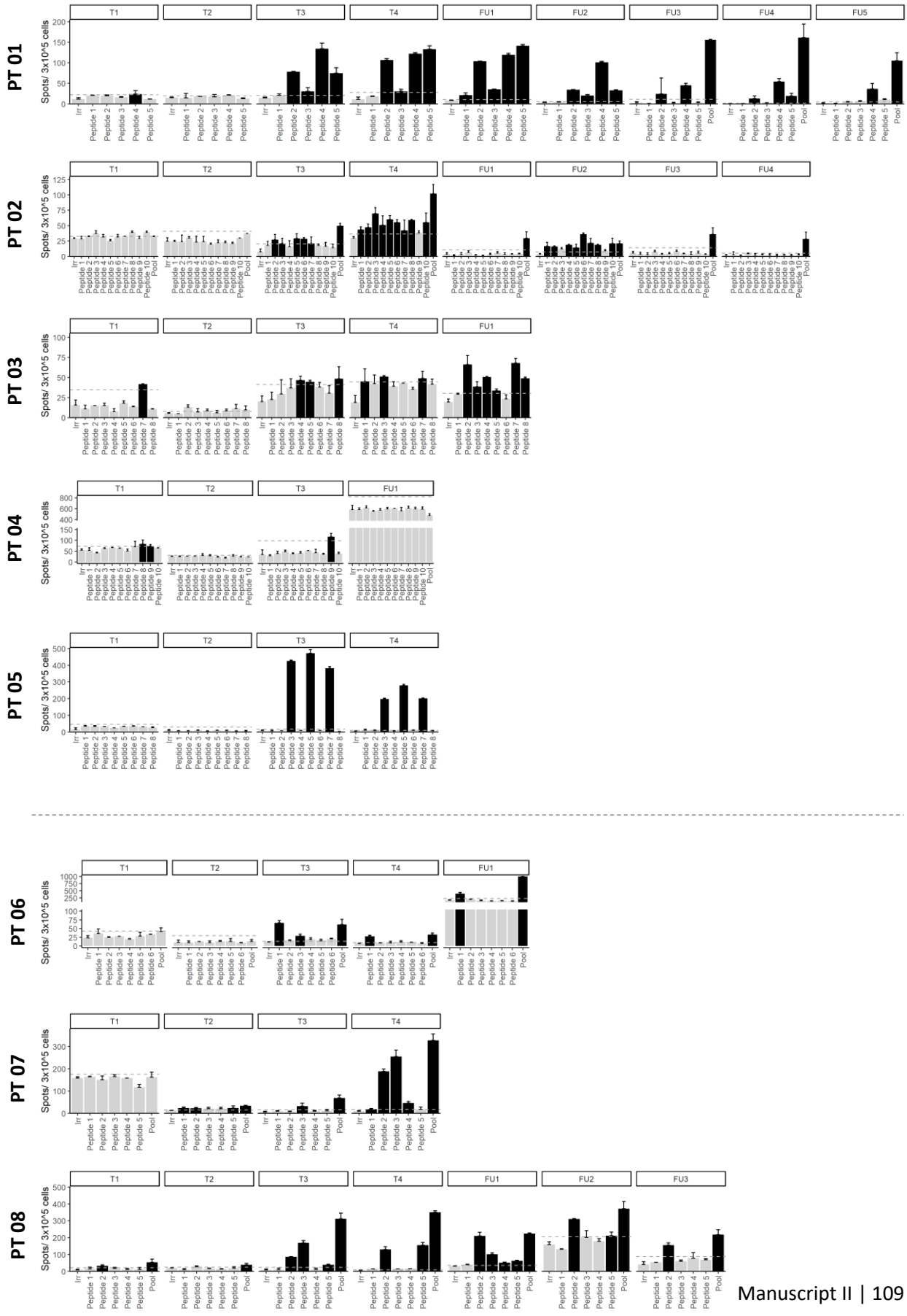
PT 01
PT 02
PT 03
PT 04
PT 05
PT 06
PT 07
PT 08
T1
T2
T3
T4
FU1
FU2
FU3
FU4
FU5
Spots/ 3x10^5 cells
Irr
Peptide 1
Peptide 2
Peptide 3
Peptide 4
Peptide 5
Peptide 6
Peptide 7
Peptide 8
Peptide 9
Peptide 10
Pool

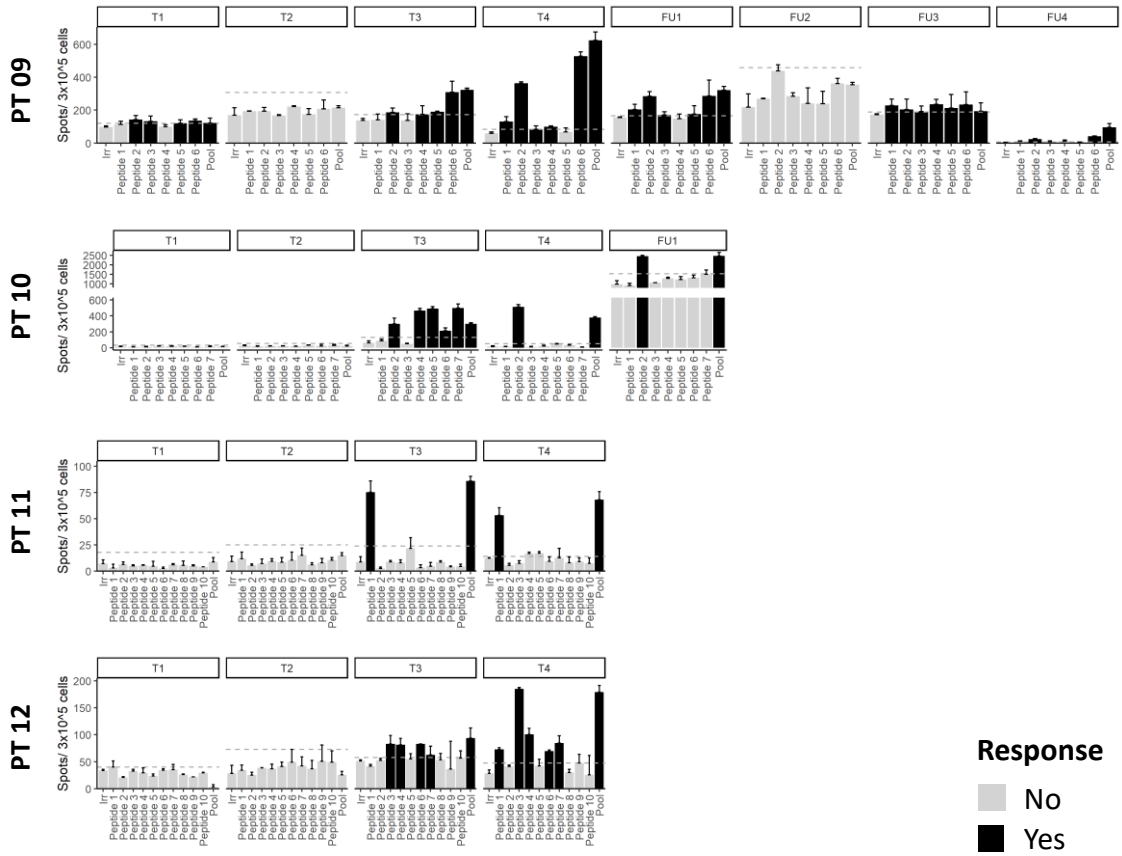

Supplementary Figure 2 | EVX-01-specific PBMC derived T cell responses analyzed by Elispot. PBMC have been pre-stimulated with patient-specific vaccine-peptide pool, for 10-14 days prior to Elispot analysis. Each graph represents one patient, divided in following time points, T1; before ICI, T2; after ICI, before vaccine, T3; after vaccine, 3 IP injections, T4; after additional 3 IM vaccine injections, and FU; follow up samples. The x-axis shows the peptides used for re-stimulation, including single vaccine peptides (Peptide 1, Peptide 2 and so on), pooled vaccine peptides (pool) and an irrelevant peptide (Irr). Black bars represent significant responses, grey bars are not significant. The dotted line indicated the threshold value for a significant response; background(irrelevant peptide) plus 3xSD of the background and at least 10 spots over background response. Note! y-axis differs between patients.

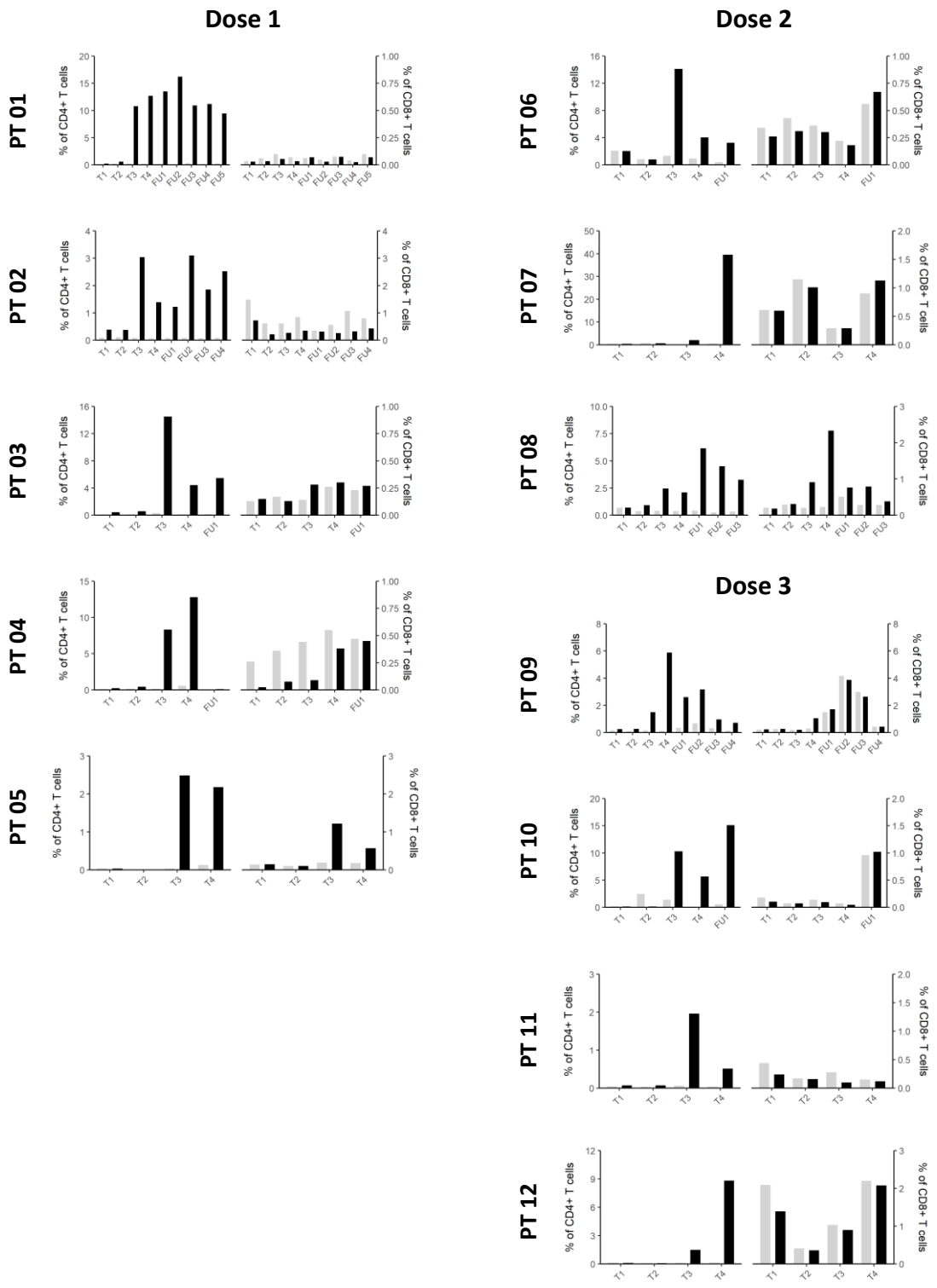

Supplementary Figure 3 | EVX-01 induced CD4+ and CD8+ T cell responses in PBMCs before and after vaccination. PBMC have been pre-stimulated with patient-specific vaccine-peptide pool, for 10-14 days prior to analysis. T cell responses showed after re-stimulation with pool vaccine peptides and stained intracellularly for IFN-γ, TNF-α, CD107a and CD137. The bars shows the percentage of cells, which are positive for at least two of above-mentioned markers. CD4+ T cells responses are shown to the left and CD8+ T cell responses to the right. Grey bars shows response after re-stimulation with irrelevant peptide, thus showing background response. Black bars shows response after re-stimulation with pooled vaccine peptides. A response exceeding background response is defined as a vaccine-specific response.

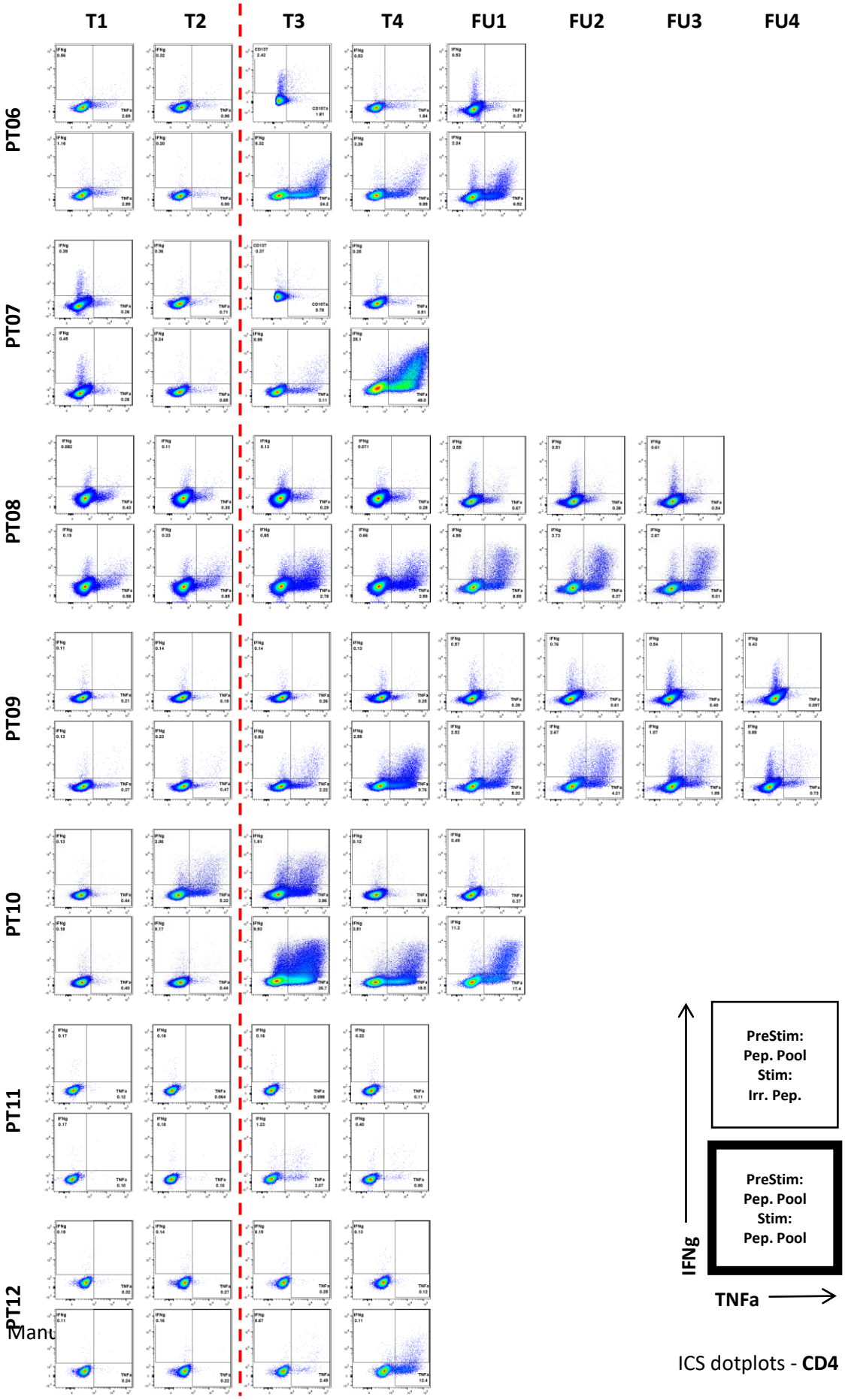

ICS dotplots - **CD4**

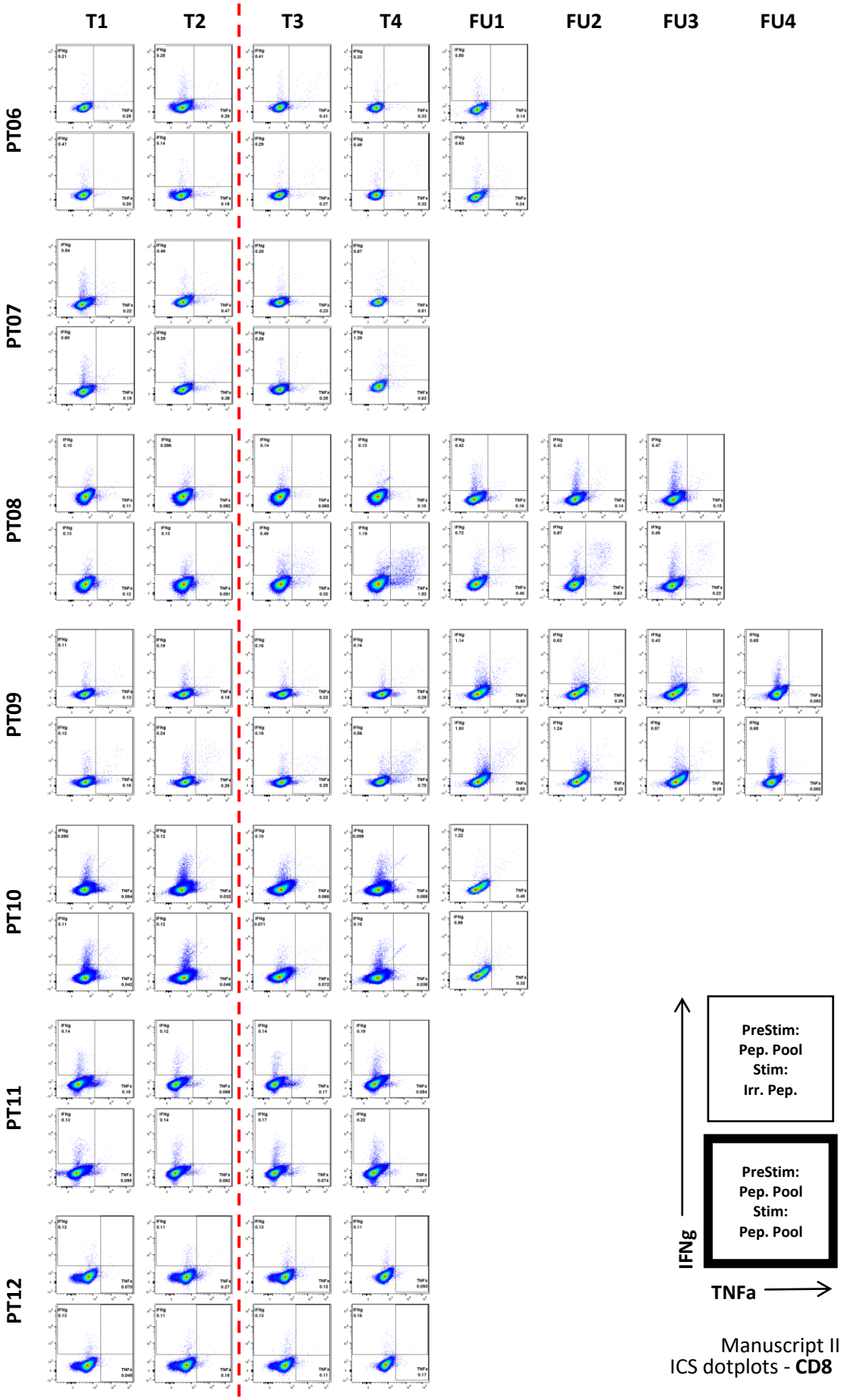

ICS dotplots - **CD8**

Supplementary Figure 4 | ICS flow cytometry dotplots. PBMC have been pre-stimulated with patient-specific vaccine-peptide pool, for 10-14 days prior to analysis. T cell responses showed after re-stimulation with pool vaccine peptides and stained intracellularly for IFN-γ, TNF-α, CD107a and CD137. Flow cytometry dotplots are shown for each patient. The top row per patient show responses to irrelevant peptide and the bottom shows responses towards peptide pool. Flow cytometry dotplots are shown for CD4+ and CD8+ T cell expression of INF-g and TNF-a. The red dotted line separate time points before and after EVX-01 vaccination

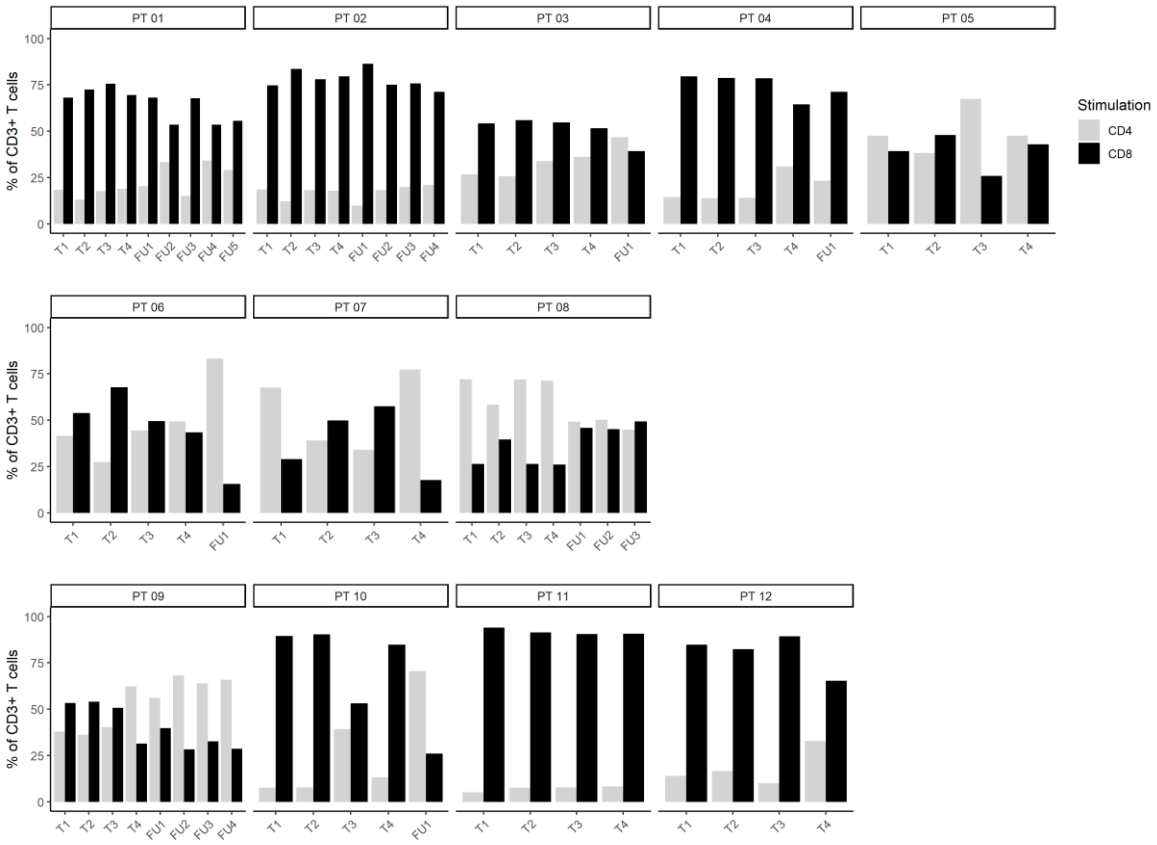

Supplementary Figure 5 |Distribution of CD4+ and CD8+ T cells after vaccine prestimulation. Graphs showing percentage of CD4+ T cells (grey) and CD8+ T cells (black) in pre-stimulated and re-stimulated PBMC cultures. Cultures were pre-stimulated for 10-14 days and re-stimulated for 8 hours, both with pooled vaccine peptides.


PT 01
Peptide 01 (50 µg)
C5orf42
S2747F
Peptide 02 (100 µg)
SLC25A28
P107L
Peptide 03 (100 µg)
SNAP47
H261Y
Peptide 04 (100 µg)
STOML2
G31A
Peptide 05 (100 µg)
VPS13A
T979I
HLA
a A0101
a A2402
a B0702
a B0801
a C0701
a C0702
a NA
PT 02
Peptide 01 (50 µg)
IFT80
Q510H
Peptide 02 (50 µg)
GPR180
I430L
Peptide 03 (50 µg)
HMGXB4
S89L
Peptide 04 (50 µg)
RBMS3
M332I
Peptide 05 (50 µg)
DDX10
S557F
Peptide 06 (50 µg)
ABCA8
P649S
Peptide 07 (50 µg)
DIDO1
P1523S
Peptide 08 (50 µg)
RBAK
H339Y
Peptide 09 (50 µg)
MAP4
D305N
Peptide 10 (50 µg)
CRCP
T119I
HLA
a A0201
a A2402
a B1501
a C0401
a NA
PT 03
Peptide 01 (50 µg)
FLNB
E1128K
Peptide 02 (50 µg)
CUL9
G2433D
Peptide 03 (50 µg)
AGTPBP1
D36N
Peptide 04 (50 µg)
UPF1
F558L
Peptide 05 (100 µg)
ATP10D
P55S
Peptide 06 (50 µg)
COL22A1
R271Q
Peptide 07 (50 µg)
LIG3
P535S
Peptide 08 (50 µg)
PEAK1
P1633S
HLA
a A1101
a B3501
a C0401
a NA
PT 04
Peptide 01 (50 µg)
HTT
P2579S
Peptide 02 (50 µg)
VPS13D
S2068F
Peptide 03 (50 µg)
TMEM132A
P94L
Peptide 04 (50 µg)
FZD3
C73S
Peptide 05 (50 µg)
ZNF461
H397P
Peptide 06 (50 µg)
RRBP1
L783F
Peptide 07 (50 µg)
TCN1
K233N
Peptide 08 (50 µg)
FAM193B
E91K
Peptide 09 (50 µg)
FZD5
E202K
Peptide 10 (50 µg)
ERN1
P75S
HLA
a A0201
a B1801
a C0701
a NA
PT 05
Peptide 01 (50 µg)
CD3EAP
P157L
Peptide 02 (50 µg)
C2CD2
V296A
Peptide 03 (100 µg)
SEZ6L
H457Y
Peptide 04 (50 µg)
CD3EAP
P473S
Peptide 05 (50 µg)
SLC15A4
M179I
Peptide 06 (50 µg)
HIST1H1C
L107R
Peptide 07 (50 µg)
NUP188
A627G
Peptide 08 (50 µg)
ZBTB33
P140T
HLA
a A0101
a A0201
a B3503
a B4001
a C0304
a NA


PT 06
Peptide 01 (100 µg)
KNTC1
S2177L
Peptide 02 (100 µg)
SBF1
P877L
Peptide 03 (200 µg)
CDK13
L552M
Peptide 04 (200 µg)
NUPL2
N212Y
Peptide 05 (200 µg)
ZNF774
S43F
Peptide 06 (200 µg)
ACSM3
G53R
HLA
a A0201
a A1101
a B1501
a B5101
a C0304
a NA
PT 07
Peptide 01 (200 µg)
MLLT6
P386L
Peptide 02 (200 µg)
TONSL
D688E
Peptide 03 (200 µg)
ROBO4
G69R
Peptide 04 (200 µg)
RIF1
P392S
Peptide 05 (200 µg)
KMT2B
P1854S
HLA
a A2402
a B1501
a C0102
a NA
PT 08
Peptide 01 (200 µg)
TMF1
P113L
Peptide 02 (200 µg)
ABCD1
E155V
Peptide 03 (200 µg)
NUDT9
H324P
Peptide 04 (200 µg)
POGZ
T270I
Peptide 05 (200 µg)
TCF4
P156S
HLA
a A0201
a A0301
a B3501
a B4001
a C0304
a C0401
a NA

Supplementary Figure 6 | information on vaccine peptides, and screened vaccine-related minimal peptides. Information on vaccine peptides; vaccpep number, intended vaccination dose, gene origin, and amino acid mutation (incl site) is noted above each vaccine peptide. The wild type sequence is shown in the top and the mutated (vaccine peptide) is shown below (black sequences). All screened vaccine-related, minimal peptides are aligned to each vaccine peptide. Minimal peptides are colored according to HLA-binding and mutated minimal peptides are marked in *italic*.

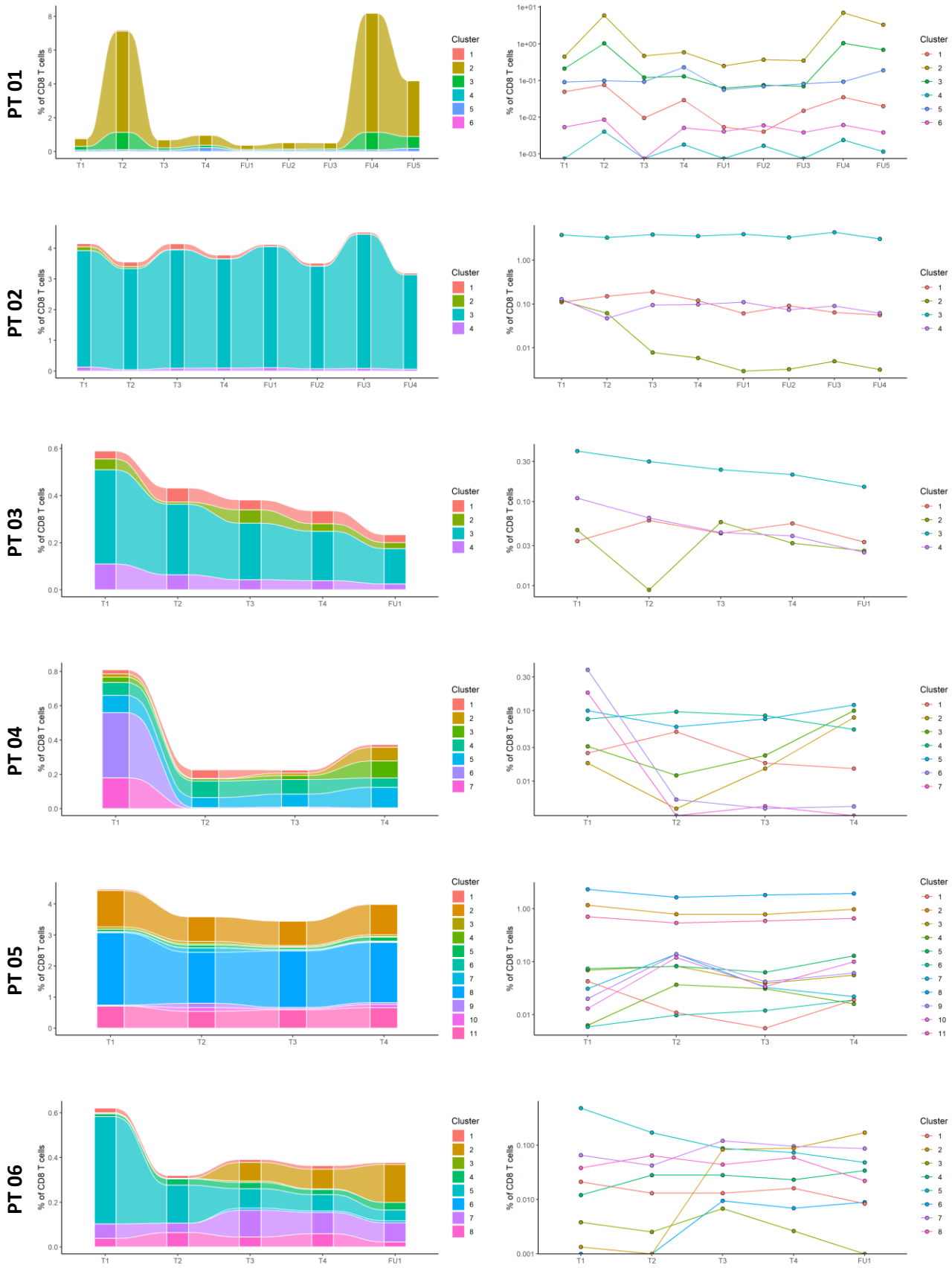
PT 01
PT 02
PT 03
PT 04
PT 05
PT 06
% of CD8 T cells
Cluster

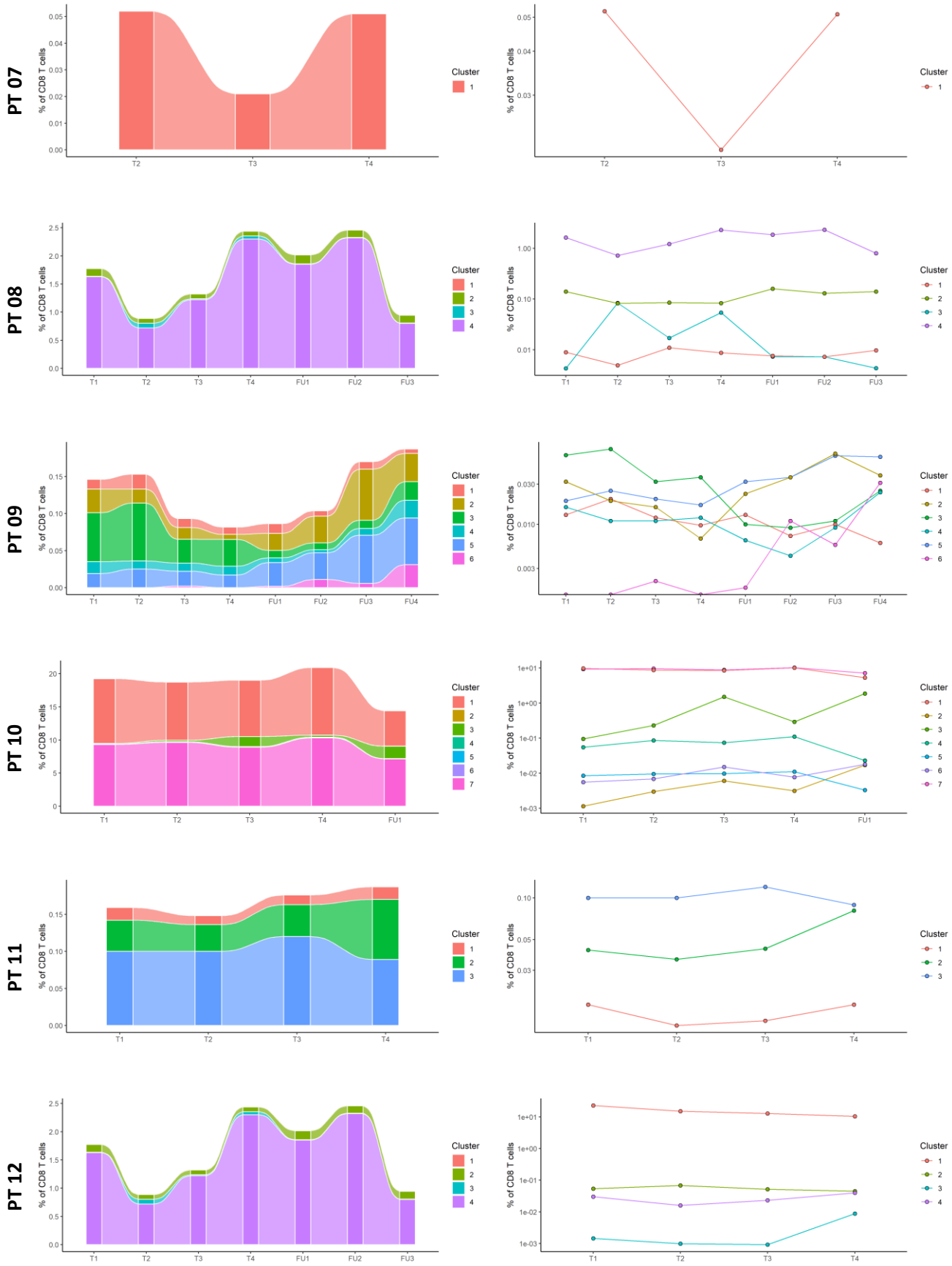
PT 07
PT 08
PT 09
PT 10
PT 11
PT 12
% of CD8 T cells
Cluster

Supplementary Figure 7 | VaccNART screening results per patient and cluster. EVX-01 prestimulated PBMC were screened for EVX-01 specific CD8 T cells (VaccNARTs) using fluorochrome labelled pMHC-multimers. VaccNARTs are gated in clusters with one or more specificities due to overlap cross reactivity between sequences. The frequency of VaccNART clusters detected in EVX-01 expanded PBMC from different time point. To the left, a flow plot showing the collected frequency per patient. Each color represents a single cluster. To the right, plot showing the frequency of single clusters, which are connected with lines between time point.

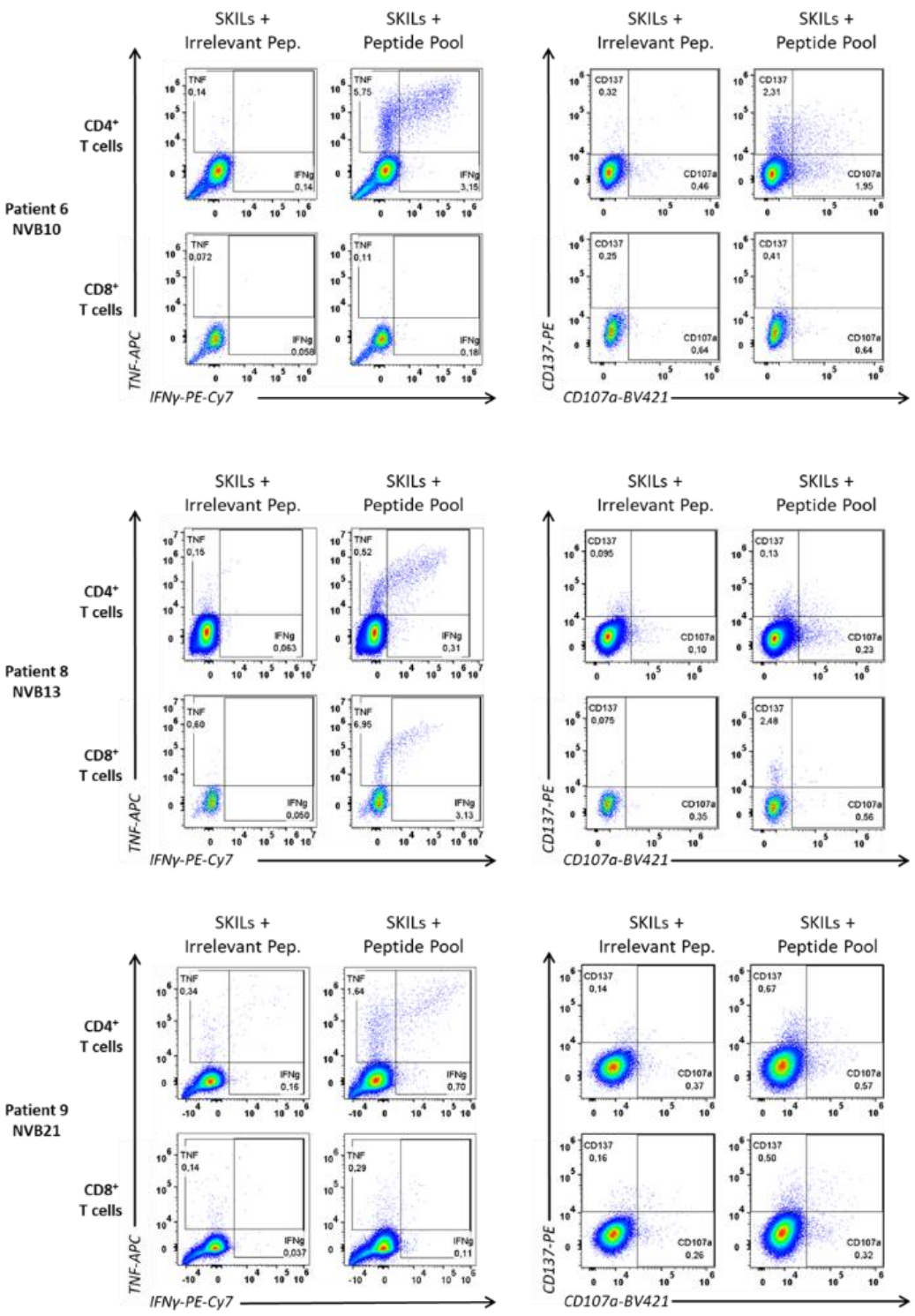

Supplementary Figure 8 | EVX-01-specific T cell responses in SKILs (skin-test infiltrating lymphocytes) EVX-01-specific CD8+ and CD4+ T cells were identified by intracellular cytokine stain in the SKILs isolated from patients 6, 8 and 9.

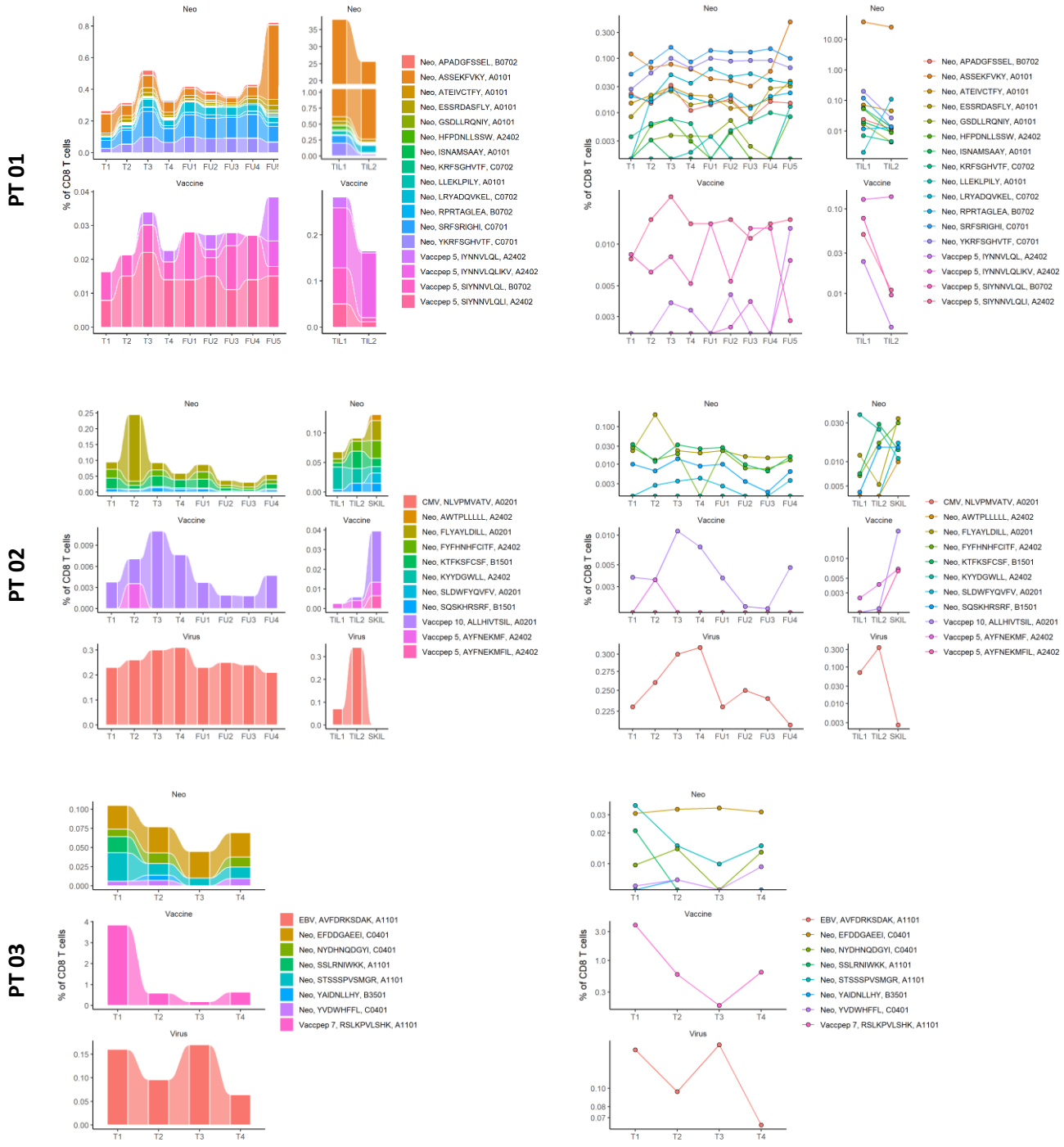
PT 01
PT 02
PT 03
Neo
Vaccine
Virus
% of CD8 T cells
Neo, APADGFSSEL, B0702
Neo, ASSEKFVKY, A0101
Neo, ATEIVCTFY, A0101
Neo, ESSRDASFLY, A0101
Neo, GSDLLRQNIY, A0101
Neo, HFPDNLLSSW, A2402
Neo, ISNAMSAAY, A0101
Neo, KRFSGHVTF, C0702
Neo, LLEKLPILY, A0101
Neo, LRYADQVKEL, C0702
Neo, RPRTAGLEA, B0702
Neo, SRFSRIGHI, C0701
Neo, YKRFSGHVTF, C0701
Vaccpep 5, IYNNVLQL, A2402
Vaccpep 5, IYNNVLQLIKV, A2402
Vaccpep 5, SIYNNVLQL, B0702
Vaccpep 5, SIYNNVLQLI, A2402
CMV, NLVPMVATV, A0201
Neo, AWTPLLLLL, A2402
Neo, FLYAYLDILL, A0201
Neo, FYFHNHFCITF, A2402
Neo, KTFKSFCSF, B1501
Neo, KYYDGWLL, A2402
Neo, SLDWFYQVFV, A0201
Neo, SQSKHRSRF, B1501
Vaccpep 10, ALLHIVTSIL, A0201
Vaccpep 5, AYFNEKMF, A2402
Vaccpep 5, AYFNEKMFIL, A2402
EBV, AVFDRKSDAK, A1101
Neo, EFDDGAEEI, C0401
Neo, NYDHNQDGYI, C0401
Neo, SSLRNIWKK, A1101
Neo, STSSSPVSMGR, A1101
Neo, YAIDNLLHY, B3501
Neo, YVDWHFFL, C0401
Vaccpep 7, RSLKPVLSHK, A1101

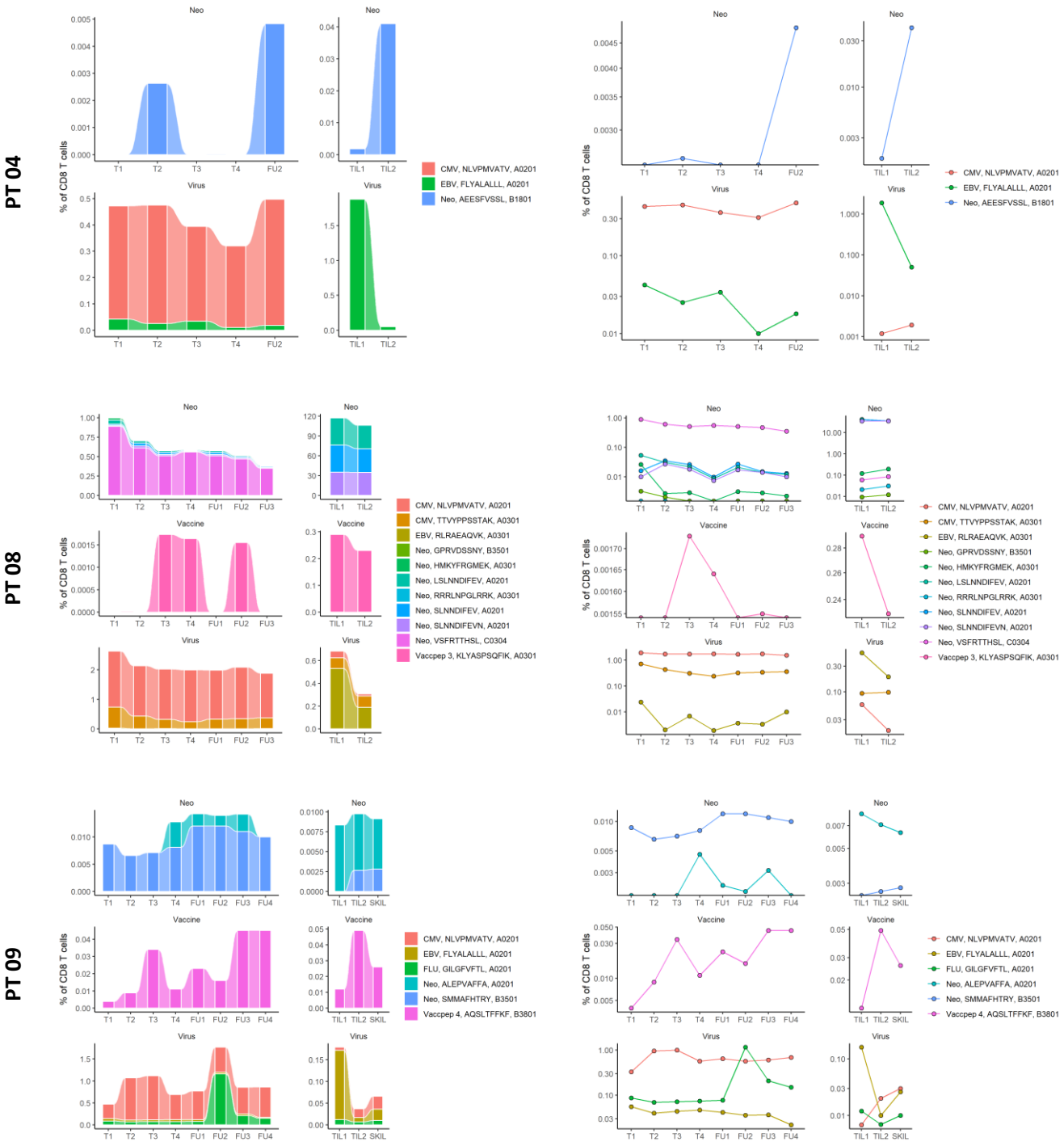

Supplementary Figure 9 | Patient specific results for analysis of epitope spreading detected in *ex vivo* PBMCs, and expanded TILs and SKILs. *Ex vivo* PBMC and expanded TILs and SKILs were screened for neoepitope specific CD8+ T cells and virus specific CD8+ T cells (VARTs). Neoepitope specific CD8+ T cells were split into two categories; CD8+ T cells recognizing EVX-01-embedded neopeptides, are referred to as VaccNARTs and CD8+ T cells recognizing the remaining non-EVX-01-embedded neopeptides, are referred to as NARTs. The frequency of NARTs (neo), VaccNART (Vaccine) and VARTs (virus) populations detected in *ex vivo* PBMCs and expanded TILs is shown for each patient. To the left, a flow plot showing the collected frequency per patient. Each color represents a single specificity. To the right, plot showing the frequency of single specificities, which are connected with lines between time point.

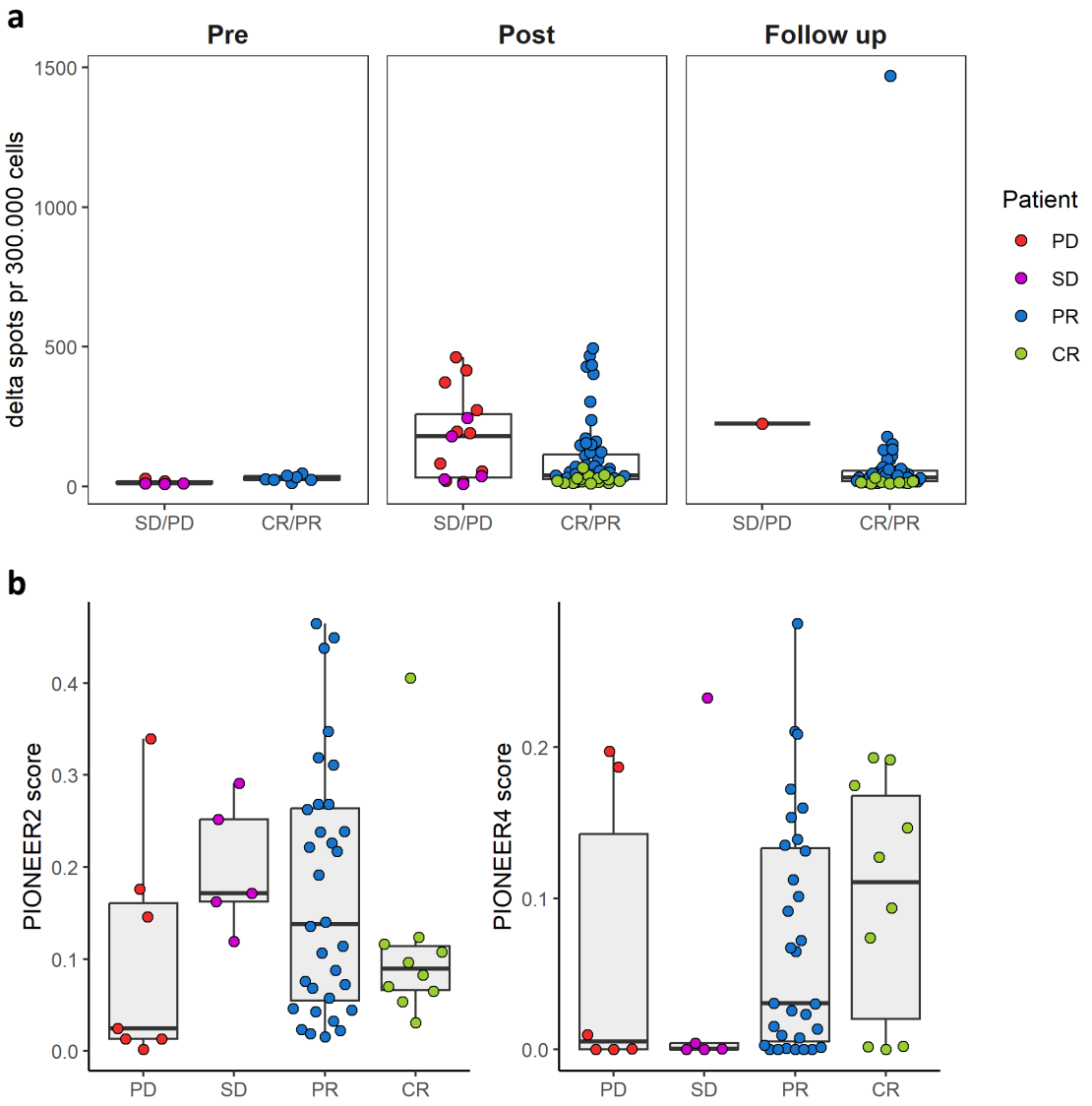

Supplementary Figure 10 | Clinical responses reflected immune analyses and prediction scores. Patient clinical outcomes was grouped in good response; CR- Complete Response and PR - Partial Response, and bad response; SD -Stable Disease and PD – Progressive Disease. **a)** Delta spots detected by Elispot for peptides with T cell response (background stimulated with irrelevant peptide has been subtracted) compared to clinical responses. Immune responses detected before vaccination (Pre), during and after vaccination (Post) and in follow up samples are grouped. **b)** The prediction scores (both from PIONEER2 and PIONEER4) for immunogenic peptides compared between patients different clinical responses.

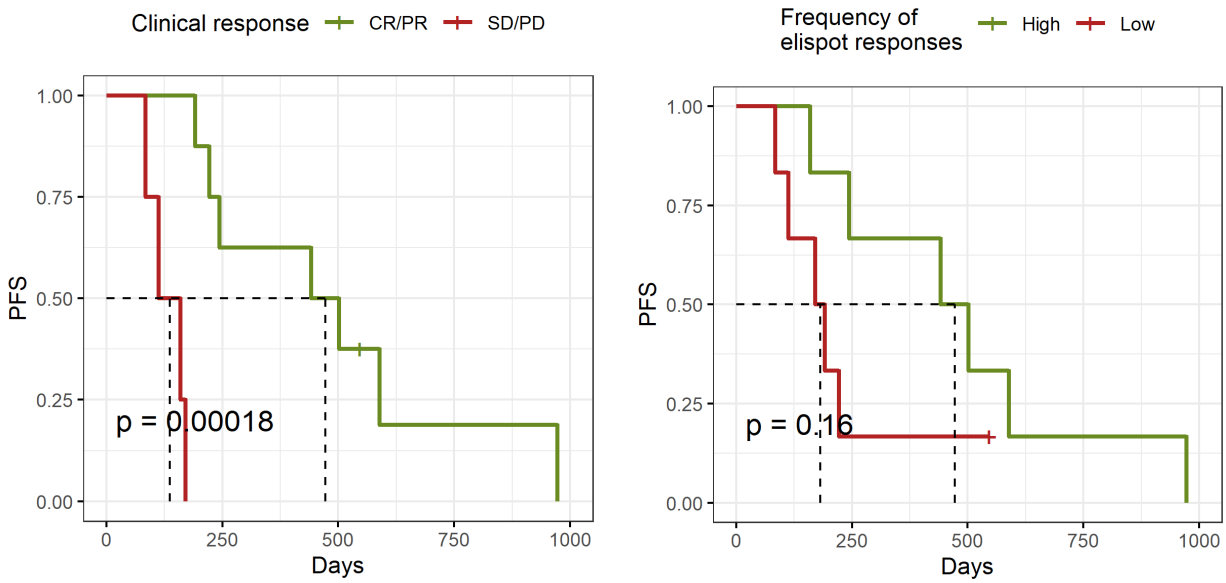

Supplementary Figure 11 | Progression free survival (PFS) compared with best objective response and the fraction of immunogic EVX-01 responses. Kaplan-Meier curve of progression free survival (PFS) for patients with **a)** good (CR/PR) vs bad(SD/PD) best objective responses and **b)** high and low fractions of single vaccine peptides with a INF-γ T cell response out of total peptides detected by Elispot.

Supplementary Table 1 | Cluster information

Patient	Cluster	Peptide sequence	HLA	Mutated	EVX-01 peptide	Color 1	Color 2
NPV02	1	GPEFKKTL	B0801	no	1	BV650	PE
NPV02	1	GPEFKKTL	B0702	no	1	BV711	PE-CF594
NPV02	1	IGPVDHIEF	A2402	no	1	PE	PE-CF594
NPV02	1	GPVDHIEFF	B0702	yes	1	BUV737	PE-CF594
NPV02	1	SGPEFKKTL	C0701	no	1	BUV737	PE-Cy7
NPV02	1	LAARYRNVL	B0702	yes	2	PE	PE-Cy7
NPV02	1	RYRNVLEAL	A2402	no	2	PE-CF594	PE-Cy7
NPV02	1	SPYEISIRQRF	B0702	no	3	BV650	PE-CF594
NPV02	1	SALPRNTVV	C0701	no	4	BV711	PE
NPV02	1	SIYNNVLQL	C0701	yes	5	BV650	PE-Cy7
NPV02	1	SIYNNVLQL	C0701	yes	5	BV650	PE-Cy7
NPV02	1	DLKSIYNNV	B0801	yes	5	BUV737	PE
NPV02	2	GPEFKKTL	B0801	no	1	BV650	PE
NPV02	3	SGPEFKKTL	B0801	no	1	BV421	BV786
NPV02	3	GPEFKKTL	B0801	no	1	BV650	PE
NPV02	3	SGPEFKKTL	C0702	no	1	BUV395	BV650
NPV02	3	SLQPDLAARY	A0101	yes	2	APC	PE
NPV02	3	RYRNVLEALW	A2402	no	2	APC	BUV395
NPV02	3	VKTRMQSL	B0801	no	2	BUV395	PE
NPV02	3	DVDDIKVYSPY	A0101	yes	3	APC	BV421
NPV02	3	YEISIRQRF	C0702	no	3	BUV737	BV786
NPV02	3	ALPRNTVVL	C0702	yes	4	BV421	BV650
NPV02	3	APRRASSAL	B0702	yes	4	BV421	PE
NPV02	3	RAPRRASSAL	B0702	yes	4	BV786	PE
NPV02	3	SIYNNVLQL	B0801	yes	5	BUV395	BV421
NPV02	3	IYNNVLQL	C0702	yes	5	BV650	BV786
NPV02	3	IYNNVLQL	C0701	yes	5	APC	BV650
NPV02	3	NVPDLKSIY	A0101	yes	5	APC	BV786
NPV02	4	LPRNTVVL	B0801	no	4	BV786	PE-Cy7
NPV02	5	QSLQPDLAARY	A0101	yes	2	APC	PE-CF594
NPV02	6	LAARYRNVL	B0702	yes	2	PE	PE-Cy7
NPV04	1	HYINSIKNL	A2402	yes	1	BV421	PE
NPV04	1	AIGEIDKVHY	B1501	yes	1	BV650	PE
NPV04	1	YYGDILSL	A2402	yes	3	BV650	PE-CF594
NPV04	1	MIGPLTQQM	A0201	yes	4	BV421	PE-CF594
NPV04	1	IFLLDEPTAGL	C0401	no	6	BV421	BV650

NPV04	1	LLDEPTAGL	A0201	no	6	PE	PE-CF594
NPV04	2	AAIGEIDKVHY	B1501	yes	1	BUV737	PE
NPV04	2	TQQMNHLSL	B1501	no	4	BV786	PE-Cy7
NPV04	2	YFNEKMFIL	A2402	yes	5	BV786	PE
NPV04	2	AYFNEKMFI	A2402	yes	5	PE	PE-Cy7
NPV04	2	LLDEPTAGL	A0201	no	6	PE	PE-CF594
NPV04	2	FLLDEPTAGL	A0201	no	6	PE-CF594	PE-Cy7
NPV04	2	SFSRHQVW	A2402	yes	6	BUV737	PE-CF594
NPV04	2	MSSPPKSSL	C0401	yes	7	BUV737	BV786
NPV04	2	LPTEKEVAL	C0401	no	9	BUV737	PE-Cy7
NPV04	2	ALLHIVTSI	A0201	yes	10	BV786	PE-CF594
NPV04	3	YFNEKMFIL	C0401	yes	5	BUV395	BV650
NPV04	4	HYINSIKNL	A2402	yes	1	BV421	PE
NPV04	4	AIGEIDKVHY	B1501	yes	1	BV650	PE
NPV04	4	VHYINSIKNL	A2402	yes	1	BUV395	PE-CF594
NPV04	4	YYGDILSL	A2402	yes	3	BV650	PE-CF594
NPV04	4	YYYGDILSL	A2402	yes	3	BUV395	PE
NPV04	4	MIGPLTQQM	A0201	yes	4	BV421	PE-CF594
NPV04	4	YFNEKMFIL	C0401	yes	5	BUV395	BV650
NPV04	4	IFLLDEPTAGL	C0401	no	6	BV421	BV650
NPV04	4	LLDEPTAGL	A0201	no	6	PE	PE-CF594
NPV04	4	RTYSGEKPY	B1501	yes	8	BUV395	BV421
NPV06	1	PFDPSKVV	C0401	no	1	BUV737	BV421
NPV06	1	MPFDPSKVV	C0401	no	1	BUV737	BV786
NPV06	1	HFSYFSRSL	C0401	no	7	BV421	BV650
NPV06	1	LPRIPFRSSY	B3501	yes	8	BV421	BV786
NPV06	1	RADLPRIPF	C0401	no	8	BV650	BV786
NPV06	2	AIDSPVSLL	C0401	yes	4	BUV395	BV650
NPV06	3	EVHIPGSPFK	A1101	no	1	APC	PE-CF594
NPV06	4	SPVSLLAL	B3501	yes	4	PE	PE-Cy7
NPV07	1	YQAWDSVPSL	A0201	yes	1	BV650	PE-CF594
NPV07	1	HLYQAWDSV	A0201	yes	1	BUV737	PE-CF594
NPV07	1	EEQGAQLGV	B1801	no	3	BV711	PE-CF594
NPV07	1	EEQGAQLGVVL	B1801	yes	3	PE	PE-Cy7
NPV07	1	SSFSHHQKI	C0701	no	5	BV711	PE
NPV07	1	IRTFQEQL	C0701	yes	6	BUV737	PE-Cy7
NPV07	1	YTKSLVEKI	C0701	no	7	BV650	PE-Cy7
NPV07	1	ILSEKNENGL	A0201	yes	7	PE	PE-CF594
NPV07	1	DELLEFINST	B1801	no	8	BV650	PE
NPV07	1	DELLEFINS	B1801	no	8	BUV737	PE
NPV07	1	ELLEFINST	A0201	no	8	PE-CF594	PE-Cy7

NPV07	1	KSHPLYNKV	C0701	yes	9	BV711	PE-Cy7
NPV07	2	ENIATHHLY	C0701	no	1	BV421	BV650
NPV07	2	YQAWDSVPSL	A0201	yes	1	BV650	PE-CF594
NPV07	2	QAWDSVPSL	C0701	yes	1	BUV395	BV650
NPV07	2	HLYQAWDSV	A0201	yes	1	BUV737	PE-CF594
NPV07	2	LFAGFPGTF	C0701	no	2	BUV395	BV421
NPV07	2	LQPSHLRSL	C0701	no	3	BUV737	BV421
NPV07	2	EEQGAQLGV	B1801	no	3	BV711	PE-CF594
NPV07	2	MEPFHPMV	B1801	no	4	BV421	PE
NPV07	2	SSRDFRPFL	C0701	yes	4	BUV395	BUV737
NPV07	2	SSFSHHQKI	C0701	no	5	BV711	PE
NPV07	2	QLQGKIRTF	C0701	yes	6	BUV395	BV711
NPV07	2	ILSEKNENGL	A0201	yes	7	PE	PE-CF594
NPV07	2	KNENGLIGNTF	B1801	yes	7	BUV395	PE
NPV07	2	FINSTKPKV	A0201	yes	8	BV421	PE-CF594
NPV07	2	DELLEFINST	B1801	no	8	BV650	PE
NPV07	2	DELLEFINS	B1801	no	8	BUV737	PE
NPV07	2	ILKKSHPLY	C0701	yes	9	BV421	BV711
NPV07	2	FLSDPNDGSL	A0201	yes	10	BUV395	PE-CF594
NPV07	3	ENIATHHLY	C0701	no	1	BV421	BV650
NPV07	3	YQAWDSVPSL	A0201	yes	1	BV650	PE-CF594
NPV07	3	QAWDSVPSL	C0701	yes	1	BUV395	BV650
NPV07	3	HLYQAWDSV	A0201	yes	1	BUV737	PE-CF594
NPV07	3	LFAGFPGTF	C0701	no	2	BUV395	BV421
NPV07	3	LQPSHLRSL	C0701	no	3	BUV737	BV421
NPV07	3	EEQGAQLGV	B1801	no	3	BV711	PE-CF594
NPV07	3	MEPFHPMV	B1801	no	4	BV421	PE
NPV07	3	SSRDFRPFL	C0701	yes	4	BUV395	BUV737
NPV07	3	SSFSHHQKI	C0701	no	5	BV711	PE
NPV07	3	QLQGKIRTF	C0701	yes	6	BUV395	BV711
NPV07	3	ILSEKNENGL	A0201	yes	7	PE	PE-CF594
NPV07	3	KNENGLIGNTF	B1801	yes	7	BUV395	PE
NPV07	3	FINSTKPKV	A0201	yes	8	BV421	PE-CF594
NPV07	3	DELLEFINST	B1801	no	8	BV650	PE
NPV07	3	DELLEFINS	B1801	no	8	BUV737	PE
NPV07	3	ILKKSHPLY	C0701	yes	9	BV421	BV711
NPV07	3	FLSDPNDGSL	A0201	yes	10	BUV395	PE-CF594
NPV07	4	ENIATHHLY	C0701	no	1	BV421	BV650
NPV07	4	QAWDSVPSL	C0701	yes	1	BUV395	BV650
NPV07	4	ENIATHHLY	B1801	no	1	BV786	PE-Cy7
NPV07	4	LFAGFPGTF	C0701	no	2	BUV395	BV421

NPV07	4	AGFPGTFFL	C0701	yes	2	BUV737	BV786
NPV07	4	FLFAGFPGT	A0201	no	2	APC	PE
NPV07	4	VLLQPSHLRSL	A0201	yes	3	APC	BV421
NPV07	4	LQPSHLRSL	C0701	no	3	BUV737	BV421
NPV07	4	LLQPSHLRSL	A0201	yes	3	APC	PE-Cy7
NPV07	4	EEQGAQLGVVL	B1801	yes	3	PE	PE-Cy7
NPV07	4	MEPFHPMV	B1801	no	4	BV421	PE
NPV07	4	AMEPFHPMV	A0201	no	4	APC	BV786
NPV07	4	SRDFRPFL	C0701	no	4	BUV395	BV786
NPV07	4	AMEPFHPMVNL	A0201	no	4	APC	BUV395
NPV07	4	SSRDFRPFL	C0701	yes	4	BUV395	BUV737
NPV07	4	KAFSYPSSF	C0701	yes	5	BV650	BV786
NPV07	4	FSYPSSFSH	C0701	yes	5	APC	BV650
NPV07	4	SSFSHHQKI	C0701	no	5	BV711	PE
NPV07	4	QLQGKIRTF	C0701	yes	6	BUV395	BV711
NPV07	4	LENGPNTQL	B1801	no	6	BV786	PE
NPV07	4	QLENGPNTQL	A0201	no	6	APC	BUV737
NPV07	4	IRTFQEQL	C0701	yes	6	BUV737	PE-Cy7
NPV07	4	YTKSLVEKI	C0701	no	7	BV650	PE-Cy7
NPV07	4	GLIGNTFST	A0201	no	7	APC	BV711
NPV07	4	KNENGLIGNTF	B1801	yes	7	BUV395	PE
NPV07	4	NENGLIGNTF	B1801	yes	7	BUV395	PE-Cy7
NPV07	4	DELLEFINST	B1801	no	8	BV650	PE
NPV07	4	DELLEFINS	B1801	no	8	BUV737	PE
NPV07	4	ILKKSHPLY	C0701	yes	9	BV421	BV711
NPV07	4	REPFVPIL	B1801	no	9	BV421	PE-Cy7
NPV07	4	KSHPLYNKV	C0701	yes	9	BV711	PE-Cy7
NPV07	4	THVEEPAFL	C0701	no	10	BV421	BV786
NPV07	5	THVEEPAFL	C0701	no	10	BV421	BV786
NPV07	6	SLSPATTGA	A0201	no	1	APC	PE-CF594
NPV07	7	FLFAGFPGT	A0201	no	2	APC	PE
NPV08	1	YNATIGRVL	C0304	yes	3	BV421	BV786
NPV08	2	LVTGPRSAL	C0304	yes	1	BV786	PE-Cy7
NPV08	2	RSALAPNLL	C0304	no	1	BUV395	PE-Cy7
NPV08	2	YNATIGRVL	C0304	yes	3	BV421	BV786
NPV08	2	NATIGRVL	C0304	no	3	BUV395	BV421
NPV08	2	WTDLRHTGF	C0304	no	7	BUV395	BV786
NPV08	2	AQDGNTEPL	B4001	no	8	BV421	PE-Cy7
NPV08	3	QESRMSETV	B4001	yes	4	BV650	PE
NPV08	3	VPQEEMPGPPL	B3503	no	4	BV650	PE-CF594
NPV08	3	RMSETVPQEEM	A0201	yes	4	PE	PE-CF594

NPV08	3	LPTDSGDKNL	B3503	yes	8	BV421	PE
NPV08	3	AQDGNTEPL	A0201	no	8	BV421	PE-CF594
NPV08	4	DPAQRFSSTL	B3503	yes	2	BUV737	PE-CF594
NPV08	4	QESRMSETV	B4001	yes	4	BV650	PE
NPV08	4	VPQEEMPGPPL	B3503	no	4	BV650	PE-CF594
NPV08	4	RMSETVPQEEM	A0201	yes	4	PE	PE-CF594
NPV08	4	QEEMPGPPL	B4001	no	4	BUV737	PE
NPV08	4	RIDEQSHRL	B3503	yes	5	BV711	PE-CF594
NPV08	4	RIDEQSHRL	A0201	yes	5	PE-CF594	PE-Cy7
NPV08	4	NPGKVWTDL	B3503	yes	7	PE	PE-Cy7
NPV08	5	QLNDPAQRF	A0101	yes	2	APC	PE-CF594
NPV08	5	ATIGRVLSPSY	A0101	no	3	APC	PE
NPV08	5	RMSETVPQEEM	A0201	yes	4	PE	PE-CF594
NPV08	6	NPLVTGPRSAL	B3503	yes	1	BV786	PE-CF594
NPV08	7	NATIGRVL	C0304	no	3	BUV395	BV421
NPV08	8	LVTGPRSAL	C0304	yes	1	BV786	PE-Cy7
NPV08	9	SETVPQEEM	B4001	yes	4	BUV395	PE
NPV08	10	LVTGPRSAL	B3503	yes	1	BUV395	PE-CF594
NPV08	10	NATIGRVL	C0304	no	3	BUV395	BV421
NPV08	10	QESRMSETV	B4001	yes	4	BV650	PE
NPV08	10	VPQEEMPGPPL	B3503	no	4	BV650	PE-CF594
NPV08	10	RMSETVPQEEM	A0201	yes	4	PE	PE-CF594
NPV08	10	SETVPQEEM	B4001	yes	4	BUV395	PE
NPV08	10	LPTDSGDKNL	B3503	yes	8	BV421	PE
NPV08	10	AQDGNTEPL	A0201	no	8	BV421	PE-CF594
NPV08	11	LVTGPRSAL	C0304	yes	1	BV786	PE-Cy7
NPV08	11	RSALAPNLL	C0304	no	1	BUV395	PE-Cy7
NPV08	11	YNATIGRVL	C0304	yes	3	BV421	BV786
NPV08	11	NATIGRVL	C0304	no	3	BUV395	BV421
NPV08	11	WTDLRHTGF	C0304	no	7	BUV395	BV786
NPV08	11	AQDGNTEPL	B4001	no	8	BV421	PE-Cy7
NPV10	1	PPLQVTKV	B5101	no	3	BV421	BV786
NPV10	2	RIPEYFNFAK	A1101	yes	6	BV650	PE-CF594
NPV10	3	EALVLITEY	B5101	yes	1	BV650	PE
NPV10	3	ALVLITEY	B1501	yes	1	BV711	PE-CF594
NPV10	3	LPIQKPKL	B5101	yes	2	BV786	PE-Cy7
NPV10	3	RLLPIQKPK	A1101	yes	2	PE	PE-CF594
NPV10	3	MQRESRRLL	B1501	yes	2	PE	PE-Cy7
NPV10	3	MIVDKATKK	A1101	yes	3	PE-CF594	PE-Cy7
NPV10	3	YQAAPAFGF	B1501	yes	4	BV786	PE
NPV10	3	KVALLSDVK	A1101	no	4	BV786	PE-CF594

NPV10	3	RPSVIFQPEQK	A1101	yes	5	BUV737	PE-CF594
NPV10	3	RIPEYFNFAK	A1101	yes	6	BV650	PE-CF594
NPV10	3	KQDFKLRIPEY	B1501	yes	6	BUV737	PE
NPV10	4	SLDEALVLI	A0201	yes	1	APC	PE-CF594
NPV10	5	EALVLITEY	B5101	yes	1	BV650	PE
NPV10	5	ALVLITEY	B1501	yes	1	BV711	PE-CF594
NPV10	5	RLLPIQKPK	A1101	yes	2	PE	PE-CF594
NPV10	5	RIPEYFNFAK	A1101	yes	6	BV650	PE-CF594
NPV10	6	LPIQKPKL	B5101	yes	2	BV786	PE-Cy7
NPV10	7	LSLDEALVL	C0304	yes	1	BUV395	BV421
NPV10	7	LPIQKPKLL	C0304	yes	2	BUV737	BV421
NPV10	7	ISRPSVIF	C0304	yes	5	BUV395	BUV737
NPV10	8	LSLDEALVL	C0304	yes	1	BUV395	BV421
NPV10	8	EALVLITEY	B5101	yes	1	BV650	PE
NPV10	8	LPIQKPKLL	C0304	yes	2	BUV737	BV421
NPV10	8	RLLPIQKPK	A1101	yes	2	PE	PE-CF594
NPV10	8	KVENNMIVDK	A1101	yes	3	BV421	PE-CF594
NPV10	8	GVYQAAPAF	B1501	yes	4	BV421	PE
NPV10	8	GISRPSVIF	B1501	yes	5	BUV395	PE
NPV10	8	SVIFQPEQK	A1101	yes	5	BUV395	PE-CF594
NPV10	8	RPSVIFQPEQK	A1101	yes	5	BUV737	PE-CF594
NPV10	8	ISRPSVIF	C0304	yes	5	BUV395	BUV737
NPV10	8	RIPEYFNFAK	A1101	yes	6	BV650	PE-CF594
NPV10	8	KQDFKLRIPEY	B1501	yes	6	BUV737	PE
NPV11	1	PSAPPSPSAL	C0102	yes	1	BUV395	BV421
NPV13	1	FVNSAIRYL	A0201	no	2	APC	PE-Cy7
NPV13	1	VDINDKLKL	B4001	no	3	BV421	PE-Cy7
NPV13	1	KLYASPSQFI	A0201	yes	3	APC	BV421
NPV13	1	NEVAKLVNIL	B4001	yes	4	BV421	BV786
NPV13	1	GENSNEVAKL	B4001	no	4	BV786	PE-Cy7
NPV13	1	KLVNILNTI	A0201	yes	4	APC	BV786
NPV13	2	KSLVVSKPPAK	A0301	yes	1	BV421	PE
NPV13	2	NILNTIPSL	C0401	yes	4	BV421	BV650
NPV13	2	KPGSQYYQY	B3501	no	5	BV650	PE
NPV13	3	KLYASPSQFIK	A0301	yes	3	BV786	PE-CF594
NPV13	4	QTIQKSLVV	C0304	yes	1	BUV395	BV421
NPV13	4	KSLVVSKPPAK	A0301	yes	1	BV421	PE
NPV13	4	FVNSAIRYL	C0304	no	2	BUV737	BV421
NPV13	4	LPATFVNSA	B3501	no	2	BUV395	PE
NPV13	4	YASPSQFIKL	C0304	yes	3	BUV395	BUV737
NPV13	4	DINDKLKLY	B3501	no	3	BUV737	PE

NPV21	1	KLSEFFLL	A0201	yes	1	APC	PE-Cy7
NPV21	1	DTEKKLSEF	B3501	no	1	PE	PE-CF594
NPV21	1	FLLKTSSSHEA	A0201	yes	1	APC	PE-CF594
NPV21	1	LMNDTEKKL	A0201	no	1	APC	PE
NPV21	1	MTIPVYTTL	B3501	yes	2	PE-CF594	PE-Cy7
NPV21	1	MTIPVYTTL	A0201	yes	2	APC	BV786
NPV21	1	HHILSGKEF	B3801	no	3	PE	PE-Cy7
NPV21	1	HQVQIPLYNF	B3801	yes	5	BV786	PE-Cy7
NPV21	1	FPQSPPAQY	B3501	no	5	BV786	PE-CF594
NPV21	2	DTEKKLSEF	B3501	no	1	PE	PE-CF594
NPV21	2	KKLSEFFLL	B3801	yes	1	BV650	PE-CF594
NPV21	2	SPFDMKILL	B3501	yes	3	BV421	PE-CF594
NPV21	2	LHHILSGKEF	B3801	no	3	BV421	PE
NPV21	2	AQSLTFFKF	B3801	yes	4	BV650	PE
NPV21	3	LMNDTEKKL	C0401	no	1	BUV395	BV421
NPV21	3	MTIPVYTTL	C0401	yes	2	BUV737	BV421
NPV21	3	PFDMKILL	C0401	yes	3	BUV395	BV786
NPV21	3	SPFDMKILL	C0401	yes	3	BUV395	BUV737
NPV21	3	RHFERFDRNI	B3801	yes	6	BV421	BV786
NPV21	4	MTIPVYTTL	A0201	yes	2	APC	BV786
NPV21	5	LMNDTEKKL	C0401	no	1	BUV395	BV421
NPV21	5	KKLSEFFLL	B3801	yes	1	BV650	PE-CF594
NPV21	5	DTEKKLSEF	B3501	no	1	PE	PE-CF594
NPV21	5	MTIPVYTTL	C0401	yes	2	BUV737	BV421
NPV21	5	MTIPVYTTL	B3801	yes	2	BV711	PE-CF594
NPV21	5	LHHILSGKEF	B3801	no	3	BV421	PE
NPV21	5	SPFDMKILL	B3501	yes	3	BV421	PE-CF594
NPV21	5	SPFDMKILL	B3801	yes	3	BUV395	PE
NPV21	5	SPFDMKILL	C0401	yes	3	BUV395	BUV737
NPV21	5	AQSLTFFKF	B3801	yes	4	BV650	PE
NPV21	5	SQGAQSLTF	B3801	no	4	BUV737	PE
NPV21	5	AQPPHQVQI	C0401	yes	5	BV711	PE
NPV21	5	YNFPQSPPAQY	B3501	no	5	BUV395	PE-CF594
NPV21	5	KTIEDVREF	B3501	no	6	BUV737	PE-CF594
NPV21	6	KKLSEFFLL	B3801	yes	1	BV650	PE-CF594
NPV21	6	DTEKKLSEF	B3501	no	1	PE	PE-CF594
NPV21	6	MTIPVYTTL	B3801	yes	2	BV711	PE-CF594
NPV21	6	MTIPVYTTL	B3501	yes	2	PE-CF594	PE-Cy7
NPV21	6	HHILSGKEF	B3801	no	3	PE	PE-Cy7
NPV21	6	AQSLTFFKF	B3801	yes	4	BV650	PE
NPV21	6	SQGAQSLTF	B3801	no	4	BUV737	PE

NPV21	6	AQPPHQVQI	C0401	yes	5	BV711	PE
NPV21	6	FERFDRNIASF	C0401	yes	6	BV650	PE-Cy7
NPV21	6	KTIEDVREF	B3501	no	6	BUV737	PE-CF594
NPV21	6	RFDRNIASF	C0401	no	6	BUV737	PE-Cy7
NPV21	7	MTIPVYTTL	C0401	yes	2	BUV737	BV421
NPV21	7	LHHILSGKEF	B3801	no	3	BV421	PE
NPV21	7	AQSLTFFKF	B3801	yes	4	BV650	PE
NPV21	7	SQGAQSLTF	B3801	no	4	BUV737	PE
NPV26	1	EAKKTLTEL	B0702	no	1	BUV395	PE-CF594
NPV26	1	QWDEDSVKY	C0702	yes	2	BV421	BV786
NPV26	1	MPANPVRIAF	B0702	no	2	BUV737	PE-CF594
NPV26	1	SGKEKLISL	C0702	yes	3	BUV395	BV421
NPV26	1	MHLELREGL	C0702	no	5	BUV737	BV421
NPV26	1	RISSFLGKK	A0301	yes	6	BV421	PE-CF594
NPV26	1	SFLGKKPSL	C0702	yes	6	BUV395	BV786
NPV26	1	INWDAVFQK	A0301	no	7	BV786	PE-CF594
NPV26	1	SQLSDVQNF	C0702	no	7	BUV395	BUV737
NPV26	2	KLDKEQAAL	C0501	no	1	BV421	PE
NPV26	2	APVDSGKEKL	B0702	no	3	BV650	PE-CF594
NPV26	2	SLLQGPSDTK	A0301	yes	3	PE	PE-CF594
NPV26	2	STDLKNNLL	C0501	yes	5	BV650	PE
NPV26	2	GLTRMSTDLK	A0301	yes	5	PE-CF594	PE-Cy7
NPV26	2	RISSFLGKK	A0301	yes	6	BV421	PE-CF594
NPV26	2	HIDIPRISSF	C0501	yes	6	BV421	PE-Cy7
NPV26	2	IPRISSFL	B0702	yes	6	BV711	PE-CF594
NPV26	2	TPIQGGIPAL	B0702	yes	8	PE	PE-Cy7
NPV26	3	EAKKTLTEL	B0702	no	1	BUV395	PE-CF594
NPV26	4	IPRISSFL	B0702	yes	6	BV711	PE-CF594
NPV26	5	KLDKEQAAL	A0201	no	1	APC	PE-CF594
NPV26	6	GLTRMSTDLK	A0301	yes	5	PE-CF594	PE-Cy7
NPV26	7	INWDAVFQK	A0301	no	7	BV786	PE-CF594
NPV27	1	RRVQKQLEV	C0702	no	4	BV421	BV786
NPV27	2	GRNVKSRKL	C0702	no	1	BV786	PE-Cy7
NPV27	2	KADVVEAW	B5701	no	2	BV421	PE-CF594
NPV27	2	RSEPFLAPLLL	B5701	no	3	BV786	PE-CF594
NPV27	2	RRSEPFLAPL	C0702	no	3	BUV395	PE-Cy7
NPV27	2	RRVQKQLEV	C0702	no	4	BV421	BV786
NPV27	2	HKAQHISRF	C0702	no	5	BUV395	BV421
NPV27	2	ATQPNPAVFIF	B5701	no	5	BUV395	PE-CF594
NPV27	2	AWKPESPFW	C0702	yes	9	BUV395	BV786
NPV27	2	HRQPPPLQQ	C0602	no	10	BV421	PE-Cy7

NPV27	2	RPTLPAAPAF	B0702	yes	10	PE-CF594	PE-Cy7
NPV27	3	RSEPFLAPLLL	B5701	no	3	BV786	PE-CF594
NPV28	1	FQSDDHPQF	B4001	yes	1	PE	PE-Cy7
NPV28	1	MLFYNPAQL	C0304	yes	2	BV421	PE-Cy7
NPV28	1	YVLGQNSPL	C0304	yes	3	BV786	PE-Cy7
NPV28	1	WELEGSTL	B4001	yes	4	BV421	PE
NPV28	1	AAVHRTRYF	C0304	yes	5	BUV395	PE-Cy7
NPV28	1	MAAMTPALL	C0304	yes	6	BV421	BV786
NPV28	1	GEIPLDMRL	B4001	no	6	BV786	PE
NPV28	1	SAKSSLSQI	C0304	no	7	BUV395	BV421
NPV28	1	TQEPPYQVL	B4001	no	8	BUV395	PE
NPV28	1	KVLQSHMSL	C0304	no	9	BUV395	BV786
NPV28	2	MAAMTPALL	C0304	yes	6	BV421	BV786
NPV28	3	FQSDDHPQF	C0304	yes	1	BV650	PE
NPV28	3	FQSDDHPQF	B4001	yes	1	PE	PE-Cy7
NPV28	3	FQSDDHPQF	B1501	yes	1	PE-CF594	PE-Cy7
NPV28	3	MLFYNPAQL	C0304	yes	2	BV421	PE-Cy7
NPV28	3	SVPEVIHYY	B1501	no	3	BV421	PE-CF594
NPV28	3	WELEGSTL	B4001	yes	4	BV421	PE
NPV28	3	AAVHRTRYF	C0304	yes	5	BUV395	PE-Cy7
NPV28	3	SAKSSLSQI	C0304	no	7	BUV395	BV421
NPV28	3	SQIFSAATSH	B1501	yes	7	BUV395	PE-CF594
NPV28	3	TQEPPYQVL	C0304	no	8	BUV737	BV421
NPV28	3	TQEPPYQVL	B4001	no	8	BUV395	PE
NPV28	3	TQEPPYQVL	B1501	no	8	BUV737	PE-CF594
NPV28	3	KVLQSHMSL	B1501	no	9	BV650	PE-CF594
NPV28	3	DEEEVLPLL	B4001	yes	9	BUV737	PE
NPV28	3	ELLQGLAYF	B1501	yes	10	BV711	PE-CF594
NPV28	3	GLAYFPETI	A0201	yes	10	PE	PE-CF594
NPV28	3	IAGSDAPSL	C0304	no	10	BUV395	BUV737
NPV28	4	FQSDDHPQF	B4001	yes	1	PE	PE-Cy7
NPV28	4	MLFYNPAQL	C0304	yes	2	BV421	PE-Cy7
NPV28	4	YVLGQNSPL	C0304	yes	3	BV786	PE-Cy7
NPV28	4	SPLFDSVPEV	A0201	yes	3	APC	PE
NPV28	4	WELEGSTL	B4001	yes	4	BV421	PE
NPV28	4	FLDQLAKFWEL	A0201	no	4	APC	PE-Cy7
NPV28	4	NMSESMAAV	A0201	yes	5	APC	BV421
NPV28	4	AAVHRTRYF	C0304	yes	5	BUV395	PE-Cy7
NPV28	4	MAAMTPALL	C0304	yes	6	BV421	BV786
NPV28	4	ALLGGEIPL	A0201	yes	6	APC	BV786
NPV28	4	GEIPLDMRL	B4001	no	6	BV786	PE

NPV28	4	SAKSSLSQI	C0304	no	7	BUV395	BV421
NPV28	4	SLSQIFSAA	A0201	yes	7	APC	BUV395
NPV28	4	TQEPPYQVL	B4001	no	8	BUV395	PE
NPV28	4	KVLQSHMSL	C0304	no	9	BUV395	BV786

Epilogue

Within this PhD thesis I have presented two individual studies, each of which addresses the challenges encountered in the use of immunotherapy for cancer treatment. Based on prior research within the field, it has become increasingly evident that there is a considerable degree of heterogeneity in response rates of cancer patients to immunotherapy both across different types of cancer and even within the same cancer form. Many factors comes into play, among others the TMB has been found to correlate with the response to ICI therapy (173). The research carried out in this thesis covers cancers in both ends of the TMB scale(90). In **Manuscript I** samples from patients with recurrent GBM are evaluated in the context of ICI therapy, while **Manuscript II** investigates the immune response towards a neopeptide vaccine in advanced melanoma patients. Furthermore, the common immune cells of interest within the two studies are the T cells, including the CD8 T cells, which are believed to be the main drivers in elimination of cancer.

The survival rates for GBM is particularly poor with a median survival of 15 months, when treated with the standard of care treatment consisting of neurosurgical resection followed by radiotherapy and adjuvant chemotherapy (Temozolomide) (174). Thus, immunotherapy has been studied intensively hoping to increase survival for these patients. Pre-clinical studies in mice have shown promising responses to treatment with e.g. ICI (175,176). However, when this is translated into a human setting the impressive response rate does not appear (177). In **Manuscript I** we examined samples from patients with recurrent GBM treated with neoadjuvant a-PD1 ICI therapy prior to neurosurgery, in order to understand the overall absence of response to ICI therapy in these patients. Generally, an important consideration of GBM treatment is the ability of drugs to pass the blood brain barrier (BBB) into the tumor lesion (178). However, the BBB has been shown to be leaky with a compromised BBB within GBM lesions (179,180). We found that the PD-1 targeting ICI drug, Nivolumab, had reached the tumor in a concentration able to saturate the PD-1 molecules expressed on both tissue resident and non-resident T cells. This finding is of considerable importance as this indicates that ICI drugs can indeed reach the TME of primary brain cancer type, GBM. Thus, failure to respond clinically is likely not due to absence of the ICI drug in the tumor lesion, but rather the TME and the phenotypical state of infiltrated immune cells. We reported that the intratumoral T cells had changed their phenotypical profile significantly, following the ICI therapy. These changes comprised both increased activation, but also a compensatory upregulation of other inhibitory checkpoint molecules, especially TIGIT. We therefore concluded that Nivolumab was able to induce an anti-cancer response, but anti-inflammatory factors, potentially caused by an induced reactivity, could

further hamper a clinical response. Interestingly, unlike GBM and other primary brain tumors, ICI therapy has considerably improved the overall survival for patients with metastatic brain tumors (181,182). T cell infiltration appears to be generally lower in GBM compared to brain metastases of solid cancer (183). We were unfortunately not able to estimate the T cell infiltration, but for future studies this should be prioritized. Several factor could cause an impaired immune infiltration, including the BBB, or a high infiltration of inhibitory immune cells, such as TAMs or MDSCs (184). Additionally, corticosteroids are used in GBM patients for a symptomatic relief of tumor-related edema, but these drugs function with an antagonistic effects to the ICI therapy by immunosuppression, in addition to strengthening the integrity of the BBB (185). The use of corticosteroids should therefore be considered carefully in the context of immunotherapy. Alternatively, an anti-VEGF drug, Bevacizumab, functions by suppressing endothelial growth and is also used to treat GBM patients to reduce edema, but does not have a direct immunosuppressive function. Patient in the clinical trial CA9UP studied in **Manuscript I** also received adjuvant treatment with Bevacizumab. Moreover, the resident immune cell of the brain, microglia, has been suggested to contribute to tumor growth, due to an altered gene expression within the microglia caused by an interaction with GBM cells (186). Hence, many factors can overshadow a T cell mediated anti-cancer response, therefore it may not have an overall effect on tumor regression. Consequently, ICI therapy is likely not efficient as a monotherapy. There is a need for increased T cell infiltration, inhibition of anti-inflammatory cells and a blockade of the anti-inflammatory interaction between cancer cells and immune cells. Though ICI has not shown any overall induced clinical effect, including patients in the CA209-9UP trial, few long-term GBM survivors and ICI responder have been reported (187). We described that ICI treated patients with tumor reactive TILs had a longer survival (not significant) than patients without tumor reactive TILs. This argues that there is indeed some GBM patients that could benefit from ICI therapy, however methods need to be established in order to identify these patient. We suggested that upregulation of CD28 on T cells could be a marker of induced T cell activity upon anti-PD-1 ICI therapy. However, this was only evident for intratumoral and not peripheral T cells. Hence, this could be used to argue for continuing aPD-1 therapy for patients, with this intratumoral T cells profile, after neurosurgical resection. Though, it needs to be verified in a much larger patient cohort. We also showed that neoantigen reactive CD8 T cells (NARTs) could also be detected in blood from TIL reactive GBM patients. In addition, upregulation of the chemokine receptors, CCR5 and CXCR3 on T cells from blood and CSF is associated with neuroinflammation and CNS homing(188,189), which was also supported by our results. It would therefore be interesting to examine the GBM NART repertoire also in CSF samples, especially in relation

to mapping out the infiltration route of T cells to the GBM TME. Understanding the T cell infiltration of GBM is an important key to improve T cell targeted immunotherapy.

As opposed to GBM, Immune therapy has changed the survival rates immensely for patients with advanced melanoma, a previously incurable disease. The impressive responses to e.g. ICI therapy has also been connected to the high TBM, within this patient group. However a group of melanoma patients still fails to respond to ICI therapy. In **Manuscript II** we address the challenges which still occur in ICI treatment of melanoma, and aimed to increase the repertoire of NARTs. An AI predicted neopeptide vaccine was tested in combination with PD-1 targeting ICI therapy in a phase I clinical trial with advanced melanoma patients. An important advantage for neopeptide vaccines, as mentioned in the introduction, is the comparably low level of side effects, which has been shown within different cancer types (165,170,190), presumably due to the high tumor specificity. In **Manuscript II** we also reported that the neopeptide vaccine in combination with ICI therapy was safe to use and that the few high grade irAE, was caused by the ICI therapy, rather than the vaccine. In line, similar safety results have been reported from recent trials with a comparable clinical setup (NCT03313778(191), NCT02897765(171)). However, it is difficult to assess the clinical effect of the vaccine, as it is administered in combination with ICI therapy. We included two patient groups in our trial; a group that was ICI naïve and a group with stable disease after ICI therapy. The latter was a preferred group to investigate a clinical response elicited by the vaccination. One patient in the ICI-experienced group had an encouraging response following the neopeptide vaccination, with increasing tumor regression over time but progressed in the end. Interestingly, PBMC samples from this patient correspondingly had a comparably high *in vitro* immune response towards the vaccine peptides, comprising both CD4 and especially CD8 T cell reactivity. However, our cohort size was unfortunately too small to conclude on vaccine induced clinical responses. The vaccine peptides were predicted with the AI platform, which both included prediction for CD8 and CD4 T cells epitopes. Criteria for a vaccine peptide was that they embedded a CD8 or/and a CD4 T cell epitope, that the epitope was only expressed in cancer cells, i.e. a neoepitope, and that the neoepitope was expressed in the tumor cells. Generally we found that T cell responses was induced and/or boosted after initiation of vaccination. However, in most patients we primarily detected CD4 T cell responses, but this is a common observation in peptide vaccines with long peptides (165,166). Nevertheless, we were able to detect a small NART population that were specific for vaccine embedded MHC-I peptides, with fluorochrome-labelled pMHC-multimer. Widely used screening methods for vaccine responses including Intracellular cytokine staining (ICS) or IFN-γ Elispot, are perhaps not sensitive enough to verify these small responses, especially due to a high and variable background reactivity, and the prestimulation with either short or long peptides could also skew the

measured reactivity towards either a CD8 or CD4 T cells response. Therefore in order to get a clear view of the response to the peptide vaccines, a comprehensive but also expensive methological pipeline can be proposed. This could include identification of the recognized peptides binding to both MHC-I and MHC-II. We included vaccine and other predicted neopeptides in our analysis, however only for MHC-I peptides. Additionally, identification of the TCRs binding to the given vaccine peptides is of interest, to observe the clonality within the pool of TCR clones on vaccine-reactive T cells. Identification of TCR clonotypes could also provide information on long-lasting memory responses, as shown by Hu et al. (161). The effector function of the vaccine induced T cells are also important to verify, either through single cell RNA analysis, or through functional assay upon *in vitro* stimulation with peptides. Fuchs et al. showed that peptide induced TCR stimulation resulted in a down regulation of TCR expression, but an upregulation of surface markers of T cell activation, including CD137 and CD355 (192). These dynamics of activation can be used as an alternative to ICS, to identify true immunogenic vaccine peptides, but after the identification of recognized vaccine peptides, rather than as a screening method. An indirect measurement of a successful vaccination resulting in tumor cytotoxicity, is epitope spreading. Ott. et al exemplified this by showing that non-vaccine related NARTs could be detected in tumor tissue after vaccination. Such NARTs were detected in tumors with infiltrated vaccine-specific NARTs, additionally this observation was also associated with a longer PFS (171). We were however not able to show this trend, in non-vaccine related NARTs after vaccination. We were also not able to show de novo CD8 T cell responses post vaccination. However, this is perhaps due to the prediction methods, as the highest ranked neopeptide has been chosen as peptide vaccine candidates, thus these neoepitopes are theoretically peptides that has already created an immune response. The vaccines can however boost an immune response instead. Peptide immunogenicity data on a single cell level vaccine can be used to optimize the AI prediction pipeline, also in context of self-similarity to wild type and thus avoid to induce tolerance to the vaccine peptides. In addition, multiple biopsies of different sides of a cancer lesion may be important to cover the overall mutational landscape of the cancer due to intra-lesion diversity. A correct prediction of immunogenic neopeptides is important for a successful clinical outcome. It has been established that the number of NARTs is correlated with a good clinical outcome to in relation to ICI therapy, to a higher extend than the TMB (193). We also found a correlation between number of immunogenic vaccine peptides and a positive clinical response. However, evolutional changes in the mutational landscape should also be followed over time, and potentially adjust the vaccine to the mutational profile of the cancer over time. Finally, for personal therapies, such as neopeptide vaccines, a well-structured manufacturing process is essential to

ensure the short delivery time to avoid disease progression during the production time, as it cannot be produced as an “off-the-shelf” product.

The studies presented in **Manuscript I** and **Manuscript II** collectively demonstrate the intricate nature of cancer treatment. They underscore the significance of conducting a comprehensive examination of the immunological condition of the tumor and advocate for personalized treatment strategies that account for the variability in response rates and the complex interplay between cancer cells and the immune system. These personalized approaches may comprise personalized immunotherapeutic drugs like neopeptide vaccines and/or a tailored combination of various “off-the-shelf” immunotherapies. Nevertheless, safety and toxicity should be given considerable weight in this context.

Bibliography

1. Parkin J, Cohen B. An overview of the immune system. Lancet. 2001;357(9270).

2. Clark M, Kroger CJ, Tisch RM. Type 1 diabetes: A chronic anti-self-inflammatory response. Front Immunol. 2017;8(DEC).

3. Baecher-Allan C, Kaskow BJ, Weiner HL. Multiple Sclerosis: Mechanisms and Immunotherapy. Neuron. 2018;97(4).

4. Rajabi F, Drake LA, Senna MM, Rezaei N. Alopecia areata: a review of disease pathogenesis. Br J Dermatol. 2018;179(5).

5. Amarante-Mendes GP, Adjemian S, Branco LM, Zanetti LC, Weinlich R, Bortoluci KR. Pattern recognition receptors and the host cell death molecular machinery. Front Immunol. 2018;9(OCT).

6. Gordon S, Plüddemann A. Macrophage clearance of apoptotic cells: A critical assessment. Front Immunol. 2018;9(JAN).

7. Zhang C, Yang M, Ericsson AC. Function of Macrophages in Disease: Current Understanding on Molecular Mechanisms. Front Immunol. 2021;12.

8. Banchereau J, Briere F, Caux C, Davoust J, Lebecque S, Liu YJ, et al. Immunobiology of dendritic cells. Annu Rev Immunol. 2000;18.

9. Sallusto F, Lanzavecchia A. The instructive role of dendritic cells on T-cell responses. Arthritis Res. 2002;4.

10. Vinuesa CG, Tangye SG, Moser B, Mackay CR. Follicular B helper T cells in antibody responses and autoimmunity. Nat Rev Immunol. 2005;5(11).

11. Lo Nigro C, Macagno M, Sangiolo D, Bertolaccini L, Aglietta M, Merlano MC. NK-mediated antibody-dependent cell-mediated cytotoxicity in solid tumors: biological evidence and clinical perspectives. Ann Transl Med. 2019;7(5).

12. Li Y, Li G, Zhang J, Wu X, Chen X. The Dual Roles of Human γδ T Cells: Anti-Tumor or Tumor-Promoting. Front Immunol. 2021;11.

13. Lanier LL. Shades of grey-the blurring view of innate and adaptive immunity. Nat Rev Immunol. 2013;13(2).

14. Paul S, Lal G. The molecular mechanism of natural killer cells function and its importance in cancer immunotherapy. Front Immunol. 2017;8(SEP).

15. Krijgsman D, Hokland M, Kuppen PJK. The role of natural killer T cells in cancer-A phenotypical and functional approach. Front Immunol. 2018;9(FEB).

16. Park JH, Lee HK. Function of γδ T cells in tumor immunology and their application to cancer therapy. Exp Mol Med. 2021;53(3).

17. Klein L, Kyewski B, Allen PM, Hogquist KA. Positive and negative selection of the T cell repertoire: What thymocytes see (and don't see). Nat Rev Immunol. 2014;14(6).

18. Nishana M, Raghavan SC. Role of recombination activating genes in the generation of antigen receptor diversity and beyond. Immunology. 2012;137(4).

19. Germain RN. T-cell development and the CD4-CD8 lineage decision. Nat Rev Immunol. 2002;2(5).

20. Xing Y, Hogquist KA. T-Cell tolerance: Central and peripheral. Cold Spring Harb Perspect Biol. 2012;4(6).

21. Robinson J, Barker DJ, Georgiou X, Cooper MA, Flicek P, Marsh SGE. IPD-IMGT/HLA Database. Nucleic Acids Res. 2020;48(D1).

22. Embgenbroich M, Burgdorf S. Current concepts of antigen cross-presentation. Front Immunol. 2018;9(JUL).

23. Wieczorek M, Abualrous ET, Sticht J, Álvaro-Benito M, Stolzenberg S, Noé F, et al. Major histocompatibility complex (MHC) class I and MHC class II proteins: Conformational plasticity in antigen presentation. Front Immunol. 2017;8(MAR).

24. Leone P, Shin EC, Perosa F, Vacca A, Dammacco F, Racanelli V. MHC class i antigen processing and presenting machinery: Organization, function, and defects in tumor cells. J Natl Cancer Inst. 2013;105(16).

25. ten Broeke T, Wubbolts R, Stoorvogel W. MHC class II antigen presentation by dendritic cells regulated through endosomal sorting. Cold Spring Harb Perspect Biol. 2013;5(12).

26. Roche PA, Furuta K. The ins and outs of MHC class II-mediated antigen processing and presentation. Nat Rev Immunol. 2015;15(4).

27. Andersen MH, Schrama D, Thor Straten P, Becker JC. Cytotoxic T cells. J Invest Dermatol. 2006 Jan;126(1):32–41.

28. Shah K, Al-Haidari A, Sun J, Kazi JU. T cell receptor (TCR) signaling in health and disease. Signal Transduct Target Ther. 2021;6(1).

29. Li Y, Yin Y, Mariuzza RA. Structural and biophysical insights into the role of CD4 and CD8 in T cell activation. Front Immunol. 2013;4(JUL).

30. Basu A, Ramamoorthi G, Albert G, Gallen C, Beyer A, Snyder C, et al. Differentiation and Regulation of TH Cells: A Balancing Act for Cancer Immunotherapy. Front Immunol. 2021;12.

31. Vignali DAA, Collison LW, Workman CJ. How regulatory T cells work. Nat Rev Immunol. 2008;8(7).

32. Barry M, Bleackley RC. Cytotoxic T lymphocytes: All roads lead to death. Nat Rev Immunol. 2002;2(6).

33. ElTanbouly MA, Noelle RJ. Rethinking peripheral T cell tolerance: checkpoints across a T cell's journey. Nat Rev Immunol. 2021;21(4).

34. Schwartz RH. T cell anergy. Annu Rev Immunol. 2003;21.

35. Kumar B V., Connors TJ, Farber DL. Human T Cell Development, Localization, and Function throughout Life. Immunity. 2018;48(2).

36. Courtney AH, Shvets AA, Lu W, Griffante G, Mollenauer M, Horkova V, et al. CD45 functions as a signaling gatekeeper in T cells. Sci Signal. 2019;12(604).

37. Henson SM, Riddell NE, Akbar AN. Properties of end-stage human T cells defined by CD45RA re-expression. Curr Opin Immunol. 2012;24(4).

38. Yan Y, Chen R, Wang X, Hu K, Huang L, Lu M, et al. CCL19 and CCR7 Expression, Signaling Pathways, and Adjuvant Functions in Viral Infection and Prevention. Front Cell Dev Biol. 2019;7.

39. Sallusto F, Lenig D, Förster R, Lipp M, Lanzavecchia A. Two subsets of memory T lymphocytes with distinct homing potentials and effector functions. Nature. 1999;401(6754):708–12.

40. Martin MD, Badovinac VP. Defining memory CD8 T cell. Front Immunol. 2018;9(NOV).

41. Corgnac S, Boutet M, Kfoury M, Naltet C, Mami-Chouaib F. The Emerging Role of CD8+ Tissue Resident Memory T (TRM) Cells in Antitumor Immunity: A Unique Functional Contribution of the CD103 Integrin. Front Immunol. 2018;9(AUG).

42. Cibrián D, Sánchez-Madrid F. CD69: from activation marker to metabolic gatekeeper. Eur J Immunol. 2017;47(6):946.

43. Kragten NAM, Behr FM, Vieira Braga FA, Remmerswaal EBM, Wesselink TH, Oja AE, et al. Blimp-1 induces and Hobit maintains the cytotoxic mediator granzyme B in CD8 T cells. Eur J Immunol. 2018;48(10).

44. Wherry EJ. T cell exhaustion. Nat Immunol. 2011;12(6):492–9.

45. Blackburn SD, Shin H, Haining WN, Zou T, Workman CJ, Polley A, et al. Coregulation of CD8+ T cell exhaustion by multiple inhibitory receptors during chronic viral infection. Nat Immunol. 2009;10(1).

46. Scott AC, Dündar F, Zumbo P, Chandran SS, Klebanoff CA, Shakiba M, et al. TOX is a critical regulator of tumour-specific T cell differentiation. Nature. 2019;571(7764).

47. Blank CU, Haining WN, Held W, Hogan PG, Kallies A, Lugli E, et al. Defining 'T cell exhaustion.' Nat Rev Immunol. 2019;19(11).

48. Kallies A, Zehn D, Utzschneider DT. Precursor exhausted T cells: key to successful immunotherapy? Nat Rev Immunol. 2020;20(2).

49. Cura Daball P, Ventura Ferreira MS, Ammann S, Klemann C, Lorenz MR, Warthorst U, et al. CD57 identifies T cells with functional senescence before terminal differentiation and relative telomere shortening in patients with activated PI3 kinase delta syndrome. Immunol Cell Biol. 2018;96(10).

50. Akbar AN, Henson SM, Lanna A. Senescence of T Lymphocytes: Implications for Enhancing Human Immunity. Trends Immunol. 2016;37(12).

51. Wu S, Zhu W, Thompson P, Hannun YA. Evaluating intrinsic and non-intrinsic cancer risk factors. Nat Commun. 2018;9(1).

52. Lowe SW, Cepero E, Evan G. Intrinsic tumour suppression. Nature. 2004;432(7015).

53. Hanahan D, Weinberg RA, Aplin A., Howe A, Alahari S., Juliano R., et al. The hallmarks of cancer. Cell. 2000;100(1):57–70.

54. Hanahan D, Weinberg R a. Hallmarks of cancer: The next generation. Cell. 2011;144(5):646–74.

55. Ehrlich P. Über den jetzigen stand der Karzinomforschung. In 1908.

56. Winau F, Westphal O, Winau R. Paul Ehrlich - In search of the magic bullet. Microbes Infect. 2004;6:786–9.

57. Dunn GP, Old LJ, Schreiber RD. The immunobiology of cancer immunosurveillance and immunoediting. Immunity. 2004;21(2).

58. Burnet M. Cancer-A Biological Approach* Iii. Viruses Associated With Neoplastic Conditions. Br Med J. 1957;1(5023).

59. Burnet FM. Immunological Surveillance in Neoplasia. Immunol Rev. 1971;7(1).

60. Dunn GP, Bruce AT, Ikeda H, Old LJ, Schreiber RD. Cancer immunoediting: from immunosurveillance to tumor escape. Nat Immunol. 2002;3(11):991–8.

61. Dunn GP, Old LJ, Schreiber RD. The three Es of cancer immunoediting. Annu Rev Immunol. 2004;22.

62. Shankaran V, Ikeda H, Bruce AT, White JM, Swanson PE, Old LJ, et al. IFNgamma and lymphocytes prevent primary tumour development and shape tumour immunogenicity. Nature. 2001;410(6832):1107–11.

63. Vesely MD, Kershaw MH, Schreiber RD, Smyth MJ. Natural Innate and Adaptive Immunity to Cancer. Annu Rev Immunol. 2011;29(1):235–71.

64. Raskov H, Orhan A, Christensen JP, Gögenur I. Cytotoxic CD8+ T cells in cancer and cancer immunotherapy. Br J Cancer. 2021;124(2).

65. Baghban R, Roshangar L, Jahanban-Esfahlan R, Seidi K, Ebrahimi-Kalan A, Jaymand M, et al. Tumor microenvironment complexity and therapeutic implications at a glance. Cell Commun Signal. 2020;18(1).

66. Dhatchinamoorthy K, Colbert JD, Rock KL. Cancer Immune Evasion Through Loss of MHC Class I Antigen Presentation. Front Immunol. 2021;12.

67. Kim SK, Cho SW. The Evasion Mechanisms of Cancer Immunity and Drug Intervention in the Tumor Microenvironment. Front Pharmacol. 2022;13.

68. Courau T, Nehar-Belaid D, Florez L, Levacher B, Vazquez T, Brimaud F, et al. TGF-β and VEGF cooperatively control the immunotolerant tumor environment and the efficacy of cancer immunotherapies. JCI Insight. 2016;1(9).

69. Anderson NM, Simon MC. The tumor microenvironment. Curr Biol. 2020 Aug 17;30(16):R921–5.

70. Strand S, Hofmann WJ, Hug H, Müller M, Otto G, Strand D, et al. Lymphocyte apoptosis induced by CD95 (APO-1/Fas) ligand-expressing tumor cells - A mechanism of immune evasion? Nat Med. 1996;2(12).

71. Thepmalee C, Panya A, Junking M, Chieochansin T, Yenchitsomanus P thai. Inhibition of IL-10 and TGF-β receptors on dendritic cells enhances activation of effector T-cells to kill cholangiocarcinoma cells. Hum Vaccines Immunother. 2018;14(6).

72. Lippens C, Duraes F V., Dubrot J, Brighouse D, Lacroix M, Irla M, et al. IDO-orchestrated crosstalk between pDCs and Tregs inhibits autoimmunity. J Autoimmun. 2016;75.

73. Chinen T, Kannan AK, Levine AG, Fan X, Klein U, Zheng Y, et al. An essential role for the IL-2 receptor in Treg cell function. Nat Immunol 2016 1711. 2016;17(11):1322–33.

74. Smazynski J, Webb JR. Resident memory-like tumor-infiltrating lymphocytes (TILRM): Latest players in the immuno-oncology repertoire. Front Immunol. 2018;9(JUL).

75. Qin S, Xu L, Yi M, Yu S, Wu K, Luo S. Novel immune checkpoint targets: Moving beyond PD-1 and CTLA-4. Mol Cancer. 2019;18(1).

76. Buchbinder EI, Desai A. CTLA-4 and PD-1 pathways similarities, differences, and implications of their inhibition. Am J Clin Oncol Cancer Clin Trials. 2016;39(1).

77. Chauvin JM, Zarour HM. TIGIT in cancer immunotherapy. J Immunother Cancer. 2020;8(2).

78. Graydon CG, Mohideen S, Fowke KR. LAG3's Enigmatic Mechanism of Action. Front Immunol. 2021;11.

79. Qian W, Zhao M, Wang R, Li H. Fibrinogen-like protein 1 (FGL1): the next immune checkpoint target. J Hematol Oncol. 2021;14(1).

80. Hui E, Cheung J, Zhu J, Su X, Taylor MJ, Wallweber HA, et al. T cell costimulatory receptor CD28 is a primary target for PD-1-mediated inhibition. Science (80-). 2017;355(6332):1428–33.

81. Zhu C, Anderson AC, Schubart A, Xiong H, Imitola J, Khoury SJ, et al. The Tim-3 ligand galectin-9 negatively regulates T helper type 1 immunity. Nat Immunol. 2005;6(12).

82. Anderson AC, Joller N, Kuchroo VK. Lag-3, Tim-3, and TIGIT: Co-inhibitory Receptors with Specialized Functions in Immune Regulation. Immunity. 2016;44(5).

83. Coulie PG, Van Den Eynde BJ, Van Der Bruggen P, Boon T. Tumour antigens recognized by T lymphocytes: At the core of cancer immunotherapy. Nat Rev Cancer. 2014;14(2).

84. Fisk B, Blevins TL, Wharton JT, Ioannides CG. Identification of an immunodominant peptide of HER-2/neu protooncogene recognized by ovarian tumor-specific cytotoxic t lymphocyte lines. J Exp Med. 1995;181(6).

85. Coulie PG, Brichard V, Van Pel A, Wolfel T, Schneider J, Traversari C, et al. A new gene coding for a differentiation antigen recognized by autologous cytolytic T lymphocytes on HLA-A2 melanomas. J Exp Med. 1994;180(1).

86. Kawakami Y, Eliyahu S, Sakaguchi K, Robbins PF, Rivoltini L, Yannelli JR, et al. Identification of the immunodominant peptides of the MART-1 human melanoma antigen recognized by the majority of HLA-A2-restricted tumor infiltrating lymphocytes. J Exp Med. 1994;180(1).

87. Pittet MJ, Valmori D, Dunbar PR, Speiser DE, Liénard D, Lejeune F, et al. High frequencies of naive Melan-A/MART-1-specific CD8+ T cells in a large proportion of human histocompatibility leukocyte antigen (HLA)-A2 individuals. J Exp Med. 1999;190(5).

88. De Smet C, De Backer O, Faraoni I, Lurquin C, Brasseur F, Boon T. The activation of human gene MAGE-1 in tumor cells is correlated with genome-wide demethylation. Proc Natl Acad Sci U S A. 1996;93(14).

89. van der Burg SH, Melief CJM. Therapeutic vaccination against human papilloma virus induced malignancies. Curr Opin Immunol. 2011;23(2).

90. Schumacher TN, Schreiber RD. Neoantigens in cancer immunotherapy. Science (80-). 2015;348(6230).

91. Snyder A, Makarov V, Merghoub T, Yuan J, Zaretsky JM, Desrichard A, et al. Genetic Basis for

Clinical Response to CTLA-4 Blockade in Melanoma. N Engl J Med. 2014;371(23).

92. Rizvi NA, Hellmann MD, Snyder A, Kvistborg P, Makarov V, Havel JJ, et al. Mutational landscape determines sensitivity to PD-1 blockade in non–small cell lung cancer. Science. 2015;348(6230):124.

93. Bjerregaard AM, Nielsen M, Jurtz V, Barra CM, Hadrup SR, Szallasi Z, et al. An analysis of natural T cell responses to predicted tumor neoepitopes. Front Immunol. 2017;8(NOV).

94. Maby P, Galon J, Latouche JB. Frameshift mutations, neoantigens and tumor-specific CD8+ T cells in microsatellite unstable colorectal cancers. Oncoimmunology. 2016;5(5).

95. Turajlic S, Litchfield K, Xu H, Rosenthal R, McGranahan N, Reading JL, et al. Insertion-and-deletion-derived tumour-specific neoantigens and the immunogenic phenotype: a pan-cancer analysis. Lancet Oncol. 2017;18(8).

96. McGranahan N, Swanton C. Clonal Heterogeneity and Tumor Evolution: Past, Present, and the Future. Cell. 2017;168(4).

97. McDonald KA, Kawaguchi T, Qi Q, Peng X, Asaoka M, Young J, et al. Tumor Heterogeneity Correlates with Less Immune Response and Worse Survival in Breast Cancer Patients. Ann Surg Oncol. 2019;26(7).

98. McGranahan N, Furness AJS, Rosenthal R, Ramskov S, Lyngaa R, Saini SK, et al. Clonal neoantigens elicit T cell immunoreactivity and sensitivity to immune checkpoint blockade. Science (80-). 2016;351(6280).

99. Greaves M, Maley CC. Clonal evolution in cancer. Nature. 2012;481(7381).

100. Kim H, Zheng S, Amini SS, Virk SM, Mikkelsen T, Brat DJ, et al. Whole-genome and multisector exome sequencing of primary and post-treatment glioblastoma reveals patterns of tumor evolution. Genome Res. 2015;25(3).

101. Johnson BE, Mazor T, Hong C, Barnes M, Aihara K, McLean CY, et al. Mutational analysis reveals the origin and therapy-driven evolution of recurrent glioma. Science (80-). 2014;343(6167).

102. Landau DA, Carter SL, Stojanov P, McKenna A, Stevenson K, Lawrence MS, et al. Evolution and impact of subclonal mutations in chronic lymphocytic leukemia. Cell. 2013;152(4).

103. Karpanen T, Olweus J. The potential of donor T-cell repertoires in neoantigen-targeted cancer immunotherapy. Front Immunol. 2017;8(DEC).

104. Schumacher TN, Scheper W, Kvistborg P. Cancer Neoantigens. Annu Rev Immunol. 2019;37:173–200.

105. Reynisson B, Alvarez B, Paul S, Peters B, Nielsen M. NetMHCpan-4.1 and NetMHCIIpan-4.0: Improved predictions of MHC antigen presentation by concurrent motif deconvolution and integration of MS MHC eluted ligand data. Nucleic Acids Res. 2021;48(W1).

106. Jurtz V, Paul S, Andreatta M, Marcatili P, Peters B, Nielsen M. NetMHCpan-4.0: Improved Peptide–MHC Class I Interaction Predictions Integrating Eluted Ligand and Peptide Binding Affinity Data. J Immunol. 2017;199(9).

107. Hadrup SR, Newell EW. Determining T-cell specificity to understand and treat disease. Nat Biomed Eng 2017 110. 2017;1(10):784–95.

108. Rodenko B, Toebes M, Hadrup SR, van Esch WJE, Molenaar AM, Schumacher TNM, et al. Generation of peptide-MHC class I complexes through UV-mediated ligand exchange. Nat Protoc. 2006;1(3).

109. Saini SK, Ostermeir K, Ramnarayan VR, Schuster H, Zacharias M, Springer S. Dipeptides promote folding and peptide binding of MHC class i molecules. Proc Natl Acad Sci U S A. 2013;110(38).

110. Saini SK, Schuster H, Ramnarayan VR, Rammensee HG, Stevanović S, Springer S. Dipeptides catalyze rapid peptide exchange on MHC class I molecules. Proc Natl Acad Sci U S A. 2015;112(1).

111. Saini SK, Tamhane T, Anjanappa R, Saikia A, Ramskov S, Donia M, et al. Empty peptide-receptive MHC class I molecules for efficient detection of antigen-specific T cells. Sci Immunol. 2019;4(37).

112. Altman JD, Moss PAH, Goulder PJR, Barouch DH, McHeyzer-Williams MG, Bell JI, et al. Phenotypic analysis of antigen-specific T lymphocytes. Science (80-). 1996;274(5284).

113. Hadrup SR, Bakker AH, Shu CJ, Andersen RS, van Veluw J, Hombrink P, et al. Parallel detection of antigen-specific T-cell responses by multidimensional encoding of MHC multimers. Nat Methods. 2009;6(7).

114. Bentzen AK, Marquard AM, Lyngaa R, Saini SK, Ramskov S, Donia M, et al. Large-scale detection of antigen-specific T cells using peptide-MHC-I multimers labeled with DNA barcodes. Nat

Biotechnol. 2016 Oct 1;34(10):1037–45.

115. COLEY WB. The Treatment of Sarcoma with the Mixed Toxins of Erysipelas and Bacillus Prodigiosus. Bost Med Surg J. 1908;158(6).

116. Hoption Cann SA, Van Netten JP, Van Netten C. Dr William Coley and tumour regression: A place in history or in the future. Postgrad Med J. 2003;79(938).

117. Gresser I, Bourali C. Antitumor effects of interferon preparations in mice. J Natl Cancer Inst. 1970;45(2).

118. Lotze MT, Line BR, Mathisen DJ, Rosenberg SA. The in vivo distribution of autologous human and murine lymphoid cells grown in T cell growth factor (TCGF): implications for the adoptive immunotherapy of tumors. J Immunol. 1980;125(4).

119. Yron I, Wood TA, Spiess PJ, Rosenberg SA. In vitro growth of murine T cells. V. The isolation and growth of lymphoid cells infiltrating syngeneic solid tumors. J Immunol. 1980;125(1).

120. Rosenberg SA, Lotze MT, Muul LM, Leitman S, Chang AE, Ettinghausen SE, et al. Observations on the Systemic Administration of Autologous Lymphokine-Activated Killer Cells and Recombinant Interleukin-2 to Patients with Metastatic Cancer. N Engl J Med. 1985;313(23).

121. Kirkwood JM, Strawderman MH, Ernstoff MS, Smith TJ, Borden EC, Blum RH. Interferon alfa-2b adjuvant therapy of high-risk resected cutaneous melanoma: The Eastern Cooperative Oncology Group trial EST 1684. J Clin Oncol. 1996;14(1).

122. Atkins MB, Lotze MT, Dutcher JP, Fisher RI, Weiss G, Margolin K, et al. High-dose recombinant interleukin 2 therapy for patients with metastatic melanoma: Analysis of 270 patients treated between 1985 and 1993. J Clin Oncol. 1999;17(7).

123. Rosenberg SA. IL-2: The First Effective Immunotherapy for Human Cancer. J Immunol. 2014;192(12).

124. Chen DS, Mellman I, Boon T, Cerottini JC, Eynde B Van den, Bruggen P van der, et al. Oncology Meets Immunology: The Cancer-Immunity Cycle. Immunity. 2013;39(1):1–10.

125. Papaioannou NE, Beniata O V., Vitsos P, Tsitsilonis O, Samara P. Harnessing the immune system to improve cancer therapy. Ann Transl Med. 2016;4(14).

126. Leach DR, Krummel MF, Allison JP. Enhancement of antitumor immunity by CTLA-4 blockade. Science (80-). 1996;271(5256).

127. Simpson TR, Li F, Montalvo-Ortiz W, Sepulveda MA, Bergerhoff K, Arce F, et al. Fc-dependent depletion of tumor-infiltrating regulatory t cells co-defines the efficacy of anti-CTLA-4 therapy against melanoma. J Exp Med. 2013;210(9).

128. Nishimura H, Nose M, Hiai H, Minato N, Honjo T. Development of lupus-like autoimmune diseases by disruption of the PD-1 gene encoding an ITIM motif-carrying immunoreceptor. Immunity. 1999;11(2).

129. Ishida Y, Agata Y, Shibahara K, Honjo T. Induced expression of PD-1, a novel member of the immunoglobulin gene superfamily, upon programmed cell death. EMBO J. 1992;11(11).

130. Dong H, Zhu G, Tamada K, Chen L. B7-H1, a third member of the B7 family, co-stimulates T-cell proliferation and interleukin-10 secretion. Nat Med. 1999;5(12).

131. Freeman GJ, Long AJ, Iwai Y, Bourque K, Chernova T, Nishimura H, et al. Engagement of the PD-1 immunoinhibitory receptor by a novel B7 family member leads to negative regulation of lymphocyte activation. J Exp Med. 2000;192(7):1027–34.

132. Kythreotou A, Siddique A, Mauri FA, Bower M, Pinato DJ. PD-L1. J Clin Pathol. 2018 Mar 1;71(3):189–94.

133. Seidel JA, Otsuka A, Kabashima K. Anti-PD-1 and anti-CTLA-4 therapies in cancer: Mechanisms of action, efficacy, and limitations. Front Oncol. 2018;8(MAR):86.

134. Darvin P, Toor SM, Sasidharan Nair V, Elkord E. Immune checkpoint inhibitors: recent progress and potential biomarkers. Exp Mol Med. 2018;50(12).

135. Cameron F, Whiteside G, Perry C. Ipilimumab: First global approval. Drugs. 2011;71(8).

136. Twomey JD, Zhang B. Cancer Immunotherapy Update: FDA-Approved Checkpoint Inhibitors and Companion Diagnostics. AAPS J. 2021;23(2):1–11.

137. Havel JJ, Chowell D, Chan TA. The evolving landscape of biomarkers for checkpoint inhibitor immunotherapy. Nat Rev Cancer. 2019;19(3).

138. Postow MA, Sidlow R, Hellmann MD. Immune-Related Adverse Events Associated with Immune

Checkpoint Blockade. N Engl J Med. 2018;378(2).

139. Kumar V, Chaudhary N, Garg M, Floudas CS, Soni P, Chandra AB. Current diagnosis and management of immune related adverse events (irAEs) induced by immune checkpoint inhibitor therapy. Front Pharmacol. 2017;8(FEB).

140. Reck M, Rodríguez-Abreu D, Robinson AG, Hui R, Csőszi T, Fülöp A, et al. Pembrolizumab versus Chemotherapy for PD-L1–Positive Non–Small-Cell Lung Cancer. N Engl J Med. 2016;375(19).

141. Robert C, Long G V., Brady B, Dutriaux C, Maio M, Mortier L, et al. Nivolumab in Previously Untreated Melanoma without BRAF Mutation . N Engl J Med. 2015;372(4).

142. Khan O, Giles JR, McDonald S, Manne S, Ngiow SF, Patel KP, et al. TOX transcriptionally and epigenetically programs CD8+ T cell exhaustion. Nature. 2019;571(7764).

143. Siddiqui I, Schaeuble K, Chennupati V, Fuertes Marraco SA, Calderon-Copete S, Pais Ferreira D, et al. Intratumoral Tcf1 + PD-1 + CD8 + T Cells with Stem-like Properties Promote Tumor Control in Response to Vaccination and Checkpoint Blockade Immunotherapy. Immunity. 2019;50(1).

144. Jenkins RW, Barbie DA, Flaherty KT. Mechanisms of resistance to immune checkpoint inhibitors. Br J Cancer. 2018;118(1).

145. Simoni Y, Becht E, Fehlings M, Loh CY, Koo SL, Teng KWW, et al. Bystander CD8+ T cells are abundant and phenotypically distinct in human tumour infiltrates. Nature. 2018;557(7706).

146. Gupta PK, Godec J, Wolski D, Adland E, Yates K, Pauken KE, et al. CD39 Expression Identifies Terminally Exhausted CD8+ T Cells. PLoS Pathog. 2015;11(10).

147. Shevchenko I, Mathes A, Groth C, Karakhanova S, Müller V, Utikal J, et al. Enhanced expression of CD39 and CD73 on T cells in the regulation of anti-tumor immune responses. Oncoimmunology. 2020;9(1).

148. Arab S, Hadjati J. Adenosine blockage in tumor microenvironment and improvement of cancer immunotherapy. Immune Netw. 2019;19(4).

149. Herbst RS, Soria JC, Kowanetz M, Fine GD, Hamid O, Gordon MS, et al. Predictive correlates of response to the anti-PD-L1 antibody MPDL3280A in cancer patients. Nature. 2014;515(7528).

150. Liu R, Yang F, Yin JY, Liu YZ, Zhang W, Zhou HH. Influence of Tumor Immune Infiltration on

Immune Checkpoint Inhibitor Therapeutic Efficacy: A Computational Retrospective Study. Front Immunol. 2021;12.

151. Kazama A, Bilim V, Tasaki M, Anraku T, Kuroki H, Shirono Y, et al. Tumor-infiltrating immune cell status predicts successful response to immune checkpoint inhibitors in renal cell carcinoma. Sci Rep. 2022;12(1).

152. Ward EM, Flowers CR, Gansler T, Omer SB, Bednarczyk RA. The importance of immunization in cancer prevention, treatment, and survivorship. CA Cancer J Clin. 2017;67(5).

153. Pulendran B, Ahmed R. Immunological mechanisms of vaccination. Nat Immunol. 2011;12(6).

154. Kantoff PW, Higano CS, Shore ND, Berger ER, Small EJ, Penson DF, et al. Sipuleucel-T Immunotherapy for Castration-Resistant Prostate Cancer. N Engl J Med. 2010;363(5).

155. Kong HY, Byun J. Emerging roles of human prostatic acid phosphatase. Biomol Ther. 2013;21(1).

156. Van De Laar L, Coffer PJ, Woltman AM. Regulation of dendritic cell development by GM-CSF: Molecular control and implications for immune homeostasis and therapy. Vol. 119, Blood. 2012.

157. Tay BQ, Wright Q, Ladwa R, Perry C, Leggatt G, Simpson F, et al. Evolution of cancer vaccines—challenges, achievements, and future directions. Vaccines. 2021;9(5).

158. Bjerregaard AM, Nielsen M, Hadrup SR, Szallasi Z, Eklund AC. MuPeXI: prediction of neo-epitopes from tumor sequencing data. Cancer Immunol Immunother. 2017 Sep 1;66(9):1123–30.

159. Liu J, Fu M, Wang M, Wan D, Wei Y, Wei X. Cancer vaccines as promising immuno-therapeutics: platforms and current progress. J Hematol Oncol. 2022;15(1).

160. Alspach E, Lussier DM, Miceli AP, Kizhvatov I, DuPage M, Luoma AM, et al. MHC-II neoantigens shape tumour immunity and response to immunotherapy. Nature. 2019;574(7780).

161. Hu Z, Leet DE, Allesøe RL, Oliveira G, Li S, Luoma AM, et al. Personal neoantigen vaccines induce persistent memory T cell responses and epitope spreading in patients with melanoma. Nat Med. 2021;27(3).

162. Bijker MS, van den Eeden SJF, Franken KL, Melief CJM, Offringa R, van der Burg SH. CD8+ CTL Priming by Exact Peptide Epitopes in Incomplete Freund's Adjuvant Induces a Vanishing CTL Response, whereas Long Peptides Induce Sustained CTL Reactivity. J Immunol. 2007;179(8).

163. Bijker MS, van den Eeden SJF, Franken KL, Melief CJM, van der Burg SH, Offringa R. Superior induction of anti-tumor CTL immunity by extended peptide vaccines involves prolonged, DC-focused antigen presentation. Eur J Immunol. 2008;38(4).

164. Slingluff CL. The present and future of peptide vaccines for cancer: Single or multiple, long or short, alone or in combination? Cancer J. 2011;17(5).

165. Ott PA, Hu Z, Keskin DB, Shukla SA, Sun J, Bozym DJ, et al. An immunogenic personal neoantigen vaccine for patients with melanoma. Nature. 2017;547(7662).

166. Awad MM, Govindan R, Balogh KN, Spigel DR, Garon EB, Bushway ME, et al. Personalized neoantigen vaccine NEO-PV-01 with chemotherapy and anti-PD-1 as first-line treatment for non-squamous non-small cell lung cancer. Cancer Cell. 2022;40(9):1010–26.

167. Honey K. TLR3 helps DCs to cross-prime. Nat Rev Immunol. 2005;5(3).

168. Khong H, Overwijk WW. Adjuvants for peptide-based cancer vaccines. J Immunother Cancer. 2016;4(1).

169. Korsholm KS, Hansen J, Karlsen K, Filskov J, Mikkelsen M, Lindenstrøm T, et al. Induction of CD8+ T-cell responses against subunit antigens by the novel cationic liposomal CAF09 adjuvant. Vaccine. 2014;32(31).

170. Hilf N, Kuttruff-Coqui S, Frenzel K, Bukur V, Stevanović S, Gouttefangeas C, et al. Actively personalized vaccination trial for newly diagnosed glioblastoma. Nature. 2019;565(7738).

171. Ott PA, Hu-Lieskovan S, Chmielowski B, Govindan R, Naing A, Bhardwaj N, et al. A Phase Ib Trial of Personalized Neoantigen Therapy Plus Anti-PD-1 in Patients with Advanced Melanoma, Non-small Cell Lung Cancer, or Bladder Cancer. Cell. 2020;183(2):347–62.

172. Crosby EJ, Acharya CR, Haddad AF, Rabiola CA, Lei G, Wei JP, et al. Stimulation of oncogene-specific tumor-infiltrating T cells through combined vaccine and aPD-1 enable sustained antitumor responses against established HER2 breast cancer. Clin Cancer Res. 2020;26(17):4670–81.

173. Yarchoan M, Hopkins A, Jaffee EM. Tumor Mutational Burden and Response Rate to PD-1 Inhibition. N Engl J Med. 2017;377(25).

174. Stupp R, Mason WP, van den Bent MJ, Weller M, Fisher B, Taphoorn MJB, et al. Radiotherapy

plus Concomitant and Adjuvant Temozolomide for Glioblastoma. N Engl J Med. 2005;352(10):987–96.

175. Reardon DA, Gokhale PC, Klein SR, Ligon KL, Rodig SJ, Ramkissoon SH, et al. Glioblastoma eradication following immune checkpoint blockade in an orthotopic, immunocompetent model. Cancer Immunol Res. 2016;4(2):124–35.

176. Park J, Kim CG, Shim JK, Kim JH, Lee H, Lee JE, et al. Effect of combined anti-PD-1 and temozolomide therapy in glioblastoma. Oncoimmunology. 2018;8(1).

177. Reardon DA, Brandes AA, Omuro A, Mulholland P, Lim M, Wick A, et al. Effect of Nivolumab vs Bevacizumab in Patients With Recurrent Glioblastoma: The CheckMate 143 Phase 3 Randomized Clinical Trial. JAMA Oncol. 2020;6(7):1003–10.

178. Grossman SA, Romo CG, Rudek MA, Supko J, Fisher J, Burt Nabors L, et al. Baseline requirements for novel agents being considered for phase II/III brain cancer efficacy trials: Conclusions from the Adult Brain Tumor Consortium's first workshop on CNS drug delivery. Neuro Oncol. 2020;22(10).

179. Liebner S, Fischmann A, Rascher G, Duffner F, Grote EH, Kalbacher H, et al. Claudin-1 and claudin-5 expression and tight junction morphology are altered in blood vessels of human glioblastoma multiforme. Acta Neuropathol. 2000;100(3):323–31.

180. Wolburg H, Wolburg-Buchholz K, Kraus J, Rascher-Eggstein G, Liebner S, Hamm S, et al. Localization of claudin-3 in tight junctions of the blood-brain barrier is selectively lost during experimental autoimmune encephalomyelitis and human glioblastoma multiforme. Acta Neuropathol. 2003;105(6):586–92.

181. Naik GS, Buchbinder EI, Cohen J V., Manos MP, Johnson AEW, Bowling P, et al. Long-term Overall Survival and Predictors in Anti-PD-1-naive Melanoma Patients with Brain Metastases Treated with Immune Checkpoint Inhibitors in the Real-world Setting: A Multicohort Study. J Immunother. 2021;44(8).

182. Crinò L, Bronte G, Bidoli P, Cravero P, Minenza E, Cortesi E, et al. Nivolumab and brain metastases in patients with advanced non-squamous non-small cell lung cancer. Lung Cancer. 2019;129.

183. Di Giacomo AM, Mair MJ, Ceccarelli M, Anichini A, Ibrahim R, Weller M, et al. Immunotherapy for brain metastases and primary brain tumors. Eur J Cancer. 2023;179:113–20.

184. Andersen RS, Anand A, Harwood DSL, Kristensen BW. Tumor-associated microglia and macrophages in the glioblastoma microenvironment and their implications for therapy. Cancers (Basel). 2021;13(17).

185. Goldman M, Lucke-Wold B, Martinez-Sosa M, Katz J, Mehkri Y, Valisno J, et al. Steroid utility, immunotherapy, and brain tumor management: an update on conflicting therapies. Explor Target Anti-tumor Ther. 2022;3(5):659.

186. Maas SLN, Abels ER, Van De Haar LL, Zhang X, Morsett L, Sil S, et al. Glioblastoma hijacks microglial gene expression to support tumor growth. J Neuroinflammation. 2020;17(1).

187. Roth P, Valavanis A, Weller M. Long-term control and partial remission after initial pseudoprogression of glioblastoma by anti-PD-1 treatment with nivolumab. Neuro Oncol. 2017;19(3).

188. Giunti D, Borsellino G, Benelli R, Marchese M, Capello E, Valle MT, et al. Phenotypic and functional analysis of T cells homing into the CSF of subjects with inflammatory diseases of the CNS. J Leukoc Biol. 2003;73(5):584–90.

189. Teleshova N, Pashenkov M, Huang YM, Söderström M, Kivisäkk P, Kostulas V, et al. Multiple sclerosis and optic neuritis: CCR5 and CXCR3 expressing T cells are augmented in blood and cerebrospinal fluid. J Neurol. 2002;249(6):723–9.

190. Sahin U, Derhovanessian E, Miller M, Kloke BP, Simon P, Löwer M, et al. Personalized RNA mutanome vaccines mobilize poly-specific therapeutic immunity against cancer. Nature. 2017;547(7662).

191. Bauman J, Burris H, Clarke J, Patel M, Cho D, Gutierrez M, et al. 798 Safety, tolerability, and immunogenicity of mRNA-4157 in combination with pembrolizumab in subjects with unresectable solid tumors (KEYNOTE-603): an update. In 2020.

192. Fuchs YF, Sharma V, Eugster A, Kraus G, Morgenstern R, Dahl A, et al. Gene Expression-Based Identification of Antigen-Responsive CD8+ T Cells on a Single-Cell Level. Front Immunol. 2019;10.

193. Yi M, Qin S, Zhao W, Yu S, Chu Q, Wu K. The role of neoantigen in immune checkpoint blockade therapy. Exp Hematol Oncol. 2018;7(1).